New gadolinium contrast agents for MRI

Elisa Elemento

New Gadolinium Contrast Agents for MRI

Elisa Elemento

A thesis submitted for the degree of Doctor of Philosophy

Department of Chemistry
Durham University

2008

To David,

for all the support over these years

Abstract

A collaboration between Bracco Imaging S.p.A. and Durham University allowed the work described in this thesis on the design and synthesis of new contrast agents for MRI.

Significant enhancements in the relaxivity of contrast agents for MRI can be gained by increasing the complex rotational correlation time (τ_R). Incorporating a Gd^{III} ion within a ligand structure possessing a suitably large dendritic framework, inspired the first part of this project. Thus, the periphery of a Gd-DOTA derivative was adorned with carbohydrate containing wedges. The symmetry of the mono-aqua tetra-substituted structure places the gadolinium-water vector at the centre of any tumbling motion, allowing a coherent tumbling of the macromolecule and an optimization of its rotational correlation time. The carbohydrates ensured high water solubility and favoured a large second sphere hydration contribution to the relaxivity.

An increase in the hydration around the metal centre and a rapid exchange of the water molecules with the bulk solvent can also significantly increase the contrast agent efficacy, by efficiently transmitting the paramagnetic effect from the Gd^{III} to the solvent. In a second part of the work, the development was undertaken of diaqua systems based on the seven-membered heterocycle 6-amino-6-methyl-perhydro-1,4-diazepin (AMPED). The three *N*-positions were substituted with different phosphinate and carboxylate groups and lanthanide complexes (Eu^{III}, Gd^{III}, Yb^{III}) prepared and studied by multinuclear NMR methods The alkylation of the amino groups with chiral 1,5-dicarboxylate pendant arms led to complex diastereisomers, possessing different water exchange rates. The individual water exchange rates of each isomer were determined, and differed by a factor of six. Furthermore, the periphery of the isomer possessing a faster water exchange rate was adorned with carbohydrate containing wedges, and the relaxation properties studied.

Declaration

The work described herein was carried out in the Department of Chemistry, University of Durham between October 2004 and September 2007. All of the work is my own; no part has previously been submitted for a degree at this or any other university.

Statement of Copyright

Acknowledgements

I would like to thank all the people who have encouraged and given me support over these last three years. Thanks to them, this time in Durham has been a very pleasant learning experience. In particular, I thank Prof. David Parker for his constant supervision and for being a guide in every step of my studies;

Dr. Lattuada and Dr. Morosini, who nicely supervised my work during the time spent in Bracco Imaging S.p.A. (Milano); Prof. Aime and Dr. Eliana Gianolio at University of Torino and Prof. Botta at University of Oriental Piedmont "Amedeo Avogadro", for performing NMRD and VT ^{17}O NMR R_{2p} experiments and for their effective collaboration; thanks to Dr. Alan Kenwright, Catherine Hefferman and Ian McKeag, for their patient assistance with NMR spectroscopy; Dr. Mike Jones, Lara Turner and Jackie Mosely, for their constant assistance with mass spectrometry measurements; Chris Ottley, for ICP analysis.

I would also like to thank the current and past members of the Wolfson laboratory (CG 27) for their friendly advice and friendship. Thanks to Filip, Rachel, Lars, Raman, Ga-Lai, Kanthi, Junhua Yu, Ben, Craig, Liz, Kirsten, Siobhan, David, James, Susanna, Shashi, Philip, Robert, Kevin, Paul, Robert, Nicola, Jonathan. Thanks to Sawsan, Alessandra, Xanthippe and Elena for being perfect housemates and because I have found in them new friends. Thanks to Liz, for her friendship and for helping me to improve my English since I first arrived, and thanks to Pratick, Andrea, Giovanni, Kathy, Pierpa, Mita, Milena, Ann, Laura, Jesus, Jaime and Louisa for all the nice moments together!

Thanks to my friends back home, because we have managed to stay close despite the distance: thank you Laura, Cecilia, Jako, Paolone, Roby, Maka, Maurizio, Protti, Lupo, Susy.

A special thanks to my mum and dad, because they have always been supporting me with their love.

Finally, I am especially thankful to David who has provided me with immense encouragement and support throughout all my time here at Durham.

Abbreviations

AIBN	*N,N'*–Azoisobutyronitrile
AMP	Adenosine–5'–monophosphate
AMPED	6-Amino-6-methyl-perhydro-1,4-diazepin
Arg	Arginine
Asp	Aspartate
BOC	*tert*-Butyloxycarbonyl
Bz	benzyloxycarbonyl
CA	Contrast Agent
Cyclen	1,4,7,10–tetraazacyclododecane
COSY	COrrelation SpectroscopY
DCC	1,3-Dicyclohexylcarbodiimide
DCM	Dichloromethane
DiBOC	*tert*–Butyldicarbonate anhydride
DMAP	*N,N*–Dimethylaminopyridine
DMF	*N,N*–Dimethylformamide
DMSO	Dimethylsulfoxide
DOTA	tetraazacyclododecanetetraacitic acid
DTPA	diethylentriaminepentaacitic acid
EDC	1–Ethyl–3–(3–dimethylaminopropyl)carbodiimide hydrochloride
EDTA	Ethylenediamine tatraacetic acid
ES-MS	Electrospray Mass-Spectrometry
EPA	solvent mixture for low temperature optical studies; diethyl ether, isopentane and ethanol 5:5:2
Glu	Glutamate
GBCA	Gadolinium Based Contrast Agents
GPC	Gel Permeation Chromatography
HBTU	2–(1H–benzotriazole–1–yl)–1,1,3,3–tetramethyluronium hexafluorophosphate
HOBt	1-Hydroxybenzotriazole hydrate
HOPO	Hydroxypyridinone
HPLC	High Performance Liquid Chromatography
HSA	Human Serum Albumin

HSQC	Heteronuclear Single Quantum Correlation
IC	Internal Conversion
MALDI	Matrix Assisted Laser Desorption Ionisation
MeCN	Acetonitrile
$MeNO_2$	Nitromethane
MOPS	3–(*N*–morpholino)propanesulfonic acid
MRI	Magnetic Resonance Imaging
MRS	Magnetic Resonance Spectroscopy
NBS	*N*–Bromosuccinimide
NMM	*N*-Methylmorpholine
NMR	Nuclear Magnetic Resonance
NMRD	Nuclear Magnetic Resonance Dispersion
NHS	*N*-hydroxysuccinimide
NOESY	Nuclear Overhauser Effect SpectroscopY
PAMAM	dendrimer based on ethylene diamine and acrylic acid building blocks
PPA	Polyphosphoric acid
SAP	Square antiprism
Ser	Serine
TACN	triazacyclononane
TAM	terephtalamide
THF	Tetrahydrofuran
TFA	Trifluoroacetic acid
TOCSY	TOtal Correlation SpectroscopY
TOF	Time Of Flight
TRIS	tri(hydroxymethyl)methylamine
TSAP	twisted square antiprism
UV	Ultra Violet
Vis	Visible

Table of Contents

Chapter 1 - Introduction -

Chapter 2

Chapter 3

Chapter 4

Chapter 1

Introduction

I. An Outline of Contrast Agents (CA) for Magnetic Resonance Imaging (MRI)

MRI has been discovered and developed as a powerful technique for application in diagnostic clinical medicine and biomedical research. It is a non-invasive procedure that uses strong magnets and radio-frequencies to construct three dimensional images of the body. Unlike conventional radiography and computed tomographic (CT) imaging, which make use of potentially harmful (X-ray) radiation, MRI is based on the magnetic properties of hydrogen nuclei in water.

I.1 MRI in clinical diagnostic medicine

"Clinical Magnetic Resonance Imaging (MRI) is essentially an elaborate proton nuclear magnetic resonance (NMR) experiment that visualizes water molecules".[1] Water is abundant in the human body and, with MRI, the three-dimensional images of the distribution of the water protons can be observed *in vivo*, described by the values of the longitudinal relaxation time (T_1), the transverse relaxation time (T_2) and the spin density. The relaxation times T_1 and T_2 are dependent on the local environment of the water molecules and the spin density depends on the concentration of water in the tissue considered. Consequently, different types of biological tissue have different water concentrations (**Table I.1**), leading to different relaxation times.

Tissue	Water content
Kidney	81%
Liver	71%
Teeth/Bones	10%

Table I.1: Water content of some tissue types.[2]

The discovery in the 1970's that the T_1 of tumours experimentally induced in tissues of laboratory animals were significantly longer than T_1 values of the corresponding normal tissues, led to an extension of the study to humans. Soon, the NMR analysis of 106 tumours taken at surgery was completed (T_1 relaxations in some malignant and normal human tissues are reported in **Table I.2**)[3] and an NMR catalogue of human neoplasm was started, with the aim of forming a database to design an instrument to detect internal malignancies.

Tissue	T_1 tumour (s)	T_1 normal (s)
Bone	1.027	0.554
Breast	1.080	0.367
Liver	0.832	0.570
Lung	1.110	0.788
Skin	1.047	0.616

Table I.2: T_1 relaxation times in some malignant and normal human tissues.

There is no ionizing radiation involved in MRI, and there have been no documented significant side effects of the magnetic fields and radio waves used on the human body to date. Although MRI was initially hoped to provide a means of making definitive diagnoses non-invasively, it was found that the addition of contrast agents (CAs) in many cases improved sensitivity and/or specificity. Currently, more than 10 million MRI studies are performed each year with gadolinium based contrast agents (GBCAs),[4] which are the magnetic resonance equivalent of a dye: they are injected into the body to enhance the contrast between normal and diseased tissue. The intensity of the signal in MRI increases with the local values of the longitudinal relaxation rate of water protons ($R_1 = 1/T_1$ (s^{-1})) and contrast agents in MRI should catalytically accelerate the relaxation time of nearby water molecules in the surrounding tissue, providing contrast to those areas where the rates remain unaffected. This objective can be achieved by paramagnetic substances, and the unique magnetic properties of lanthanides (in particular gadolinium) make these

metal ions near ideal for the purpose. The most common intravenous contrast agents are based on complexes of gadolinium.

I.2 Lanthanides and their paramagnetic properties

The lanthanides are commonly thought of as trace constituents of the terrestrial environment. Although rare in comparison to the more common "earths" (the old term for water-insoluble strongly basic oxides of electropositive metals) such as lime or magnesia, these elements are as abundant in the solar system as many heavy elements (such as tungsten, tantalum, iridium).[5] For example thulium, the least common naturally-occurring lanthanoid, is more abundant than iodine, cerium is the 26th most abundant element in the Earth's crust, and neodymium is more abundant than gold.

Mendeleev's periodic classification of the elements places the lanthanides in the first period of the f-block, starting from lanthanum (Z = 57), with electronic configuration [Xe] $5d^1 6s^2$, to lutetium (Z = 71), [Xe] $4f^{14} 5d^1 6s^2$. The similar physicochemical properties shown by these elements is attributed to their common existence in the more stable oxidation state as trivalent ions, given by the loss of a single 4f electron and two 6s electrons (with the exception of lanthanum, lutetium and gadolinium which, because of the electronic configuration including 5d orbitals, lose one 5d electron and two 6s electrons). The lanthanide trications possess a Xe core electronic configuration with the addition of *n* 4f electrons, protected by closed $5s^2$ and $5p^6$ sub-shells. The shielded 4f orbitals of the lanthanides only slightly overlap with the ligand atom orbitals, suggesting a predominant electrostatic character for the interaction between the lanthanide trication and the ligand's atoms. The lanthanides behave in their complexes as "hard" acids, which interact preferentially with "hard" bases, such as fluoride, oxygen and nitrogen. The resulting complexes adopt irregular geometries, reflecting a balance between electrostatic and steric demand around the highly coordinated metal. The more common coordination numbers for lanthanides in aqueous solutions are 8 and 9, and the lanthanide contraction theory explains how the

size of the ion affects its coordination number: the smaller the ionic radius becomes along the series from La^{3+} towards Lu^{3+}, the more contracted the 5s and 5p orbitals are and a lessening in the coordination number (CN) is observed (CN ~ 10 for La^{3+}, CN ~ 8 for Lu^{3+}).

Furthermore, the one or more unpaired 4f electrons confer paramagnetic properties upon the trivalent lanthanide cations; only La^{3+} and Lu^{3+} are diamagnetic. This important characteristic has made lanthanide complexation chemistry a subject of intense study over the last 20 years. In this thesis we will mainly focus on the extraordinary properties of gadolinium complexes as potential intravenous contrast agents for enhancing image intensities in MRI. The most common intravenous CAs used in clinical practice are nowadays based on Gd^{III} which, because of its half-filled f-shell, has a large magnetic moment. Owing to the symmetric S-state which is an hospitable environment for electron spins, this metal ion possesses a high spin paramagnetism and also an exceptionally long electron spin relaxation times (~ 10^{-9} s at the magnetic field strengths of interest for MRI applications),[6] typically 3-4 orders of magnitude longer than for other lanthanides (except Eu^{II}, which is a very strong reducing agent).[7]

I.3 Characteristics for a CA suitable for medical use

In clinical applications, small dosage, reasonable aqueous solubility, good metal retention and hydrophilicity are required physico-chemical properties.

Solubility- Since the amount of metal chelate necessary for a significant increase in image contrast is relatively high (for low molecular weight Gd^{III} complexes, a typical dose is 0.05 - 0.3 mmol kg^{-1} total body weight)[8] the concentration of the injected solution must also be high. To obtain the necessary water solubility of the non-ionic Gd^{III} complex (~ 0.5 M), the introduction of hydrophilic OH groups as side chains or functional groups in the ligand structure is a typically adopted synthetic strategy (e.g. DO3A-butrol and HP-DO3A -**Figure I.1**-).

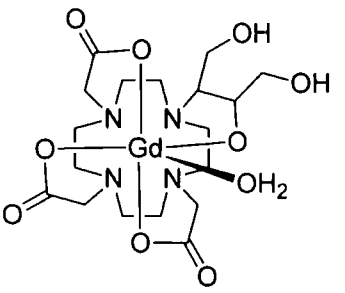

[Gd(DO3A-butrol)(H_2O)]
Gadovist™

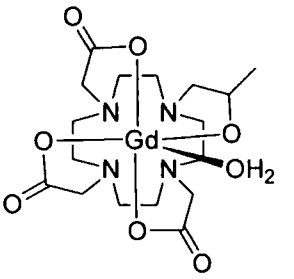

[Gd(HP-DO3A)(H_2O)]
Prohance™

Figure I.1: Structure of Gadovist™ and Prohance™, two contrast agents currently in clinical use.

Stability – On account of its high *in vivo* toxicity, $LD_{50} \approx 0.1$ mmol kg^{-1}, the Gd^{III} ion must be encapsulated by a strong multidentate organic ligand, forming a chelate stable under biological conditions. This feature should avoid the dissociation of the complex into free metal ion and ligand species once administered to the patient.[9] Since the lanthanide ions are classified as hard acids, binding to multidentate structures possessing hard σ-donor atoms (eg. nitrogen and oxygen) is favoured. This, together with the chelate effect, enhances both the thermodynamic and kinetic stability of the complex.[10] The thermodynamic stability of a metal-ligand (ML) complex is expressed by the equilibrium constant shown in **Equation (I.1)**

$$K_{ML} = [ML] / [M] [L] \qquad \textbf{(Eq. I.1)}$$

where K_{ML} refers to a specific equilibrium constant (called the stability constant), [M], [L] and [ML] are the equilibrium concentrations of the metal ion, deprotonated ligand and complex (the charges of the ions are omitted for simplicity). The classical method for determining ML stability constants is a pH-potentiometric titration of the ligand, carried out in the presence and in the absence of M. This works extremely well for systems that reach equilibrium quickly (a few minutes) after addition of acid or base.

Hydrophilicity – The biodistribution of a CA largely depends on its relative lipophilicity and/or its hydrophilic properties. Some of the most widely used first generation CA, like $[GdDTPA]^{2-}$, $[GdDOTA]^{-}$, [GdHP-DO3A] and [GdDTPA-BMA] (see **Scheme I.1**), are all relatively hydrophilic and distribute non-specifically throughout the plasma and interstitial spaces, before being excreted via the renal system. The half-time for excretion of $[GdDTPA]^{2-}$ (typical of hydrophilic CAs) is ~ 1.6 h in man. Different structures, containing lipophilic groups, are preferred for lanthanide complexes used as imaging agents for the biliary pathway and the liver, like ($[Gd(BOPTA)(H_2O)]^{2-}$, $[Gd(EOB\text{-}DTPA)(H_2O)]^{-}$, in **Figure I.3**); they are partially excreted through the hepatobiliary system.

I.4 Commercially available MRI Contrast Agents (CAs)

The steady progress accomplished over the last decades by medical research in diagnostic MRI has been translated into the large number of CAs currently in widespread clinical use, here categorized according to their magnetic properties and biodistribution.

They all work by enhancing both the longitudinal (T_1) and the transverse (T_2) relaxation times of the water protons in the examined tissue. However, they are divided into two large groups: the T_1 or *positive* contrast agents and the T_2 or *negative* contrast agents. The T_1 contrast agents, such as the paramagnetic gadolinium based ones, work on altering $1/T_1$ of tissue more than $1/T_2$, owing to the fast endogenous transverse relaxation in tissue. With most pulse sequences, this dominant T_1 lowering effect results in increases in the signal intensity.[4] Examples of the second category, the T_2 contrast agents, are the ferromagnetic large iron oxide particles,[11] which operate mainly by increasing the $1/T_2$ of the tissue, causing a reduction in the signal's intensity.

I.4.1 T_2 contrast agents

The superparamagnetic agents are made up of iron oxide particles (Fe_3O_4). When exposed to an external magnetic field, the thousands of magnetic ions mutually align, resulting in a very large magnetic moment, greater than that of a single molecule of a Gd^{III} chelate.[8] The iron oxide particles are divided into two groups, depending on their dimensions: the super paramagnetics (SPIO), with diameter (d) > 50 nm, and the ultra smalls (USPIO), d < 50 nm.

Commercial name	Type of particle	d(nm)	r_1(mM^{-1} s^{-1})	r_2(mM^{-1} s^{-1})
Endorem (Guerbet)	SPIO	200	24	107
Resovist (Schering)	SPIO	62	20	197
Abdoscan (GEHealthcare)	USPIO	3500	-	-
Lumirem (Guerbet)	USPIO	300	3.4*	3.8*

*measured at 1Tesla

Table I.3: Commercially available super-paramagnetic agents. Relaxivity measured at 37 °C, 0.5T.

I.4.2 T_1 contrast agents

The paramagnetic contrast agents consist of Gd^{III} or, less commonly, Mn^{II} [12] or Fe^{III} based complexes, where the ligand is a chelate structure which binds strongly the metal ion in a stable balance of electrostatic forces.

First generation contrast agents

The molecular structures of some "first generation" commercially available contrast agents are shown respectively in **Scheme I.1** and in **Table I.4**.

Chemical name	Generic name	Brand name	Company
$[Gd(DTPA)(H_2O)]^{2-}$	gadopentetate dimeglumine	Magnevist	Schering(Germany)
$[Gd(DOTA)(H_2O)]^{-}$	gadoterate meglumine	Dotarem	Guerbet (France)
$[Gd(DTPA\text{-}BMA)(H_2O)]$	gadodiamide	Omniscan	GE Healthcare
$[Gd(HP\text{-}DO3A)(H_2O)]$	gadoteridol	ProHance	Bracco (Italy)
$[Gd(DO3A\text{-}butrol)(H_2O)]$	gadobutrol	Gadovist	Schering(Germany)
$[Gd(DTPA\text{-}BMEA)(H_2O)]$	gadoversetamide	OptiMARK	Mallinckrodt (U. S.)

Table I.4: Extracellular contrast agents commercially available

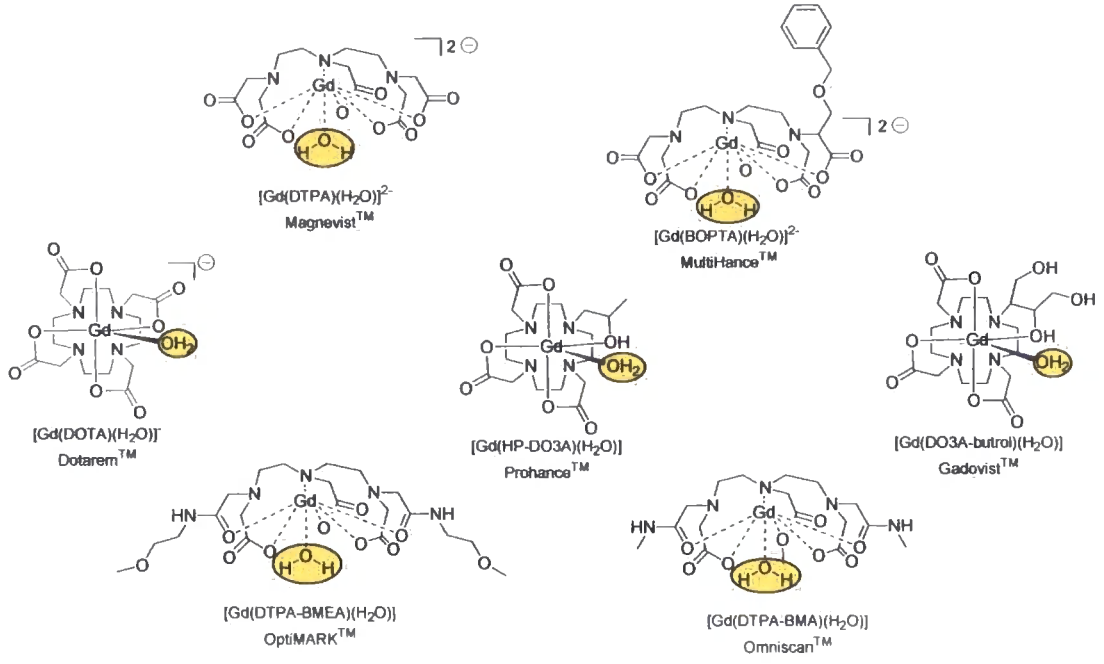

Scheme I.1: Commercially available contrst agents

All these gadolinium based contrast agents (GBCAs) are nine-coordinate complexes, in which a low molecular weight (< 1000 Da) ligand occupies eight binding sites at the metal centre and one water molecule, supplied by the solvent, corresponds to the ninth. They are all based on one of two ligand systems: DOTA (macrocycle) and DTPA (acyclic ligand system), which have proved to be very good ligand skeletons for highly kinetically and thermodynamically stable Gd^{III} complexes.[13,14] Omniscan was administered in ascending doses (from 0.05 mmol/kg to 0.3 mmol/kg) in 20 healthy male volunteers, in order to check its safety and monitor the performance. Once the gadodiamide was injected, it diffused into the interstitium with a distribution half-life of about 5 min, and the serum elimination half-life throughout the kidneys was approximately 70 min. Only mild post-injection side effects were registered on 9 of the 20 subjects, such as light-headedness, dizziness, and perversion of taste or smell.[15] Extracellular MRI contrast agents are generally considered very safe. However, patients with severe kidney insufficiency or with chronic liver disease or just before (or after) liver transplantation are considered to be at risk of developing a rare acquired disease, known as nephrogenic systemic fibrosis (NSF).[16] This

condition has been reported in the vast majority of cases (≥ 200), with Omniscan. Indeed, the DTPA-bisamide Gd^{III} complex is well known to be the least kinetically stable, with respect to acid catalysed dissociation, of all the approved contrast agents.[17] It has been proved, however, that gadolinium contrast agents can be used also in hemodialysis patients, if hemodialysis is performed immediately after the examination to get rid of the circulating residual contrast agent. From the first to the third hemodialysis session, average gadolinium-based contrast clearance rates were 78%, 96%, and 99%, respectively.[18]

Five gadolinium-based contrast agents have been approved for clinical use in Europe and in the United States: Magnevist (gadopentetate dimeglumine, $[Gd(DTPA)(H_2O)]^{2-}$), Omniscan (gadodiamide, $[Gd(DTPA\text{-}BMA)(H_2O)]$), OptiMARK (gadoversetamide, $[Gd(DTPA\text{-}BMEA)(H_2O)]$), MultiHance (gadobenate dimeglumine, $[Gd(BOPTA)]^{2-}$) and Prohance (gadoteridol, $[Gd(HP\text{-}DO3A)(H_2O)]$). Among these, Multihance is classified as a "second generation" contrast agent.

GdIII is the lanthanide ion most commonly used for the synthesis of MRI contrast agents, but other lanthanide ions (and different oxidation states i.e. +2) are also increasingly considered as alternatives.19 An example is the [Mn(H2DPDP)]4-, commercially produced by GE Healthcare and known as "Telescan" (molecular structure illustrated in Figure I.2).[20]

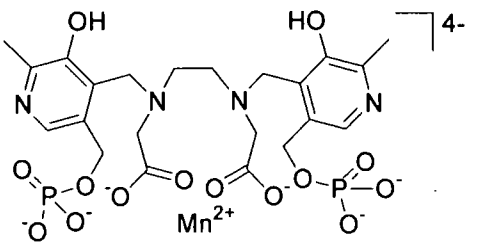

Figure I.2: "Telescan" molecular structure.

Second generation contrast agents

Known as "smart" agents, they are Gd^{III} based systems endowed with higher efficacy (quantified in higher relaxivity values). They show responsive behaviour to their physiochemical environments: their relaxivities can be modulated by changes in the pH of the solution,[21, 22, 23, 24] by a metal ion concentration (such as calcium,[25] zinc,[26,27] copper [28]), by enzyme activity [29, 30, 31, 32, 33] or they can be responsive to changes in the partial oxygen pressure (pO_2 responsive CA).[1] Furthermore, these contrast agents can be "*organ specific*": they are selectively taken up by a particular kind of cell, e.g. hepatocytes, before being excreted through the bile. An image enhancement is verified only in the organs where these cells are present, such as the liver, spleen or lymph nodes.[28]

Based on a DTPA backbone, adorned with hydrophobic substituents, are the structures of two of the most widely used "smart" contrast agents: gadobenate dimeglumine, $[Gd(BOPTA)]^{3-}$ and $[Gd(EOBDTPA)]^{3-}$ (**Figure I.3**).

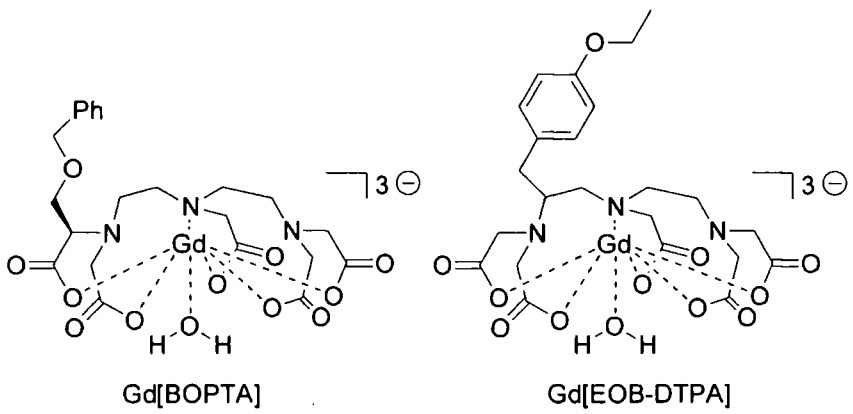

Figure I.3: **Gd(BOPTA) and Gd(EOBDTPA) molecular structures.**

The pharmacological and MRI contrast-enhancing properties of $[Gd(BOPTA)]^{2-}$ are based both on its utility in the imaging of the liver and the myocardium and on its efficiency, greater than $[Gd(DTPA)]^{2-}$ for those applications which require an extracellular agent. Currently ($[Gd(BOPTA)]^{2-}$) is produced by Bracco Imaging, Italy,

with the commercial name "MultiHance", and detailed physiochemical and pharmacokinetic studies have been undertaken since the synthesis of the molecule in the early 1990s.[34] The performances of MultiHance have been compared to the conventional gadolinium chelate $[Gd(DTPA)]^{2-}$ for MR imaging in brain tumours. In a crossover study of 22 patients with brain metastases, $[Gd(BOPTA)]^{2-}$ consistently improved the depiction of tumour margins, revealing larger areas of contrast enhancement compared to $[Gd(DTPA)]^{2-}$.[35] MultiHance has also found applications in perfusion cardiac MRI for the diagnosis of coronary artery disease, cardiac tumours, inflammations and different forms of cardiomyopathies. It has been demonstrated that, in comparison to the conventional coronary angiography, perfusion cardiac MRI considerably increases the specificity and sensitivity of the diagnosis.[36]

Again based on the DTPA ligand structure, is another hepatotropic agent: $[Gd(EOB\text{-}DTPA)]^{2-}$, whose molecular structure is reported in **Figure I.3**. It is produced by Schering (Germany) and known on the market as "Eovist™". It increases the signal intensity of normal liver parenchyma on T_1 - weighted images, before being excreted through both the renal and biliary routes. Eovist injection provides additional information regarding lesion detection, their classification and characterization, and it also exhibits an acceptable safety profile in clinical trials.[37] In addition to its use as a liver-specific MRI contrast agent, $[Gd(EOB\text{-}DTPA)]^{2-}$ has been tested successfully in patients as a potential contrast agent for computed tomography (CT).[38]

A new class of MRI contrast agents is represented by the blood-pool agents. They display larger size compared to the extracellular fluid agents, which prevents their leakage into the interstitium and enhances their efficacy, making the tumbling of the macromolecule (τ_R) slower. They work by selectively reducing the T_1 relaxation time of blood, and their relatively long half vascular life translates into longer image acquisition time and therefore higher image resolution. These "blood pool contrast agents" have been initially developed for use in magnetic resonance angiography (MRA). An example of commercially available blood pool agent is the

gadophostriamine trisodium, known as MS-325 and on the market as "AngioMARK", described in **Section III.2.1, q=1 systems**.

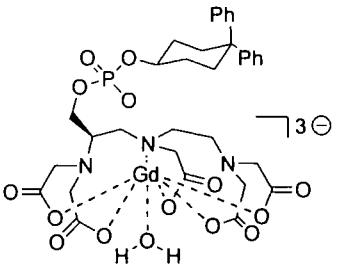

MS-325

Figure I.4: The structure of MS-323, marked under the name "AngioMARK".

II. The efficacy of a CA: its Relaxivity

II.1 Relaxation Rates and Relaxivity

The image-enhancing capability of a contrast agent, directly proportional to its ability to catalyze the relaxation rate of the surrounding water's hydrogen nuclei, is quantitatively expressed by its relaxivity.

Both longitudinal ($1/T_1$) and transverse ($1/T_2$) relaxation rates of the water protons are perturbed, but in this discussion only the longitudinal relaxation rates, R_1, more relevant for the NMR image enhancement, will be considered. In comparison to the value for pure water, R_1 is dramatically enhanced for the water protons of an aqueous solution containing a paramagnetic metal complex, such as a Gd^{III} chelate. The observed relaxation rate, $R_{1,obs}$, where $R_{1,obs} = 1/T_{1,obs}$, is the sum of a diamagnetic contribution ($1/T_{1,d}$, pure water relaxation rate) and of a paramagnetic contribution ($1/T_{1,p}$) to the water proton relaxation rates, caused by the presence of the lanthanide complex, (**Equation II.1**):

$$1/T_{1,obs} = 1/T_{1,d} + 1/T_{1,p} \qquad \textbf{(Eq. II.1)}$$

$1/T_{1,p}$ is proportional to the concentration of the paramagnetic species dissolved in solution, and the paramagnetic relaxation enhancement (R_{1p}), when referred to a 1 mM concentration of a given Gd^{III} chelate, is called its relaxivity (**Equation II.2**):

$$1/T_{1,obs} = 1/T_{1,d} + r_1[Gd] \qquad \textbf{(Eq. II.2)}$$

Many parameters affect the relaxivity value of a lanthanide complex dissolved into solution: the water molecules interact differently with the paramagnetic centre, depending on their distance from it (**Figure II.1**). The "inner sphere" water molecules directly enter the Gd^{III} coordination sphere (the water oxygen binds to the Gd^{III}) and then rapidly (nanoseconds) exchange with the bulk; the "2nd sphere" water molecules arise as a result of hydrogen bonding and similar interactions with ligand and inner sphere water molecules, creating a loosely coordinated network of water molecules intermediate between the inner and the outer spheres. They show a finite residence time which is longer than the translational diffusion time of the pure water. "Outer sphere" water molecules create interactions with second sphere and closely diffusing water molecules. Three different relaxation mechanisms may be associated with the three types of water molecules just described, respectively: the inner sphere, the second sphere and the outer sphere mechanism, which all add together in a total paramagnetic relaxation enhancement (**Equation II.3**):

$$1/T_{1,para} = 1/T_{1,is} + 1/T_{1,ss} + 1/T_{1,os} \qquad \textbf{(Eq. II.3)}$$

The same criteria can be used for the relaxivity (**Equation II.4**):

$$r_1 = r_1^{IS} + r_1^{SS} + r_1^{OS} \qquad \textbf{(Eq. II.4)}$$

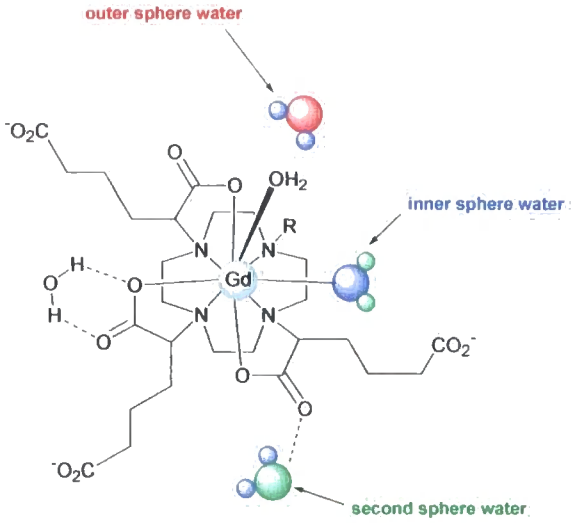

Figure II.1: Inner sphere, outer sphere, second sphere water molecules.

II.2 Inner Sphere Proton Relaxivity

The longitudinal inner sphere contribution to the relaxivity (R_{1p}^{is}) is rationalized in **Equation II.5:**[39]

$$\frac{1}{T_{1p}^{is}} = P_m \left(\frac{1}{T_{1m}^{H} + \tau_m} \right) = \frac{Cq}{55.5} \left(\frac{1}{T_{1m}^{H} + \tau_m} \right) \qquad \textbf{(Eq. II.5)}$$

where

- P_m = mole fraction of the bound water nuclei
- C = molal concentration of paramagnetic compound
- q = the number of bound water molecules per Gd^{III}
- $1 / T^{H}_{1m}$ = proton longitudinal *relaxation* rate in bound water
- $1 / \tau_m$ = inner sphere *exchange rate* for bound water molecule(s)

In order to increase the overall relaxivity of a contrast agent, the number of coordinated waters (q) can be increased (this aspect will be discussed in section V of this introduction: "Survey of *di*-aqua complexes"). Also, the relaxation of the bound water(s) can become faster by making the T^{H}_{1m} (or τ_m) as short as possible. T^{H}_{1m} and τ_m show opposite temperature dependencies: on lowering the temperature, T^{H}_{1m}

decreases while τ_m increases.[40] In the first generation contrast agents, $\tau_m << T^H_{1m}$, therefore T^H_{1m} is the limiting value for the relaxivity of these agents.[4]

The term $1/T_{1p}^{is}$ originates from dipole-dipole and scalar (or contact) mechanisms which are modulated only by electron spin relaxation and water exchange, and represent a small contribution to $1/T_{1p}^{is}$ at the low fields used in many MRI examinations (usually 1.5 T). This introduction will therefore mainly focus on understanding the dipolar interactions between paramagnetic ion and proton nuclei of directly bound water molecules; such interactions are dependent on the magnetic field and modulated by the reorientation time of the nuclear spin – electron spin vector (τ_R), by changes in the Gd^{III} electron-spin relaxation time (τ_S) and by water proton exchange times (τ_m) between the inner and the outer sphere. The dependence of the dipolar relaxation ($1/T_{1m}^{DD}$) upon the magnetic field strength, is expressed by the modified Solomon-Bloembergen equation[41] (**Equation II.6**):

$$1/T_{1m}^{DD} = \frac{2}{15} \frac{S(S+1)g^2\gamma_H^2\mu_B^2}{r^6_{GdH}}\left(\frac{\mu_0}{4\pi}\right)^2\left[\frac{7\tau_{c2}}{\left(1+\omega_s^2\tau_{c2}^2\right)}+\frac{3\tau_{c1}}{\left(1+\omega_H^2\tau_{c1}^2\right)}\right] \quad \textbf{(Eq. II.6)}$$

where

- S is the magnetic number of electron spin;
- γ_H is the nuclear gyromagnetic ratio of the proton;
- g is the electron g-factor (or Landé factor for the free electron);
- μ_B is the Bohr magneton;
- $r_{Gd\text{-}H}$ is the electron spin - proton distance;
- τ_{ci} (i = 1, 2) is the correlation time relative to the electron spin – proton coupling;
- ω_S and ω_H (rad/s) are nuclear & electron Larmor frequencies, where $\omega_S = 658\omega_H$ (and $\omega = \gamma B$).

The relaxation depends on: Gd-H distance, r_{GdH}; proton and electron Larmor frequencies, respectively ω_S and ω_H; correlation times, τ_{ci}. As a consequence of this dependence on the Gd-H distance, the directly bound waters are the most effectively

relaxed, and the rapid exchange with the bulk water spreads this effect into the bulk solution. This process is referred to as the inner sphere contribution to the overall proton relaxivity. Many different dynamic processes occurring on molecular level can modulate the electron-nuclear spin interactions (expressed by τ_{ci}), including the rotational correlation time (τ_R) of reorientation of the metal – proton vector, the water residence lifetime on the metal ion (τ_m), the Gd^{III} electronic longitudinal (T_{1e}) and transverse (T_{2e}) relaxation times (**Equation II.7**):

$$\frac{1}{\tau_c} = \frac{1}{\tau_R} + \frac{1}{T_{1,e}} + \frac{1}{T_{2,e}} + \frac{1}{\tau_m} \qquad \textbf{(Eq. II.7)}$$

To make everything even more complex, the electronic relaxation rates (like the nuclear relaxation rates) are field dependent. For Gd^{III} complexes the rates are interpreted in terms of zero-field splitting (ZFS) interaction, as described in **Eq. II.8**, **II.9** and **II.10**. These equations are referred to as the Bloembergen-Morgan Theory of paramagnetic electron-spin relaxation:

$$\left(\frac{1}{T_{1e}}\right)^{ZFS} = B\left[\frac{1}{1+\omega_S^2\tau_v^2} + \frac{4}{1+4\omega_S^2\tau_v^2}\right] \qquad \textbf{(Eq. II.8)}$$

$$\left(\frac{1}{T_{2e}}\right)^{ZFS} = B\left[\frac{5}{1+\omega_S^2\tau_v^2} + \frac{2}{1+4\omega_S^2\tau_v^2} + 3\right] \qquad \textbf{(Eq. II.9)}$$

and

$$B = \frac{1}{10\tau_{S0}} = \frac{\Delta^2}{50}[4S(S+1)-3]\tau_v \qquad \textbf{(Eq. II.10)}$$

where Δ^2 is the mean-square zero field splitting energy and τ_v is the correlation time for the modulation of the zero field splitting interaction.

Gd-H distance

Given that the dipole-dipole relaxation term (**Eq. II.6**) is proportional to $1/(r_{Gd\text{-}H})^6$, large variations in the relaxivity value could theoretically be obtained with even small changes on the metal ion-water proton distance. Experimentally, this parameter is

very difficult to measure, and only recently scientists have managed to determine it exactly using "direct" methods. In the past, this value was estimated by fitting of NMRD data, but many parameters in the fitting where unknown and therefore the measured value was not very accurate. Literature values vary over the range between 2.5 and 3.3 Å.[8,41,42] The term $1/(r_{Gd\text{-}H})^6$ originates from the anisotropic hyperfine interaction (hfi) between the electron and nuclear spins, therefore the most appropriate techniques to deal with this factor would be those of magnetic resonance because they allow the direct determination of anisotropic hfi. With 1D and 2D pulsed electron-nuclear double resonance (ENDOR) studies on glassy water/methanol solutions of Gd^{III} and one of the commercial contrast agents, Gd^{III}HPDO3A (Prohance), the Gd-H distance for a range of 8 and 9-coordinate Gd^{III} complexes has been estimated to be about 3.1 Å and it does not depend on co-ligand or total charge.[43]

An increasing in the tilt angle between the Gd-O bond and the plane of the water molecule could decrease $r_{Gd\text{-}H}$. However, in a symmetric complex structure like $[GdDOTA]^-$, it is unlikely that hydrogen bonding would form preferentially between the water molecule and an electronegative atom on a side of the chelate.

Alternatively, any electronic anisotropy could induce electron localization nearer to the water molecule. Unfortunately, this approach is also not feasible in the case of the stable, highly symmetric electronic state of Gd^{III}.[8]

Effect of τ_R on relaxivity (r_{1p}) as a function of the magnetic field strength

The efficiency of a contrast agent is dependent on the magnetic field strength. In a Nuclear Magnetic Resonance Dispersion profile (NMRD), the contrast agent's behaviour is monitored over a range of several orders of magnitude (0.01 – 120 MHz). The change of the magnetic field strength does not usually modify the chemistry of the sample, unlike other thermodynamic parameters, e.g. temperature or pressure. Furthermore, qualitative interpretation of some relaxivity mechanisms can be obtained at low magnetic fields ($\leq$ 3 MHz), for example the electronic relaxation which affects the dipole-dipole interaction and determines the relaxivity; at higher

magnetic fields, (> 4 MHz) the τ_R term can be studied, as this term is dominant at around 30 MHz , as shown in **Figure II.2.**

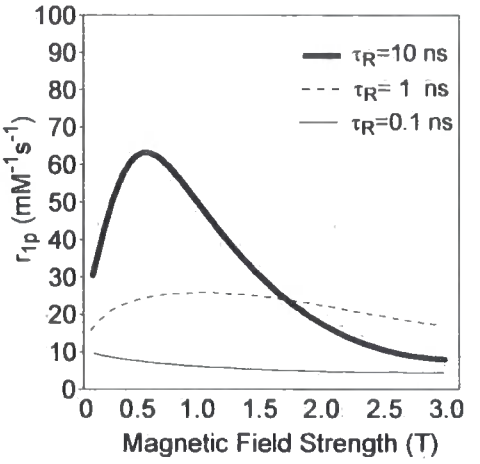

Figure II.2: Effect of rotational correlation time on relaxivity as a function of field strength.[4]

II.3 Outer Sphere Proton Relaxivity

Two types of outer-sphere relaxation mechanisms contribute to the overall relaxivity observed for a contrast agent: the first of these mechanisms, **outer sphere**, involves the modulation of the dipole-dipole interaction between the electron spin, *S*, and the proton spin, *I*, and is caused by the diffusion of water molecules nearby the paramagnetic centre (**Figure II.3**). The outer-sphere relaxivity (R_{1p}^{os}) is a complex problem in solvation dynamics and diffusion,[4] and a theory is available to treat the limiting case where no chemical (or electrostatic) interactions occur between water and metal complex.[44] The Freed equation,[45] explains how the outer sphere relaxation is dependent on the fluctuations

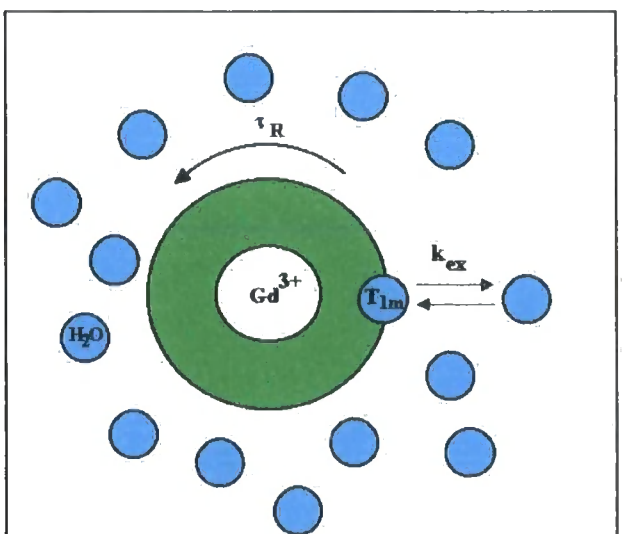

Figure II.3: Relaxation mechanisms and main relaxation parameters operating in aqueous solution containing a paramagnetic Gd^{III} chelate.[4]

due to electronic relaxation time of the metal ion (τ_{s1} and τ_{s2}), on the distance of closest approach of solute and solvent (d), on the sum of solvent and solute diffusion constants (D) and it is modulated by the magnetic field strength. **Equation II.11** shows the most general form of the theory for outer sphere relaxivity,[45] which shows some similarities with the Solomon-Bloembergen equations:

$$\left[\frac{1}{T_1}\right]_{OuterSphere} = \frac{C_\pi N_S \gamma_H^2 \gamma_S^2 \hbar^2 S(S+1)}{d^3 \tau_D} \left[7I(\omega_S, \tau_D, T_{1e}) + 3I(\omega_H, \tau_D, T_{1e})\right] \qquad \textbf{(Eq. II.11)}$$

Where C is a numerical constant that differs slightly between different models used to derive the equations, N_S is the number of metal ions per cubic centimeter, τ_D is the relative translational diffusion time, given by **Equation II.11**, where D_H and D_S are the diffusion coefficients of water and the metal complex, respectively. Diffusion coefficients can be estimated if the motion described by the Stokes-Einstein model, in which the diffusion of rigid spheres in a medium of viscosity η is considered, as shown in **Equation II.12**, where a is the molecular radius:

$$D = kT / 6\pi a\eta \qquad \textbf{(Eq.II.12)}$$

Freed equation can be modified in a form suitable for small paramagnetic metal chelates:[51]

$$R_{1p}^{OS} = C^{OS}\left(\frac{1}{aD}\right)\left[7J(\omega_S) + 3J(\omega_H)\right] \qquad \textbf{(Eq.II.13)}$$

where C^{OS} is a constant ($5.8 \cdot 10^{-13}$ $s^{-2}M^{-1}$) and the dependence on the electronic relaxation times is expressed in the non-Lorentzian spectral density functions $J(\omega_i)$.[46] The outer sphere contribution, R_{1p}^{os}, can constitute a significant contribution to the observed relaxation rate for low molecular weight Gd^{III} complexes.[46] For small-sized complexes with q = 1 [such as $Gd(DOTA)^-$ and $Gd(DTPA)^{2-}$], R_{1p}^{os} makes a contribution of roughly 40–50% to the observed relaxivity. Experimental evidence for an even greater contribution to the relaxivity from the outer sphere can be found in

the lanthanide complex [Gd-**1**]$^-$, based on the macrocyclic tetrabenzylphosphinate ligand (**Figure II.4**). Its $1/T_1$ NMRD profile is compared in **Figure II.5** with the one of a similar compound, [Gd-**2**], where one phosphinate group is substituted with a less bulky carboxoamide and the benzyl group on the remaining phosphinate pendant arms is replaced with a methyl. The shape and amplitude of the [Gd-**1**]$^-$ NMRD profile suggest that the inner sphere does not contribute to the overall relaxivity; the steric bulk of [Gd-**1**]$^-$ phosphinate groups prevents the access of the water molecules onto the metal ion, leading to a $q = 0$ system, making the outer sphere term the main contribution.[47]

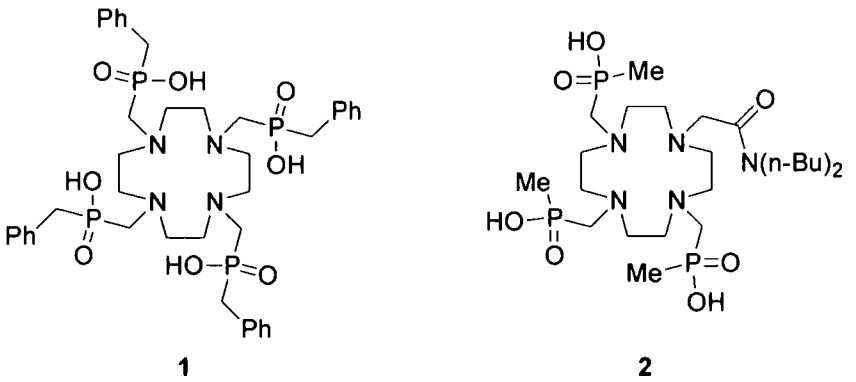

Figure II.4: Ligand structure for the complexes [Gd-1]$^-$ and [Gd-2].

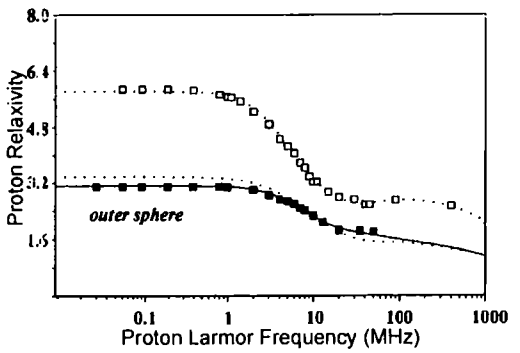

Figure II.5: NMRD profiles (25 °C) of [Gd-1]$^-$ (filled squares) and [Gd-2] (open squares) and best-fit curves; the dotted line at the bottom is the calculated outer-sphere contribution for [Gd-2][48]
(reproduced with permission of the author).

II.4 Second Sphere Proton Relaxivity

The second of these mechanisms involves a region of more strongly associated water molecules, which possess limited translational motion but exist nearby the electronic spin centre. This type of water coordination environment is referred to as the second sphere. Hydrogen bonding interactions with polar groups of the ligand leave the water molecules of the second coordination sphere free to rotate with the molecule, and exposes them to rotationally modulated magnetic field fluctuations of the dipolar electron-nuclear coupling, causing a significant enhancement in the relaxivities. This contribution to the observed relaxivity is considered separately from the diffusion controlled outer-sphere term only when the residence lifetime of the water molecules in the second sphere is longer than the diffusional correlation time τ_D ($\tau_D = a^2/D$).[48] Even if in the past more efforts have been spent in the understanding of the inner sphere and outer sphere relaxation mechanisms, there are cases where the only plausible explanation for the high relaxivity values observed can be found in the interactions of the second sphere water molecules. For example, scientists seem to agree that in the case of the anionic tetraphosphonate macrocyclic gadolinium complex **[Gd.3]**$^{5-}$ (complex structure in **Figure II.6)**, the 50% increase of the relaxivity (r_{1p} = 11.5 $mM^{-1}s^{-1}$ at 20 MHz, pH 9, 25 °C) versus **[Gd.1]**$^{-}$ (in **Figure II.4**) is a consequence of solvent molecules in the second shell of the metal ion, involved in H-bonding interactions with the oxygen atoms of the phosphonate groups.[49] The ^{17}O transverse relaxation rate profile as a function of the temperature gave further evidence in support to this theory. The shape of the profile is typical of a q = 0 complex, thus excluding any contribution from the inner sphere water molecules.

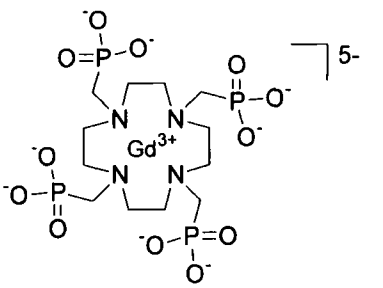

3

Figure II.6: Molecular structure for the complex [Gd-3]$^{5-}$.

Since the second sphere water molecules reside closely enough to the inner sphere water protons to be strongly relaxed, their relaxation pathways also depend on the same parameters, such as rotational correlation time (τ_R), water residence lifetime on the metal ion (τ_m), Gd^{III} electronic longitudinal (T_{1e}) and transverse (T_{2e}) relaxation times and magnetic field strength. The relaxivity value measured for the tetraphosphonate complex is in fact enhanced by slowing down its rotational mobility (*i.e.* increasing the rotational correlation time, τ_R, of the whole complex), simply by decreasing the temperature. However, unlike the inner sphere water molecules, the number of the second sphere ones can be increased without altering ligand structure and complex thermodynamic stability. A considerable enhancement in the relaxivity can be obtained by inducing electrostatic interactions between the ligand and a substrate. In the example considered here, the interactions are between the negative charges on the oxygen atoms of the phosphonate groups and the hydroxyl groups of the *N*-methyl-glucosamine (**Figure II.7**). A considerable second sphere contribution is evident in the resulting relaxivity observed, which is 15 $mM^{-1}s^{-1}$ (20 MHz, 25 °C, pH 9) for this adduct.

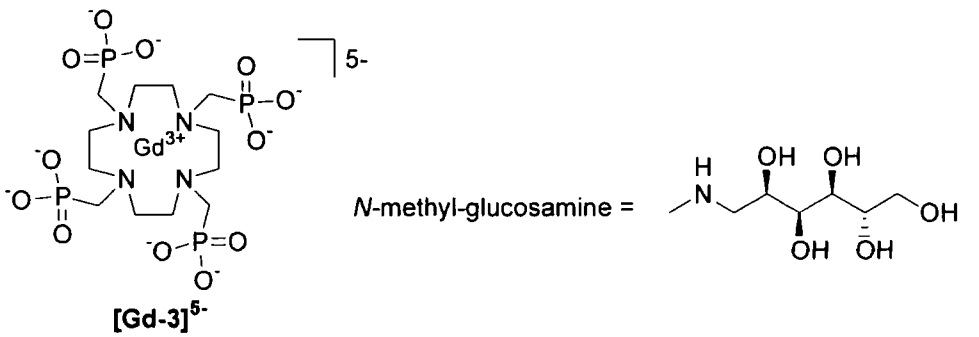

Figure II.7: *N*-methyl-glucosamine interacts with the $[Gd\text{-}3]^{5-}$ complex.

In **Figure II.8** it is illustrated how the interaction of the anionic tetraphosphonate macrocyclic gadolinium complex $[\mathbf{Gd\text{-}3}]^{5-}$ with an *N*-benzylhexa-aza-18-crown-6 analogue, (**4**) and a *β*-cyclodextrin (**5**) formes a non-covalent ternary complex, $q = 0$, where the optimized contribution of second sphere of hydration[50] results in a remarkable r_{1p} value of 18 $mM^{-1}s^{-1}$ (at 20 MHz, 25 °C). The existence of this ternary

adduct has only been attested in water, at neutral *p*H; acidic conditions could possibly weaken the interactions which keep the system assembled.

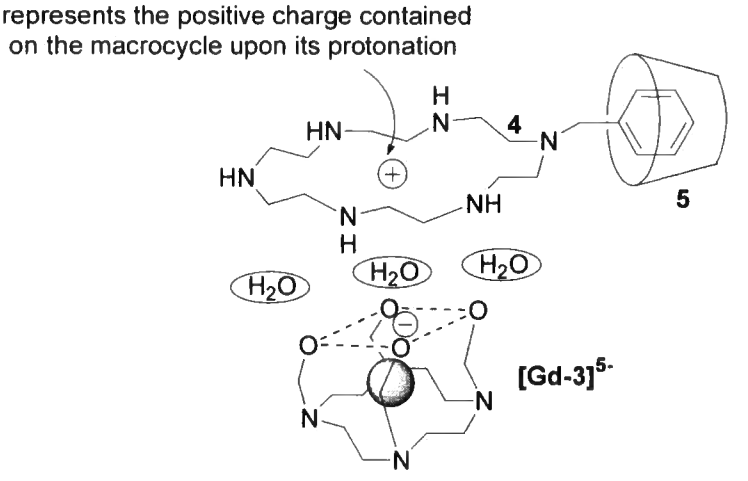

Figure II.8: Formation of a non-covalent, q = 0, ternary complex

The second sphere water molecules play an important role in determining the relaxivity of aqueous solutions of Gd^{III} complexes bearing phosphonate or anionic groups on the coordination sites of the metal ion. In the case of the DTPA complex, the second sphere is estimated to represent roughly the 25% of the observed relaxivity. This conclusion has been drawn after the X-ray structure of the complex $[Yb(DTPA)(H_2O)]^{2-}$ was determined, and variable-field and temperature NMRD studies of the corresponding Gd^{III} complex were performed. The studies led to a detailed picture of the three hydration shells around the metal ion: i) one coordinated water molecule; ii) several water molecules in the outer coordination sphere and iii) one water molecule surprisingly close to the metal centre (4.2 Å), acting as a hydrogen bond donor to ligand's proximate carboxylate groups and forming part of a linear chain of hydration.[50]

A substantial second-sphere contribution to the relaxivity has been suggested also for the highly stable $q = 2$ system $[Gd(aDO3A)(H_2O)_2]^{3-}$.[51] The efficacy of the complex in water is maintained in serum solution (r_{1p} = 12.3 $mM^{-1}s^{-1}$, pH 7.2 in serum, 65.6 MHz, 293 K) because the binding of proteins and endogenous anions (*e.g.* HCO_3^-

$/CO_3^{2-}$) is suppressed by the electrostatic repulsion of the carboxypropyl substituents (**Figure II.9**).[52]

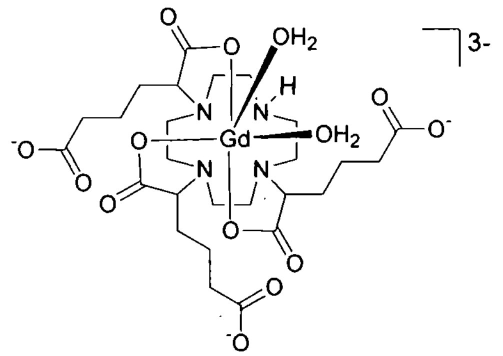

Figure II.9: Molecular structure of $[Gd(aDO3A)]^{3-}$.

In this thesis, the design and synthesis of new carbohydrate containing Gd^{III} complexes will be described (**Chapter II**), and the contribution from the second sphere water molecules will be discovered once again to be determinant in the high relaxivity values measured for the macromolecules.

III. Strategies for Enhancing Relaxivity

III.1 The crucial role of τ_m in contrast agent design

The water molecule(s) of inner sphere, directly coordinated to the metal centre of the chelate structure, must be in rapid exchange with the bulk, in order to transmit the paramagnetic effect from the Gd^{III} to the solvent. In the Solomon-Bloembergen-Morgan theory,[39, 42] this water molecule(s) exchange rate is expressed by τ_m (= $1/k_{ex}$). The value of this term can cover a range of more than four orders of magnitude, from the lowest, reported for one isomer of the $[Eu(DOTAM)(H_2O)]^{3+}$ (k_{ex}^{298} = 8.3×10^3 s^{-1}),[53, 54] to the highest, (k_{ex}^{298} = 8×10^8 s^{-1}), attributed to the aqua ion itself.

A slow water exchange rate results in a poorly transmitted relaxation effect to the bulk, this leading to a limited efficacy of the contrast agent. However, if the exchange with the bulk is too fast, the water molecule(s) could not be coordinated to the Gd^{III} ion long enough to be relaxed, thus not allowing high relaxivity either. However, the

effect of a too fast (or too slow) water exchange can considerably affect the overall relaxivity only if other parameters (eg. τ_R) are also optimized. For example, when τ_R is 0.1 ns, any residency time between 1-1000 ns will produce a relaxivity within 20% of the maximum at this value of τ_R; when τ_R is 10 ns, this range becomes 2-30 ns for τ_m, as shown in **Figure III.1.**[4]

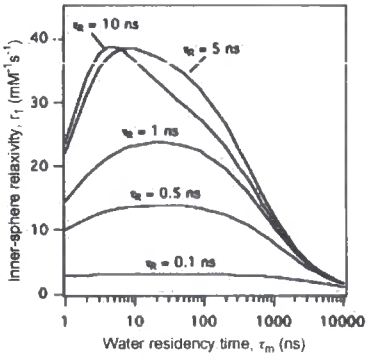

Figure III.1: Relationship between τ_R and τ_m at 1.5 T for q = 1 system with long (>10 ns) T_{1e}.[4] ***(reproduced with permission of the author).***

The water exchange can be described as a dissociative/associative mechanism closely related, together with the rate of the process, to the inner-sphere solution structure of the Gd^{III} complex.[8] **(Figure III.2).**

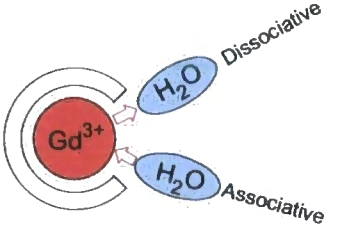

Figure III.2: Simplified representation of dissociative/associative water exchange mechanism.

For lanthanide aqua ions, the coordination number decreases from nine at the beginning of the series to eight at the end, and τ_m decreases by more than one order of magnitude between $[Gd(H_2O)_8]^{3+}$ and $[Yb(H_2O)_8]^{3+}$.[55] Only for the ions at the centre of the lanthanide series the τ_m ($=1/k_{ex}$) is relatively long (Eu = 395 ± 60 μs; Gd = 159 ± 4 μs).

Expanding our look at the lanthanide complexes, the nine coordinated Gd^{III} poly(aminocarboxylate) possess dissociatively activated water exchange, since in their coordination sphere there is no space for a second water molecule to enter before the bound water molecule has left. On progressing towards the end of the lanthanide series, the eight coordinate transition state becomes more accessible since the radius of the ions decreases, and the result is an increased water exchange rate. Also, the rigidity of the inner coordination sphere is an important factor: while in the aqua ion the rearrangement of the flexible coordination sphere is easy, the poly(aminocarboxylate) complexes show a more rigid inner shell, whose rearrangement requires higher energy. It emerges that the inner sphere structure induces different water exchange mechanisms and it also regulates the speed of the process, usually much slower in the nine-coordinate lanthanide^{III} poly(aminocarboxylate) complexes than in the eight-coordinate $[Gd(H_2O)_8]^{3+}$.[8]

The overall complex charge is also important in determining k_{ex}: generally speaking, the bound water in positively charged complexes exchanges more slowly than in neutral complexes which themselves are slower than negatively charged ones. The higher negative charge aids the leaving of the water molecule in the dissociative process. Indeed, a 50% increment in the τ_m value was found for [Gd(DOTASA) $(H_2O)]^{2-}$ (**Figure III.3**) compared to [Gd(DOTA) $(H_2O)]^{-}$,[56] whose τ_m value is already considered relatively fast and it corresponds to 15×10^6 s^{-1}, at 298 K.

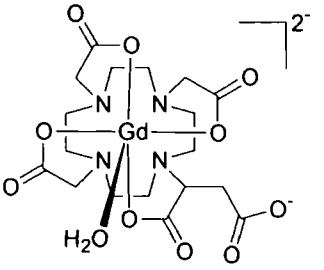

Figure III.3: [Gd(DOTASA) $(H_2O)]^{2-}$ molecular structure.

However, this assessment cannot be a rule. The steric constraints caused in the inner sphere by, for example, the introduction of bulky substituents, can destabilize the

water molecule and accelerate the water exchange. In ($[Gd(EGTA)(H_2O)]^{2-}$, in fact, the water exchanges ten time faster than in $[Gd(DTPA)(H_2O)]^{2-}$). [57]

Indeed, structure dependent factors can affect the τ_m value. For a series of cationic DOTA-tetra-amide europium complexes, it has been proved that τ_m depends on the extent of second sphere of hydration, determined by the complex hydrophobicity:[58, 59] the introduction of more hydrophobic substituents inhibits the formation of the hydrogen bonded structure which creates the metal ion's second sphere, determinant for the water interchange process.

Large differences in the τ_m values have been found even in isomers of the same compound. For example, the lanthanide^{III} DOTA-based complexes exist as two different diastereoisomers: **M** and **m**, which assume a squared antiprismatic and a twisted square antiprismatic geometry,[60, 55] respectively.

In agreement with the observations on water exchange dynamics on related Eu^{III}-amide complexes,[54] the rate of water exchange at a Gd^{III} centre is determined by the proportion of the isomer with the fastest water exchange rate in solution which, in the case of the DOTA systems (eg. GdDOTA, GdDOTMA, GdgDOTA), is the **m** isomer, obtained mainly through a rotation of the amide arms in an interchange mechanism, as shown in **Figure III.4**.

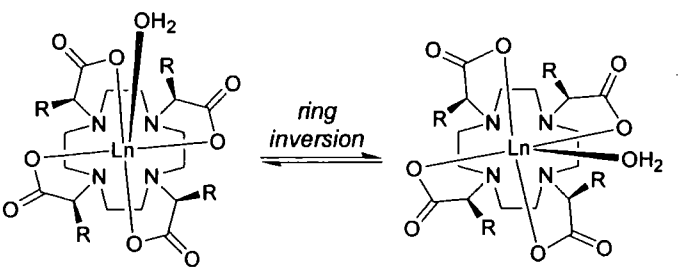

Figure III.4: The interconversion of DOTA-based complexes.

These observations were confirmed by the diastereomeric gadolinium complexes of tetra(carboxyethyl)DOTA, where a significant difference has been found between the

water exchange rate of the (*RRRR-SSSS*)-GdgDOTA (τ_m = 68 ns, 298 K) and the other isomers, *RRRS*- and *RSRS*-GdgDOTA (τ_m = 140 and 270 ns, respectively).[61]

The contribution given by these studies to the design of new contrast agents is fundamental, since they revealed the necessity of synthesizing complexes which exist in solution in well defined isomeric form.

III.2 Working on τ_R

At the magnetic field strengths typically employed in clinical imaging (1.5 T, 64 MHz proton Larmor frequency),[4] the longitudinal relaxation time of the inner sphere water protons, T_{1M}, is dominated by the molecular reorientational correlation time, τ_R. Contrast agents possessing a compact structure and high molecular weight should exhibit slow molecular tumbling. The slower the Gd^{III} complex tumbles, the longer the correlation time (τ_R) becomes, leading to faster relaxation rates and hence higher relaxivities.[1] Some different approaches have been considered for decreasing the tumbling rates, and the most effective one seems to be the linking of a Gd^{III} complex to a slowly tumbling macromolecule (such as dendrimers),[62] or to examine molecular complexes conjugated to polysaccharides[63] or proteins.[64, 65]

The best relaxivity enhancements have been achieved in non-covalently bound systems,[66] such as those based on binding of Gd^{III} complexes to serum albumins.

III.2.1 Non-Covalent Systems

- **q = 2 systems**

The changes in the relaxivity values generated by the binding interactions of DO3A based gadolinium chelates (**Figure III.5**) to HSA have been investigated by Aime *et al.*[69]

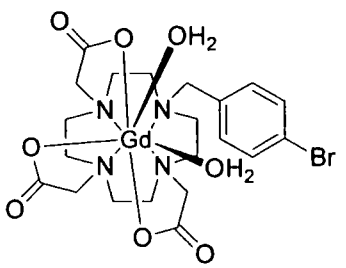

Gd-4

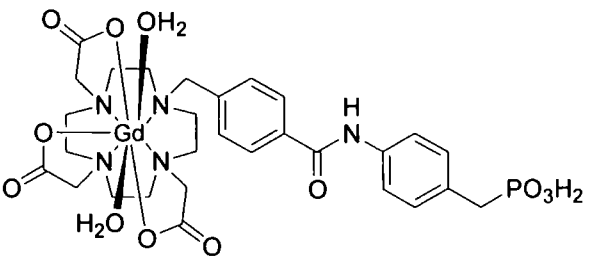

Gd-5

Figure III.5: DO3A based Gd^{III} complexes.

Given that both the systems are endowed with $q = 2$ and short τ_m values (for **Gd-4**, τ_m = 15 ns and for **Gd-5**, τ_m = 12 ns, at 298 K) surprisingly low relaxivities were reported for the macromolecular adducts with HSA: 24 and 21 $mM^{-1}s^{-1}$ for **Gd-4/HSA** and **Gd-5/HSA**, respectively.[67] Luminescence measurements and emission spectra of the europium analogue adducts with HSA, made clear that the expected relaxation enhancement was not observed because of the displacement of the two inner sphere water molecules by donor groups (such as a carboxylate group from Glu or Asp side chains) of the proteins and phosphate ions, possibly of the buffer solution. Conversely, when the interactions of the **Gd-4** and **Gd-5** complexes with poly-β-cyclodextrin were investigated, no changes in the hydration state of the metallic centre were observed and, in spite of a much lower τ_R value, the observed relaxivities were higher (28.3 and 27 $mM^{-1}s^{-1}$). Recently, the non-covalent interactions between Gd^{III}-complexes and β– or γ–cyclodextrin units (CDs) have been revisited, and supra-molecular adducts of chitosan (obtained by deacetylation of chitin, natural polymer of β-(1-4)-D-glucosamine) functionalized with cyclodextrins were bound to negatively charged Gd^{III} chelates bearing hydrophobic substituents (**Figure III.6**).[68]

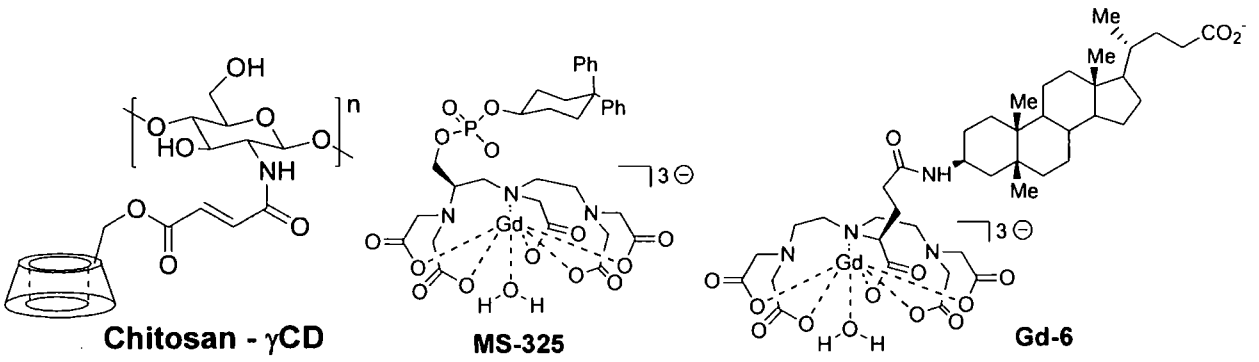

Figure III.6: Gd^{III} chelates and CDs adduct.

Compared to the corresponding analogues with monomeric cyclodextrins, the chitosan functionalized ones showed large increases both in terms of their binding affinities towards Gd^{III} complexes and in the relaxivity values ($r_{1p(\text{Chitosan }\beta\text{-CD / MS-325})}$ = 27.5; $r_{1p(\text{Chitosan }\gamma\text{-CD / Gd-6})}$ = 21.6 $mM^{-1}s^{-1}$). Furthermore, the binding affinity (K_A) of the

gadolinium chelates towards the exogenous polymer was evaluated, and the chitosan γ-CD / **Gd-6** adduct could be considered for in vivo applications as, it remains mainly bound to the polymer even in solution where the concentration of HSA is equal to the albumin in human serum (0.58 mM).

Further interesting studies focused on the change of the relaxivity values of Gd^{III}-diaqua-triphosphate complexes in the presence of a protein.[69] The relaxivity of the triphosphonate (**Figure III.7**), based upon the molecule aDO3A, was found to be significantly enhanced from 7.9 mM^{-1} s^{-1} to 30.0 $mM^{-1}s^{-1}$ in the presence of HSA (at a concentration 0.6 mM, similar to the *in vivo* protein concentration).

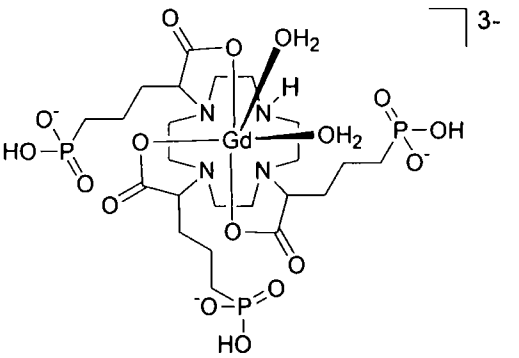

Figure III.7: Molecular structure of $[Gd(aDO3AP)(H_2O)_2]^{3-}$.

Phosphate anions were then added to the protein solution to understand if the complex was able to withstand competition from competing anions when strongly bound to serum albumin. The results showed that, unfortunately, the phosphate anions were able to displace the complex from the protein adduct, as well as displacing bound water in the complex, resulting in a marked reduction of the observed relaxivity.

It emerges from the previously examined examples that it is not straightforward to realize the expected relaxivity enhancement upon non-covalent binding of $q = 2$ systems to macromolecules. The water molecules of the Gd^{III} ion seem, in fact, to make the complex particularly reactive towards other coordinating groups, which can replace the metal-bound waters.

The highest observed r_{1p} value for non-covalent paramagnetic adducts with slow-moving substrates has been shown, so far, by the lipophilic Gd^{III}-AAZTAC17 complex (shown in **Figure III.8**) bound to HSA.[70]

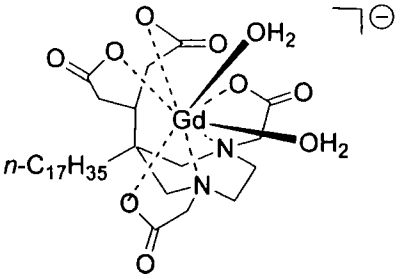

Figure III.8: Molecular structure of Gd^{III}-AAZTAC17.

Functionalisation of the AAZTA ligand[71] (which synthesis and magnetic properties of the corresponding Gd^{III} complex will be discussed in detail in **Chapter III - Section III.1** and **III.4** -) with a C17 aliphatic chain induces the formation of micelles already at submillimolar concentrations (greater than 0.1 mM). A sharp increase in the relaxivity value is observed when the system evolves from the monomeric state to micellar aggregates: at 20 MHz, 37 °C the r_{1p} of Gd^{III}-AAZTAC17 below the critical micellar concentration (cmc) is 10.2 $mM^{-1}s^{-1}$ whereas the r_{1p} of the self-assembled complex above the cmc is 30 $mM^{-1}s^{-1}$.[72] The interaction with HSA has been investigated for both the monomeric gadolinium complex (below the cmc) and the aggregated micellar system. While a slight increase in the relaxivity value was registered for the bound to HSA form with respect to the free micellar system, very similar relaxivity values were observed when the micellar system was bound to fatted or defatted HSA. Alternatively, the binding affinity of monomeric Gd^{III}-AAZTAC17 for defatted HSA (nK_A = (2.3 ± 0.7) · 10^4 M^{-1}) is significantly higher than for fatted HSA (nK_A = (7.1 ± 0.7) · 10^4 M^{-1}), whereas the relaxivity of the paramagnetic macromolecular adduct with defatted HSA is markedly higher and reaches the 84 $mM^{-1}s^{-1}$ (at 20 MHz, 25 °C); these differences in the relaxivity of fatted and defatted HSA adducts has been mainly ascribed to changes in the contribution of the second

sphere of hydration. The macromolecular adduct given by the binding of monomeric Gd^{III}-AAZTAC17 to defatted HSA is by far the most efficient reported to date.

- **$q = 1$ systems**

The compound MS 325 (**Figure III.9**) developed by Epix Medical (USA), is an example of a *non-covalently bound system.*[72] The molecule, linked via a phosphate ester to the DTPA chelate of Gd(III), bears a diphenyl substituted cyclohexyl group for non-covalent binding to the human serum albumin (HSA) protein in the blood pool. The rotational rigidity in the protein adduct imparted by this arrangement results in an increase in relaxivity for the protein bound complex (24 $mM^{-1}s^{-1}$, 310 K, 64 MHz).

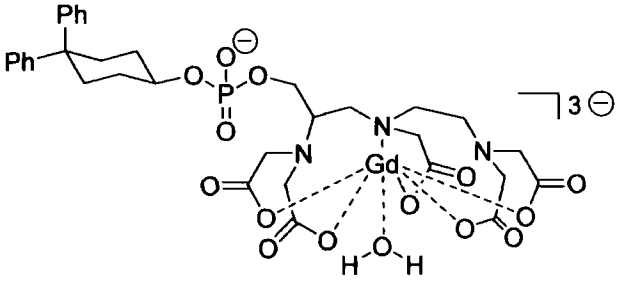

Figure III.9: Structure of MS 325 (Epix Medical).

The highest enhancements in the relaxivity values for q = 1 systems reported to date were exhibited by a GdEGTA[73] derivative, characterized by small size and compactness of the structure, one inner sphere, fast exchanging water molecule ($\tau_m \approx$ 17 ns at 298 K), and a rigid targeting moiety (an aromatic group) capable of forming non-covalent interactions with the hydrophobic sites of HSA (**Figure III.10**).[74]

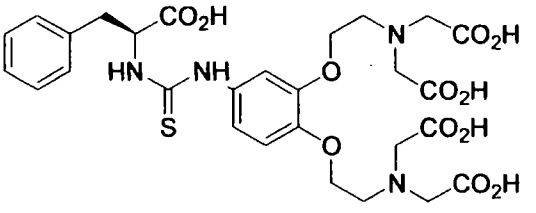

Figure III.10: GdEGTA phenylalanine derivative.

The relaxivity of this adduct reaches 68 mM^{-1} s^{-1} (at 298 K, 20 MHz), even higher than the value previously reported for the host-guest hydrophobic interaction between a [Gd(DOTA)]$^-$ system bearing three benzyloxy-propionic substituents and human serum albumin (HSA): ca. 56 $mM^{-1}s^{-1}$ at 310 K, 20 MHz. In this case, the increase in relaxivity is explained as a consequence of interactions with nearby water molecules from the macromolecular hydration sphere and perhaps from exchangeable protein protons.

Remarkably good results have also been obtained with Gd^{III}-TTDA-BOM derivatives bound to HSA (**Figure III.11**):[75] r_{1p} value of 65.8 $mM^{-1}s^{-1}$ has been registered for the adduct $[Gd^{III}(TTDA\text{-}BOM)(H_2O)]^{2-}$ / HSA and 61.5 $mM^{-1}s^{-1}$ for $[Gd^{III}(TTDA\text{-}N'\text{-}BOM)(H_2O)]^{2-}$ / HSA.

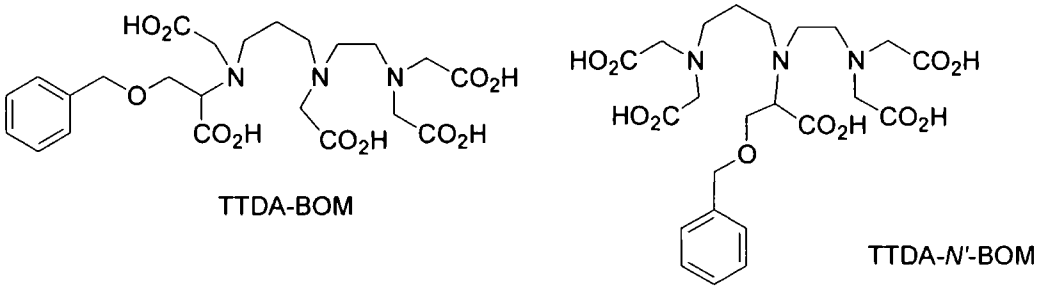

Figure III.11: $[Gd(TTDA\text{-}BOM)(H_2O)]^{2-}$ and $[Gd(TTDA\text{-}BOM)(H_2O)]^{2-}$.

III.2.2 Covalently Linked Systems

An alternative strategy to enhance the intrinsic τ_R of a contrast agent is to construct a higher molecular volume complex. However, despite several different attempts, most *covalently-linked* high molecular weigh conjugates do not significantly increase the relaxivity of the macromolecule. In a 2001 study,[76] the attachment of Gd^{III} complexes to polymers was performed in order to increase the value of τ_R. For example, poly(ethylene glycol) (PEG) moieties of average molecular weights 2000 and 5000 Da respectively were attached to the ligand TREN-HOPO-TAM (**Figure III.12**).

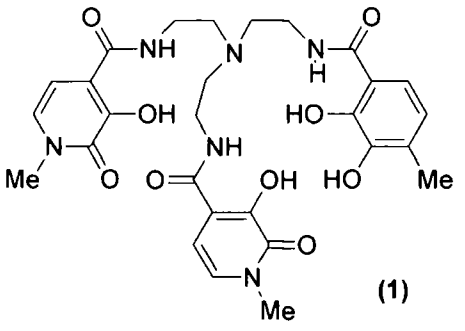

(1)

H_4TREN-HOPO-TAM

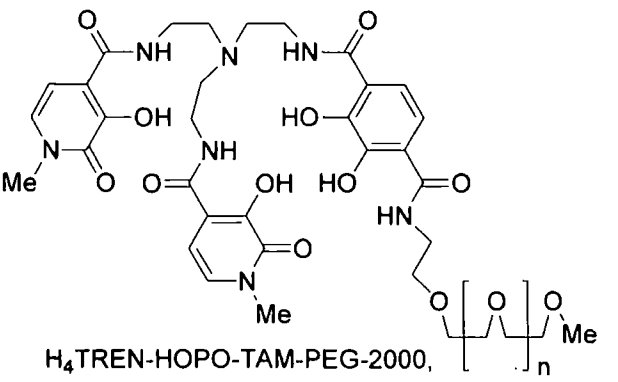

H_4TREN-HOPO-TAM-PEG-2000, median n = 43

H_4TREN-HOPO-TAM-PEG-5000, median n = 121 **(2)**

Figure III.12: The ligands TREN-HOPO-TAM (1) and TREN-HOPO-TAM-PEG (2).

The high water solubility of PEG chains increased the rather low solubility of the ligand, and it was also demonstrated that PEG chains can bind to human serum albumin across a wide pH range.[77] The complexes [Gd-TREN-HOPO-TAM-PEG-2000] (**1**) and [Gd-TREN-HOPO-TAM-PEG-5000] (**2**) were found to be highly soluble in H_2O. The τ_M and the number of coordinated water molecules (q = 1) were determined by a variable temperature ^{17}O NMR R_{2p} study of the transverse relaxation rate of H_2 ^{17}O (R_2) at 2.1 T. The observed increase in τ_M as the PEG chain is lengthened (with values of ~19 and ~31 ns for (**1**) and (**2**), respectively), can be accounted for by considering the concentration of water molecules in the immediate vicinity of the Gd^{III} complex. The increase in relaxivity observed upon addition of the PEG chain, however, was very modest considering the large increase in molecular weight, largely because of inefficient motional coupling between the Gd-centre and the macromolecular complex as a whole. Indeed, the relaxivity of the Gd^{III}-complex with "PEG-5000 chain" at pH 7.5 is 9.1 $mM^{-1}s^{-1}$ (20 MHz, 25 °C), which compares to 8.8 $mM^{-1}s^{-1}$ (20 MHz, 25 °C) for the "simple" Gd^{III}-complex.

Recent research has focused on increasing the efficiency of motional coupling between the Gd^{III} centre and the motion of the whole complex, by placing the metal ion at the barycentre of the structure. In this way, the Gd^{III} should always lie on any axis of reorientational motion and be always coupled to the motion of the macromolecule as a whole. Such a situation will exist in a dendrimer as it approaches a spherical overall shape, wherein the Gd^{III} ion resides at the centre.

IV. Dendrimers

IV.1 Structure and strategies of synthesis

Dendrimers are monodisperse polymeric macromolecules with a high degree of molecular uniformity and a highly branched three-dimensional structure, consisting of three major architectural components: core, branches and end groups.[78] The structure of the dendrimers is often represented as being symmetrical, with all dendritic arms radiating outwards from the core and all end groups located at the surface. Some studies,[79, 80] however, revealed the occurrence of a considerable degree of backfolding, which can cause a distribution of terminal functionalities throughout the volume of the dendrimer.

Dendrimers are synthesised by iterative reaction sequences, with each sequence leading to increasingly higher generations of dendrimers.

The convergent and the divergent synthesis approach

Two different strategies have been introduced for the synthesis of these macromolecules. The first example of a divergent synthesis was reported by Vögtle,[81] followed by the poly(amido-amine) (PAMAM) dendrimers (**Figure IV.1**) of Tomalia[82, 83] and Newkome's arborol systems.[84] To prepare the PAMAM dendrimer, a multifunctional core was iteratively functionalised and extended to form the various generations. PAMAM dendrimers represent a class of macromolecular architecture called "dense star" polymers which feature larger molecular diameters, twice the

number of reactive surface sites, and approximately double the molecular weight of their preceding smaller generation.

The opposite convergent approach was introduced by Fréchet in 1990,[85, 86] where the synthesis is commenced at the periphery and iteratively elaborated inwards to the core. Both the convergent and the divergent approaches to dendrimer synthesis involve the repetition of reaction steps, but purities of the resulting products can be very different. With divergent synthesis, the dendrimer is constructed outwards from a central core. Increasing numbers of functional groups are introduced at the periphery and extended outwards successfully in the subsequent step, to achieve the next generation; this strategy can lead to defects and imperfections, even for reactions with high yield and selectivity. Unfortunately, the small structural differences between defective and defect free molecules do not allow easy purification of the resulting products, which will consequently show a number of statistical imperfections.

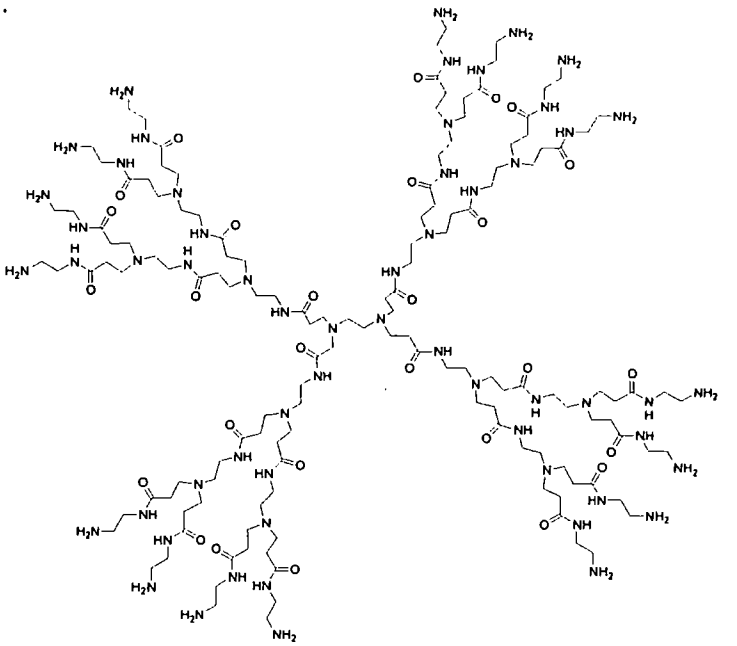

Figure IV.1: Generation 2 PAMAM Dendrimer.

The synthesis of dendrimers by the convergent approach starts at the periphery and grows inwards to the core. There is only one reaction site at the focal point of the

growing dendron to couple to the monomer, producing the next generation. Defective partially substituted monomers are often easily separable from the pure product by chromatography.

In principle, dendritic contrast agents may be devised either with the complex at the periphery or in the core of the macromolecule. Examples of each case will be considered.

IV.2 Gd^{III} complexes at the periphery of a dendrimeric structure

In a recent study, only a moderate increase of the reorientational correlation time, τ_R, of Gd^{III} complexes was obtained by conjugating them to the surface of polyamidoamine (PAMAM) dendrimers.[87] The relaxivity gains display a "saturation effect" and a consequent "quench" of the relaxivity for Gd^{III} complexes linked to the dendrimeric backbone upon increasing the size of the complex-dendrimer adducts. This observation was explained in terms of the undesired mobility of the anchoring spacer and flexibility of the skeleton. In order to understand more about this phenomenon, a new series of PAMAM conjugates with Gd-DO3AP^{ABn} on the periphery of the dendrimers was synthesised (**Figure IV.2**).[88] The [Gd-DO3AP] complex was selected, as it possesses a fast water exchange rate. Typically, the G2-PAMAM conjugate had an empirical molecular mass in the region of 13500 Da, with 16 Gd complexes bound at its periphery.

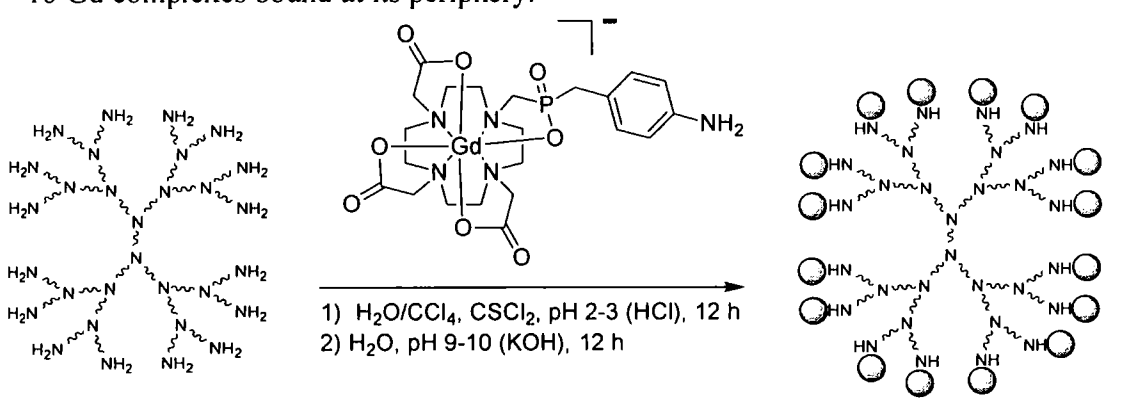

Figure IV.2: Simplified representation of the reaction sequence leading to G2-PAMAM dendrimeric conjugate.

An enhancement in the relaxivity was observed by rigidifying the internal frame of Gd-containing PAMAM dendrimers following protonation of the dendrimer or the formation of supramolecular adducts with cationic polyaminoacids. From an initial relaxivity value of 20.4 $mM^{-1} s^{-1}$ (at 25 °C, 20 MHz) at pH < 6, an increase to *ca.* 24.8 $mM^{-1} s^{-1}$ was observed (25 °C, 20 MHz), and the relaxivity reached a plateau of *ca.* 34 $mM^{-1} s^{-1}$ (25 °C, 20 MHz) during the titration of an aqueous solution of the paramagnetic dendrimer with poly(Arg) (degrees of polymerization, dp ~ 56 and 320).

IV.3 Gd^{III} complexes at the core of the dendrimeric structure

A different synthetic approach to prepare dendritic contrast agents is to conjugate dendritic wedges to a Gd^{III} complex core, placing the metal ion at the barycentre of the molecular complex and efficiently coupling the local motion of the Gd–OH_2 vector with the rotational motion of the whole complex.[89]

A compound prepared by this synthetic strategy is P760-Gd (**Figure IV.3**), a hydrophilic derivative of Gd^{III}DOTA with a molecular mass of 5.6 kDa.[90] This conjugate has been characterized in various media: aqueous solution, protein-containing solution, and Zn^{2+} - containing solution.

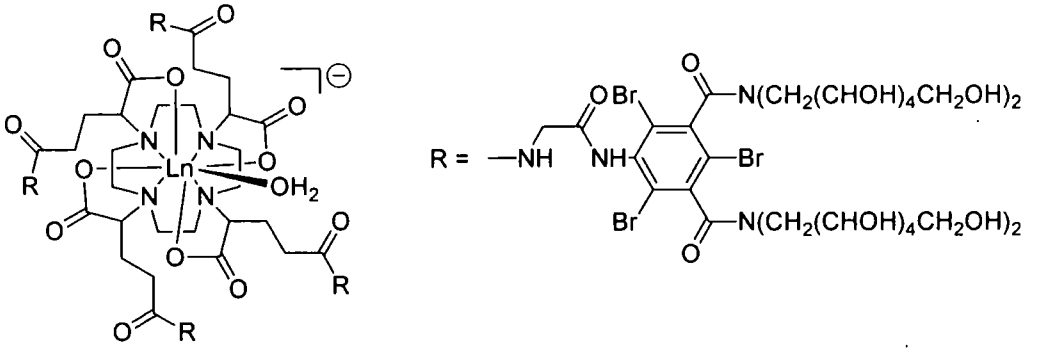

Figure IV.3: The structure of the Gd^{III}-centered dendrimer P760-Gd.

Like its parent complex Gd-DOTA, P760-Gd does not undergo transmetallation by Zn^{II} ions and, furthermore, analysis of the non-covalent binding of P760-Gd to serum proteins by proton relaxometry showed that the complex does not interact with human serum albumin. The relaxivity of P760-Gd is one of the highest reported in the

literature for a gadolinium complex not displaying protein binding;[91] its large longitudinal and transverse proton relaxivities (r_{1p} ~ 25.0 $s^{-1}mM^{-1}$ and r_{2p} ~ 29.5 $s^{-1}mM^{-1}$ at 310 K and 0.94 T) are a consequence of its increased rotational correlation time (τ_R ~ 2 ns at 310 K). Unfortunately, the proton NMRD data obtained show that the benefits from the increased τ_R are not completely achieved because of sub-optimal water-exchange rate, and the relatively high relaxivity is likely to be associated with a large second sphere contribution.

New types of dendritic framework have been synthesised based on a central Gd^{III} complex.[92] These dendrimers, containing four or twelve (**Figure IV.4**) glucose moieties at their peripheries, were synthesized by conjugating diethylenetriaminepentaacetic (DTPA) to carbohydrate-containing dendritic wedges. This extended ligand was complexed to a gadolinium ion to afford a contrast agent containing a single bound water molecule. Despite its acetylated glycosides, which may reinforce its hydrophobicity, this dendrimer shows a good solubility in aqueous solutions. However, its diamides containing core possesses rather slow water exchange rates, quenching any relaxivity gains that might otherwise have been obtained.

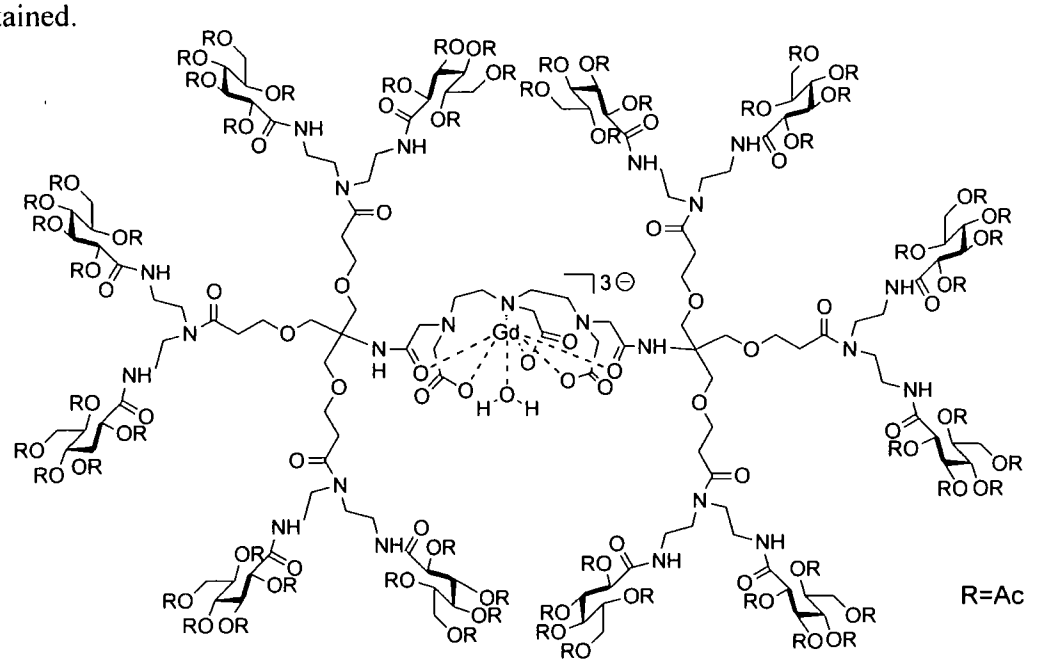

Figure IV.4: Structure of Gd^{III}–dendrimer chelate |Gd(D2)|(H_2O).

Unfortunately, relaxivity studies were not reported on this dendrimer or its deacylated analogue. Nevertheless, gadolinium centred spherically dendritic macromolecules are interesting and stimulating subjects to be studied as new potential candidates for MRI contrast agents. The important role played by carbohydrates in many recognition processes on cell surfaces make them candidates for the site-specific delivery of the contrast agents at a molecular level.

The design and synthesis of new carbohydrate-containing dendrons has been the aim of the research during the first year of this project, and it will be discussed in **Chapter II** of this thesis.

IV.4 Gd^{III} complexes incorporating hydrophilic dendrons

Significant enhancements in the relaxivity values were recently obtained in dendrimers constructed upon the (*RRRR/SSSS*)-[GdgDOTA(H_2O)]$^{5-}$ complex. The macromolecules are synthesized by conjugating dendritic wedges to the C_4-related peripheral carboxylate groups of the (*RRRR/SSSS*)-[GdgDOTA(H_2O)]$^{5-}$ complex. An example of such a dendrimer is illustrated in **Figure IV.5**:

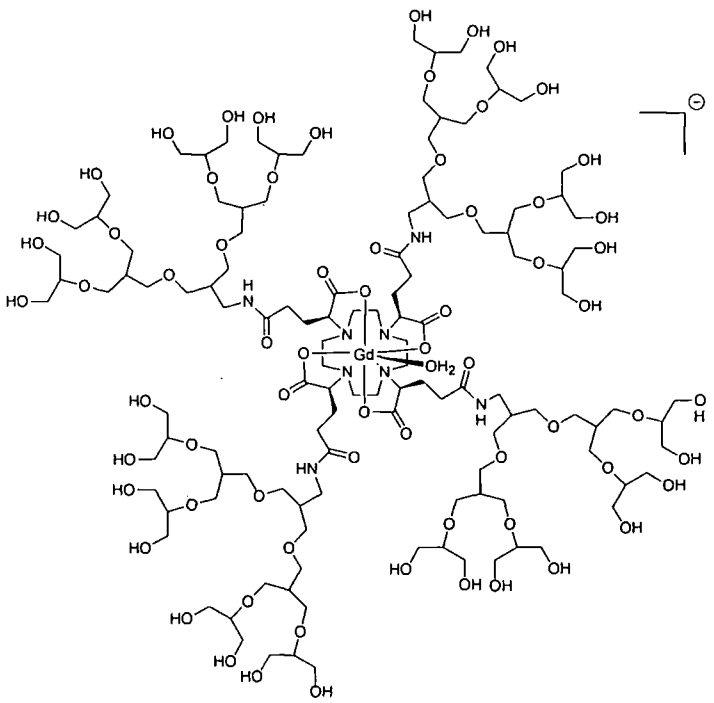

Figure IV.5: Structure of a dendrimer based upon [GdgDOTA(H_2O)]$^{5-}$.

The Gd^{III} ion resides at the focal point of this spherical complex, which possesses an overall maximum density at the centre surrounded by a hydrophilic dendritic structure. The observed relaxivity (r_{1p} = 19.6 $mM^{-1}s^{-1}$, at 25 °C, 20 MHz) is thought to be dominated by a large second sphere contribution, that increases linearly with the molecular volume, and a fast inner sphere water exchange rate is also maintained (τ_m = 85 ns).[89]

An attractive example of dendrimeric chelate possessing optimal water residence time (τ_m = 10 ns), slow molecular tumbling (τ_R = 238 ps) and good water solubility (≥ 15 mM), is the q = 2 system Gd-TREN-bisHOPO-TAM-Asp-Asp_2-12OH,[93] illustrated in **Figure IV.6**.

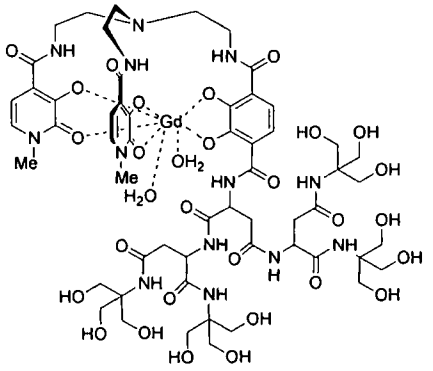

Figure IV.6: Structure of [Gd-TREN-bisHOPO-TAM-Asp-Asp_2-12OH$(H_2O)_2$], MW 1576 $gmol^{-1}$.

However, all these optimized parameters result in an observed efficacy measured at 20 MHz, 25 °C, of 14.3 $mM^{-1}s^{-1}$, inferior to the value observed at the same magnetic field strenght for the previously described q = 1 Gd-gDOTA based dendrimer. An explanation of this data can be found in the field dependent magnetic properties of the HOPO-based complexes, which will be discussed in **section V** of this introduction.

IV.5 Glycodendritic Complexes: taking advantage of the sugar moiety?

An interesting recent study reported the *in vitro* relaxivity of some Gd^{III}-glycoconjugates (**Figure IV.1**) based on the DOTA ligand.[94] DOTA like ligands form Ln^{III} chelates of high thermodynamic and kinetic stability, which is of crucial

importance for *in vivo* applications, and DOTA-monoamides are easy to prepare. However, they also usually possess a rather slow water exchange rate so the relaxivity gains in non-covalent adducts are sub-optimal.

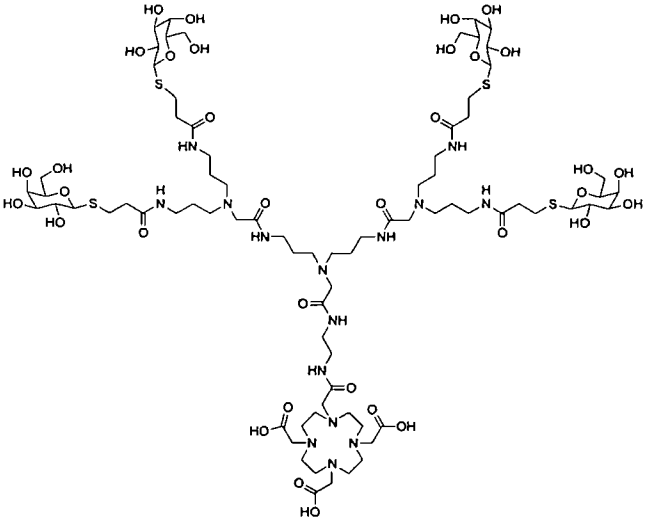

Figure IV.1: A tetravalent galactoside based upon a mono-amide derivative of DOTA.[94]

A ^{1}H NMRD profile study was undertaken and the interaction of these glycoconjugates with lectins (carbohydrate binding proteins) was examined. The flexibility of the glycodendrimer moiety in solution was found to limit the relaxivity of the Gd^{III} complex to a value lower than expected from its molecular weight. Precise details of the relaxivity of this system have not been reported, but it is likely to be low because of the slow water exchange rate and the high degree of flexibility inherent to the structure. The lectin–glycoconjugate interaction was found to slow down the tumbling rate and increase the relaxivity of the Gd^{III} chelates, but this effect was modest and the increase in relaxivity was only 8% in the lectin conjugate.

An increase in the relaxivity value of a gadolinium contrast agent can be registered upon slowing down its molecular tumbling (τ_R), insofar as its inner water molecule's exchange rate (τ_m) is also close to an optimal value, which is of ~ 30 ns.[95] A q = 1, small gadolinium complex, based on 1,2-HOPO chelate, GdH(2,2)-1,2-HOPO[96] has been recently synthesized (the ligand structure is shown in **Figure IV.2**), whose relaxivity value (r_{1p} = 8.2 $mM^{-1}s^{-1}$, 20 MHz, 37°C), is approximately double that of

both $[Gd(DOTA)(H_2O)]^-$ and $[Gd(DTPA)(H_2O)]^{2-}$, and rises from the optimization of all the relevant parameters: long rotational correlation time (τ_R = 107 ps), Δ^2 is small (1.0×10^{19} s^{-2}) and τ_v is long (47 ps), allowing an estimation of a very favourable longitudinal electronic correlation time T_{1e} (~ 70 ns at 60 MHz).

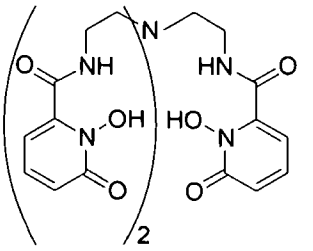

Figure IV.2: H(2,2)-1,2-HOPO structure

Extra enhancement to the overall relaxivity can be achieved by further increasing the rotational correlation time, grafting the small gadolinium-HOPO-chelate to large and rigid macromolecules. The toxicity of the compound has been also examined, and the pM values obtained from competition batch titration versus DTPA have shown a very high stability of the Gd(III) complex and excellent selectivity for Gd(III) binding over Zn(II) and Ca(II); the luminescence spectroscopy experiments on the analogues europium-HOPO-chelate revealed no affinity for the Zn(II) and Ca(II) ions either. The exceptionally good relaxometric properties for a q = 1, small gadolinium complex, and the very low affinity for endogenous anions, renders GdH(2,2)-1,2-HOPO a promising extracellular contrast agent for MRI.

V. Survey of *Di*-aqua complexes

V.1 General considerations

The commercially available poly(amino-carboxylate)-based chelates of first generation possess only one coordinated water molecule in their inner sphere (q = 1), which can exchange sufficiently slow with the bulk solvent to limit the image-

enhancing efficacy of macromolecular derivatives (typical r_{1p} value ~ 4 $mM^{-1}s^{-1}$).[8] According to the Solomon-Bloembergen-Morgan equation, a bigger number of inner sphere water molecules, with fast exchange rate, should significantly increase the relaxivity of the system. A straightforward way of testing this theory is to decrease the ligand's denticity, although the use of heptadentate ligands can lead to a substantial drop in the thermodynamic stability and kinetic inertness that are essential to guarantee the non-toxicity of the complex, or to a change of the chelate's selectivity towards physiological anions, with consequent possible formation of ternary complexes. With regard to this, [Gd(DO3A)] and several functionalized derivatives based upon it have been investigated in detail. The complex $[Gd(aDO3A)]^{3-}$, synthesized a few years ago in our laboratory[52] (its molecular structure is reported in **Figure II.9**), is an example of DO3A based q = 2 system whose efficacy (r_{1p} = 12.5 mM^{-1} s^{-1}) has been proved not to be perturbed by the presence of endogenous cations (*e.g.* Zn^{III}), or anions (*e.g.* HCO_3/CO_3^{2-}). $[Gd(aDO3A)]^{3-}$ showed a kinetical inertness ten times superior to the clinically used $[GdDTPA]^{2-}$ (Magnevist).

However, among other examined DO3A-based systems,[97] evidence has been found for the displacement of one or both of the coordinated water molecules by endogenous anions (eg. carbonate, lactate, malonate, citrate). In addition the formation of ternary Gd^{III}L-human serum albumin (HSA) adducts has been defined with coordinating groups on the surface of the HSA displacing the inner sphere water molecules.[67]

Studies have therefore been oriented towards other classes of heptacoordinated Gd^{III} chelates.

V.2 HOPO derivatives

Hydroxypyridinate (HOPO) monoanions have been employed as a base structure in the synthesis of q = 2 Gd(III) complexes: they become effective multidentate chelating agents (especially for metal ions, such as Gd^{III}) when the ring carbon in α-

position to the hydroxyl (or carbonyl) group is functionalized and attached to a suitable backbone through amide bond formation[98] (**Figure V.1**).

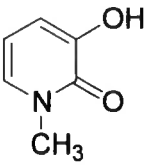

Figure V.1: HOPO structure

In 1995, the first HOPO derivative was synthesized: Gd(TREN-1-Me-3,2-HOPO)(H_2O)$_2$ = tris[(3-hydroxy-1-methyl-2-oxo-1,2-didehydropyridine-4-carboxyamido)ethyl]amine (**1** in **Table V.I**).[99] The purely oxygen donor ligand allows two coordinated water molecules at the metal centre, without destroying the chelate stability or affecting the efficacy of the complex. The relaxivity is 10.5 $mM^{-1}s^{-1}$ (at 37 °C, 20 MHz), double that of the commercial CAs.[100] Since then, an entire "HOPO-based family" of MRI contrast agents has been created: it includes complexes with chelating HOPO moieties and various caps, in which the lanthanide ion is coordinated to six oxygen donors. The complex accommodates two water molecules, which exchange at a fast, near optimal speed with the bulk solvent (molecular structures are reported in **Table V.1** and a comparison of the τ_m of some HOPO-based complexes versus commercial agents is shown in **FigureV.2**).

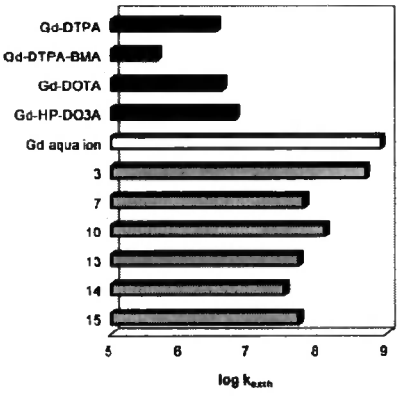

FigureV.2: Water exchange rate of HOPO-based Gd^{III} complexes (grey) vs commercial agents(black)[99] ***(reproduced with permission of the author).***

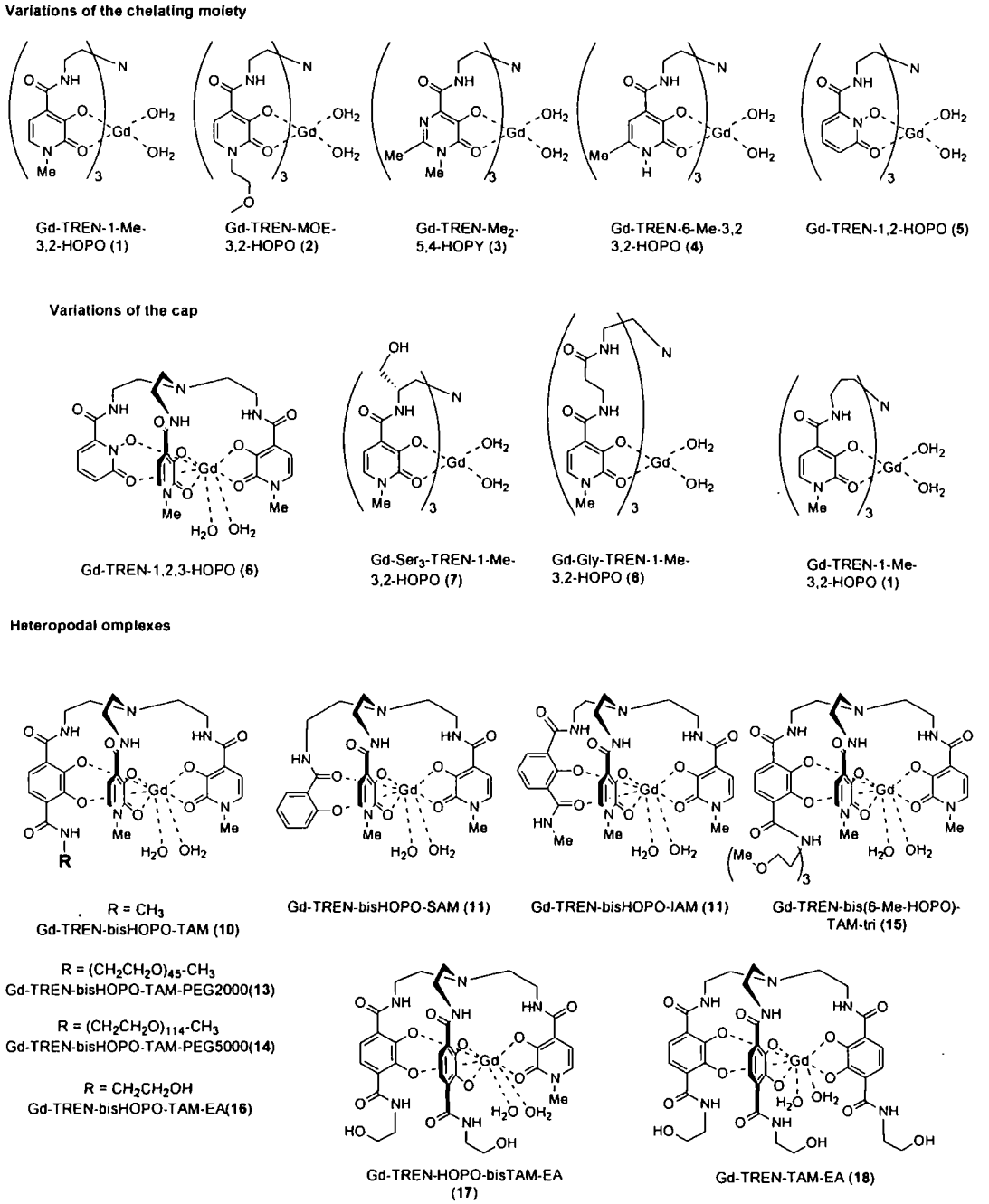

Table V.1. Structure of hydroxypyridinone-based Gd^{III} complexes.[101]

Besides a significant improvement in the τ_m values, the HOPO-based Gd^{III} complexes show a substantial difference in the relaxivity dependency upon magnetic field strength. Thus, in their $1/T_1$ NMRD profiles, a distinctive peak in the relaxivity value

is registered at high fields, between 20 and 100 MHz. This behaviour is opposite to that observed for the contrast agents commercially available, which usually present higher relaxivities at magnetic fields below 10 MHz. The recently synthesized Gd-TREN-bisHOPO-TAM-Asp-Asp$_2$-12OH(H$_2$O)$_2$ (**Figure V.3 *a*, Gd-2**),[90] where the Gd^{III} chelate is grafted onto a dendron consisting of four tris(hydroxymethyl)aminomethane (TRIS) groups linked by three aspartic acids, presents the best NMRD profile (in **Figure V.3 *b***) for such a HOPO-derivative gadolinium complex.

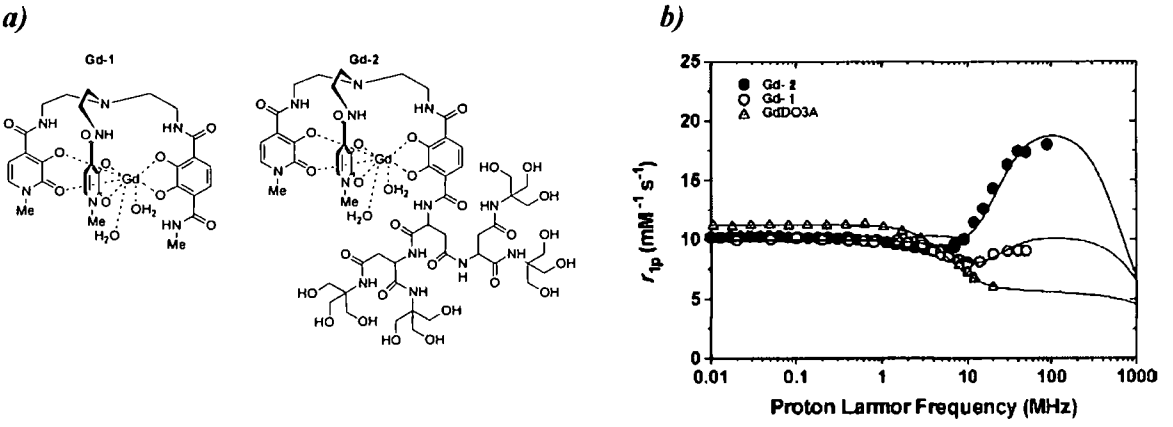

Figure V.3: *a)* Gd-TREN-bisHOPO-TAM-Me(H$_2$O)$_2$ (Gd-1) and Gd-TREN-bisHOPO-TAM-Asp-Asp$_2$-12OH(H$_2$O)$_2$ (Gd-2) and *b)* relative $1/T_1$ NMRD profiles (at 298 K) [90]
(reproduced with permission of the author).

The relaxivity value of 14.3 mM^{-1}s^{-1} (20 MHz, pH 7.2, 25 °C) exhibited by this dendrimer is three times greater than that of the comparative q = 2 commercial agent Gd-DO3A[102] and 1.6 times that of the monomer Gd(TREN-1-Me-3,2-HOPO)(H$_2$O)$_2$ [Gd**1**]. At 90 MHz, the relaxivity value reaches 18 mM^{-1}s^{-1}. The enhancement is explained in terms of the increased rotational correlation time: the higher molecular weight (1576 g/mol) and compactness of the structure (guaranteed by the short linker between two branching points of each aspartic moiety) ensure a slower tumbling, without affecting the fast water exchange rate (τ_m = 10 ns) of the two inner sphere water molecules or the short electronic relaxation time. Furthermore, the alcohols on

the dendritic moieties offer a solution to a problem associated to the use of HOPO-derivatives in general as contrast agents: their *poor solubility* in water. Many structural changes have been investigated to circumvent this drawback, such as the insertion into the ligand's structure of methoxy derivatives (as shown in **2**), or salicylamide (**11**), or isophthalamide (in **12**). Noticeable water solubility enhancement has been found with complexes based on another class of bidentate chelating groups: the 6-carboxamido-5,4-hydroxypyrimidinones. An example is Gd-TREN-Me_2-5,4-HOPY (**3**), which showed a very much improved solubility (up to 100 mM) and exceptionally short water residence time (τ_m ~ 2 ns); the absence of binding interactions towards endogenous anions has been confirmed by titration of a 1 mM L^- [1] solution of the complex with acetate, lactate and malonate, at 20 MHz, 25 °C and pH 7.2. The accessibility of the anions towards the metal centre is hindered by the tight coordination of the ligand donor groups, which probably presents a high steric constraint at the water binding sites.[103] A comparison of relaxivity measurements in water and in blood serum reveals that the relaxivity is approximately 35% higher in the latter, this suggesting the presence of a weak interaction between the complex and human serum albumin.

However, the complexes currently claimed to be the most promising relaxometric and solubility properties rely on a heteropodal bis-HOPO-TAM ligand, incorporating a triazacyclononane (TACN) derivative as a "cap" (**Figure V.4**).[98]

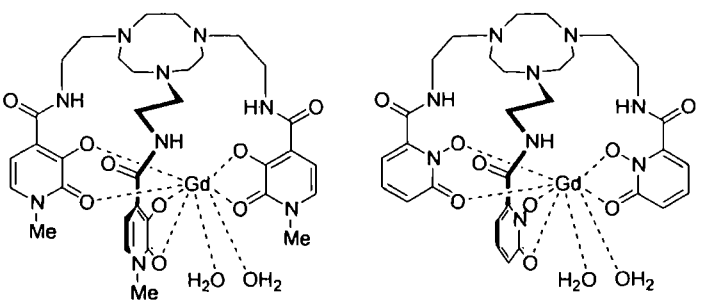

Figure V.4: Gd^{III}-TACN-3,2-HOPO (**3**) and Gd^{III}-TACN-1,2-HOPO (**4**).

To determine if the TACN capping scaffold has any influence on the number of coordinated water molecules, the europium analogue complex was synthesized and luminescence lifetime measurements confirmed what had previously been predicted by molecular mechanic techniques: the system is a q = 3 complex. The relaxivity values for **3** and **4** are respectively of 13.1 and 12.5 $mM^{-1}s^{-1}$ (20 MHz, 298 K, pH 7), one of the highest registered so far for low molecular weight mononuclear gadolinium complexes. The τ_m value has been measured of ca. 2.0 ns and the Δ^2 value obtained from the NMRD fits are the lowest yet determined for any HOPO-based gadolinium complex (*i.e.* longer electronic relaxation time is expected).

Given the very high toxicity of the gadolinium ion, it becomes crucial to examine the stability of the chelate structures in their environments. Studies of the effect of the ligand basicity on the thermodynamic stability of the gadolinium HOPO-based complexes demonstrated that maximum stability is gained with the intermediate basicity displayed by the heteropodal ligand TREN-bis-HOPO-TAM,[104] (**10**, **Table V.1**). Acidic or negatively charged substituents drastically decrease the stability of the complex, which is enhanced if the overall charge is maintained as close to zero as possible and the ligand's basicity is optimized (**Figure V.5**).

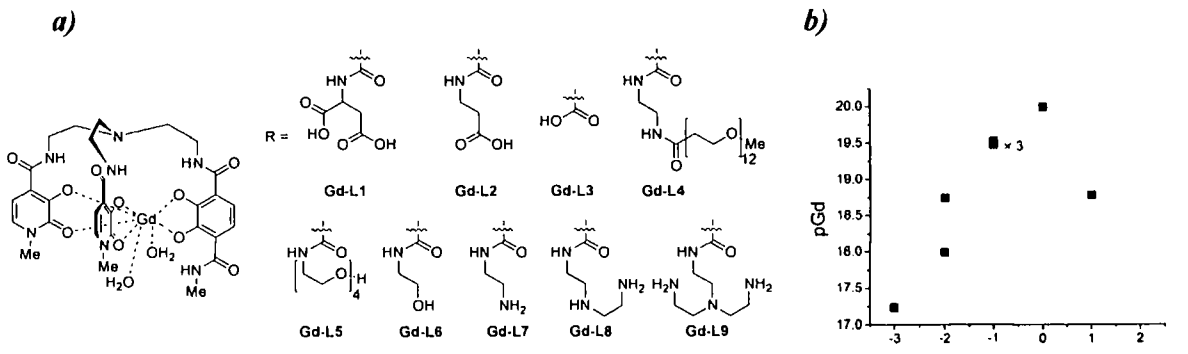

Figure V.5: (*a*) Functionalized Gd^{III}-TREN bisHOPO-TAM complexes and (*b*) effect of the charge of the Gd^{III} complex on their stability [103] *(reproduced with permission of the author).*

The stability of HOPO-based gadolinium complexes in the presence of Cu^{II}, Ca^{II} and Zn^{II} is important, as these metal cations, present in the human serum in non-negligible concentrations, potentially could displace toxic gadolinium from the complex. Titration studies on a representative complex, **Gd-L5**,[105] indicate that the compound is of comparable stability and toxicity to commercial MRI contrast agents.

Endogenous anions (e.g. carbonate, phosphate, citrate, malonate), present in serum and other biological fluids, can also decrease the contrast enhancing effectiveness by displacing the water molecules coordinated to the metal. Only hydrogenphosphate and oxalate exhibit a significant effect on the relaxivity of both the complexes **Gd-L5** and **Gd-L9**: in each case, phosphate replaces one of the two bound water molecules, while the bidentate oxalate anion seems to replace both waters in **Gd-L5** but only one in **Gd-L9**. It should be noted that the equilibrium stability studies reported by Raymond (e.g. pM/anion affinity) are perhaps not as important as kinetic stability profiles, examining the pH or pM dependence of the rate of complex dissociation. It is these experiments that predict more accurately whether a complex is suitable for *in vivo* use.

Macromolecules with higher number of coordinated water molecules

Upon the principle of the supramolecular self-assembly is based the recent work which led Raymond and collaborators to obtain the macromolecules in **Figure V.6**: self-assembled supramolecular clusters of Gd^{III} hydroxypyridinone (HOPO) complexes, templated by a Fe^{III} terephthalamide (TAM) centre.[106] The peripheral Gd^{III} ions coordinate two water molecules which exchange rapidly with the bulk solvent; the cylindrical architecture of the self-assemblies and the high rigidity of the supramolecules, contribute to efficiently increase the τ_R of the cluster, resulting in elevated relaxivities at high magnetic fields, with a maximum centred around 60 – 100 MHz. The relaxivity of the trinuclear assembly **Fe, 2Gd-3L$_C$** at 90 MHz is r_{1p} = 42 $mM^{-1}s^{-1}$ (*i.e.* 14 $mM^{-1}s^{-1}$ per Gd^{III}), a value maintained also at physiological pH and when dissolved in human serum.

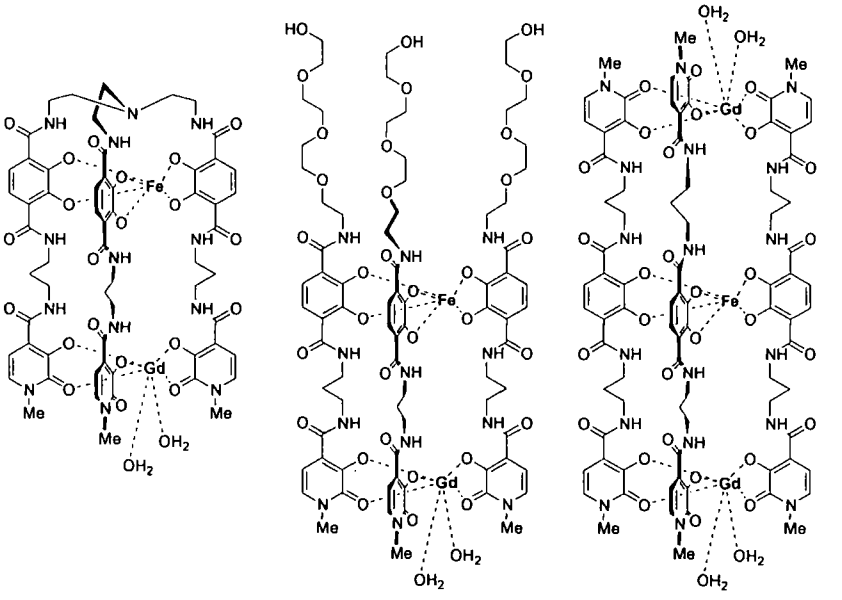

Figure V.6: Self-assembled supramolecular clusters of Gd^{III} hydroxypyridinone (HOPO) complexes.

An alternative q = 2 system based on the DTPA structure has been developed by Ruloff et al.,[107] shown in **Figure V.7**.

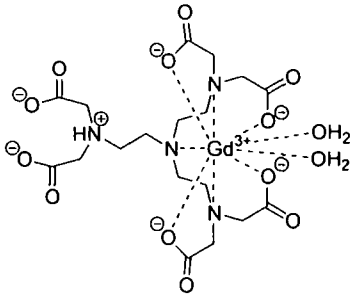

Figure V.7: Suggested structure for the Gd^{III} complex of $TTAHA^{6-}$ in aqueous solution pH 7.

A fast water exchange rate was found for this system (k_{ex}^{298} = (8.6 ± 0.6) × 10^6 s^{-1}), which has been recently revisited for its incorporation into a novel heterotritopic ligand, LH_8, or metallostar, which comprises two poly(aminocarboxylate) groups (the *N*-tris-(2-aminoethyl)amine-*N',N',N'',N'',N''',N'''*-hexaacetate ligand or TTAHA) for binding to Gd^{III} ions and a 2,2'-bipyridine moiety for specific binding to Fe^{II} ions.

By following a convergent approach, the complex $\{Fe[Gd_2L(H_2O)_4]_3\}^{4-}$ was obtained, and its molecular model is reported in **Figure V.8.**[108] The heterometallic, self-assembled metallostar possesses six efficiently relaxing paramagnetic centers confined into a small space, and the concurrent chelation of the ligand to Fe^{II} and Gd^{III} ions forces the rotational correlation time of the Gd^{III}-water proton vector to be close to that of the entire assembly, minimizing the internal flexibility. Each of these feature lead to particularly high relaxivity values (27.0 and 33.2 mM^{-1} s^{-1} at 20 and 60 MHz, respectively, at 25 °C), and the $1/T_1$ NMRD profile shows the high field peak, typical of a slowly rotating complex (similar to HOPO-based systems). The negative charge of $\{Fe[Gd_2L(H_2O)_4]_3\}^{4-}$ ensures its high water solubility, but at the same time implies a higher osmotic load, not viable for gadolinium complexes for medical applications.[109]

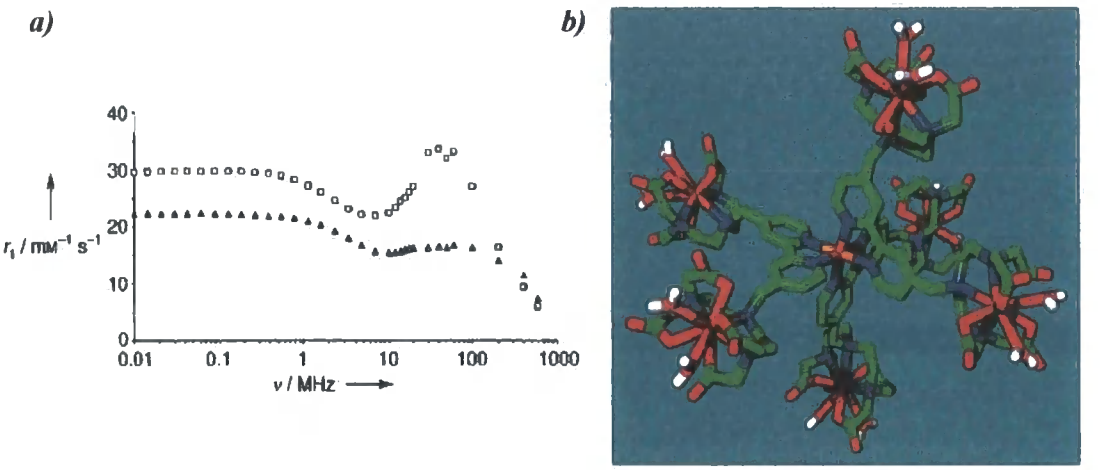

Figure V.8: ***a)*** **$1/T_1$ NMRD profiles of $[Gd_2L(H_2O)_4]^{2-}$ (▲) and $\{Fe[Gd_2L(H_2O)_4]_3\}^{4-}$(□) pH 6, 25 °C; *b)* Framework molecular model of $\{Fe[Gd_2L(H_2O)_4]_3\}^{4-}$** [106]

(reproduced with permission of the author).

VI. General remarks and outline of the presented work

Some theoretical principles fundamental to the application of contrast agents to MRI have been examined in this chapter, to understand better how the gadolinium chelate structure can be modified in order to improve the MRI contrast agent performances. A difficult balance between different parameters has to be respected in the design of any new structure that seeks to replace the commercially available contrast agents. Despite many attempts, some of which have been reported earlier in this introduction, it is a big challenge to prepare a new system where all the parameters (*eg.* fast τ_m, slow τ_R, $q > 1$, kinetic / thermodynamic stability) act synergically to increase the overall relaxivity value.

Indeed, even in the promising and largely examined HOPO based structures, where nearly optimal water(s) exchange rate (τ_m), slow molecular tumbling (τ_R) and reasonably high water solubility (*eg.* **Gd-2** [90] and the heteropodal bis-HOPO-TAM ligand incorporating a triazacyclononane (TACN) as a "cap" [98]) gave rise to reasonably good relaxivity values (~ 14 $mM^{-1}s^{-1}$, at 20 MHz, 25 °C), kinetic stability measurements need to be performed before any *in vivo* experiments. The non-trivial synthetic procedures needed for the preparation of these compounds require the patient work of expert chemists and quite high costs.

In the highly engineered work of the self-assembled supramolecular clusters of Gd^{III}HOPO complexes, containing an Fe^{III} terephthalamide (TAM) centre,[104] questions about the post-injection toxicity (*i.e.* thermodynamic / kinetic stability) of the compound still need to be answered.

The concerns about the heterometallic, self-assembled metallostars[105] are identical: will the water molecules stay bound to the metal ions, even in the body? Will the negative charges confer to the compound, apart from good water solubility, a higher osmotic load?

The technique of non-covalently binding $q = 1$ systems (the displacement of the inner sphere water molecule(s) in $q = 2$ systems to macromolecules has exhibited good

results, especially in the case of a GdEGTA complex linked to HSA.[71] In this case, the replacement of the coordinated water molecules or displacement of the complex itself from the protein adduct have to be carefully investigated, to test the stability of the supramolecular assembly. As for $q = 2$ systems conjugates to macromolecules, the displacement of the inner sphere water molecule(s) by endogenous anions or by donor groups of the protein has been demonstrated to be very likely to happen. [68, 69]

Based upon the discovery that high molecular weight dendrimeric structures, synthesized by attaching hydrophilic moieties[86] (*i.e.* sugars[89, 91]) to a paramagnetic centre (*eg.* GdDTPA, GdgDOTA, GdDOTA), can lead to slowly tumbling, highly water soluble macromolecular structures, it was considered worthwhile to explore the design of new dendrimeric structures.

The collaboration between Bracco Imaging S.p.A. and Durham University allowed the herein described work of design and synthesis of new contrast agents for MRI. Two different approaches have been followed: at first, efforts were focused on the synthesis of a new, medium molecular weight (~ 2080 $gmol^{-1}$) dendritic structure, bearing sugar moieties at the periphery of a GdgDOTA core. The gadolinium-water vector should be placed at the centre of any tumbling motion, thus allowing a coherent tumbling of the macromolecule and an optimization of its rotational correlation time. The carbohydrate wedges should also guarantee high water solubility and favour a large second sphere of hydration.

Thereafter, we focused on the development of $q = 2$ systems based on the alternative heptadentate core structure 6-amino-6-methyl-perhydro-1,4-diazepin (AMPED).[110] This core structure possesses three reactive amino positions available for further functionalization. Different diastereisomers can be obtained by alkylating the amino groups, and different water exchange rates can be found, as already shown in the GdgDOTA system.[61] Once synthesized, the thermodynamic and kinetic stability of these new $q = 2$ gadolinium chelates needs to be proved, also at variable pH and in the presence of endogenous salts.

List of references

[1] Lowe, M. P. *Aust. J. Chem.* **2002**, *55*, 551.

[2] Diem, K.; Leutner, C. *Documenta Geigy Scientific Tables*; Gregory Ed.: Basel, 1970.

[3] Damadian, R. *Proc. Nat. Acad. Sci. USA* **1974**, *71*, 1471.

[4] Caravan, P. *Chem. Soc. Rev.* **2006**, *35*, 512.

[5] Bünzli J.-C. G.; Choppin, G. R. *Lanthanide Probes in Life, Chemical and Earth Science,* Elsevier **1989,** pp. 391.

[6] Aime, S.; Botta, M.; Fasano, M.; Terreno, E. *Chem. Soc. Rev.* **1998**, *27*, 19.

[7] Sharp, R. R. *Nuclear Magnetic Resonance* **2005**, Vol. 34, (The Royal Society of Chemistry).

[8] Merbach A. E.; Toth, É. (Eds), *The Chemistry of Contrast Agents in medicinal magnetic resonance Imaging*, 1st ed., Wiley, Chichester **2001**.

[9] Raymond, K. N.; Pierre, V. C. *Bioconjugate Chem.* **2005**, *16*, 3.

[10] Schwarzenbach, G. *Helv. Chim. Acta.* **1952**, *35*, 2344.

[11] Weissleder, R.; Hahn, P. F.; Stark D. D., Elizondo, G.; Saini, S.; Todd, L. E.; Wittenberg, J.; Ferrucci, J. T. *Radiology*, **1988**, *169*, 399.

[12] Elizondo, G.; Fretz, C. J.; Stark, D. D.; Rocklage, S. M.; Quay, S. C.; Hahn, F. E.; Raymond, K. N. *Inorg. Chem.* **1989**, *28*, 477.

[13] Desreux, J. F. *J. Am. Chem. Soc.* **1980**, *19*, 1319.

[14] Loncin, M. F.; Desreux, J. F.; Merciny, E. *Inorg. Chem.* **1986**, *25*, 2646.

[15] Van Wagoner, M.; Worah, D. *Invest. Radiol.* **1993**, *28*, S44.

[16] FDA News, May 23 **2007**.

[17] Khurana, A.; Runge, Val M.; Narayanan, M.; Greene, J. F.; Nickel, A. E. *Investigative Radiology* **2007**, *42 (2)*, 139 - 145.

[18] Okada, S.; K. Atagiri, K.; Kumazaki, T.; Yokoyama, H. *Acta Radiol.* **2001**, *42(3)*, 339.

[19] Bottrill, M.; Kwok, L.; Long, N. J. *Chem. Soc. Rev.* **2006**, *35*, 557 – 571.

[20] Rocklage, S. M.; Cacheris, W. P.; Quay, S. C. ; Hahn, F. E. ; Raymond, K. N. *Inorg. Chem.* **1989**, *28*, 477.

[21] Woods, M.; Kiefer, G. E.; Bott, S.; Castillo-Muzquiz, A.; Eshelbrenner, C.; Michaudet, L.; McMillan, K. ; Mudigunda, S. D. K. ; Ogrin, D.; Tircso′, G.; Zhang, S.; Zhao, P.; Sherry, A. D. *J. Am. Chem. Soc.* **2004**, *126*, 9248 - 9256.

[22] Lowe, M. P.; Parker, D.; Reany, O.; Aime, S.; Botta, M.; Castellano, G.; Gianolio, E.; Pagliarin, R. *J. Am. Chem. Soc.* **2001**, *123*, 7601 - 7609.

[23] Woods, M.; Zhang, S.; Ebron, V. H.; Sherry, A. D. *Chem. Eur. J.* **2003**, *9*, 4634.

[24] Aime, S.; Botta, M.; Geninatti Crich, S.; Giovenzana, G.; Palmisano, G.; Sisti, M. *Chem. Commun.* **1999**, 1577.

[25] Li, W.; Fraser, S. E.; Meade, T. J. *J. Am. Chem. Soc.* **1999**, *121*, 1413.

[26] Hanaoka, K.; Kikuchi, K.; Urano, Y.; Nagano, T. *J. Chem. Soc.* **2001**, *2*, 1840.

[27] Hanaoka, K.; Kikuchi, K.; Urano, Y.; Nagano, T. *J. Chem. Soc., Perkin Trans. 2* **2001**, 1840.

[28] Que, E. L.; Chang, C. J. *J. Am. Chem. Soc.* **2006**, *128*, 15942.

[29]Moats, R. A.; Fraser S. E.; Meade, T. J. *Angew. Chem.*, Int. Ed. Engl. **1997**, *36*, 726.

[30]Louie, A. Y.; Huber, M. M.; Ahrens, M. M.; Rothbächer, U.; Moats, R.; Jacobs, R. E.; Fraser, S. E.; Meade, T. J. *Nat. Biotechnol.* **2000**, *18*, 321.

[31] Duimstra, J. A.; Femia, F. J.; Meade, T. J. *J. Am. Chem. Soc.* **2005**, *127*, 12847.

[32] Nivorozhkin, A. L.; Kolodziej, A. F.; Caravan, P.; Greenfield, M. T.; Lauffer, R. B.; McMurry, T. J. *Angew. Chem.*, Int. Ed. **2001**, *40*, 2903.

[33] Aime, S.; Cabella, C.; Colombatto, S.; Crich, S. G.; Gianolio, E.; Maggioni, F. *J. Magn. Reson. Imaging* **2002**, *16*, 394.

[34] Uggeri, F.; Aime, S.; Anelli, P.L.; Botta, M.; Brocchetta, M.; de Haën, C.; Ermondi, G.; Grandi, M.; Paolio, P. *Inorg. Chem.* **1995**, *34*, 633.

[35] Jansen, O. *Eur. Radiol. Suppl.* **2004**, *14*, 05.

[36] Schneider, G.; Saedi, D.; Massmann, A.; Fries, P.; Boehm, M.; Kramann, B.; Winter, H. *Eur. Radiol. Suppl.* **2004**, *14*, 71.

[37] Mintorovitch, J.; Shamsi, K. *Oncology* (Williston Park, N.Y.) **2000**, *14*, 37.

[38] Schmitt-Willich, H.; Brehm, M.; Ewers, Ch. L. J.; Michl, G.; Müller-Fahrnow, A.; Petrov, O.; Platzek, J.; Radüchel, B.; Sülzle, D. *Inorg. Chem.* **1995**, *38*, 1134.

[39] Bloembergen, N.; Morgan, L. O. *J. Chem. Phys.* **1961**, *34*, 842.

[40] Caravan, P.; Ellison, J. J.; McMurry, T. J. ; Lauffer, R. B. *Chem. Rev.* **1999**, *99*, 2293.

[41] Solomon, I.; Bloembergen, N. *J. Chem. Phys.* **1956**, *25*, 261.

[42] Koenig, S. H.; Brown, R. D. *Prog. Nuc. Magn. Reson. Spectros.* **1990**, *22*, 487.

[43] Astashkin, A. V.; Raitsimring, A. M.; Caravan, P. *J. Phys. Chem. A* **2004**, *108*, 1990.

[44] Lauffer, R.B. *Chem. Rev.* **1987**, *87*, 901.

[45] Freed, J. H. *J. Chem. Phys.* **1978**, *68(9)*, 4034.

[46] Aime, S.; Botta, M.; Ermondi, G. *J. Magn. Reson.* **1991**, *92*, 572.

[47] Aime, S.; Batsanov, A. S.; Botta, M.; Howard, J. A. K.; Parker, D.; Senanayake, K.; Williams, J. A. G. *Inorg. Chem.* **1994**, *33*, 4696.

[48] Botta, M. *Eur. J. Inorg. Chem.* **2000**, 399.

[49] Botta, M. First COST D1 European Workshop, Coimbra **1995**, Abstract book: p 24.

[50] Hardcastle, K. I.; Botta, M.; Fasano, M.; Digilio, G. *Eur. J. Inorg. Chem.* **2000**, 971.

[51] Parker, D.; Dickins, R. S.; Puschmann, H.; Crossland, C.; Howard, J. A. K. *Chem. Rev.* **2002**, 102, 1977.

[52] Messeri, D.; Lowe, M. P.; Parker, D.; Botta, M. *Chem. Commun.* **2001**, 2742.

[53] Aime, S.; Barge, A.; Botta, M.; De Sousa, A. S.; Parker, D. *Angew. Chem., Int. Ed. Engl.* **1998**, *37*, 2673.

[54] Aime, S.; barge, A.; Bruce, J. I.; Botta, M.; Howard, J. A. K.; Moloney, J. M.; Parker, D.; De Sousa, A. S.; Woods, M. *J. Am. Chem. Soc.* **1999**, *121*, 5762.

[55] Cossy, C.; Helm, L.; Merbach, A. E. *Inorg. Chem.* **1989**, *28*, 2699.

[56] André, J. P.; Maecke, H. R.; Tóth, E.; Merbach, A. E. *J. Biol. Inorg. Chem.* **1999**, *4*, 341.

[57] Aime, S.; Barge, A.; Borel, A.; Botta, M.; Chemerisov, S.; Merbach, A.; Mueller, U.; Pubanz, D. *Inorg. Chem.* **1997**, 36, 5104.

[58] Parker, D. *Chem. Soc. Rev.* **2004**, 33, 156.

[59] Aime, S.; Barge, A.; Batsanov, A. S.; Botta, M.; Delli Castelli, D.; Fedeli, F.; Mortillaro, A.; Parker, D.; Puschmann, H. *Chem. Commun.* **2002**, 1120.

[60] Taliaferro, C. H.; Motekaitis, R. J.; Martell, A. E. *Inorg. Chem.* **1984**, *23*, 1188.

[61] Woods, M.; Aime, S.; Botta, M.; Howard, J. A. K.; Moloney, J. M.; Navet, M.; Parker, D.; Port, M.; Rousseaux, O. *J. Am. Chem. Soc.* **2000**, *122*, 9781 – 9792.

[62] Tóth, E.; Pubanz, D.; Vauthey, S.; Helm, L.; Merbach, A. E.; *Chem. Eur. J.* **1996**, *2*, 1607.

[63] Corsi, D.M.; Van der Elst, L.; Muller, R.N.; Van Bekkun, H.; Peters, J. A.; *Chem. Eur. J.* **2001**, *7*, 64.

[64] Aime, S.; Botta, M.; Crich, S. G.; Giovenzana, G.; Palmisano, G.; Sisti, M.; *Bioconjugate Chem.* **1999**, *10*, 192.

[65] Thompson, N. C.; Parker, D.; Schmitt-Willich H.; Sülzle, D.; Muller, G.; Riehl, J. P. *Dalton Trans.* **2004**, *12*, 1892.

[66] Aime, S.; Barge, A.; Botta, M.; Terreno, E. *Metal Ions in Biological Systems*, ed. H. Sigel and A. Sigel, Marcel-Dekker, New York **2003**, *vol. 40*, 643.

[67] Aime, S.; Gianolio, E.; Terreno, E.; Giovenzana, G. B.; Pagliarin, R.; Sisti, M.; Palmisano, G.; Botta, M.; Lowe, M. P.; Parker, D. *J. Biol. Inorg. Chem.* **2000**, *5*, 488.

[68] Aime, S.; Gianolio, E.; Uggeri, F.; Tagliapietra, S.; Barge, A.; Cravotto, G. *J. Inorg. Biochem.* **2006**, *100*, 931.

[69] Thompson, N. C., PhD Thesis, University of Durham **2005**.

[70] Gianolio, E.; Giovenzana, G. B.; Longo, D.; Longo, I.; Menegotto, I.; Aime, S. *Chem. Eur. J.* **2007**, *13*, 5785.

[71] Aime, S.; Calabi, L.; Cavallotti, C.; Gianolio, E.; Giovenzana, G. B.; Losi, P.; Maiocchi, A.; Palmisano, G.; Sisti, M. *Inorg. Chem.* **2004**, *43*, 7588.

[72] Dunham, S. U.; Tyeklar, Z.; Midlefort, K. S.; McDermid, S. A.; McMurry, T. J.; Lauffer, R. B. COST D1 Meeting, The Hague **1996**.

[73] Aime, S.; Barge, A.; Borel, A.; Botta, M.; Chemerisov, S.; Merbach, A. E.; Muller, U.; Pubanz, D. *Inorg. Chem.* **1997**, *36*, 5104.

[74] Avedano, S.; Tei, L.; Lombardi, A.; Giovenzana, G. B.; Aime, S.; Longo, D.; Botta, M. *Chem. Commun.* **2007**, 4726.

[75] Ou, M. H.; Tu, C. H.; Tsai, S. C. ; Lee, W. T. ; Lin, G. C. ; Wang, Y. M. *Inorg. Chem.* **2006**, *45*, 244.

[76] Doble, D. M., J.; Botta, M.; Wang, J.; Aime, S.; Barge, A.; Raymond, K. N. *J. Am. Chem. Soc.* **2001**, *123*, 10758.

[77] Azegami, S.; Tsuboi, A.; Izumi, T.; Hirata, M.; Dubin, P. L.; Wang, B.; Kokufta, E.; *Langmuir* **1999**, *15*, 940.

[78] Newkome, G. R.; Moorefield, C. N.; Vögtle, F. "Dendrimers and Dendrons", VCH Verlagsgesellschaft, Weinheim, **2001**.

[79] Bosnan, A. W.; Janssen, H. M.; Meijer, E. W. *Chem. Rev.* **1999**, *99*, 1665.

[80] Mourey, T. H.; Turner, S. R.; Rubinstein, M.; Frechet, J. M. J.; Hawker, C. J.; Wooley, K. L. *Marcomolecules* **1992**, *25*, 2401.

[81] Buhleier, E.; Wehner, W.; Vogtle, F. *Synthesis* **1978**, 155.

[82] Tomalia, D.A.; Baker, H.; Dewald, J. R.; Hall, M.; Kallos, G.; Martin, S.; Roek, J.; Smith, P. *Polym. J. (Tokyo)* **1985**, *17*, 117.

[83] Tomalia, D.A.; Baker, H.; Dewald, J. R.; Hall, M.; Kallos, G.; Martin, S.; Roek, J.; Smith, P. *Macromolecules* **1986**, *19*, 2566.

[84] Newkome, G. R.; Yao, Z.; Baker, G. R.; Gupta, K. *J. Org. Chem.* **1985**, *50*, 2003.

[85] Hawker, C. J.; Frechet, J. M. J. *J. Am. Chem. Soc.* **1990**, *112*, 7638.

[86] Hawker, C. J.; Frechet, J. M. J. *J. Chem. Soc., Chem. Commun.* **1990**, 1010.

[87] Esfand, R.; Tomalia, D. A. *Drug. Discov. Today* **2001**, *6*, 427.

[88] Rudovský, J.; Hermann, P.; Botta, M.; Aime, S.; Lukeš, I. *Chem. Commun.* **2005**, 2390.

[89] Fulton, D. A.; O'Halloran, M.; Parker, D.; Senanayake, K.; Botta, M.; Aime, S. *Chem. Commun.* **2005**, *127*, 474.

[90] Van der Elst, L.; Port, M.; Raynal, I.; Simonot, C.; Muller, R.N. *Eur. J. Inorg. Chem.* **2003**, 2495.

[91] Bertini, I.; Galas, O.; Luchinat, C.; Parigi, G. *J. Magn. Reson.* **1995**, *113*, 151.

[92] Takahashi, M.; Hara, Y.; Aoshima, K.; Kurihara, H.; Oshikava, T.; Yamashita, H.; *Tetrahedron Lett.* **2000**, *41*, 8485.

[93] Pierre, V. C.; Botta, M.; Raymond, K. N. *J. Am. Chem. Soc.* **2005**, *127*, 504.

[94] André, J. P.; Geraldes, C. F. G. C.; Martins, J.A.; Merbach, A. E.; Prata, M. I. M.; Santos, A. C.; de Lima, J. J. P.; Tóth, E. *Chem. Eur. J.* **2004**, *10*, 5804.

[95] Nicolle, G.M.; Toth, E.; Schmitt-Willich, H.; Raduchel, B.; Merbach, A. E. *Chem. Eur. J.* **2002**, *8*, 1040.

[96] Jocher, C. J.; Botta, M.; Avedano, S.; Moore, E. G.; Xu, Jide; Aime, S.; Raymond, K. N. *Inorg. Chem.* **2007**, *46*, 4796.

[97] Aime, S.; Botta, M.; Geninatti Crich, S.; Giovenzana, G. B.; Pagliarin, R.; Sisti, M.; Terreno, E. *Magn. Reson. Chem.* **1998**, *36*, S200.

[98] Durbin, P. W.; Kullgren, B.; Xu, J.; Raymond, K. N. *Radiat. Prot. Dosim.* **1994**, *53*, 305.

[99] Xu, J.; Franklin, S. J.; Whisenhunt, Jr. D. W.; Raymond, K. N. *J. Am. Chem. Soc.* **1995**, *117*, 7245.

[100] Werner, E. J.; Avedano, S.; Botta, M.; Hay, B. P.; Moore, E. G.; Aime, S.; Raymond, K. N. *J. Am. Chem. Soc.* **2007**, *129*, 1870.

[101] Raymond, K. N.; Pierre, V. C. *Bioconjugate Chem.* **2005**, *16*, 3.

[102] Aime, S.; Botta, M.; Crich, S. G.; Giovenzana, G.; Pagliarin, R.; Sisti, M.; Terreno, E. *Magn. Reson. Chem.*, **1998**, *36*, S200.

[103] Sunderland, C. J.; Botta, M.; Aime, S.; Raymond, K. N. *Inorg. Chem.* **2001**, *40*, 6746.

[104] Doble, D. M. J.; Melchior, M.; O'Sullivan, B.; Siering, C.; Xu, J.; Pierre, V. C.; Raymond, K. N. *Inorg. Chem.* **2003**, *42*, 4930.

[105] Pierre, V. C.; Botta, M.; Aime, S.; Raymond, K. N. *Inorg. Chem.* **2006**, *45(20)*, 8355.

[106] Pierre, V. C.; Botta, M.; Aime, S.; Raymond, K. N. *J. Am. Chem. Soc.* **2006**, *128*, 9272.

[107] Ruloff, R.; Muller, R. N.; Pubanz, D.; Merbach A. E. *Inorg. Chim. Acta 275 – 276* **1998**, 15.

[108] Livramento, J. B.; Toth, E.; Sour, A.; Borel, A.; Merbach, A. E.; Ruloff, R. *Angew. Chem. Int. Ed.* **2005**, 44, 1480.

[109] Laus, S.; Ruloff, R.; Toth, E.; Merbach, A. E. *Chem. Eur. J.* **2003**, *9*, 3555.

[110] Aime, S.; Calabi, L.; Cavallotti, C.; Gianolio, E.; Giovenzana, G. B.; Losi, P.; Maiocchi, A.; Palmisano, G.; Sisti, M. *Inorg. Chem.* **2004**, *43*, 7588.

Chapter 2

Design and synthesis of new Gd^{III} dendrimer chelates

II.1 Design of new Gd^{III} dendrimer chelates

The design and synthesis of a new, medium molecular weight gadolinium dendrimer chelate will be described in this chapter. Field dependent relaxivities have been monitored and compared to the behaviour of structurally similar dendrimers, thereby exploring the potential application of such compounds as novel contrast agents for diagnostic MRI.

A tetra(carboxyethyl) DOTA derivative, the (*RRRR/SSSS*) diastereoisomer of the $[Gd(gDOTA)]^{5-}$ complex, was chosen to be the core of the molecular structures. It is a mono-aqua complex (q = 1) with a fast water exchange rate (τ_m = 68 ns at 298K, the fastest among the GdgDOTA diastereoisomers) [1] and possesses a high thermodynamic stability ($\log\beta_{110}$ = 24.03) [2] comparable to that of $[Gd(DOTA)]^-$ ($\log\beta_{110}$ = 25.58, 0.1M Me_4NCl, 25 °C). Moreover, it is kinetically inert with respect to Gd^{III} dissociation, consistent with a low *in vivo* toxicity. Structurally, the complex possesses four pendant carboxyl groups on the glutarate arms which allow further functionalisation via amide bond-forming reactions. Inspired by the work of Stoddart *et al.*[6] describing the convergent synthesis of carbohydrate dendrimers, the carbohydrate-containing dendrons illustrated in **Figure II.1.1** were chosen as substituents to be attached to the $[Gd(gDOTA)]^{5-}$ core.

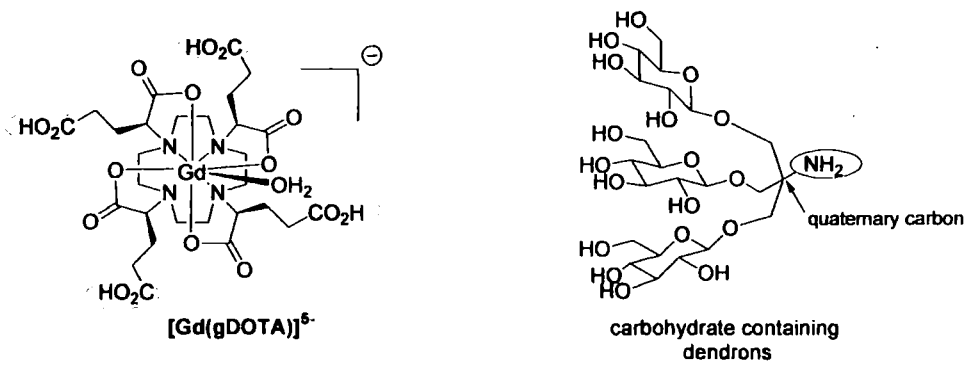

Figure II.1.1: Molecular structure of $[Gd(gDOTA)]^{5-}$ and dendrons. The reactive sites are depicted in yellow and red, respectively.

Symmetrical tetra-substitution is desirable, since it is considered important to maximise the electronic relaxation time and to ensure that the gadolinium ion lies at the barycentre of the macromolecular structure, allowing the gadolinium-water vector to be at the centre of any tumbling motion.[3] The numerous hydroxyl groups of the dendrons should guarantee the water solubility of the complex (an idea already considered in the past)[4, 5] and favour the formation of a well defined second sphere of hydration. The quaternary carbon within the carbohydrate dendrons also provides a high degree of structural rigidity, which should keep the motion of the gadolinium-core efficiently coupled to the rest of the macromolecule, as presented schematically in **Figure II.1.2**. The high molecular weight of the structure should be translated into a decrease of the molecular tumbling rate (*i.e.* an increase of the rotational correlation time, τ_R), with a consequent elevation of the overall relaxivity.

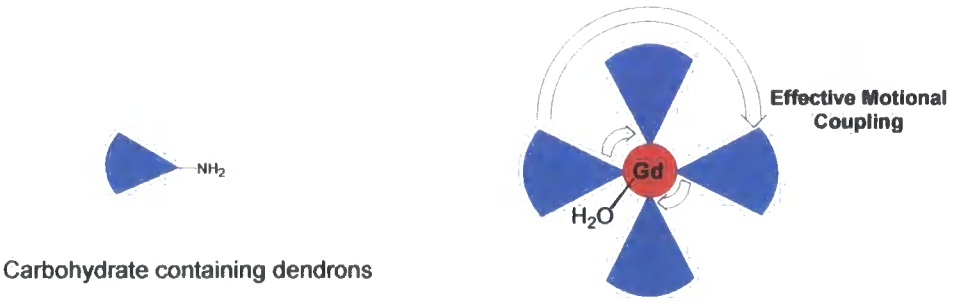

Figure II.1.2: Effective motional coupling of GdgDOTA-core to the all system.

Furthermore, as carbohydrates are involved in many biological recognition[6] processes, they could also promote the site-specific delivery of the contrast agent at a molecular level, for example targeting cell-surface lectins *e.g.* the asialoglycoprotein receptor found on the surface of mammalian hepatocytes.[7]

II.2 Convergent synthesis of carbohydrate containing dendrons

The target Gd^{III}-dendrimer chelates were assembled following a convergent growth approach: the triglucosylated dendrons of TRIS were synthesized rapidly and in reasonable quantities, and then conjugated to the $[Gd(gDOTA)]^{5-}$ core in the final step. Initial work focused on the carbohydrate dendron **6**,[8] which was envisioned as a useful intermediate in the synthesis not only of Gd^{III}-centered carbohydrate dendrimers, but also for other synthetic projects within our laboratory. In order to achieve a stereo-selective glycosylation of the hydroxyl groups of TRIS, its amino group was first protected as its benzyloxycarbonyl derivative (**Scheme II.2.1**) under Schotten-Baumann conditions.

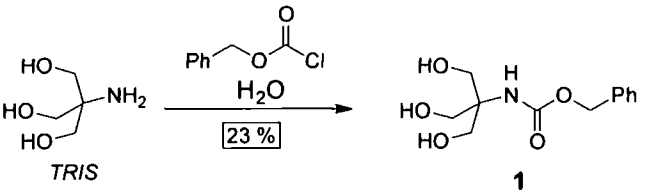

Scheme II.2.1: The preparation of an N-protected derivative of TRIS.

This protection was achieved by reacting TRIS with benzyloxycarbonyl chloride in water, where a slightly basic pH was maintained by addition of Na_2CO_3; although only a moderate yield was obtained under these conditions ample quantities of product could still be easily obtained. The product (**1**) was then glycosylated with 2,3,4,6–tetrabenzoyl-α-D-glucopyranosyl bromide (**3**), prepared in two steps from D-glucose (**Scheme II.2.2**).[9]

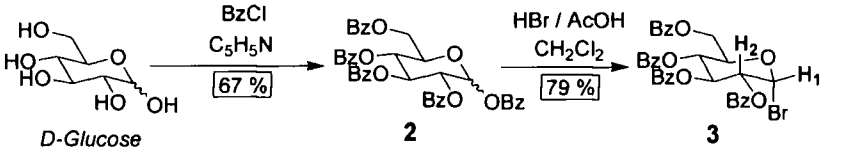

Scheme II.2.2: Synthesis of 2,3,4,6 –tetrabenzoyl-α D-glucopyranosyl bromide. [3]

The initial step involves the protection of the hydroxyl groups of D-glucose as their benzoate esters by addition of benzoyl chloride to a suspension of the sugar in pyridine, to afford the fully protected product as a mixture of α- and β–anomers. The pentabenzoate product was then dissolved in freshly distilled

CH_2Cl_2, and displacement of the benzoyl group in the α-position was performed by treatment with 33 % hydrogen bromide in acetic acid. Recrystallisation from diethyl ether and petroleum ether afforded **3** as a crystalline compound in good yield. ^{1}H NMR analysis (**Figure II.2.3**) showed a single anomeric signal at δ = 6.88 ppm with a coupling constant of 4 Hz. The magnitude of this coupling constant is consistent the presence of the α–anomer, an observation which can be rationalized by examination of the Newman projections of both the α- and β-anomers (**Figure II.2.4**). The equatorial position of H1 in the α-anomer makes possible only a partial overlap of its σ–orbital with the synclinal H2 (as shown in **Figure II.2.4a**). Consequently the corresponding signal in the ^{1}H NMR is a doublet with a small coupling constant J ~ 4 Hz, as predicted by the Karplus equation. The β-anomer displays an antiperiplanar relationship of H1 to H2 (**Figure II.2.4b**), resulting in greater overlap with the orbitals of H2, and a consequent increased J value of 12 Hz.

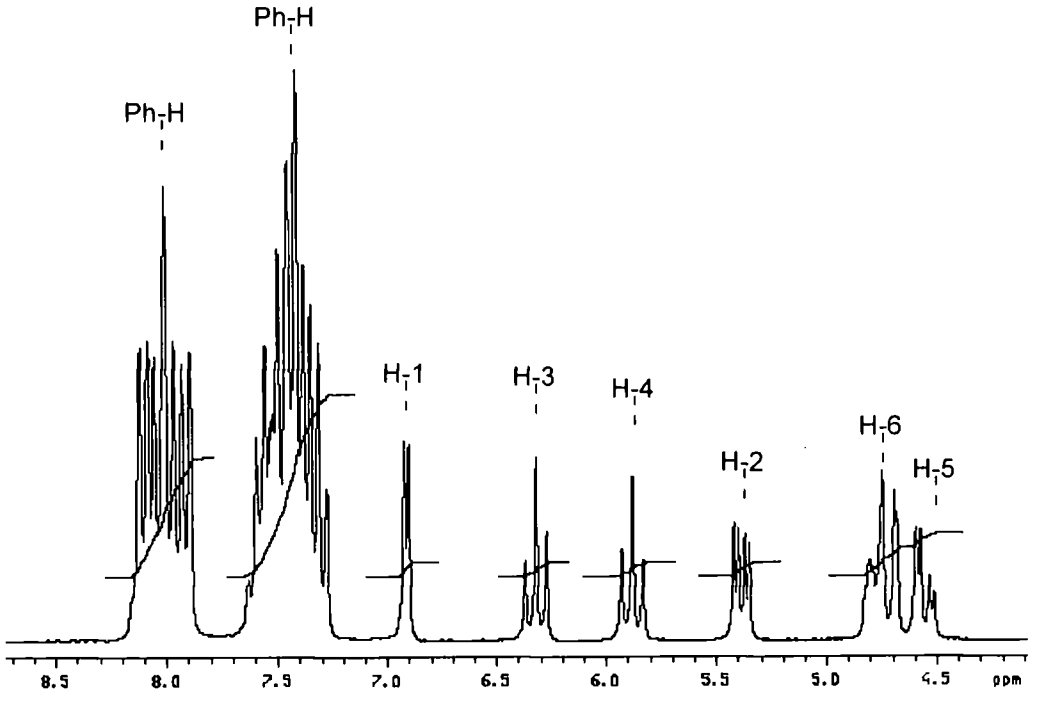

Figure II.2.3: ^{1}HNMR (300 MHz, $CDCl_3$) of 2,3,4,6 –tetrabenzoyl-α D-glucopyranosyl bromide.

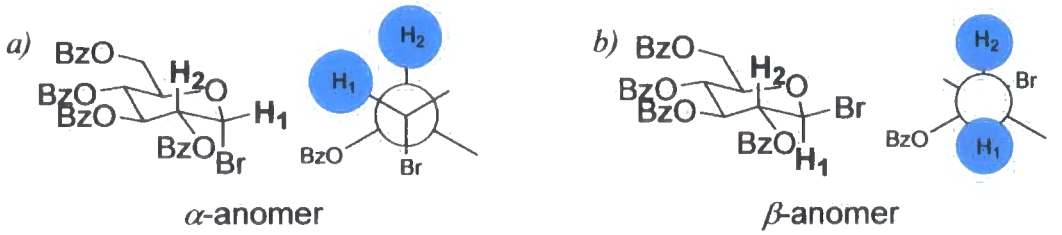

Figure II.2.4: Newman projections for α- and β-anomers of 2,3,4,6 –tetrabenzoyl-α D-glucopyranosyl bromide.

Glycosylation of **1** with 2,3,4,6–tetrabenzoyl-α-D-glucopyranosyl bromide **3** was accomplished in $CH_2Cl_2/MeNO_2$, using AgOTf as the promoter and 2,4,6-collidine as the base to afford the triglycosylated product **4** (**Scheme II.2.3**).

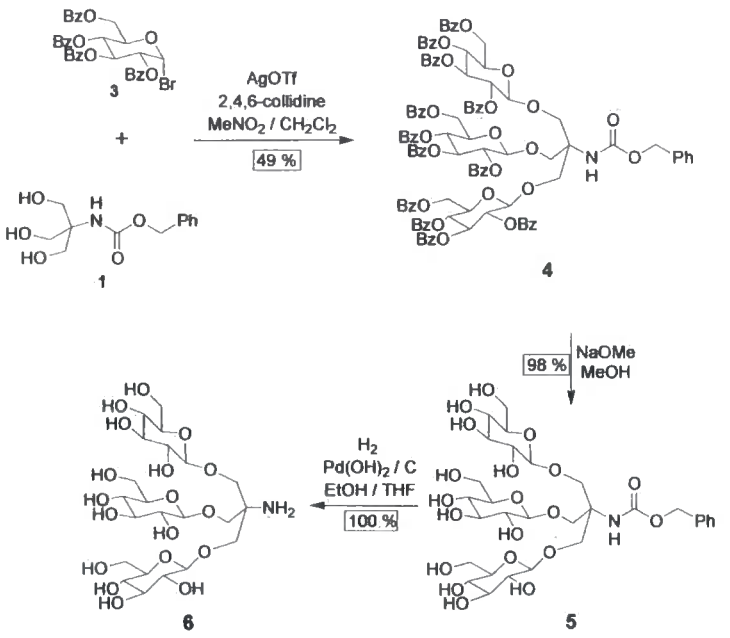

Scheme II.2.3: Synthesis of tris(β-D-glucopyranosyloxymethyl)-methylamine (6).

After purification of the crude product (**4**) by column chromatography, the initial yield was not very high, and the experimental conditions were modified carefully in order to optimize the overall reaction yield. Perfectly anhydrous conditions and an atmosphere of dry argon are strictly necessary for the synthesis of **4**, with the solution of 2,3,4,6–tetrabenzoyl-α-D-glucopyranosyl-bromide added over a period of 20 min. The temperature of the reaction mixture was required to be kept at

approximately -30°C, in order to avoid the formation of undesired side products such as hemiacetals or mixtures containing α-anomers. Evidence for the excellent anomeric selectivity of the reaction was obtained by ^{1}H NMR analysis of the product: each of the three simultaneous glycosylations afford β-glycosidic linkages only. A single anomeric signal integrating to three protons was observed as a doublet (J = 10.5 Hz) at δ = 4.3 ppm, indicating that each hydroxyl in **1** was glycosylated to form a β-linkage.

The deprotection of the hydroxyl groups was carried out using sodium methoxide in methanol, under Zemplén conditions. The reaction's progress was monitored by TLC (SiO_2) and, along with the desired product (**5**), methylbenzoate was detected as the side-product. Once completed, quenching of the reaction with Amberlite resin and subsequent filtration gave the pure glucopyranosyloxymethyl Cbz-protected amine. Hydrogenolysis over $Pd(OH)_2/C$ led to the final amine (**6**) in quantitative yield.

Other work within our laboratory, however, led to concerns about the low reactivity of this dendron's amino group. With the amino group at a quaternary centre, the nitrogen is a relatively poor nucleophile as a consequence of both steric hindrance and the unfavourable σ–polarization effect of the three β-oxygens.

Therefore, the coupling reaction between the carbohydrate wedges and the $[Gd(gDOTA)]^{5-}$ carboxylic acids (**Scheme II.2.4)** proved to be troublesome, with large amounts of the coupling agent HBTU and an excess of **6** needing to be added. [8]

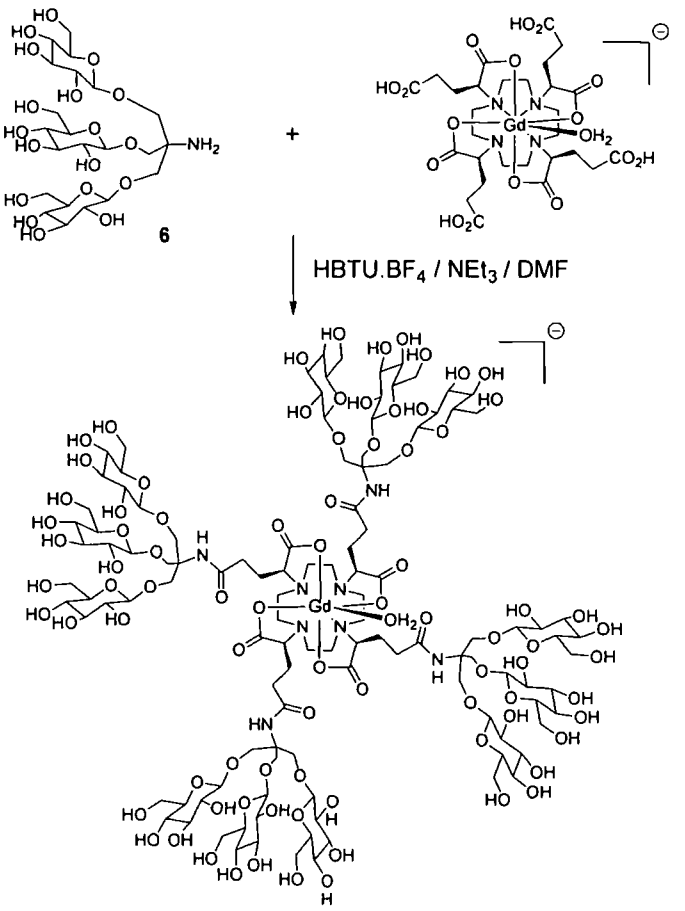

Scheme II.2.4. Synthesis of a tetra-amide $[Gd(gDOTA)]^{5-}$ complex, [10] prepared within our group.

The crude product obtained was identified by ES-MS as a mixture of the fully substituted tetraamide (major product), the under-substituted tri-amide and di-amide (minor products), and a lactone derived from the undesired competitive lactonization of a sugar hydroxyl by the fourth carboxyl group of the Gd^{III} complex. The most probable structure of this lactone sub-product is illustrated in **Figure II.2.5**.

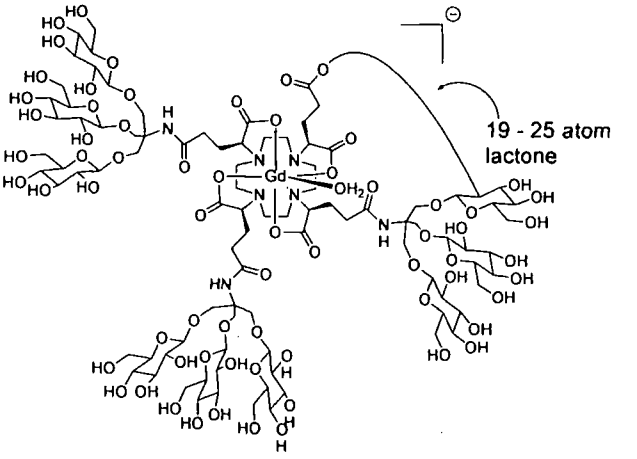

Figure II.2.5: Proposed structure of undesired lactone product.

It was therefore decided to prepare a modified carbohydrate wedge, containing a more reactive amino function. The incorporation of a glycine spacer onto the amino group of TRIS should result in a new wedge containing a more nucleophilic amino group, even though it probably enhances the local flexibility of the resulting dendritic structure. This idea had already been explored, [6] but the adopted synthetic strategy to obtain the glycine extended dendrons is different to that used in the Stoddart laboratories, where the glycine spacer was introduced directly on the primary amine of the derivative of **4** where the *N*-protecting group had been removed. The strategy adopted (**Scheme II.2.5**) was to form initially the amide bond between TRIS and carbobenzyloxyglycine to yield **7**, undertaken using the amide bond coupling reagents 1,3-dicyclohexylcarbodiimide (DCC) and 1-hydroxybenzotriazole (HOBT).

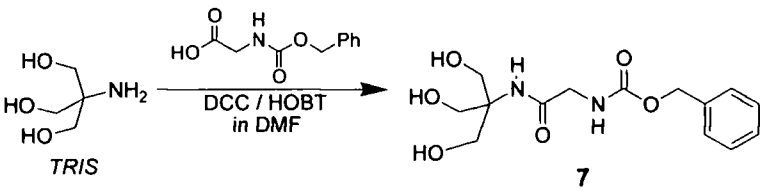

Scheme II.2.5: The synthesis of a glycine-extended derivative of TRIS.

Purification of the crude reaction mixture was performed by column chromatography, where polar solvent mixtures were needed for the elution of the pure *tris*-glycinamide compound **7**, which was obtained in 28% yield.

The procedure followed for the synthesis of the branched dendron (**10**), in **Scheme II.2.6**, was identical to that described for the synthesis of (**6**). It involved the stereoselective glycosylation of (**7**) with 2,3,4,6–tetrabenzoyl-α-D-glucopyranosyl bromide (**3**), deprotection of the hydroxyl groups using sodium methoxide in methanol and followed by hydrogenolysis over $Pd(OH)_2/C$ in order to remove the benzyloxycarbonyl protecting group to afford the product, **10**.

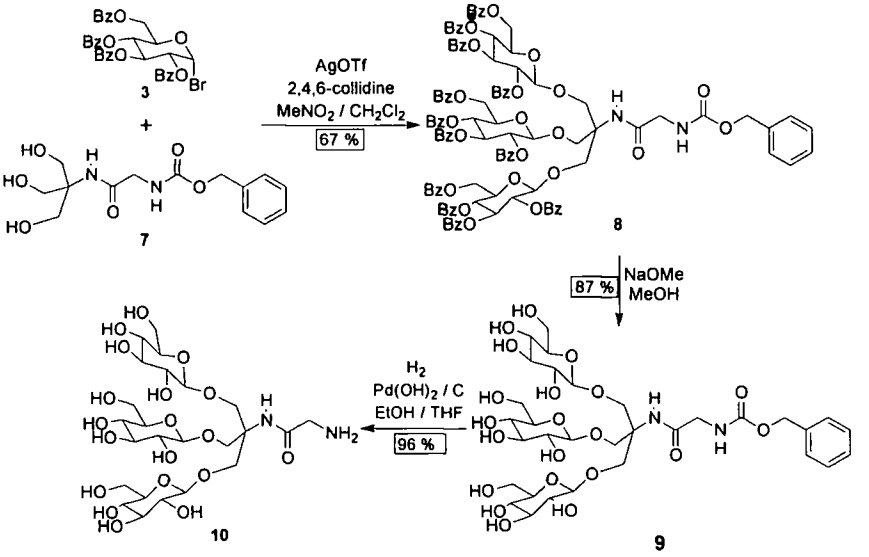

Scheme II.2.6: Synthesis of N-[tris(β-D-glucopyranosyloxymethyl)methyl]glycinamide10.

The glycosylation of the three primary hydroxyl groups of TRIS has already been investigated by other groups [6, 11, 12, 13] in the preparation of cluster glycosides and other glycoconjugates. The success of the reaction can be easily confirmed by ^1H NMR spectroscopy. In the spectrum of compound **8** (**Figure II.2.6**) the signal corresponding to the three equivalent CH_a α– to the quaternary carbon appears as a doublet (J = 10.2 Hz) at 3.50 ppm, equal to the coupling constant of the doublet at 4.24 ppm (J = 10.2), representing the three equivalent CH_b. Further evidence that the glycosylation leads selectively to β-substitution on the anomeric carbons, comes once again from the ^1H NMR spectrum, which displays a doublet ($^3J_{1,2}$ = 9.0 Hz) at 4.16 ppm corresponding to the three anomeric protons. The symmetry of this molecular structure is demonstrated by the fact that only 7 signals are present for the three carbohydrate units.

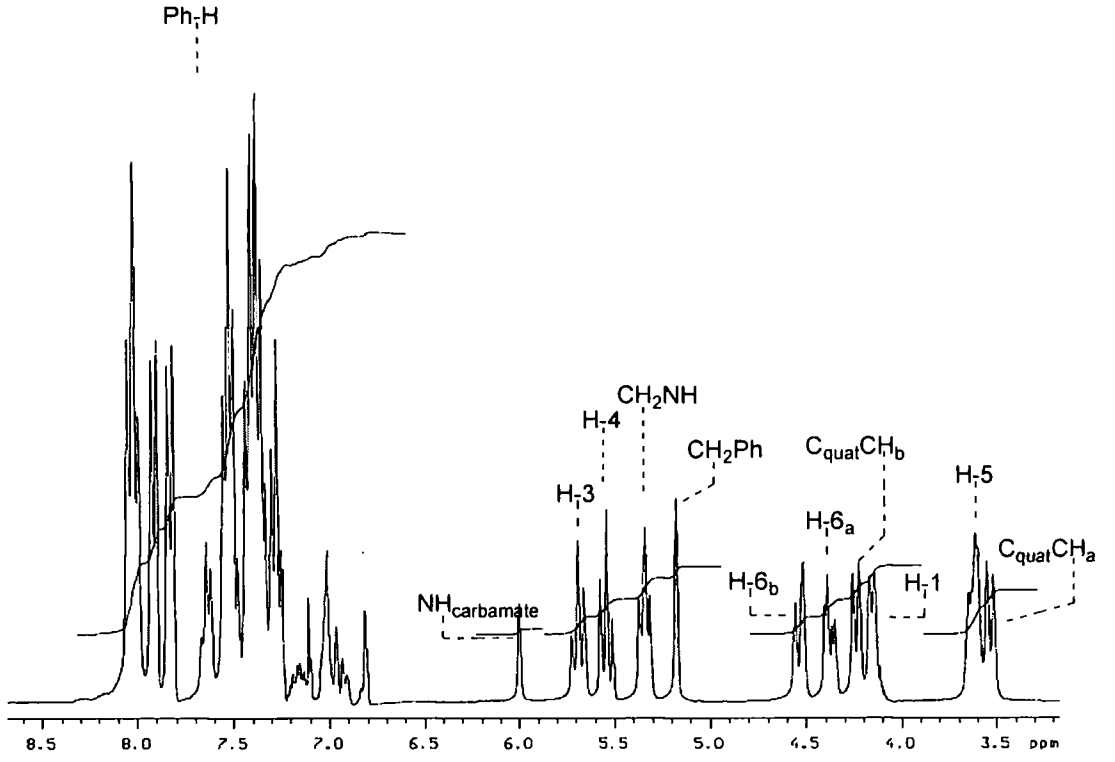

Figure II.2.6: ^{1}H NMR spectrum of the product of glycosylation, 8.

The following two deprotection steps were performed in the particular order illustrated in **Scheme II.2.6** because this sequence proved the most effective way to obtain the final triglycosylated amine product **10**, whose ^{1}H NMR spectrum is shown in **Figure II.2.7**.

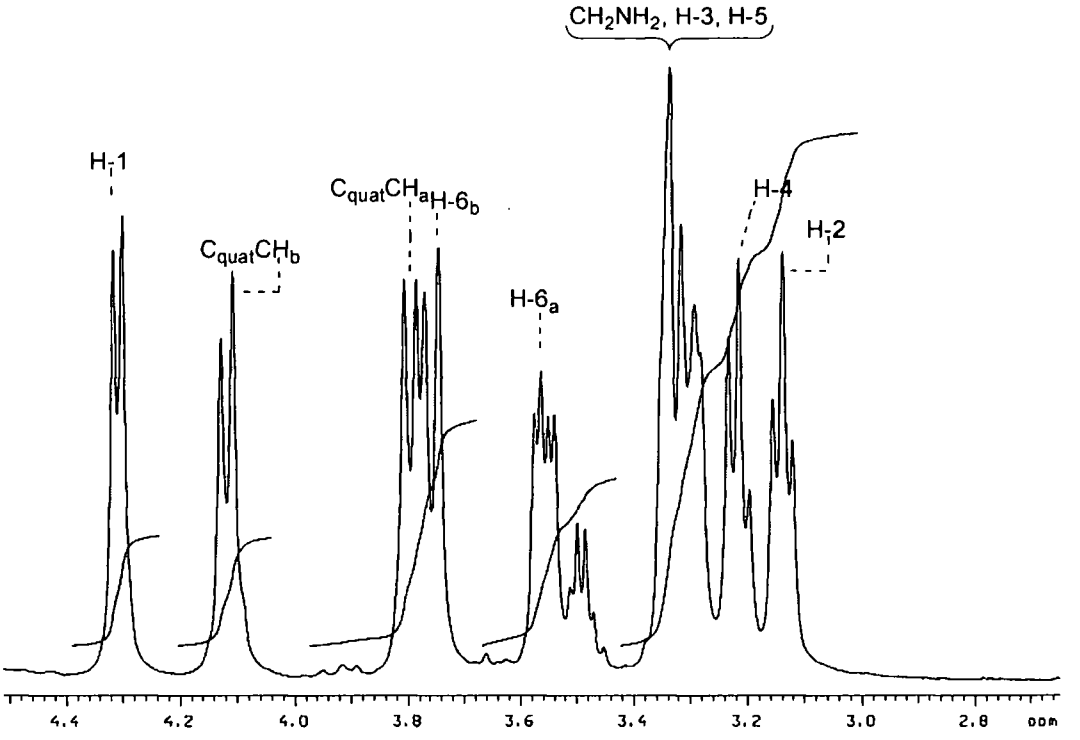

Figure II.2.7: ^{1}H NMR spectrum (300 MHz, D_2O) of the ligand structure.

The coupling reaction between the complex $[Gd(gDOTA)]^{5-}$ and the trisaccharide wedge (**10**) to obtain the final dendrimer (**Scheme II.2.7**) was performed in the polar aprotic solvent DMF, using *N*-methylmorpholine as the base and HBTU·BF_4 as the coupling agent. The solution was allowed to stir overnight under an atmosphere of dry argon and the crude product was identified by ES-MS as a mixture of the fully substituted tetraamide (major product), the under-substituted tri-amide and some di-amide (minor product). The lactonization observed in the previously described coupling of **6** to the $[GdgDOTA]^{5-}$ core did not occur to a significant extent, in this case. The mixture was purified by gel permeation chromatography (GPC) to afford the pure dendrimer, **11**.

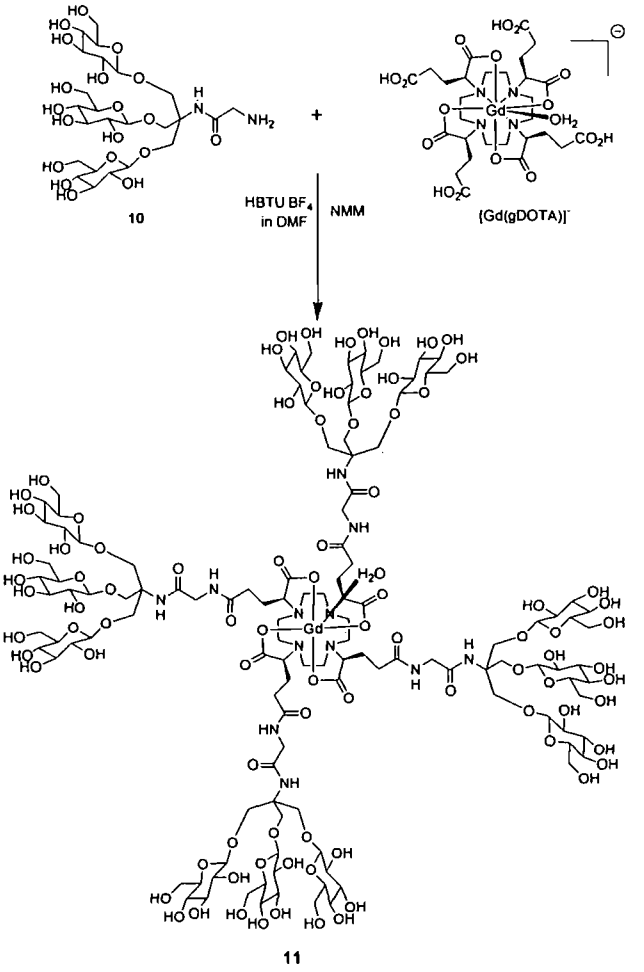

Scheme II.2.7: Preparation of the tetra-amide dendrimer.

Although this purification technique did not allow a complete separation of the desired tetra-substituted product from the lower mass under-substituted products, analysis of the GPC fractions by MALDI-TOF or electrospray mass spectrometry (ES-MS) ensured that only those fractions containing the desired tetra-substituted product were combined to afford the final sample. The exact molecular mass of the compound (MW 3448) was confirmed by ES-MS (the full spectrum is shown in the **Appendix**) and an expansion highlighting the isotopic pattern of the molecular ion $[M]^{3-}$ is shown in **Figure II.2.8**.

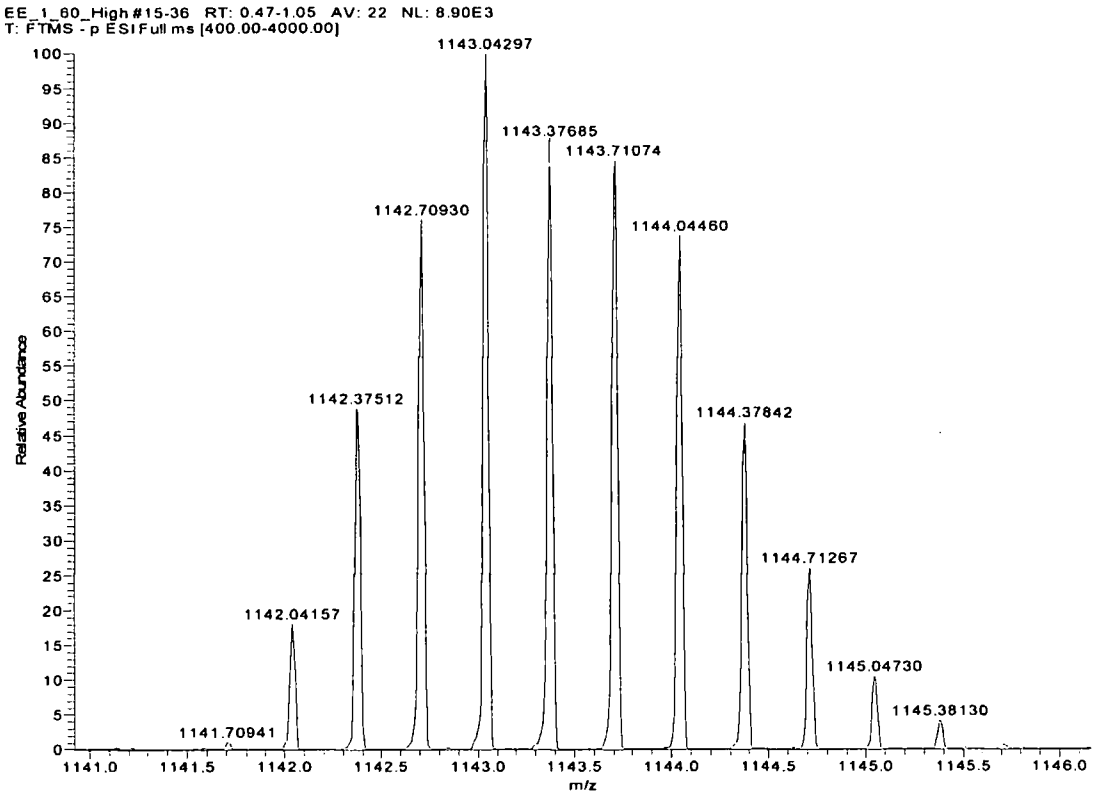

Figure II.2.8: Expansion of the electrospray mass-spectrum of the tetra-amide dendrimer, 11, highlighting the isotopic pattern of the molecular ion $[M]^{3-}$.

II.3 NMR studies

II.3.1 Determining τ_m: VT ^{17}O NMR R_{2p} analysis

The water exchange rate at the Gd^{III} centre of the $[GdgDOTAGlu_{12}Gly_4(H_2O)]^-$ dendrimer **11** was determined by a variable temperature (VT) ^{17}O NMR R_{2p} study. The profile obtained, showing the variation of T_2 with temperature at 2.1 T, is displayed in **Figure II.3.1.** The concentration of Gd^{III} in the sample, 3 mM, was determined by mineralization with 37% HCl at 120 °C overnight.

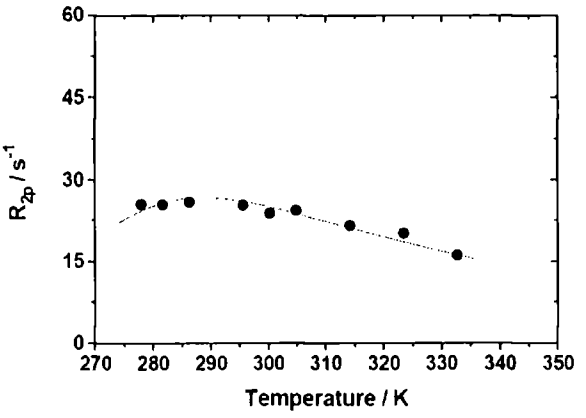

Figure II.3.1: VT ^{17}O NMR R_{2p} profile for tetra-amide dendrimer (11), $[Gd^{III}]$ = 3.0 mM.

The concave shape of this profile suggests a reasonably fast water exchange, which after curve fitting gave a value for τ_m = 221 ns. This value is close to that measured for the analogous complex without glycine spacer arms $[GdgDOTAGlu_{12}(H_2O)]^-$ (τ_m = 198 ns)[4] but it is twice as slow as in $[GdgDOTA\text{-}TRIS_4(H_2O)]^-$ (τ_m = 93 ns), [4] the structurally analogous complex, which lacks peripheral pyranose groups. The molecular structure and VT ^{17}O NMR R_{2p} profile of $[GdgDOTA\text{-}TRIS_4(H_2O)]^-$ is shown in **Figure II.3.2**, for purposes of comparison.

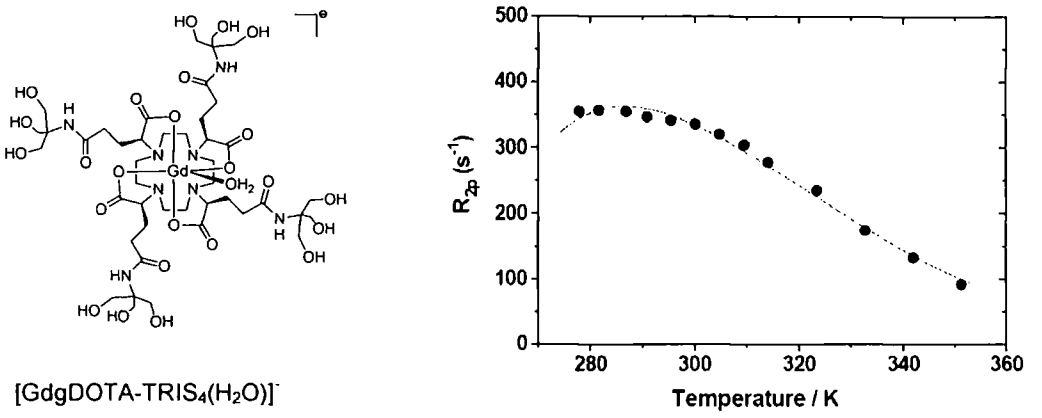

Figure II.3.2: *a)* **Molecular structure and** *b)* **VT ^{17}O NMR R_{2p} profile of [GdgDOTA-TRIS$_4$(H$_2$O)]$^-$, showing the fitted curve to the experimental data.**

It is possible that in the case of the complexes [GdgDOTAGlu$_{12}$Gly$_4$(H$_2$O)]$^-$, **11,** and [GdgDOTAGlu$_{12}$(H$_2$O)]$^-$ the introduction of the trisaccharide wedges allows greater interactions of the second sphere water molecules localized between the glucose groups and the metal centre. Although an overall relaxivity enhancement is in this way generated, the rate of exchange of the inner sphere water molecule with the bulk of the solvent can be limited.

Stronger evidence for a well defined second sphere network is given by the shape and analysis of the $1/T_1$ NMRD profiles of the complexes [GdgDOTAGlu$_{12}$Gly$_4$(H$_2$O)]$^-$ (**11**) and [GdgDOTAGlu$_{12}$(H$_2$O)]$^-$ over the frequency range 0.1 to 70 MHz (shown in **Figure II.3.3**, **II.3.4** and in the comparative **Figure II.3.5**).

II.3.2 $1/T_1$ NMRD studies

The proton relaxivities for the Gd^{III} glycoconjugate **11** were measured over the proton Larmor frequency range 0.01 to 70 MHz. In **Figure II.3.3** the nuclear magnetic relaxation dispersion profile of the tetra-amide dendrimer (**11**) at 25 °C is reported. The concentration of Gd^{III} in the sample was determined by ICP-mass spectrometry and also by mineralization with 37% HCl at 120 °C overnight; the relaxivity has been corrected for the diamagnetic contribution.

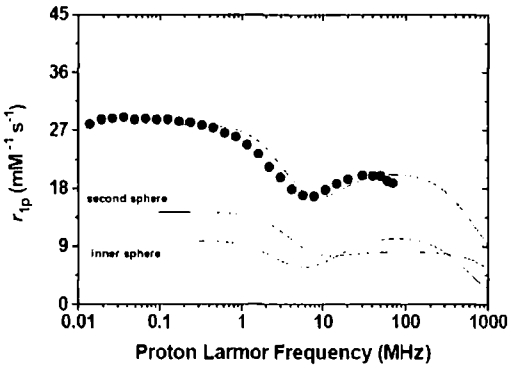

Figure II.3.3: $1/T_1$ **NMRD profile for tetra-amide dendrimer, 11. [Gd^{3+}] = 3 mM.**

The relaxivity value for this Gd^{III} complex at the temperature of 25 °C, pH 7, 20 MHz, is 19.6 mM^{-1} s^{-1}. The value increases in the higher field region of the $1/T_1$ NMRD profile (from approximately 5 to 70 MHz), a feature which suggests that the compound does possess a relatively slow rotational correlation time. By fitting the observed profile using standard methods,[14, 15, 16, 17, 18] the τ_R value was estimated to be 318 ns. From a comparison of the $1/T_1$ NMRD profiles of complex **11** and the structural analogue without glycine spacer arms (shown in **Figure II.3.4**), it can be deduced that both curves possess a similar overall form. However, the lower relaxivity exhibited by $[GdgDOTAGlu_{12}Gly_4(H_2O)]^-$ compared to $[GdgDOTAGlu_{12}(H_2O)]^-$ (23.5 $mM^{-1}s^{-1}$, at 25 °C, pH 7, 20 MHz), notwithstanding its higher molecular weight (3448 g/mol and 3220 g/mol, respectively), suggests that the extra flexibility imparted to the complex by the glycine spacers reduces the efficiency of motional coupling, with a consequent detrimental effect on the overall relaxivity.

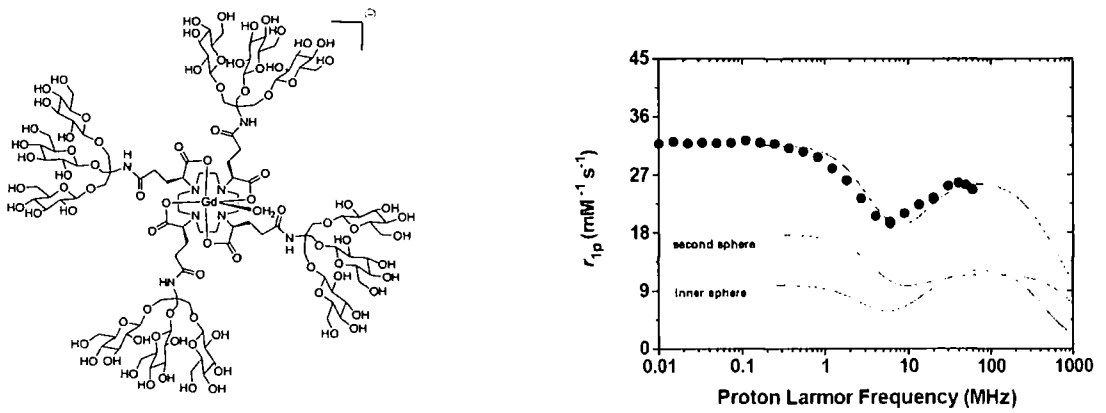

Figure II.3.4: *a)* **Molecular structure and** *b)* $1/T_1$ **NMRD profile for the complex** $[GdgDOTAGlu_{12}(H_2O)]^-$ **(298 K).**

Fitting of the NMRD profiles was undertaken by Prof. Mauro Botta (University of the Oriental Piedmont "Amedeo Avogadro" -Italy-) to define the contributions given to the overall relaxivity separately by the inner, second and outer sphere water molecules. The predominant second sphere contribution is evident in the systems where the carbohydrate wedges have been attached, as shown in **Figure II.3.5**.

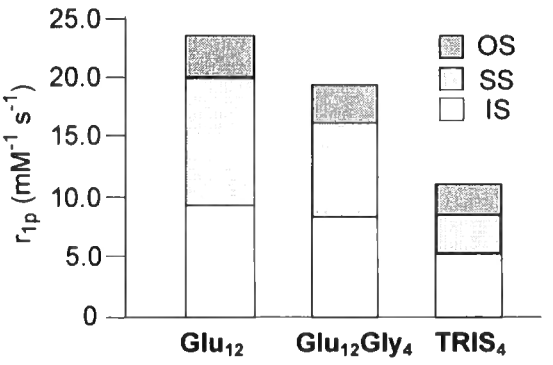

Figure II.3.5: Relative contributions to the relaxivity for $[GdgDOTAGlu_{12}(H_2O)]^-$, ($Glu_{12}$), $[GdgDOTAGlu_{12}Gly_4(H_2O)]^-$, ($Glu_{12}Gly_4$), $[GdgDOTA\text{-}TRIS_4(H_2O)]^-$, ($TRIS_4$).

In **Table II.3.1**, some of the relaxation parameters assessed from ^{17}O NMR and by the iterative fitting of the ^1H NMRD profiles are reported. The values relative to complex **11,** $[GdgDOTAGlu_{12}Gly_4(H_2O)]^-$, are compared to those found for other GdgDOTA based dendrimers and for the core structure itself.

Chemical Name	MW (g mol^{-1})	r_{1p} ($mM^{-1}s^{-1}$, 20 MHz, 25 °C)	τ_V (ps)	τ_R (ps)	τ_m (ns)
$[GdgDOTA(H_2O)]^{5-}$	860	7.1	10.0	94	68
$[GdgDOTAGlu_{12}(H_2O)]^-$	3220	23.5	20.0	390	198
$[GdgDOTAGlu_{12}Gly_4(H_2O)]^-$	3448	19.6	20.1	318	221
$[GdgDOTA\text{-}TRIS_4(H_2O)]^-$	1267	11.3	13.0	173	93

Table II.3.1: Relaxation parameters for $[GdgDOTAGlu_{12}Gly_4(H_2O)]^-$, GdgDOTA and other DOTA based dendrimers synthesiszed in our laboratoty.

It is very clear that there is an enhancement of τ_R following the increase of the structures molecular weight and hence molecular volume. The slow molecular

tumbling obtained with the $[GdgDOTAGlu_{12}(H_2O)]^-$ complex is the result of the structural rigidity and compactness of this system, where the local motion of the Gd^{III}-water vector resides close to any axis of reorientational motion and is effectively coupled to the overall tumbling motion of the whole complex.

In the case of $[GdgDOTAGlu_{12}Gly_4(H_2O)]^-$, the glycine spacers have been introduced to increase the reactivity of the carbohydrate-containing dendrons reactive amine, making their conjugation to $[GdgDOTA(H_2O)]^{5-}$ easier. They have also enhanced the conformational freedom of the system, to such an extent that the compact molecular tumbling is limited.

II.4 Relaxivity dependence on pH variation and enzyme activity

Before exploring the *in vivo* behaviour of the gl ycoconjugates of gadolinium complexes, the stability of their *O*-glycoside bonds under physiological conditions was investigated since there is evidence that glycopyranosides can be susceptible to acid- or enzymatically catalyzed hydrolysis.[19, 20]

A simple NMR procedure has been used to estimate the kinetic stability of the gadolinium chelates under acidic conditions. The variation in the relaxivities of the gadolinium conjugates, at various pH values, were estimated over a period of at least 72 h. The measurement of the T_1 values was undertaken at 60 MHz, 25 °C for the following solutions at known Gd^{III} concentrations (measured by inductively coupled plasma mass spectrometry):

- aqueous $[GdgDOTAGlu_{12}(H_2O)]^-$ solution in the pH range from 10 to 2;
- aqueous $[GdgDOTAGlu_{12}Gly_4(H_2O)]^-$ solution in the pH range from 10 to 2;
- $[GdgDOTAGlu_{12}(H_2O)]^-$ in ammonium acetate buffer (pH 5.08) / human serum albumin solution (1:1).

No changes in the T_1 value were registered in any of the reported solutions either at neutral or slightly acidic pH, even over a period of 96 h; only at pH ~ 3.5 did the T_1 value drop slightly (from 230 ms at pH 4 to 215 ms at pH 3.5), suggesting some decomposition of the complex, such as cleavage of the glycosidic bonds.

Also, the presence in solution of components found in blood plasma could result in a significant change in the gadolinium chelate efficacy: enzymes, such as the glycoside hydrolases (or glycosidases) can, for example, break the glycosidic bonds (i.e. catalyze their hydrolysis). These enzymes are located in the lysosomes, where most glycoconjugates are degraded, and present their maximum activity in acidic environment (between pH 4.0 and 5.5). [21, 22]

Based upon these considerations, it seemed appropriate to test the stability of the dendrimers in the presence of selected enzyme. No changes in the T_1 observed were registered upon titration of the $[GdgDOTAGlu_{12}(H_2O)]^-$, $[GdgDOTAGlu_{12}Gly_4(H_2O)]^-$ and $[GdgDOTAGal_{12}Gly_4(H_2O)]^-$ ammonium acetate buffer (pH 5.08) solutions with β–glucosidase (from almonds) and β–galactosidase, respectively, even when the concentration of the added enzyme was half that of the paramagnetic chelate (**Figure II.4.1**).

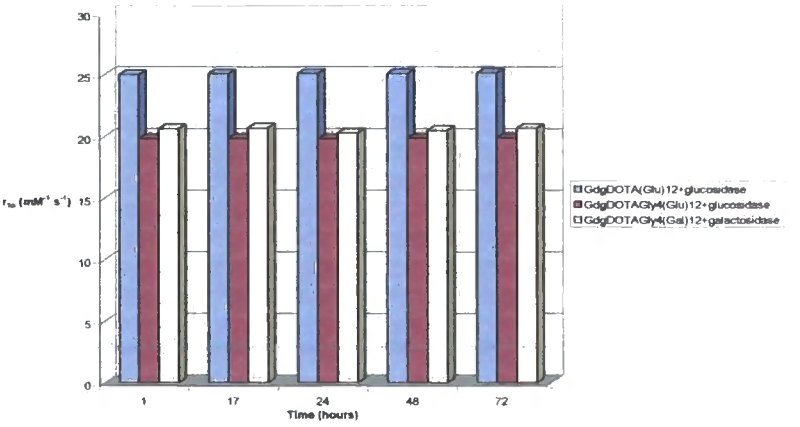

Figure II.4.1: Variation of T_1 relaxivity (60 MHz, 37 °C) with time for:

- $[GdgDOTAGlu_{12}(H_2O)]^-$: $[Gd^{3+}]$ 0.105 mM + 3.5 mM β-glucosidase solution
- $[GdgDOTAGlu_{12}Gly_4(H_2O)]^-$: $[Gd^{3+}]$ 0.12 mM + 4 mM β-glucosidase solution
- $[GdgDOTAGal_{12}Gly_4(H_2O)]^-$: $[Gd^{3+}]$ 0.12 mM + 3 mM β-galactosidase solution

As a control, the previously described tests to verify the stability of the compounds upon pH variation and enzyme activity, were repeated for the individual trisaccaride wedges. The experiments were monitored by ES-MS and ^{1}H-NMR, and once again only under very acidic ($\leq$ pH 3.5) environmental conditions was any cleavage of the glycosidic bonds evident. Summarizing, the glycoconjugates appear to be stable in dilute acid solutions and to glucosidase enzymes.

II.5 *In vivo* studies

The *in vivo* behaviour of $[GdgDOTAGlu_{12}Gly_4(H_2O)]^-$ and of $[GdgDOTAGlu_{12}(H_2O)]^-$ was examined by our collaborators in Italy (Bracco Imaging S.p.A and University of Torino), and their performance compared to the clinically used complex Pro-Hance. $[GdgDOTAGlu_{12}(H_2O)]^-$ was administered in a dose equal to 0.1 μmol/g to a female mouse over-expressing the transforming activated rat HER-2/neu oncogene under the control of the mouse mammary tumour virus promoter. The contrast agent induced a 50 - 60% enhancement in the MRI signal, and the signal enhancement was maintained over a post-injection period of time between 5 and 45 minutes. The $[GdgDOTAGlu_{12}(H_2O)]^-$ caused a signal intensity enhancement that lasted longer than that created by Prohance, whose efficiency had decayed below 20%, 35 minutes after the injection. A similar profile was exhibited by the glycine spacer analogue complex $[GdgDOTAGlu_{12}Gly_4(H_2O)]^-$. Both Gd^{III} dendrimer chelates were excreted mainly via the renal system, with little or no evidence for clearance or retention in the liver.

The first row of **Figure II.5.1** shows five scans of mouse kidneys without contrast agents, over 12 minute intervals up to 1h. In the second row, the excretion of Prohance through the kidneys is monitored over the same period of time and compared with the glucose dendrimer $[GdgDOTAGlu_{12}(H_2O)]^-$, in the third row.

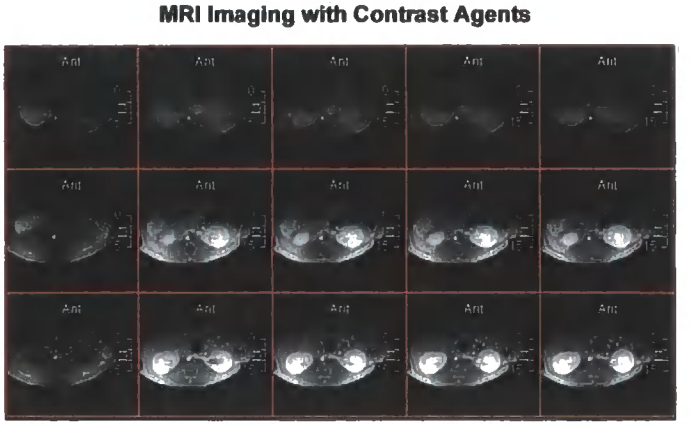

Figure II.5.1: MRI images (12, 24, 36, 48, 60 minutes) of mouse kidneys without CA (upper), with Prohance (centre) and with $[GdgDOTAGlu_{12}(H_2O)]^-$ (lower).

II.6 Conclusions

A new medium molecular weight contrast agent with carbohydrate-containing dendrons attached to a $[Gd(gDOTA)]^{5-}$ core has been synthesized and its magnetic properties carefully evaluated and compared to the behaviour of similar gadolinium dendrimer chelates, also synthesized in Durham. The second sphere contribution has once again [23, 24] played a critical role in determining the overall relaxivity enhancement. In the design of new dendritic systems, the carbohydrate containing dendrons should be conserved, while the glycine spacers need to be replaced with more rigid moieties. Dendrons containing more reactive hydrazide functions, for example, could be prepared (**Figure II.6.1**). They should contain suitably reactive amino functions without increasing significantly the overall flexibility of the target dendrimers.

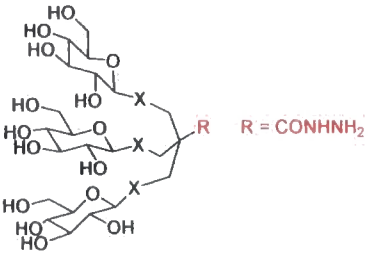

Figure II.6.1: example of a more rigid spacer arm.

With this aim in mind, a new carbazate derivative has been synthesized and the reactivity of its two carboxylic groups towards amide coupling tested in an attempt reaction coupling to TRIS, as shown in **Scheme II.6.1**.

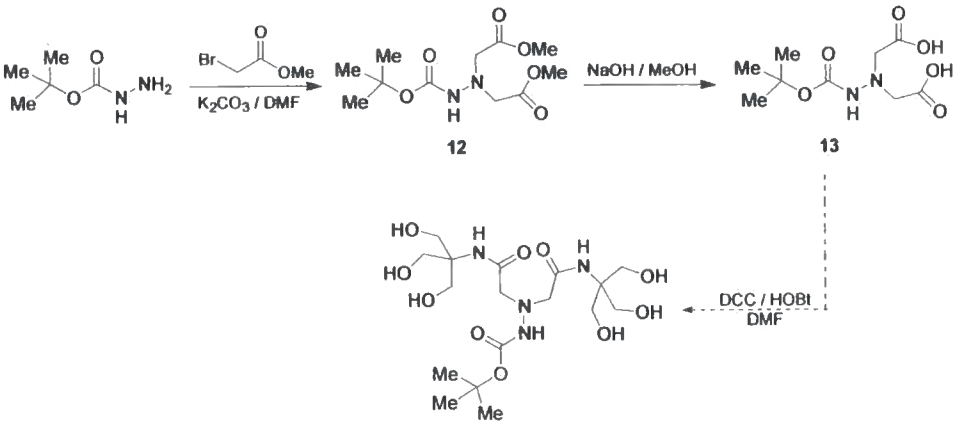

Scheme II.6.1: Synthesis of dicarboxycarbazate 13.

While the synthesis of the diacid **13** proceeded well, problems were encountered in the final coupling reaction, and the target molecule was not obtained. However, this idea is further developed in a parallel project in Durham.

Furthermore, instead of $[Gd(gDOTA)]^{5-}$, alternative Gd^{III}-complexes, possessing even faster water exchange rate could be placed as a core element for the Gd^{III}-dendritic complexes. A suitable example could be the 6-amino-6-methylperhydro-1,4-diazepine (AMPED) structure, which has already been studied as the core structure for the lanthanide chelates discussed in **Chapter III** of this thesis.

References

[1] Woods, M.; Aime, S. ; Botta, M.; Howard, J. A. K.; Moloney, J. M.; Navet, M.; Parker, D.; Port, M.; Rousseaux, O. *J. Am. Chem. Soc.*, **2000**, *122*, 9781 – 9792.

[2] Moreau, J.; Guillon, E.; Aplincourt, P.; Pierrard, J.-C.; Rimbault, J.; Port, M.; Aplincourt M. *Eur. J. Inorg. Chem.*, **2003**, 3007.

[3] Fulton, D. A.; O'Halloran, M.; Parker, D.; Senanayake, K.; Botta, M.; Aime, S. *Chem. Commun.* **2005**, 474.

[4] Caravan, P.; Ellison, J. J.; McMurry, T. J. ; Lauffer, R. B. *Chem. Rev.* **1999**, *99*, 2293.

[5] Parker, D.; Dickins, R. S.; Puschmann, H.; Crossland, C.; Howard, J. A. K. *Chem. Rev.* **2002**, *102*, 1977.

[6] (a) Lis, H.; Sharon, N. *Chem. Rev.* **1998**, *98*, 637 – 674. (b) Lis, H.; Sharon, N. *Glycobiology* **2004**, *14*, 53R-62R.

[7] Weigel, P. H.; Yik, J. H. N. *Biochim. Biophys. Acta (General Subjects)* **2002**, *1572*, 341.

[8] Ashton, P. R.; Boyd, S. E., Brown, C. L.; Jayaraman, N.; Nepogodiev, S. A.; Stoddart, J. F. *Chem. Eur. J.* **1996**, *2*, 1115.

[9] Lichtenthaler, F. W.; Kaji, E.; Weprek, S. *J. Org. Chem.* **1985**, *50*, 3505.

[10] Fulton, D. A.; Elemento, E. M.; Aime, S.; Chaabane, L.; Botta, M.; Parker, D. *Chem. Commun.* **2006**, 1064.

[11] Pucci, B.; Polidori, A.; Rakotomanomana, N.; Chorro, M; Pavia, A. A. *Tetrahedron Lett.* **1993**, *34*, 4185 – 4188.

[12] Kempeo, H. J. M.; Hoes, C.; van Boom, J. H. ; Spanjer, H. H.; de Lange, J.; Langendoen, J. A.; van Berkel, T. J. C. *J. Med. Chem.* **1984**, *27*, 1306 - 1312.

[13] Biessen, E. A. L.; Beuting, D. M.; Roelen, H, C. P. F.; G. **A.** van de Marel, van Boom, J. H.; van Berkelf, T. J. C. *J. Med. Chem.* **1995**, *38*, 1538 - 1546.

[14] Koenig, S. H. *J. Magn. Res.* **1978**, *31*, 1.

[15] Powell, H. D.; Ni Dhubhghaill, O. M.; Pubanz, D.; Helm, L.; Lebedev, Y.; Schlaepfer, W.; Merbach, A. E. *J. Am. Chem. Soc.* **1996**, *118*, 9333.

[16] Tóth, É.; Helm, L.; Merbach, A. E.; Hedinger, R.; Hegetschweiler, K.; Jánossy, A. *Inorg. Chem.* **1998**, *37*, 4104.

[17] Tóth, É.; Connac, F.; Helm, L.; Adzamli, K.; Merbach, A. E. *Eur. J. Inorg. Chem.* **1998**, 2017.

[18] Tóth, É.; van Uffelen, I.; Helm, L.; Merbach, A. E.; Ladd, D.; Briley-Saebo, K.; Kellar, K. E. *Magn. Res. Chem.* **1998**, *36*, S200.

[19] Capon, B. *Chem. Rev.* **1969**, *69 (4)*, 407-498.

[20] Bochkov, A. F.; Zaikov, G. E. *Chemistry of the O-Glycosidic Bond: Formation & Cleavage*, Pergamon Press: Oxford, **1979**.

[21] Varki, A. *et al.* Essentials of Glycobiology. Cold Spring Harbor Laboratory Press; **1999**.

[22] Duimstra, J. A.; Femia, F. J.; Meade, T. J. *J. Am. Chem. Soc.* **2005**, *127*, 12847 – 12855.

[23] Messeri, D.; Lowe, M. P.; Parker, D.; Botta, M. *Chem. Commun.* **2001**, 2742.

[24] Parker, D.; Dickins, R.; Puschmann, H.; Crossland, C.; Howard, J. A. K. *Chem. Rev.* **2002**, *102*, 1977 – 2010.

Chapter 3

New Ligands for $q = 2$ systems

III.1 New ligands for *q* = 2 systems

At the outset of this project, the synthesis of diaqua Gd^{III} complexes was already being pursued in our laboratory. As already mentioned above (**Introduction Section II.2** and **Section V**), an increase in the hydration around the metal centre can significantly enhance the contrast agent efficacy. Diaqua systems can be prepared by reducing the denticity of the core ligand structure, although the complex stability can in this way be compromised. Indeed, the use of heptadentate ligands can reduce the kinetic and thermodynamic stability of the gadolinium chelate with respect to cation mediated or acid catalyzed dissociation, or favour the interaction with endogenous anions or protein coordinating groups present in human serum[1] resulting in a displacement of inner sphere water molecule(s).[2, 3] Based upon the same principle that inspired the previous work realized in our laboratory with $[GdaDO3A]^{3-}$,[4] where the anionic side chains electrostatically inhibit encounter of the complex with negatively charged species (such as protein and endogenous anions), are the two ideas of synthesising a $[GdaDO3AP]^{3-}$ phosphonate, analogous to the $[GdaDO3A]^{3-}$ complex (**Figure III.1**, ***a***),[5] and $[Gd(aDO3Aasp)(H_2O)_2]^{3-}$, given by the incorporation onto the DO3A core of amino acid side arms, based on *N*-Boc-aspartic acid-benzyl ester (**Figure III.1**, ***b***). Both compounds were designed to bind non-covalently to serum albumin proteins: the overall relaxivity of the system should be enhanced by its slower tumbling motion.

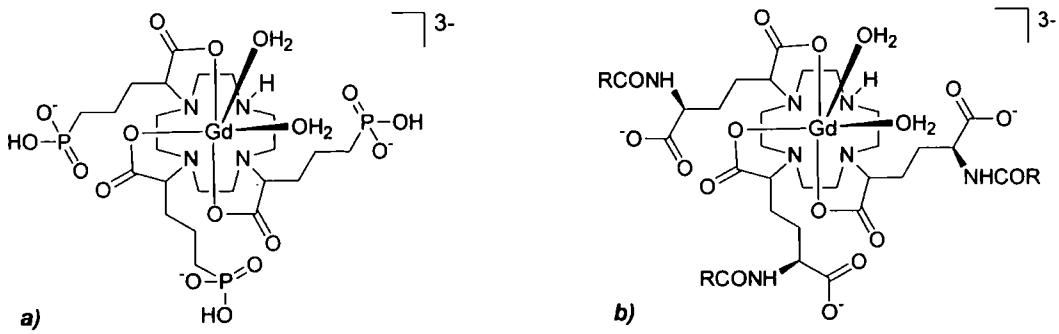

Figure III.1: ***a)*** **Molecular structure of $[Gd(aDO3AP)(H_2O)_2]^{3-}$ and** ***b)*** **of $[Gd(aDO3Aasp)(H_2O)_2]^{3-}$.**

Further work focused on the synthesis of new $q = 2$ systems built upon a different core ligand structure: the triamino 6-amino-6-methyl-perhydro-1,4-diazepin (AMPED). This compound is readily prepared from low-cost starting materials in a synthesis that proceeds in two steps in near quantitative yield. [6] The synthesis of AMPED, illustrated in **Scheme III.1**, was performed starting from the reaction of *N,N'*-dibenzyl-ethylenediamine with *para*-formaldehyde, and successive reaction of the intermediate Schiff base with deprotonated nitroethane. The deprotection of the amino groups and the reduction of the nitro group was achieved by hydrogenolysis. This seven ring heterocycle possesses two differently reactive amino groups (primary and secondary), which can be used for further functionalisation *e.g.* introduction of pendant arms by alkylation. The alkylation of each of the nitrogen atoms was undertaken with *tert*-butylbromoacetate in the presence of potassium carbonate, followed by treatment with trifluoroacetic acid, yielding 6-amino-6-methylperhydro-1,4-diazepinetetraacetic acid, AAZTA. This ligand was complexed in the presence of stoichiometric amounts of $Ln^{(III)}$ trichlorides ($EuCl_3$ or $GdCl_3$).

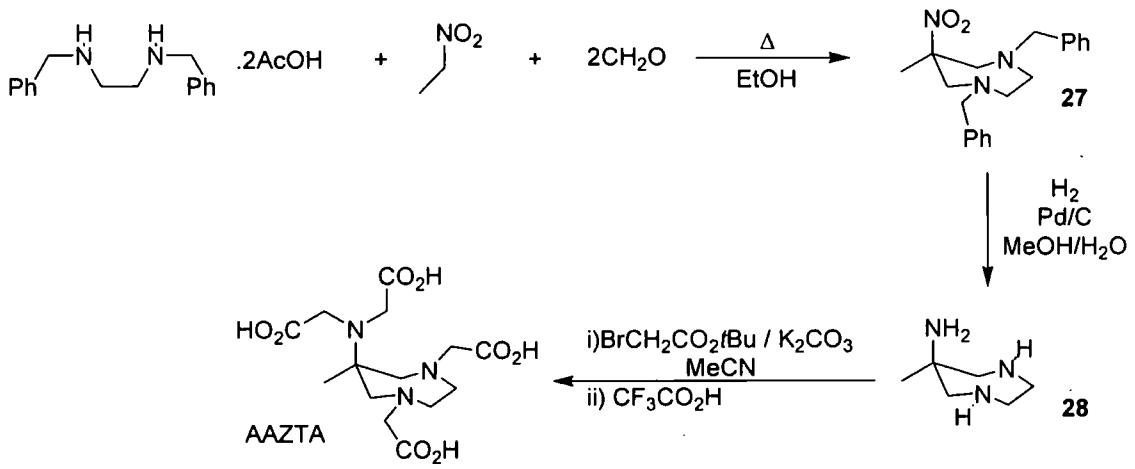

Scheme III.1: Preparation of the core of the complex (AMPED).

The [Gd-AAZTA]$^-$ complex is reported [7] to show promising relaxometric properties, a favourable kinetic inertness profile (the r_{1p} value 7.1 $mM^{-1}s^{-1}$ at 20 MHz, 298 K was

maintained over the pH range 2 - 11) and a thermodynamic stability comparable to that of $[Gd\text{-}DTPA]^{2-}$. It exhibits a remarkable inertness towards endogenous anion binding: [7] no changes in the relaxivity values (*i.e.* no replacement of the coordinated water molecules) were registered during titration in the presence of lactate or phosphate at concentrations even 200 times higher than the gadolinium chelate. Furthermore, the fitting of the data [8] obtained by measuring ^{17}O NMR R_{2p} as function of temperature allowed the estimation of a τ_m^{298} value of 90 ns. The exceptionally good magnetic properties and the stability shown by this new AMPED-based gadolinium chelate encouraged further studies. In association with Bracco Imaging S.p.A. (Italy), the design and synthesis of new systems was planned.

Phosphine and phosphonate based structures were envisaged as new pendant arms for the core ring strucure AMPED, to explore the different reactivity of phosphinate (eg. ***a)*** and ***b)*** in **Figure III.2**) analogues of the previously mentioned carboxylate AAZTA complexes.

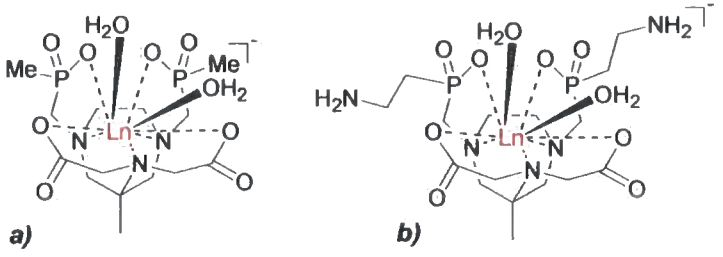

Figure III.2: Target Phosphinate (*a*) and (*b*) AMPED based strutures.

However, the original structure bearing carboxylate pendant arms was not abandoned: suitable 1,5-dicarboxylate pendant arms (**Scheme III.2**) were also synthesized and attached to the core ring (this work will be discussed in detail in **Chapter 4**). Different diastereomeric structures were considered and their magnetic properties determined separately. It was surmised, at the outset, that as in the case of GdgDOTA,[9] an isomer possessing faster water exchange rate (τ_m) may be isolated. Furthermore, the complexes obtained were adorned with glycosidic wedges, with the

aim of increasing the molecular volume of the system, and hence increasing the relaxivity by slowing down the overall molecular tumbling motion (*i.e.* larger τ_R).

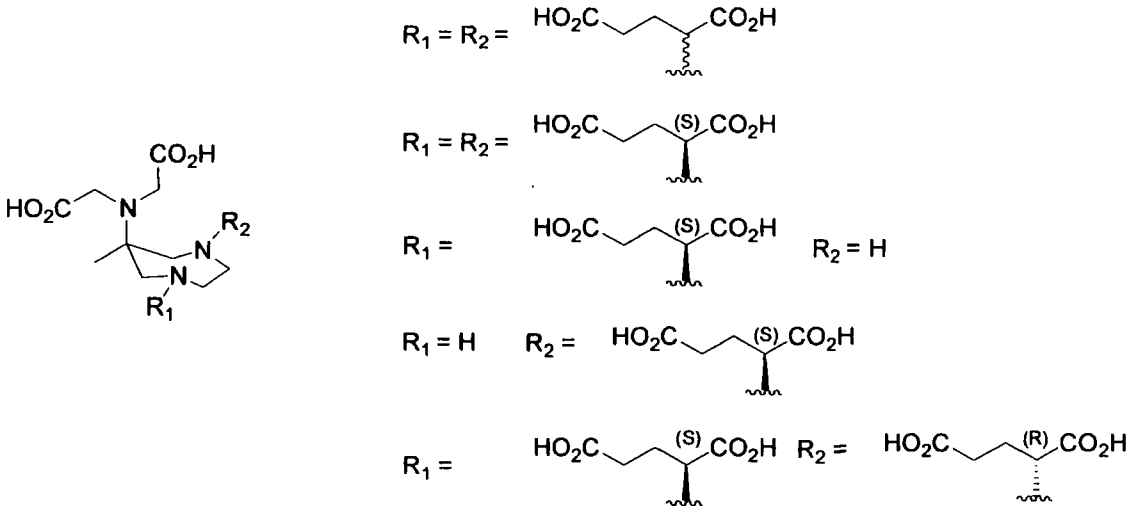

Scheme III.2: Target ligand structures based on AMPED inorporating 1,5-dicarboxylates pendant arms.

III.2 Synthesis of ligands based on the core ring structure DO3A

III.2.1 Phosphonate based macrocyclic compounds

The synthetic pathway to the target triphosphonate complex $[Gd(aDO3AP)(H_2O)_2]^{3-}$ (**Figure III.3**) began with the synthesis of the appropriate "pendant arms" to be reacted with an *N*-Boc protected cyclen.

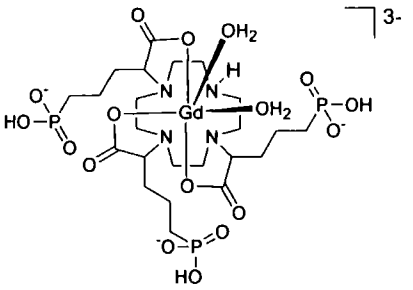

Figure III.3: The structure of $[Gd(aDO3AP)(H_2O)_2]^{3-}$.

The first step in the preparation of the phosphonate moieties involved the protection of 5-bromopentanoic acid as its *t*-butyl ester, following the method of Schmidt *et al.*:[10] stirring of the acid in oxalyl chloride gave the acid chloride, which was then esterified to **14** by treatment with *t*-butanol in the presence of pyridine, as shown in **Scheme III.3**. The pyridine acts as a nucleophilic promoter of reaction and as a base, preventing the generation of a high acid concentration. Removal of the white pyridinium salts by column chromatography gave the ester **14**, whose bromo-functionality was converted into the phosphonate ester **15** using excess triethylphosphite, according to the Michaelis - Arbusov reaction mechanism.[11]

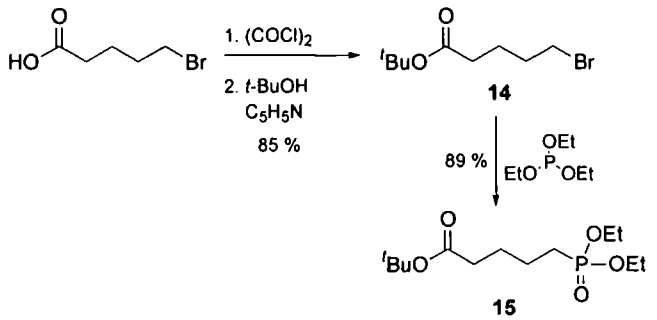

Scheme III.3: Synthesis of *tert*-butyl-5-(diethoxy-phosphonyl)-pentanoate (15).

Deprotection of the *t*-butyl group with trifluoroacetic acid afforded the carboxylic compound (**16**) in quantitative yield, which was used directly in the following Hell-Volhardt-Zelinski reaction, performed by carefully adding molecular bromine to the acid chloride derived from **17**. The reaction was quenched by pouring the crude mixture into cold ethanol and the final bromoester (**18**) was obtained as a yellow, oily product (**Scheme III.4**).

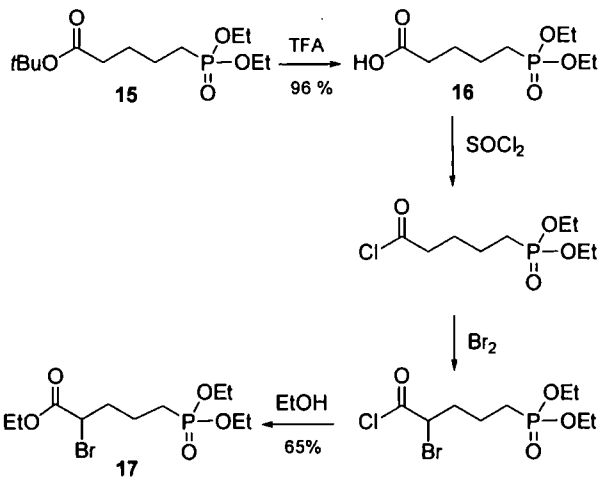

Scheme III.4: Synthesis of (±) Ethyl-2-bromo-5-(diethoxy-phosphonyl)-pentanoate (17).

Among the many strategies attempted,[5] the best results in the alkylation of the 1,4,7,10-tetraazacyclododecane with the α-bromo-phosphonate ester were achieved with the sequence of reactions reported in **Scheme III.5**. The trisubstituted cyclen was prepared by a slightly modified method of Yang *et al.*[12] from reaction of 1,4,7,10-tetraazacyclododecane with ethyl trifluoroacetate in the presence of triethylamine. The product 1,4,7-tris-trifluoromethylcarbonyl-12-N-4 (**18**) was isolated in good yield, by purification through a short silica gel column.

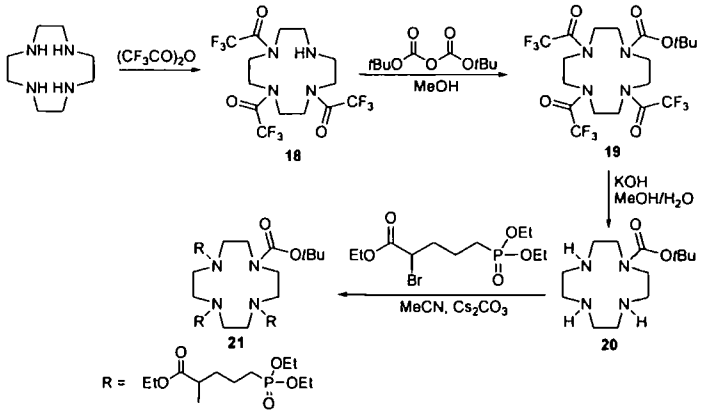

Scheme III.5: Synthesis of tri-substituted phosphonate derivative of the aDO3A ligand.

The next steps involved the BOC-protection of the free amino group of **18** a nd deprotection of the trifluoroacetamide **19** with aqueous potassium hydroxide, to afford the monocarbamate **20** as a clear oil. The alkylation of the macrocyclic secondary amine groups was performed with an excess of (±) ethyl-2-bromo-5-(diethoxy-phosphonyl)-pentanoate (**17**) in the presence of caesium carbonate as base. The final product **(21)** was isolated in low yield after purification by column chromatography. The completion of the synthesis was then performed in our laboratory [5] and data were obtained from spectroscopic analysis and from experiments in solution and also in the presence of HSA. The final steps of the Gd^{III}-complex synthesis are briefly illustrated in **Scheme III.6**. The BOC protecting group was removed by the use of trifluoroacetic acid in the presence of dichloromethane and the hydrolysis of the ethyl ester groups was achieved using hydrogen bromide solution in acetic acid.[19]

The complexation with gadolinium and europium were accomplished in aqueous solution at pH 6 as shown in **Scheme III.6**.

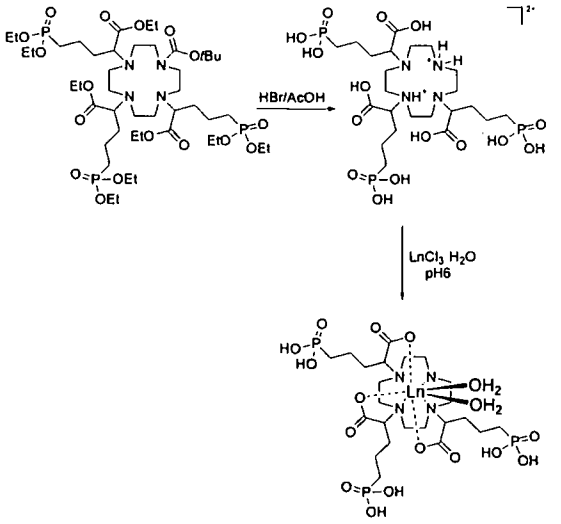

Scheme III.6: Final steps in the synthesis of $[Gd(aDO3AP)(H_2O)_2]^{3-}$.

The relaxivity observed for $[Gd(aDO3AP)(H_2O)_2]^{3-}$ was 7.3 $mM^{-1}s^{-1}$ at 60 MHz, 37 °C, pH 6.8. This relaxivity is in the range expected for similarly sized complexes with two bound water molecules.[13, 14] It is higher than the values found in diaqua complexes containing macrocyclic heptadentate ligands such as $[Gd(DO3A)(H_2O)_2]$ (6.1 mM^{-1} s^{-1} at 60 MHz, 25 °C) and $[Gd(PCTA[12])(H_2O)_2]$ (6.9 mM^{-1} s^{-1} at 60 MHz, 25 °C).[15, 16]

In vitro experiments involving binding to proteins were also performed. [5] It was found that the relaxivity of this complex increased from 7.3 mM^{-1} s^{-1} to ~ 30 mM^{-1} s^{-1} when the gadolinium chelate is in the presence of human serum albumin at a concentration of 0.6 mM, similar to the *in vivo* concentration. However, when phosphate anions were added to the complex-protein solution, it was found that these anions were able to displace the inner sphere water molecules, resulting in a significant reduction of the observed relaxivity.

The failure to develop suitable diaqua species as contrast agents is often due to their intrinsic kinetic and thermodynamic stabilities with respect to premature decomplexation or to their tendencies to react with anionic species in solution (*i.e.* HCO_3^-, lactate or phosphate in biofluids) with displacement of one or both of the bound water molecules. Evidently, this phosphonate complex suffers from these

anion-binding problems, precluding its usage *in vivo*. Work on this system was therefore curtailed.

III.2.2 A new kind of pendant arm for Gd^{III} complexes

In order to circumvent the problems of anion binding encountered with the previously described $[Gd(aDO3AP)(H_2O)_2]^{3-}$ complex, a new type of pendant arm was designed to be incorporated into the DO3A based core structure. It was resolved that the resulting $q = 2$ target complex (shown in **Figure III.4**) should possess three pendant amino acid moieties. The systematic variation of the substituent group should allow the protein binding affinity of the complex to be modulated, and the presence of the carboxylate anionic groups was proposed to inhibit the anion binding problems which had afflicted the phosphonate system discussed above.

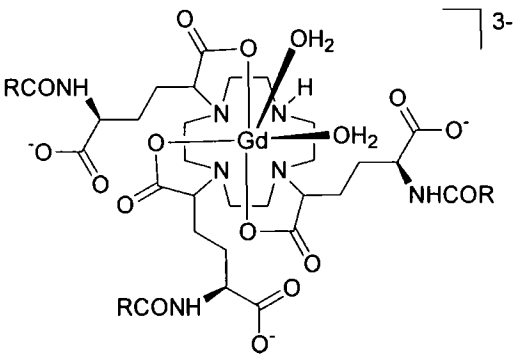

Figure III.4: Target $[Gd(aDO3A)(H_2O)_2]^{3-}$ complex.

The synthetic pathway to the amino-acid based pendant arm is outlined in **Scheme III.7**.

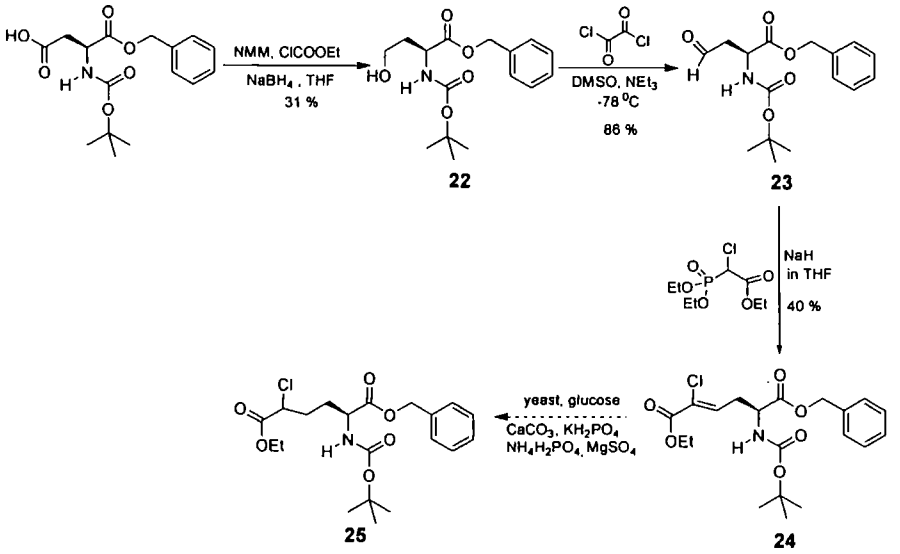

Scheme III.7: Synthesis of a new pendant arm to incorporate to the $[Gd(aDO3A)(H_2O)_2]^{3-}$.

The *N*-Boc-aspartic acid-benzyl ester was reduced to the corresponding homoserine derivative (**22**) following the procedure of Johns *et al.*[17] The *t*-butyl ester of *γ*-hydroxy amino acids is reported to be stable toward lactonization. However, side products such as the lactone (***a***) or the methyl ester (***b***) reported in **Figure III.5** were isolated during the preparation of alcohol **22**, but were obtained in fairly low yields.

Figure III.5: Side products generated in the synthesis of 22.

It was observed that this reduction is very sensitive to moisture and consequently has to be performed under anhydrous conditions, using an argon atmosphere. Indeed, the addition of the reaction mixture to the reducing agent has to be performed as quickly as possible. After chromatographic purification, **22** was oxidised via Swern oxidation[18, 19, 20] to the corresponding aldehyde **23**, which was subsequently reacted

with the Wittig reagent [21] to give a mixture of the *Z*- and *E*-vinyl bromide in 40 % yield. The last synthetic step, involving the reduction of alkene **24**, proved to be very troublesome. A mild method was at first attempted involving the use of fermenting baker's yeast and glucose in warm aqueous solution.[22] Unfortunately no product was obtained with this approach. Hydrogenation over $Pd(OH)_2/C$ was then attempted, but this approach proved too reactive: after only 1h a mixture was obtained of the dechlorinated diester and the debenzylated acid.

The synthesis of the target molecule was therefore not accomplished, but the idea of incorporating amino-acid based moieties onto an heptadentate core ring structure has been preserved and applied in further work with the new core ring structure 6-amino-6-methyl-perhydro-1,4-diazepin (AMPED), discussed in the next section of this chapter.

III.3 Synthesis of ligands based on the core ring structure AMPED

III.3.1 Phosphinate complexes based on AMPED

Phosphinate analogues of the carboxylate AAZTA complexes were prepared with the main aim of obtaining lanthanide complexes possessing suitable physico-chemical and biochemical characteristics for use as contrast agents. Our attention focused on these systems because it was considered that they retain similar stability profiles to the parent AAZTA complexes. However, a different steric demand around the Ln^{III} ion is likely because of the longer C-P (1.8 Å vs 1.5 Å for C-C) and P-O bonds (1.5 Å vs 1.25 A for C-O). It was thought that these differing steric demands might favour the enhancement of the second sphere contribution to the overall relaxivity observed and, perhaps, modify the affinity of the complex towards anion chelation. The introduction of the phosphinate groups should allow the fast water exchange rate to be retained and favour the formation of stronger hydrogen bonds compared to

carboxylates, perhaps keeping more water molecules close to the coordination sphere of the complex.

III.3.2 Synthesis of AAZTA based complexes possessing simple phosphinate pendant arms

Phosphinate groups are attractive alternative ligating systems to carboxylates. Two different synthetic routes were investigated for the synthesis of ligand **31** (or **L1**). In the first route, shown in **Scheme III.8**, (*O*-mesylmethylene)methylphosphinic ethyl ester (**26**) was prepared in two steps by reacting methyldiethoxyphosphine with *para*-formaldehyde in THF to afford the alcohol **25**, which was subsequently converted into the mesylate by treatment with mesylchloride and triethylamine in THF.

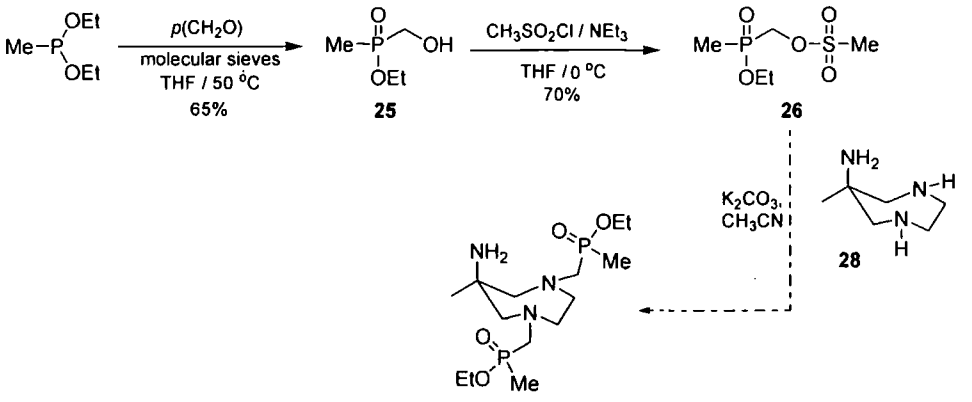

Scheme III.8: First synthetic approach for the AMPED dialkylation.

Dialkylation of AMPED was attempted with two equivalents of mesylate **26** and the progress of reaction was monitored by TLC, HPLC and ES-MS. Unfortunately the desired product was not observed and an alternative route, shown in **Scheme III.9**, was then investigated.

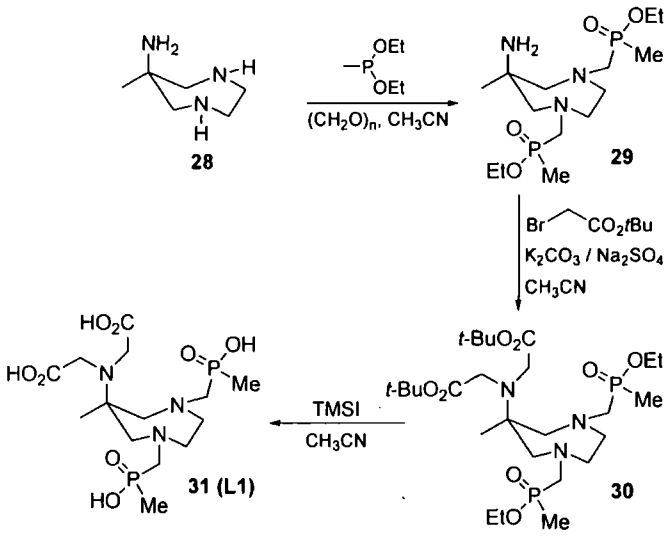

Scheme III.9: Synthesis of the AAZTAP ligand (L1).

Two equivalents of methyldiethoxyphosphine were dissolved in few millilitres of acetonitrile and this solution added directly to a suspension of AMPED and *para*-formaldehyde in acetonitrile. The desired dialkylated AMPED was obtained as the main product of reaction and was separated by column chromatography from the monoalkylated, traces of the trialkylated and the alcohol generated from the direct reaction of $MeP(OEt)_2$ with *para*-formaldehyde. Alkylation of the primary amine was performed by addition of *t*-butylbromoacetate to a solution of the dialkylated AMPED in CH_3CN at 0 °C in the presence of K_2CO_3 as base. The subsequent deprotection of the carboxy and phosphinate groups proved to be more difficult than anticipated. Initial attempts to perform this hydrolysis used 6M HCl at both room temperature and reflux for varying times (30 min to several days) but each attempt was unsuccessful in affording pure product, as monitored by ^{31}P and ^{1}H NMR analysis of the crude product. However, a sample of approximately 80% purity was obtained by refluxing **30** overnight in 6 M HCl followed by removal of solvent. The ^{31}P NMR spectrum of this sample displayed singlets at 48 ppm (ester) and 36 ppm (acid), consistent with incomplete hydrolysis. Acidic hydrolysis in $HBr/MeCO_2H$ was also attempted, but the ^{1}H NMR spectrum of the crude showed no signals corresponding to the AMPED ring protons, suggesting that the core structure might

have been destroyed. An improved method for this deprotection step was sought. Surprisingly, treatment of **30** with TMSI in MeCN proceeded smoothly and gave the target ligand **L1**. ^{31}P NMR analysis of this sample displayed only a singlet at 36 ppm indicating that the product contained no other phosphorus-containing impurities.
The complexation of ligand **L1** with lanthanide salts $(Eu(OAc)_3 \cdot 6H_2O$ and $GdCl_3 \cdot 6H_2O$, respectively) was performed in water (pH 5.5) at 60 °C. The excess lanthanide salt was removed as the corresponding hydroxide by raising the pH to 10, filtering off the $Ln(OH)_3$ and restoring to neutral pH.

III.3.3 Studies of the complexes magnetic properties and stability

The emission spectrum of $[Eu^{III}AAZTAP(H_2O)_2]^-$, here called $[Eu^{III}L1]^-$, was measured in H_2O and in D_2O at pH 7.4 (pD = pH + 0.4), 298 K exciting into the charge-transfer band at 255 nm (the emission spectrum of the complex in D_2O is shown in **Figure III.6**).

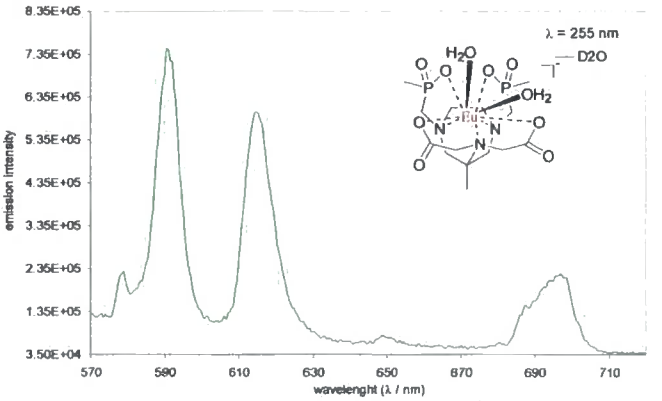

Figure III.6: Emission Spectrum of $[Eu^{III}L1]^-$ (1 mM solution in D_2O, pH 7.4).

Measurement of the luminescence lifetimes in H_2O and D_2O allowed an estimation of the hydration state of the complex. The number of bound water molecules was calculated according to the following (**Equation III.4.1**):[23]

$$q_{Eu} = 1.2 \cdot \left(k_{H2O} - k_{D2O} - 0.25\right) \qquad \textbf{(Eq. III.4.1)}$$

In this equation, $k_{(H2O)}$ and $k_{(D2O)}$ are the radiative decay rate constants in H_2O and D_2O, respectively; the term 0.25 for Eu^{III} refers to quenching due to second sphere water molecules.

Measurements of the excited state lifetime (k_{H2O} = 2.63 ms^{-1}, k_{D2O} = 0.8 ms^{-1}) established that **$[Eu^{III}L1]^-$** is a diaqua system [$q^{Eu} = (\Delta k - 0.25) \cdot 1.2 = 1.90$].

In further work, lifetime measurements of an aqueous solution of the Eu^{III} chelate (0.5 mM) in the presence of carbonate anions (20 mM aqueous Na_2CO_3) showed little change, strongly suggesting that the system remains q = 2. However, significant changes were noted in the form of the europium emission spectrum (**Figure III.7**). In particular, the ratio of the ΔJ = 2 / ΔJ = 1 band intensities at 620/590 nm increased from ~ 3:2 to 5:1, consistent with the chelation of a carbonate group, observed in several earlier studies on anion chelation.[2, 24] This observation suggests a change in the coordination sphere of the metal and is consistent with displacement of the carboxylate or the phosphinate pendant arms by the carbonate group.

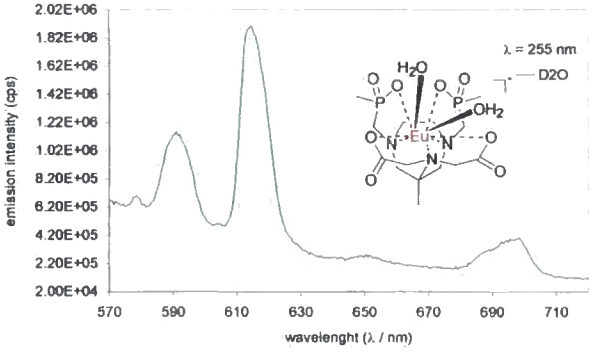

Figure III.7: Emission spectrum pH 7.4 of $[Eu^{III}L1]^-$ (1 mM solution in D_2O) + 40 mM aqueous Na_2CO_3.

A comparison of the ^1H NMR spectrum of $[Eu^{III}L1]^-$ in the absence (**Figure III.8**) and in the presence of 40 mM aqueous Na_2CO_3 solution (**Figure III.9**) was done. The

spectra observed were notably different and suggested that a large change had occurred in the coordination environment about the europium centre.

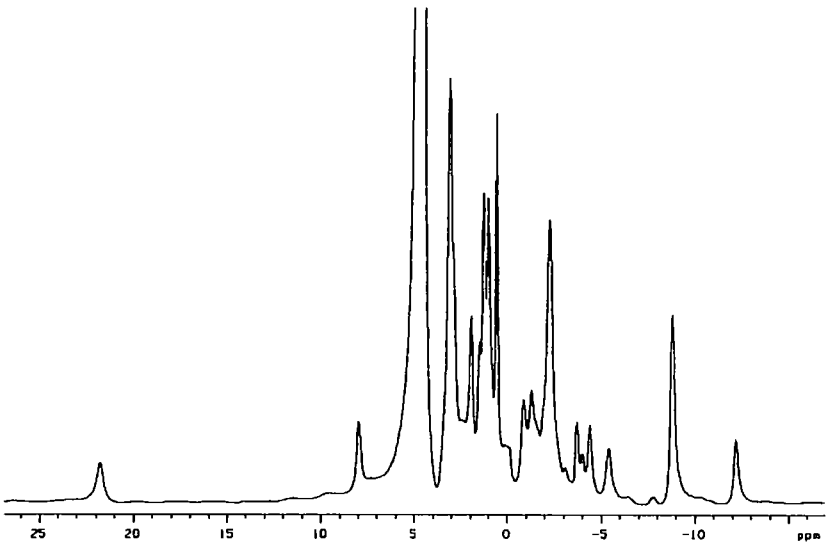

Figure III.8: ^{1}H NMR spectrum of $[Eu^{III}L1]^-$ (200 MHz, D_2O, 24 °C).

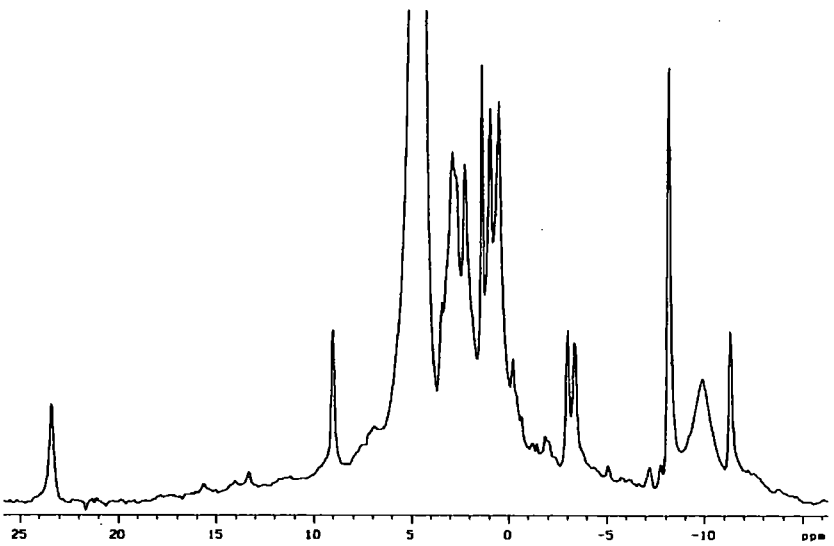

Figure III.9: ^{1}H NMR spectrum of $[Eu^{III}L1]^-$ in D_2O + 40 mM Na_2CO_3 (200 MHz, 24 °C).

6.5 to 2.2 $mM^{-1}s^{-1}$ (60 MHz, 37 °C) when aqueous carbonate (14 mM) solution was added to the gadolinium chelate solution (0.678 mM). Once again, the displacement of the phosphinate arms (or of the carboxylate ones) with carbonate was suggested. The occurrence of such a displacement is a severe drawback for the $[Ln^{III}AAZTAP(H_2O)_2]^-$ system, and compromises its *in vivo* use as a contrast agent.

III.3.4 A more functionalized phosphinate pendant arm

Other routes for adorning the AMPED periphery were considered. A more functionalized phosphinate pendant arm was synthesized (**Scheme III.10**), according to a procedure previously developed in our laboratory.[25]

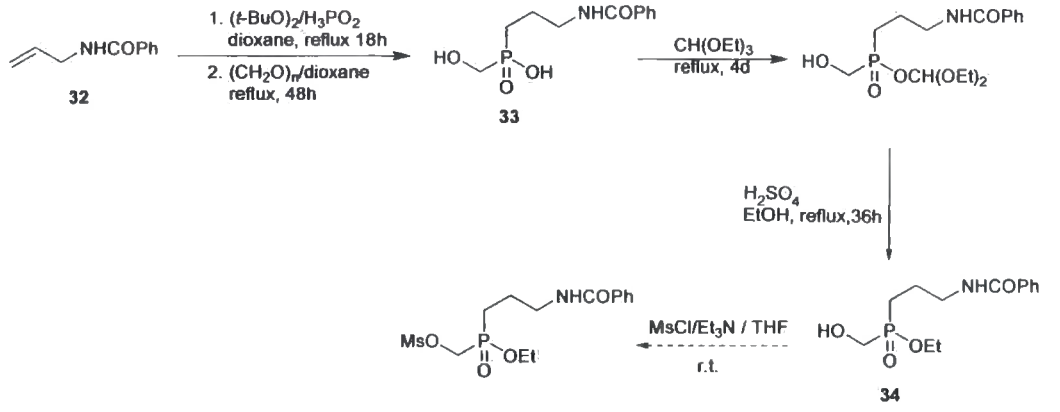

Scheme III.10: Synthesis of a more functionalized phosphinate pendant arm.

Upon completion of its synthesis, the phosphinate wedge could be incorporated onto an AMPED core, affording a ligand suitable for a target complex such as that shown in **Figure III.12.**

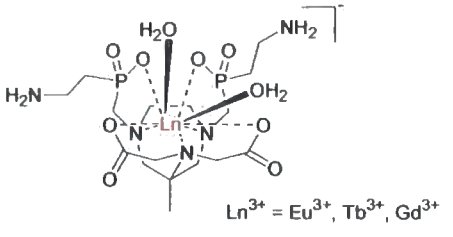

Figure III.12: The target complex $[Ln^{III}AAZTAPN(H_2O)_2]^-$.

On the basis of the results previously obtained with the $[Ln^{III}AAZTAP(H_2O)_2]^-$ complexes, the synthesis of $[Ln^{III}AAZTAPN(H_2O)_2]^-$ was not pursued. It was expected that the coordination sphere of the metal ion would have not been significantly changed, therefore the system could have exhibited similar affinity towards anion binding.

III.4 Conclusions

The design and synthesis of di-aqua gadolinium complexes based on the heptadentate structures DO3A and AMPED has been described in this chapter. None of the chelate structures developed has exhibited the thermodynamic stability and inertness towards anion chelation necessary for the possible future use of the complexes as probes in MRI. The high relaxivity value of ~30 $mM^{-1}s^{-1}$ observed for the $[Gd(aDO3AP)(H_2O)_2)^{3-}$/HSA system dropped when phosphate anions were added to the complex / protein solution, at a concentration similar to that found *in vivo*. The anions are able to displace the inner sphere water molecules, thereby precluding the usage of the system *in vivo*. Similar results were obtained for the $[GdAAZTAP(H_2O)]^-$ system. Carbonate anions were found to displace the ligating groups of the complex, leading to a drop of the relaxivity value. The radical change in the coordination sphere of the metal ion was apparent from the ^1H NMR and emission spectrum of the analogue Eu^{III} complex. Given the behaviour with the phosphinate groups, research was directed towards di-aqua systems based on the novel AMPED core, adorned with carboxylic acid side arms. This work is described in Chapter 4 of this thesis.

List of references

[1] Aime, S.; Gianolio, E.; Terreno, E.; Giovenzana, G. B.; Pagliarin, R.; Sisti, M.; Palmisano, G.; Botta, M.; Lowe, M. P.; Parker, D. *J. Biol. Inorg. Chem.* **2000**, *5*, 488.

[2] Bruce, J. I.; Dickins, R. S.; Govenlock, L. J.; Gunnlaugsson, T.; Lopinski, S.; Lowe, M. P.; Parker, P.; Peacock, R. D.; Perry, J. J. B.; Aime, S.; Botta, M. *J. Am. Chem. Soc.* **2000,** *122,* 9674.

[3] Burai, L.; Kiraly, R.; Toth, E.; Brucher, E. *Magn. Reson. Imaging* **1997**, *38*, 146.

[4] Messeri, D.; Lowe, M. P.; Parker, D.; Botta, M. *Chem. Commun.* **2001**, 2742.

[5] Thompson, N. C., PhD Thesis, University of Durham **2005**.

[6] Aime, S.; Calabi, L.; Cavallotti, C.; Giovenzana, G. B.; Palmisano, G.; Sisti, M. PCT Int. Patent Appl. W00308390, **2003**, *138*, 146684.

[7] Aime, S.; Calabi, L.; Cavallotti, C.; Gianolio, E.; Giovenzana, G. B.; Losi, P.; Maiocchi, A.; Palmisano, G.; Sisti, M. *Inorg. Chem.* **2004**, *43*, 7588.

[8] Swift, T. J.; Connick, R. E. J. *J. Chem. Phys.* **1962**, *37*, 307.

[9] Woods, M.; Aime, S.; Botta, M.; Howard, J. A. K.; Moloney, J. M.; Navet, M.; Parker, D.; Port, M.; Rousseaux, O. *J. Am. Chem. Soc.* **2000**, *122*, 9781.

[10] Schmidt, U.; Braun, C.; Sutoris, H. *Synthesis*, **1996**, 223.

[11] Bruice, P. Y.; Organic Chemistry, 3rd Edition, Prentice Hall Inc., **2001**, 786.

[12] Yang, W.; Giandomenico, C. M.; Sartori, M.; Moore, D. A. *Tetrahedron Lett.* **2003**, 44, 2481.

[13] Jocher, C. J.; Botta, M.; Avedano, S.; Moore, E. G.; Xu, J.; Aime, S.; Raymond, K. N. *Inorg. Chem.* **2007**, *46*, 4796.

[14] Aime, S.; Gianolio, E.; Corpillo, D.; Cavallotti, C.; Palmisano, G.; Sisti, M.; Giovenzana, G. B.; Pagliarin, R. *Helv. Chim. Acta* **2003**, *86*, 615.

[15] Aime, S.; Botta, M.; Crich, G. S.; Giovenzana, G. B.; Pagliarin, R.; Sisti, M.; Terreno, E. *Magn. Reson. Chem.* **1998**, *36*, S200.

[16] Aime, S.; Botta, M.; Crich, G. S.; Giovenzana, G. B.; Jommi, G.; Pagliarin, R.; Sisti, M. *Inorg. Chem.* **1997**, *36*, 2992.

List of references

[1] Aime, S.; Gianolio, E.; Terreno, E.; Giovenzana, G. B.; Pagliarin, R.; Sisti, M.; Palmisano, G.; Botta, M.; Lowe, M. P.; Parker, D. *J. Biol. Inorg. Chem.* **2000**, *5*, 488.

[2] Bruce, J. I.; Dickins, R. S.; Govenlock, L. J.; Gunnlaugsson, T.; Lopinski, S.; Lowe, M. P.; Parker, P.; Peacock, R. D.; Perry, J. J. B.; Aime, S.; Botta, M. *J. Am. Chem. Soc.* **2000,** *122,* 9674.

[3] Burai, L.; Kiraly, R.; Toth, E.; Brucher, E. *Magn. Reson. Imaging* **1997**, *38*, 146.

[4] Messeri, D.; Lowe, M. P.; Parker, D.; Botta, M. *Chem. Commun.* **2001**, 2742.

[5] Thompson, N. C., PhD Thesis, University of Durham **2005**.

[6] Aime, S.; Calabi, L.; Cavallotti, C.; Giovenzana, G. B.; Palmisano, G.; Sisti, M. PCT Int. Patent Appl. W00308390, **2003**, *138*, 146684.

[7] Aime, S.; Calabi, L.; Cavallotti, C.; Gianolio, E.; Giovenzana, G. B.; Losi, P.; Maiocchi, A.; Palmisano, G.; Sisti, M. *Inorg. Chem.* **2004**, *43*, 7588.

[8] Swift, T. J.; Connick, R. E. J. *J. Chem. Phys.* **1962**, *37*, 307.

[9] Woods, M.; Aime, S.; Botta, M.; Howard, J. A. K.; Moloney, J. M.; Navet, M.; Parker, D.; Port, M.; Rousseaux, O. *J. Am. Chem. Soc.* **2000**, *122*, 9781.

[10] Schmidt, U.; Braun, C.; Sutoris, H. *Synthesis*, **1996**, 223.

[11] Bruice, P. Y.; Organic Chemistry, 3rd Edition, Prentice Hall Inc., **2001**, 786.

[12] Yang, W.; Giandomenico, C. M.; Sartori, M.; Moore, D. A. *Tetrahedron Lett.* **2003**, 44, 2481.

[13] Jocher, C. J.; Botta, M.; Avedano, S.; Moore, E. G.; Xu, J.; Aime, S.; Raymond, K. N. *Inorg. Chem.* **2007**, *46*, 4796.

[14] Aime, S.; Gianolio, E.; Corpillo, D.; Cavallotti, C.; Palmisano, G.; Sisti, M.; Giovenzana, G. B.; Pagliarin, R. *Helv. Chim. Acta* **2003**, *86*, 615.

[15] Aime, S.; Botta, M.; Crich, G. S.; Giovenzana, G. B.; Pagliarin, R.; Sisti, M.; Terreno, E. *Magn. Reson. Chem.* **1998**, *36*, S200.

[16] Aime, S.; Botta, M.; Crich, G. S.; Giovenzana, G. B.; Jommi, G.; Pagliarin, R.; Sisti, M. *Inorg. Chem.* **1997**, *36*, 2992.

---

[17] Valerio, R. M.; Alewood, P. F.; Johns, R. B. *Synthesis* **1988**, 786.

[18] Werner, R. M.; Shokek, O.; Davis, J. T. *J. Org. Chem.* **1997**, *62*, 8243.

[19] Ramsamy, K.; Olsen, R. K.; Emery, T. *Synthesis* **1982**, 42.

[20] Omura, K.; Swern, D. *Tetrahedron* **1978**, *34*, 1651.

[21] Märkl, G. *Chem. Ber.* **1962**, *95*, 3003.

[22] Utaka, M.; Satoshi, K.; Takeda, A. *Tetrahedron Lett.* **1986**, *27*, 4737.

[23] Beeby, A.; Clarkson, I. M.; Dickins, R. S.; Faulkner, S.; Parker, D.; Royle, L.; de Sousa, A. S.; Williams, J. A. G.; Woods, M. *J. Chem. Soc., Perkin Trans. 2* **1999**, 493.

[24] Dickins, R. S.; Aime, S.; Batsanov, A. S.; Beeby, A.; Botta, M.; Bruce, J. I.; Howard, J. A. K.; Love, C. S.; Parker, D.; Peacock, R. D.; Puschmann, H. *J. Am. Chem. Soc.* **2002**, *124*, 12697.

[25] Broan, C. J.; Cole, E.; Jankowski, K. J.; Parker, D.; Pulukkody, K.; Boyce, B. A.; Beeley, N. R. A.; Millar, K.; Millican, A. T. *Synthesis* **1992**, 63.

Chapter 4

Carboxylated AAZTA complexes as relaxation agents

IV.1 AMPED based complexes with carboxylic acid side arms

The initial idea[1] of an AMPED core bearing carboxylic acid side arms was revisited. Inspired by observations from the GdaDO3A system,[2] it was thought that an AMPED based complex bearing carboxylate anionic groups could also inhibit anion binding.

A simple racemic α-bromo diester (**Figure IV.1**, ***a***) and an enantiopure amino-acid ester (**Figure IV.1**, ***b***) were considered at the outset as precursors to 1,5-carboxylates prepared for incorporation into the AMPED core structure. Introduction of a metal ion (Eu^{III}, Gd^{III}, Yb^{III}) into the ligand structures led to AAZTA lanthanide chelates, whose different magnetic and physico-chemical properties were determined and studied.

The work in this chapter focuses on the enhancement of the carboxylated AAZTA complexes efficacy as relaxation agents. Their molecular volumes were increased by attachment to dendrimeric wedges, in an attempt to enhance the contribution of the second coordination sphere to their relaxivities and to slow down the overall molecular tumbling rate ($1/\tau_R$).[3] Carbohydrate containing dendrons were envisaged as suitable candidates to be attached to the gadolinium AMPED based chelates by an amide coupling reaction on the carboxylic side arm.

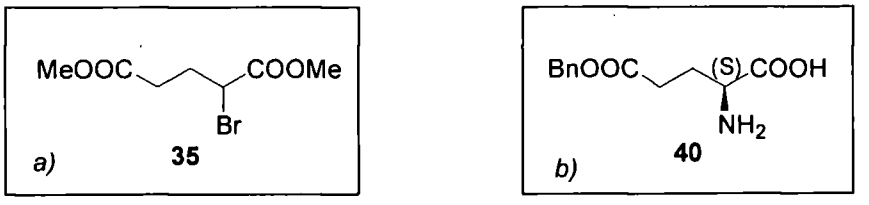

Figure IV.1: Precursors to 1,5-carboxylate pendant arms: *a)* Simple racemic α-bromo ester; *b)* enantiopure amino-acid ester.

IV.2 Simple racemic α-bromo diester as AMPED side arm

IV.2.1 Preparation of $[Ln^{III}(Glu)_2$*racemic*-AAZTA$]^{3-}$

The racemic dimethyl α-bromoglutarate, **35**, was prepared via a Hell-Volhardt-Zelinski reaction, where molecular bromine was carefully added to a solution of the acid chloride derived from the monomethylglutaric acid (**Scheme IV.1**).[4] The reaction was quenched by adding methanol to the mixture cooled at 0 °C. Sequential extraction gave the crude product, together with significant amounts of 2,4-dibromodimethylglutarate. The product was obtained as a clear oil and was separated from the dibromide by disti llation under reduced pressure using a long Vigreux column.

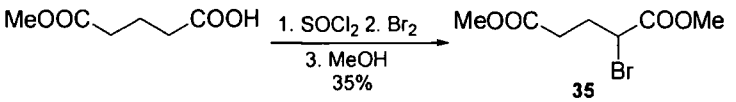

Scheme IV.1: Synthesis of (±)dimethyl-2-bromo-pentanedioate.

The second step in the preparation of the ligand structure **39** (**Scheme IV.2**) involved the *N*-alkylation of the AMPED secondary amines with the racemic bromide **35**. This reaction proceeded selectively at the less hindered secondary amine sites, and the product (**36**) was obtained in good yield and used directly for the next step.

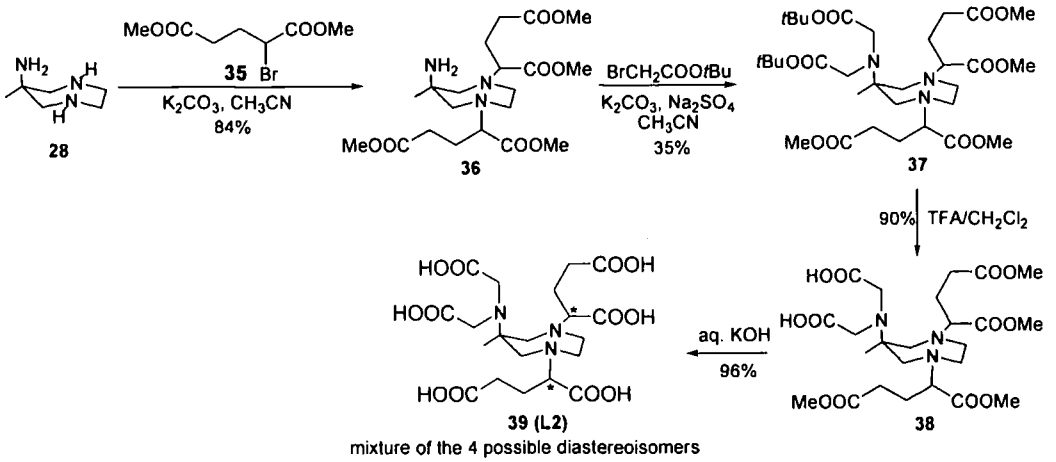

Scheme IV.2: Synthesis of the diglutarate AAZTA ligand, L2, as a racemic mixture.

Dialkylation of the primary amine with *tert*-butyl bromoacetate gave the fully functionalized ligand structure, **39**. This may exist as four different stereoisomers (*RR/SS*/two meso stereoisomers *RS+SR*), determined by the configuration at each of the labelled stereogenic centres. However, neither in TLC nor from the ^{1}H NMR spectrum, shown in **Figure IV.2**, could these diastereoisomers be distinguished.

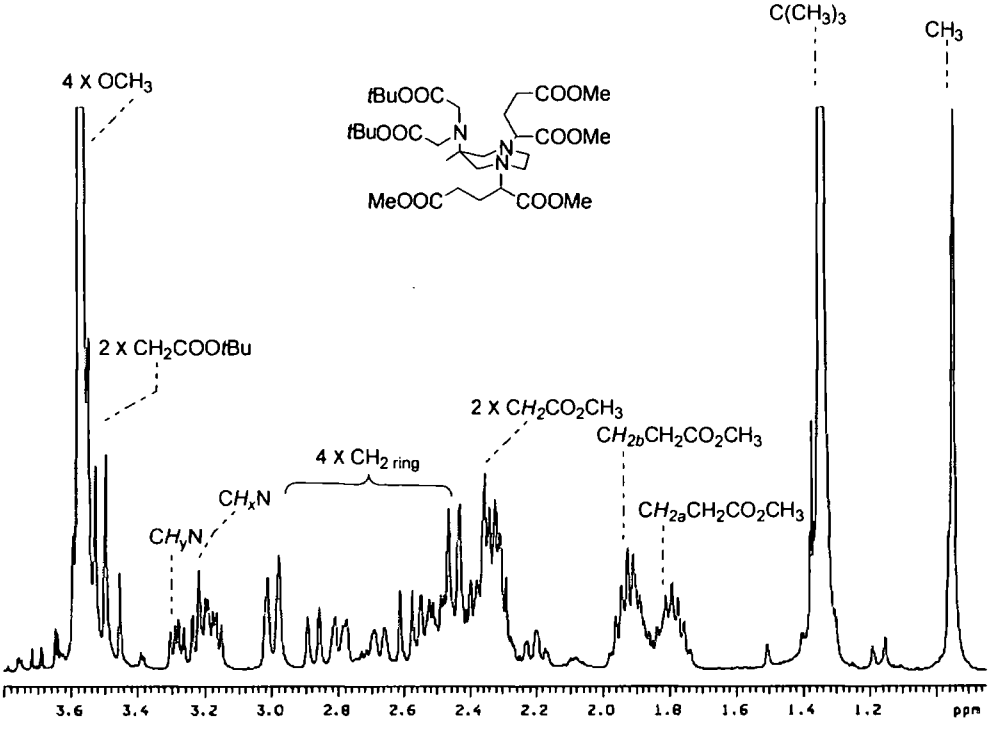

Figure IV.2: ^{1}H NMR spectrum of the ester 37 (400 MHz, in $CDCl_3$).

Removal of the *tert*-butyl esters in trifluoroacetic acid/dichloromethane (1:1) solution (**Scheme IV.2**) gave **38**, which was precipitated from diethyl ether as a white crystalline solid. The subsequent deprotection of the methyl esters was found to be a very slow reaction: hydrolysis in aqueous KOH solution (1M, 20 °C) reached completion onl y after 7 days. Complexes of Gd^{III}, Eu^{III} and Yb^{III} with **39** were prepared by reaction of stoichiometric quantities of the Ln^{III} trichloride salt with the ligand in water. The pH dropped when the metal salt was added to the ligand solution, and a white solid precipitated. The pH was maintained at ~ 5.5 by addition

of aqueous KOH solution (1M), and the reaction progress was followed by ES-MS (for the Gd^{III} chelate) and by ^1H NMR (for Eu^{III} and Yb^{III}). The liquid supernatant was separated from the precipitate by centrifugation. The resultant white solid was soluble only in aqueous HCl (2% solution), thus allowing its characterization only by ES-MS: lanthanide complex, salts and a 2:1 metal:ligand species (LM_2) were identified as the constituents of this precipitate. The separation of the small quantity of complex from the other constituents present in the precipitate was never accomplished, therefore further details cannot be provided about the nature of this isomeric structure. The lanthanide complex was also dissolved in the supernatant. The excess lanthanide was removed as its corresponding hydroxide, by raising the pH of the solution to ~ 10 with an aqueous potassium hydroxide solution. A mixture of the lanthanide complex and KCl salts was finally isolated as a white crystalline solid. The properties of the lanthanide (Yb^{III}, Eu^{III}, Gd^{III}) complexes prepared from ligand **L2** (**Figure IV.3**) were examined in the presence of the potassium salts.

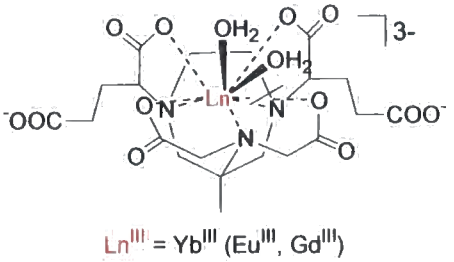

Figure IV.3: Stereoisomeric mixture of complexes synthesized from simple racemic α-bromide.

Information about the number of stereoisomers present in solution could be gathered by analysis of the ^1H NMR spectrum. Two diastereoisomeric species of $[Yb^{III}(Glu)_2$*racemic*-AAZTA$]^{3-}$ were apparent in solution, in approximately a 9:4 ratio (**Figure IV.4**). These two isomers are characterized by different dipolar shifts, exemplified by the signals of their methyl groups, resonating at 10 and 14 ppm, respectively.

The ^1H NMR spectra of the analogous $[Eu^{III}(Glu)_2$*racemic*-AAZTA$]^{3-}$ complex confirms the presence in solution of two main species in approximately the same ratio

(9:4), with dipolar shifts of lower magnitude, but in the same sense as the Yb^{III} system.

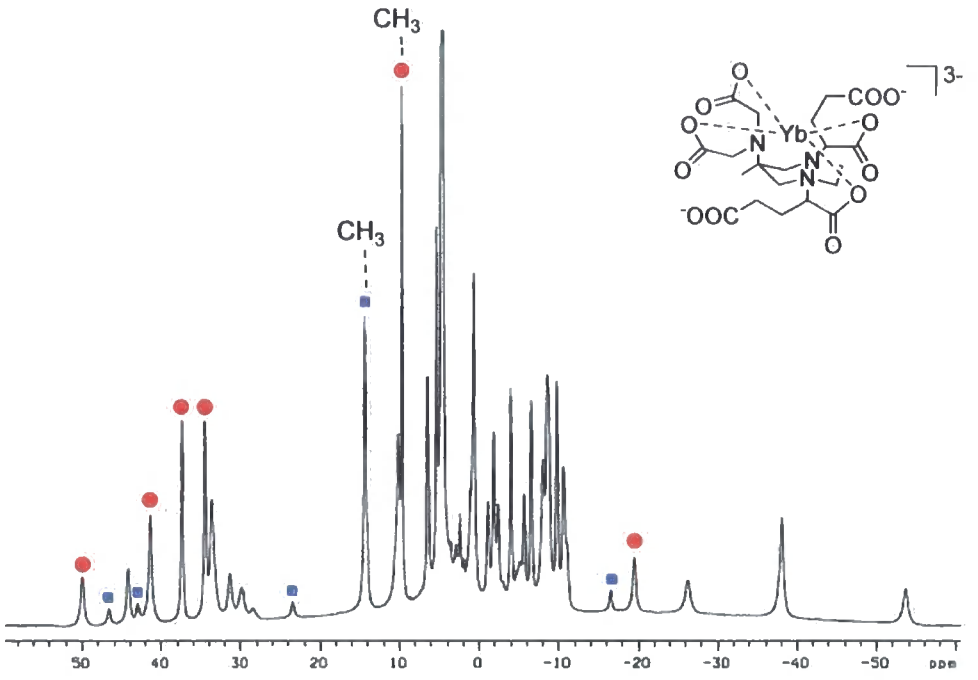

Figure IV.4: ^{1}HNMR spectrum of $[Yb^{III}(Glu)_2$*racemic*-AAZTA$]^{3-}$ (200 MHz, D_2O, pH 5.5).

Based upon previous studies on lanthanide complexes of DTPA,[5] it has been hypothesized that in solution these AAZTA complexes can be 9-coordinated, with the ligand affording seven donor atoms and two water molecules bound to the metal ion on one face of a square antiprismatic structure. Looking at $[Yb^{III}(Glu)_2$*racemic*-AAZTA$]^{3-}$ up its N_3 basal plane, two enantiomeric conformations can be distinguished, defined by three NC-CO torsion-angles (Δ: positive and Λ: negative). Different right or left handed orientations of three of the acetate arms can in this way be visualized, associated with the different Δ or Λ helicities about the metal centre (**Figure IV.5**). It is assumed that each of the NC-CO torsion angles is the same sign, in each case.

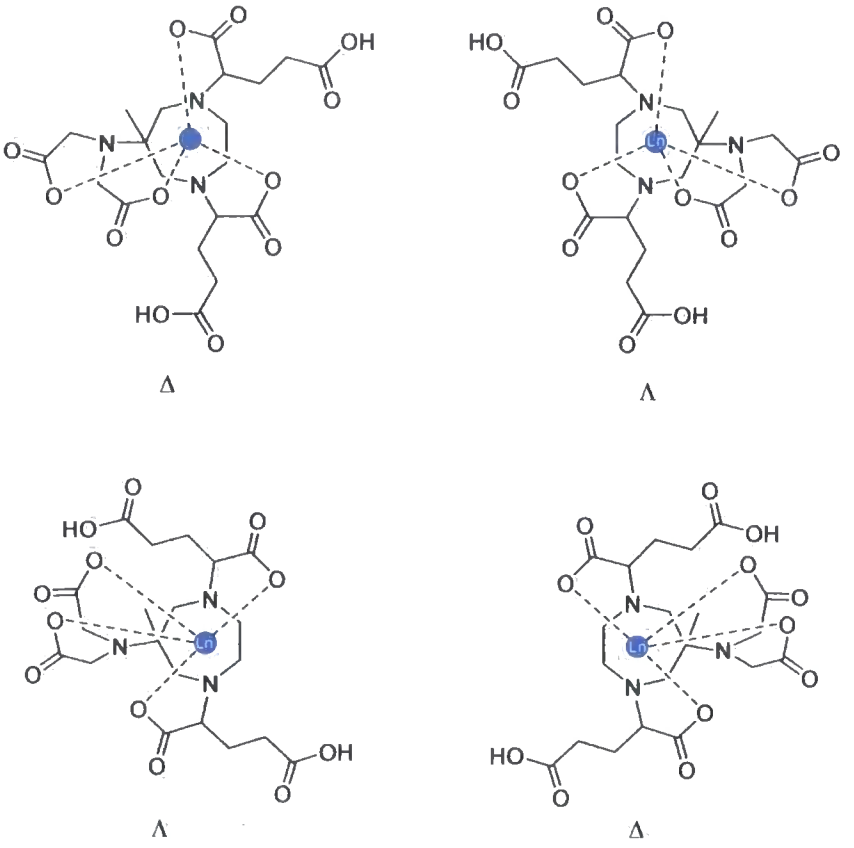

Figure IV.5: Possible stereoisomeric conformations adopted by [Yb^{III}(Glu)$_2$(*RR*)- *and (SS)*-AAZTA]$^-$ in solution, acidic pH. The two structures on the right are the enantiomers of the pair on the left.

Measurements of the radiative decay constants for deactivation of the Eu^{III} excited state in H_2O and in D_2O ($k_{(H_2O)} = 4.86$ ms^{-1}, $k_{(D_2O)} = 2.85$ ms^{-1}) allowed an estimation of the hydration state of the complex. The number of bound water molecules was calculated according to **Equation III.4.1**,[6] already discussed in **Section III.4** of this chapter: $[q^{Eu} = (\Delta k - 0.25) \cdot 1.2]$. It was in this way established that [Eu^{III}(Glu)$_2$*racemic*-AAZTA]$^{3-}$ is a diaqua system ($q = 2.06$).

The $1/T_1$ NMRD profile of the [Gd^{III}(Glu)$_2$*racemic*-AAZTA]$^{3-}$ complex was measured and the relaxivity (r_{1p}) at 20 MHz, 25 °C was determined to be 8.0 mM^{-1}s^{-1}, a value in the range of magnitude expected for a $q = 2$ system of similar volume (MW = 659).[7, 8] The water exchange rate at the Gd^{III} centre was determined by variable

temperature (VT) ^{17}O NMR R_{2p} measurements (at 600 MHz, neutral pH, 25 °C), and the τ_m value obtained was 414 ns. As demonstrated by NMR and luminescence studies on DOTA based systems,[9, 10, 11, 12, 13] the rate of water exchange at the lanthanide ion can be markedly different for two isomers of the same complex. Is this theory applicable to AMPED based systems also? This question was addressed by attempting the separation (or at least an increase of the ratio) of $[Yb^{III}(Glu)_2$*racemic*-AAZTA$]^{3-}$ isomers in solution. Attempts to epimerise the statistical $[Yb^{III}(Glu)_2$*racemic*-AAZTA$]^{3-}$ isomeric mixture in the Yb^{III} or Eu^{III} complexes were undertaken, but unfortunately this strategy did not work: over the pH range 2.5 to 6 no change was registered in the observed isomeric ratio, even after heating for a week.

IV.3 Enantiopure amino-acid α-bromo diester as AMPED side arm

Since the product (**36**) obtained from the alkylation of AMPED (**28**) secondary amines with racemic dimethyl α–bromoglutarate (**35**) was a mixture of diastereoisomers, it was decided to synthesise an enantiopure amino acid ester, wherein stereoselective alkylation of the AMPED secondary amines leads to a simplified diastereomeric mixture in the lanthanide complex.

The enantiopure 2-bromo amino acid diester **41** was prepared in two steps from L-glutamic acid 5-benzyl ester (**Scheme IV.3**).

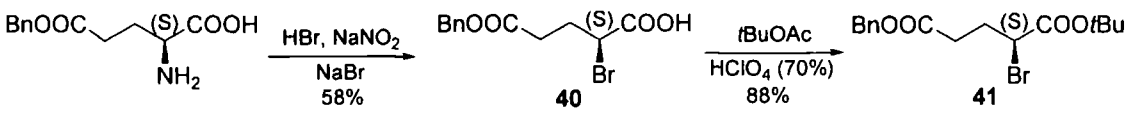

Scheme IV.3: Synthesis of (2*S*)-2-Bromo pentanedioic acid 1-(1,1-dimethylethyl) 5-(phenylmethyl) diester, 41.

The first step involved the diazotization of the amino group of L-glutamic acid-5-benzyl ester by treatment with hydrobromic acid and sodium nitrite, in the presence

of sodium bromide at -5 °C. It is hypothesized[14] that the diazonium salt immediately undergoes an intramolecular S_N2 reaction, involving nucleophilic attack of the oxygen of the carboxylic acid onto the electrophilic carbon, followed by loss of the dinitrogen leaving group (**Scheme IV.4**).

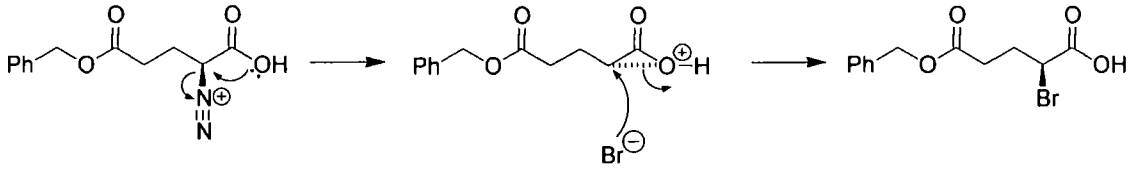

Scheme IV.4: Double inversion mechanism in the synthesis of 40.

The resulting cyclic oxonium ion is then opened by nucleophilic attack of bromide, resulting in the formation of the α-bromide (**40**) where the α-carbon possesses the same configuration as in the starting glutamic acid. The *t*-butyl ester **41** was prepared by transesterification of **40** with *t*-BuOAc in the presence of a catalytic amount of $HClO_4$ (70 %), affording the ester product (**41**) in 88% yield.

Alkylation of the AMPED secondary amines with the enantiomerically pure diester **41** (**Scheme IV.5**) led to the disubstituted AMPED derivative **44** and to the mono-substituted diastereoisomers **42** and **43**.

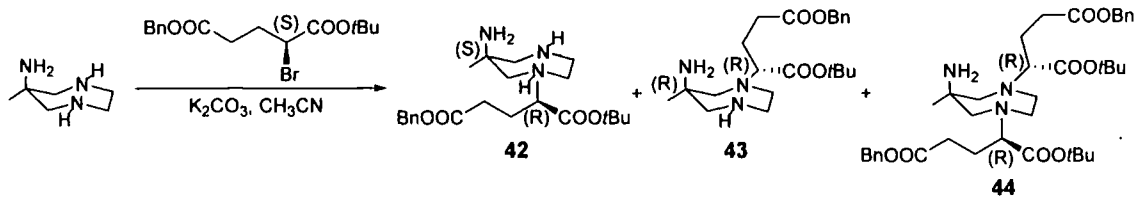

Scheme IV.5: Alkylation of AMPED secondary amines with the enantiomerically pure amino-acid diester.

The mixture of alkylated AMPED products was separated by extraction in EtOAc / aqueous HBr (1M). The disubstituted product remained dissolved in the oganic solvent, probably because of its higher lipophilicity and the decreased basicity of the alkylated secondary amines. The monoalkylated derivatives remained in the aqueous phase and were subsequently extracted into an organic layer after the pH was adjusted

to ~ 9 with ammonia solution. The mixture of the two diastereoisomers of the mono-alkylated AMPED was separated (or, at least, it was largely enriched in one of the two diastereoisomers) via crystallization from EtOH, one isomer being found to be soluble in the solvent and the other precipitating as a white crystalline solid. The purity of these two compounds was determined by ^{1}H NMR analysis. In **Figure IV.6** is shown the spectrum of the diastereomeric mixture and in **Figure IV.7** the spectrum of diastereoisomer **42** (soluble in ethanol) after crystallization. Evidence of the successful diastereomeric separation was given by observing the signal at $\delta \approx 5.10$ ppm, which corresponds to the two benzylic protons: two resonances were observed when both the diastereoisomers were in solution ($\Delta\delta_H$ = 0.008 ppm) and the signal became a > 90% one singlet when they had been separated.

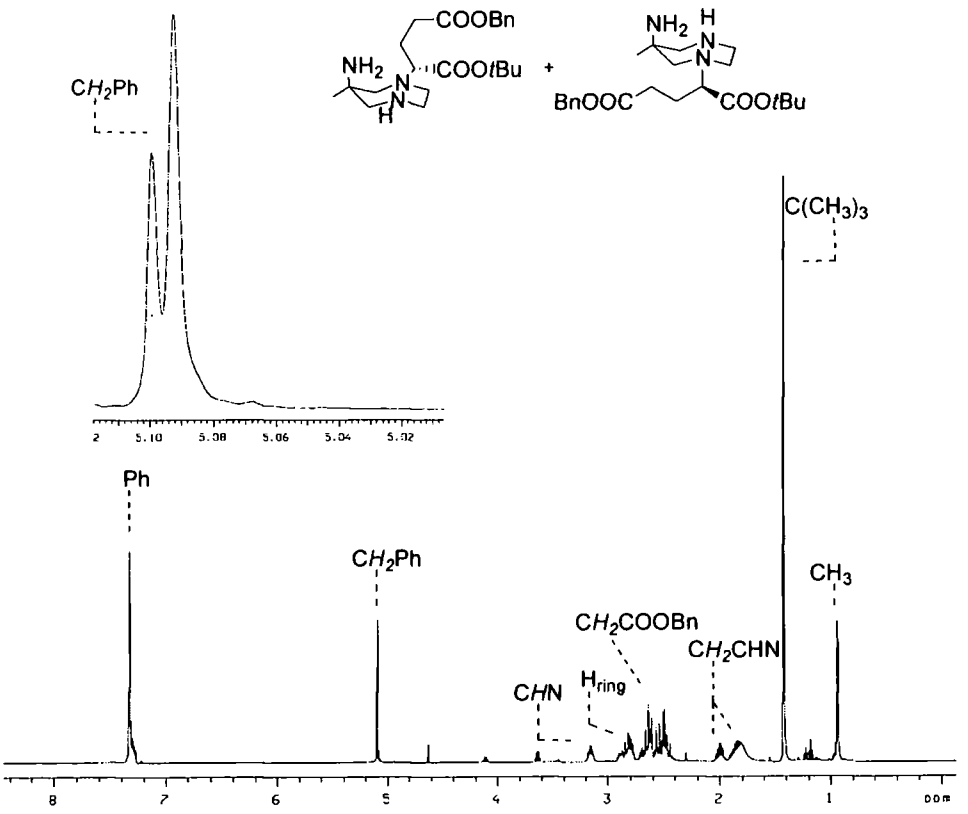

Figure IV.6: ^{1}H NMR spctrum of the mono-alkylated AMPED isomeric mixture (42 + 43) (700 MHz, $CDCl_3$).

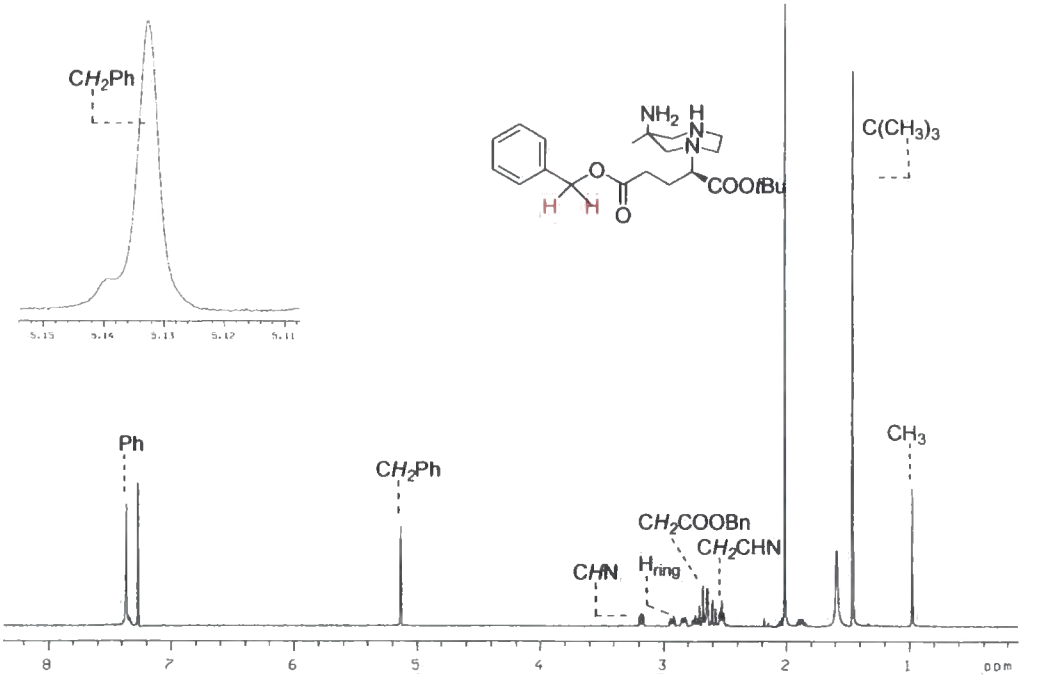

Figure IV.7: ^{1}H NMR spectrum of the mono-alkylated AMPED isomer soluble in EtOH, 42 (700 MHz, $CDCl_3$).

Unfortunately crystal structures of these compounds have not so far been obtained, and the relative / absolute configuration of the two diastereoisomers has thus not been assigned. However, ligands have been prepared either from the dialkylated and the two monoalkylated AMPED derivatives.

IV.3.1 Preparation of $[Ln^{III}(Glu)_2$*(RR)*-AAZTA$]^{3-}$

In **Scheme IV.6** is reported the synthesis of the disubstituted AMPED based ligand structure **L5**, which involved the alkylation of the primary amine of **44** with *tert*-butyl bromoacetate and two subsequent deprotection steps, where the *tert*-butyl and the benzyl protecting groups were removed by treatment with trifluoroacetic acid and hydrogenation over Pd / C, respectively.

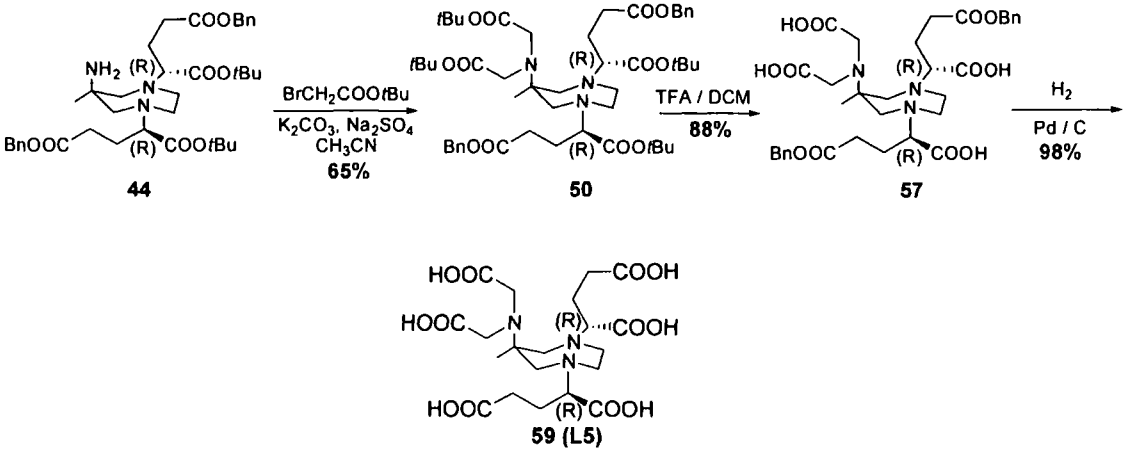

Scheme IV.6: Synthesis of the (Glu)$_2$*(RR)*-AAZTA ligand L5.

The dialkylation of the AMPED secondary amines, which led to **L5**, proceeded stereoselectively, with clean inversion at the stereogenic centre of the alkylating glutamic acid derivatives. Apart from the defined chiral centres of the carbon atoms on the pendant arms (*R* - configuration), the triply substituted nitrogen atoms of the ring structure can give rise to other possible stereoisomers. However, the configurational instability of these isomers, as a consequence of the rapid nitrogen inversion, leads to fast interconversion of these limiting structures. Hence, only a single set of signals is observed in the ^{1}H NMR spectrum (**Figure IV.8**), which can either be the average of the rapidly interconverting isomers or the more thermodynamically stable structure.

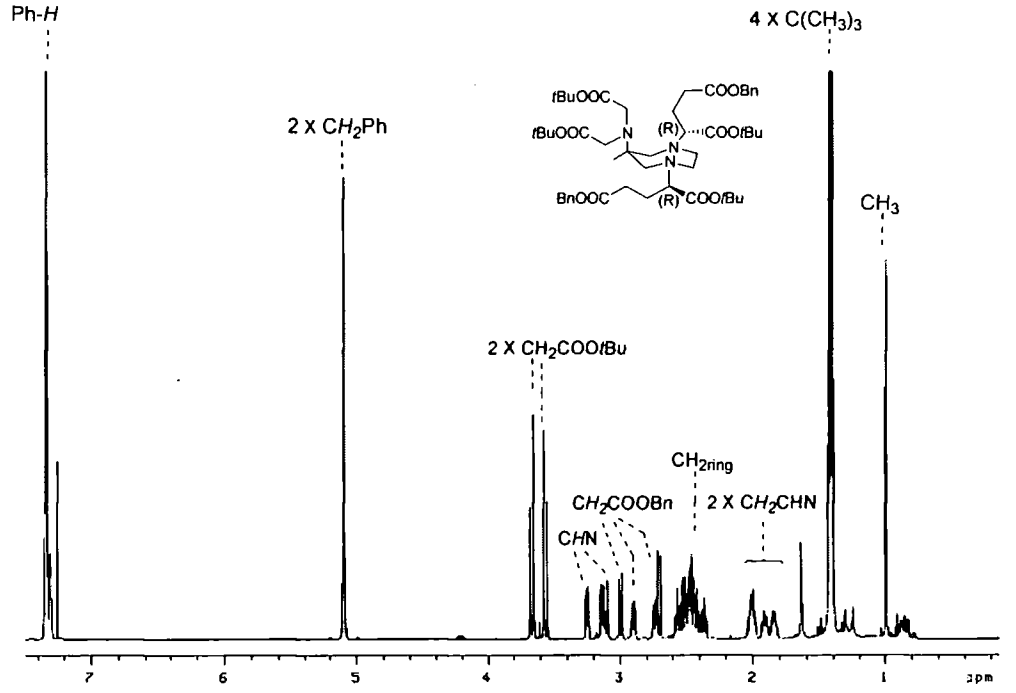

Figure IV.8: ^{1}H NMR spectrum of 50 (700 MHz, $CDCl_3$).

Gd^{III}, Eu^{III} and Yb^{III} complexes were prepared from the $(Glu)_2$*(RR)*-AAZTA ligand. Both the ^{1}H NMR spectra of $[Yb^{III}(Glu)_2$*(RR)*-AAZTA$]^{3-}$ (**Figure IV.9**) and $[Eu^{III}(Glu)_2$*(RR)*-AAZTA$]^{3-}$ (**Figure IV.10**) suggested the presence in solution of one dominant species and a second minor one, in ratio ≥ 9:1. Two dimensional ^{1}H - ^{1}H COSY NMR experiments (the one relative to the europium complex is shown in the **Appendix**) confirmed the coexistence of two species and allowed the separation of some of the related resonances.

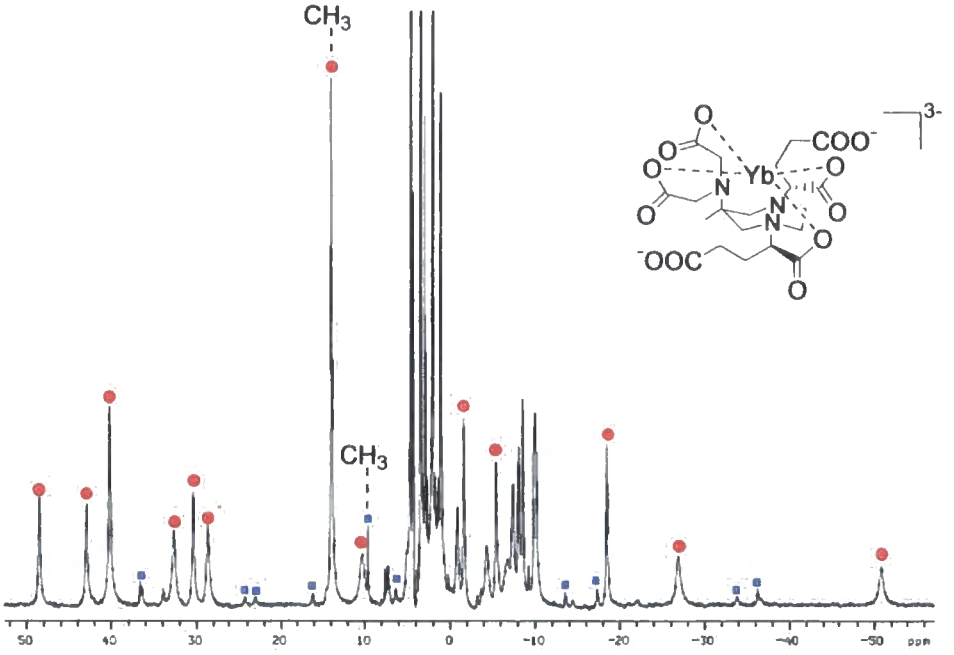

Figure IV.9: ^{1}H NMR spectrum of [$Yb^{III}(Glu)_2$*(RR)*-AAZTA]$^{3-}$ showing the major (red) and the minor species (blue) (D_2O, 700 MHz, pD 5.4, 24 °C).

It appears that in the ^{1}H NMR of the Eu^{III} complex the methyl group resonates at about 6.6 ppm in the major species, but is not obviously assigned in the minor species.

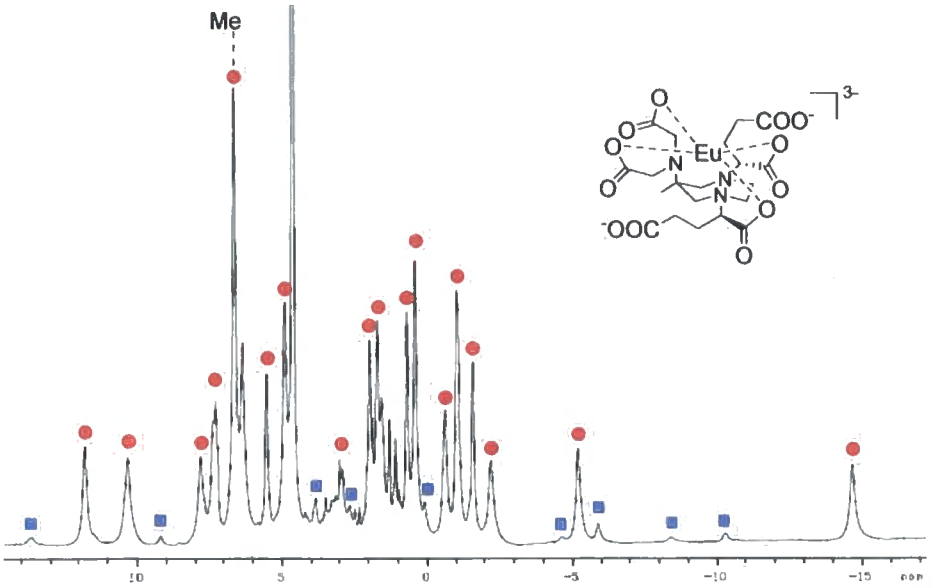

Figure IV.10: ^{1}H NMR spectrum of [$Eu^{III}(Glu)_2$*(RR)*-AAZTA]$^{3-}$ (700 MHz, D_2O, pD 5.4, 24 °C).

The emission spectrum for $[Eu^{III}(Glu)_2$*(RR)*-AAZTA$]^{3-}$ was recorded following direct excitation of the Eu^{III} ion at 397 nm (**Figure IV.11**).

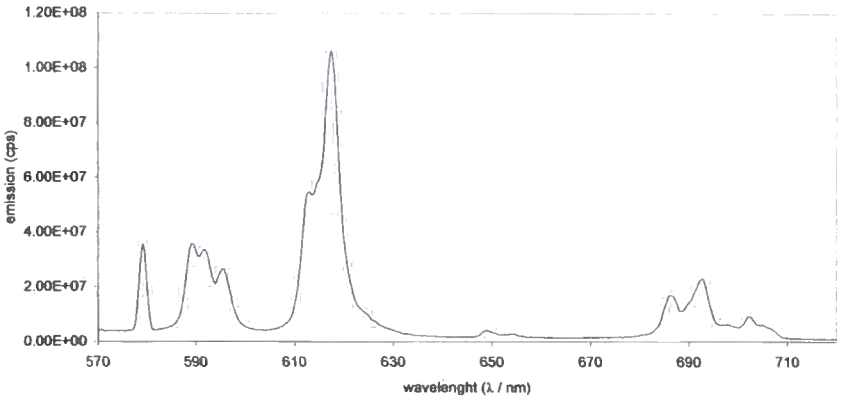

Figure IV.11: Emission spectrum of $[Eu^{III}(Glu)_2$*(RR)*-AAZTA$]^{3-}$ in D_2O, 397 nm, pH 6.

The spectral form of the europium emission in the range 570 – 720 nm is consistent with the presence of only one species in solution. The number of chemically distinct environments of the Eu^{III} ion can be estimated from the number of bands in the $\Delta J = 0$ and $\Delta J = 1$ transitions between 579 nm and 595 nm. In the spectrum considered here, only one band is distinguished at 580 nm and three bands in the $\Delta J = 1$ manifold, indicating the presence of only one species. Furthermore, the symmetry of the system can be examined by comparing the intensity ratio of the $\Delta J = 1$ and $\Delta J = 2$ bands. The dominance of the $\Delta J = 2$ transition is consistent with the lack of symmetry around the metal ion, which is further supported by the presence of three bands in the $\Delta J = 1$ manifold, as compared to the only two bands expected for a C_4 symmetric system such as Eu^{III} DOTA,[13, 6] for example.

Rate constants for the depopulation of the excited states of $[Eu^{III}(Glu)_2$*(RR)*-AAZTA$]^{3-}$ were measured in H_2O and D_2O at 20 °C. This allowed an estimation of the degree of hydration of the complex which, according to the values measured of $k_{H_2O} = 3.6\ ms^{-1}$ and $k_{D_2O} = 1.15\ ms^{-1}$ **(Equation III.4.1)** [6] is consistent with a diaqua system (calculated q value of 2.4).

The $1/T_1$ NMRD profile of the $[Gd^{III}(Glu)_2$*(RR)*-AAZTA$]^{3-}$ complex was measured and the relaxivity (r_{1p}) at 20 MHz, 25 °C was determined to be 8.65 $mM^{-1}s^{-1}$. Such a relaxivity value corresponds to that expected for such a small molecular volume (MW 659) $q = 2$ complex. The measured water exchange rate at the Gd^{III} centre was rather slow: VT ^{17}O NMR R_{2p} measurements allowed an estimation of $\tau_m = 720$ ns (at 600 MHz, neutral pH, 25 °C). This value of τ_m is much larger than is desirable: lifetimes of the order of 20 – 30 ns are required in order to get relaxivity gains as τ_R increases. Accordingly, the monoalkylated analogue was examined, for purposes of comparison.

IV.3.2 Preparation of $[Ln^{III}$Glu AAZTA$]^{2-}$ complexes

Ligands derived from the mono-alkylated AMPED diastereoisomers **42** and **43** were prepared by following an analogous experimental procedure to that employed in the preparation of the dialkylated AMPED ligand **L5** (**Scheme IV.6**). As already mentioned, the relative / absolute configuration of the two diastereoisomers **42** and **43** has not been determined, so it will be assumed that structure **42** corresponds to the isomer soluble in ethanol and structure **43** to the crystalline solid precipitated from ethanol (the molecular structures of the two compounds are shown in **Scheme IV.5**).

The alkylation of the remaining secondary and primary amines of **42** (**Scheme IV.7**) and **43** (**Scheme IV.8**) with *tert*-butyl bromo acetate proceeded slowly, over 48 hours, and heating at reflux of the reaction mixture was required to ensure the alkylation of all the three amino positions.

Ligand **L3** (**Scheme IV.7**), derived from diastereoisomer (**42**), soluble in ethanol, was easily obtained in good yield after the deprotection steps.

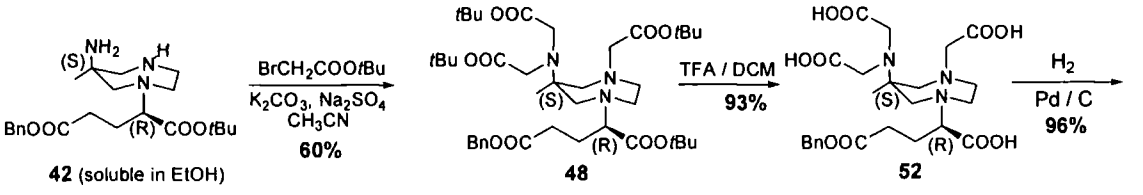

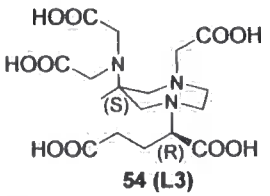

54 (L3)

Scheme IV.7: Preparation of ligand L3 from the soluble in ethanol diastereoisomer 42.

Gd^{III}, Eu^{III} and Yb^{III} complexes were prepared from the GluAAZTA ligand **L3**, and the ^1H NMR analysis of the ytterbium adduct (**Figure IV.12**) indicates the presence of only one major complex isomer species in solution (9:1 ratio with a second, minor species) with a chemical shift of 9 ppm for the methyl group. Higher resolution ^1H NMR (500 MHz) and correspondent ^1H - ^1H COSY NMR spectra which helped in the identification of the two species in solution are shown in the **Appendix**.

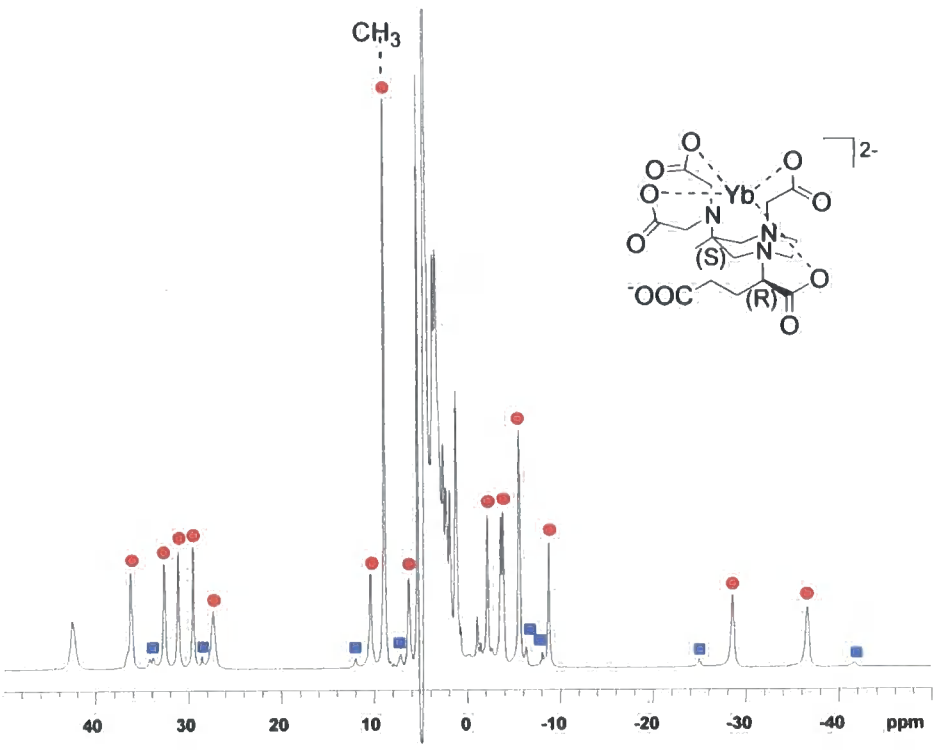

Figure IV.12: ^1H NMR spectrum of $[Yb^{III}GluAAZTA]^{2-}$ showing the major species (red) and the minor one (blue) (200 MHz, D_2O, pD 5.4, 24 °C).

The related europium complex was also formed as one main species, as confirmed by ^{1}HNMR (**Figure IV.13**) and two dimensional ^{1}H - ^{1}H COSY NMR analysis (which is shown in the **Appendix**). However, the dipolar shifts observed here do not correspond to those of the Yb^{III} complex, suggesting that there might have been a reduction in the coordination number from 9 (q = 2) to 8 (q = 1). This would lead to a change in B_0^2 -the second order crystal field coefficient that determines the dipolar shift- as well as geometric changes around the Ln^{III} ion.

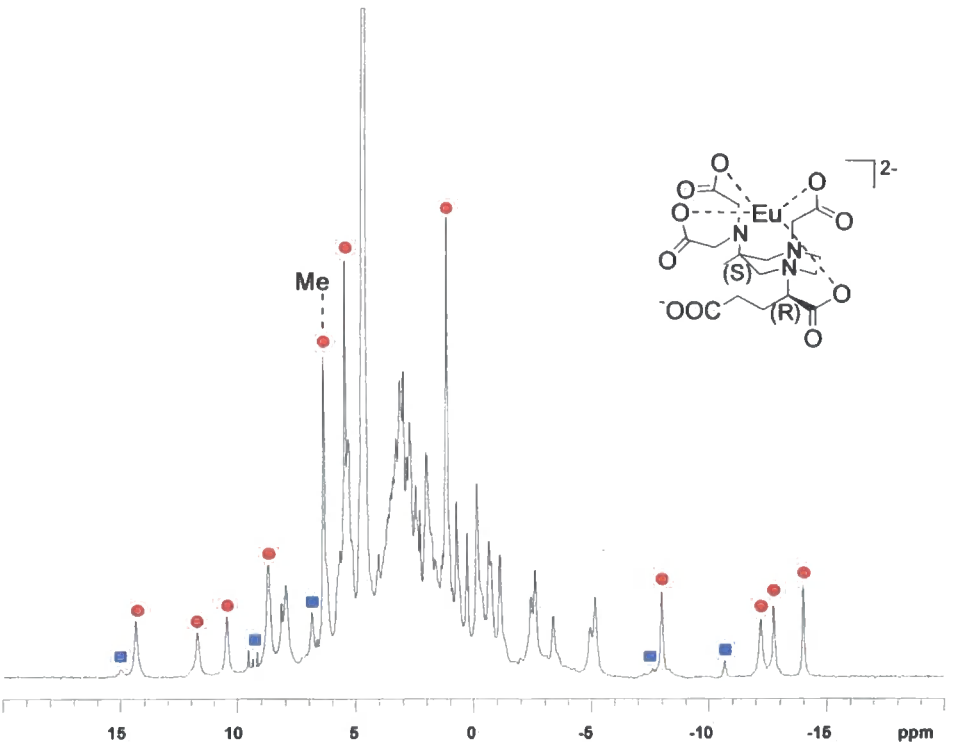

Figure IV.13: ^{1}H NMR spectrum of $[Eu^{III}GluAAZTA]^{2-}$ (500 MHz, D_2O, pD 5.4, 24 °C).

The emission spectrum of $[Eu^{III}GluAAZTA]^{2-}$ was recorded following direct excitation of the Eu^{III} ion at 397 nm (**Figure IV.14**).

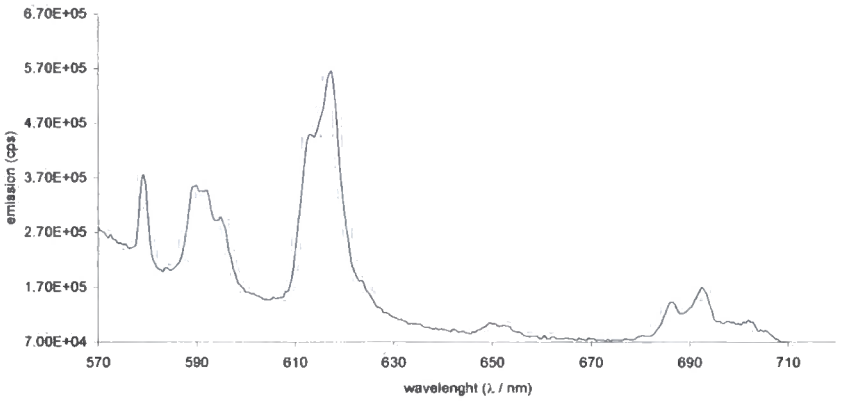

Figure IV.14: Emission spectrum of $[Eu^{III}GluAAZTA]^{2-}$ (1 mM solution in D_2O, pD 5.4, 24 °C).

The form of the emission spectrum of the monoglutarate complex $[Eu^{III}GluAAZTA]^{2-}$ in the range 570 – 720 nm was very similar to that of the diglutarate $[Eu^{III}(Glu)_2$*(RR)*-AAZTA$]^{3-}$, **43**. The presence of only one band in the $\Delta J = 0$ region at 580 nm suggested that only one species was in solution. The three bands in the $\Delta J = 1$ manifold and the dominance of the $\Delta J = 2$ band were evidence of a lack of symmetry in the coordination of the metal ion.[13, 6]

Rate constants for the population of the Eu^{III} excited state were measured as $k_{(H_2O)}$ = 3.0 ms^{-1} and $k_{(D_2O)}$ = 1.16 ms^{-1} indicating that the europium complex possessed a value of q = 1.9.[6]

The relaxivity value (r_{1p}) at 20 MHz, 25 °C of $[Gd^{III}GluAAZTA]^{2-}$ was determined to be 7.3 $mM^{-1}s^{-1}$, and a water exchange rate (τ_m) at the Gd^{III} centre of 115 ns was found by VT ^{17}O NMR R_{2p} measurements (600 MHz, neutral pH, 25 °C). This τ_m value is lower than those recorded for the related diglutaric AAZTA complexes $[Gd^{III}(Glu)_2$*(RR)*-AAZTA$]^{3-}$ and $[Gd^{III}(Glu)_2$*racemic*-AAZTA$]^{3-}$, but is still relatively long, implying that the rate of water exchange may still quench relaxivity gains in more slowly tumbling analogues.

As for the ligand prepared from diastereoisomer **43**, problems were unexpectedly encountered during the final deprotecting step (**Scheme IV.8**). Various attempts at

removing the benzyl protecting group by hydrogenation over Pd/C and also on $Pd(OH)_2/C$ failed and the lanthanide complex had to be prepared from ligand **L4**, still bearing the benzyl on the remote carboxy group.

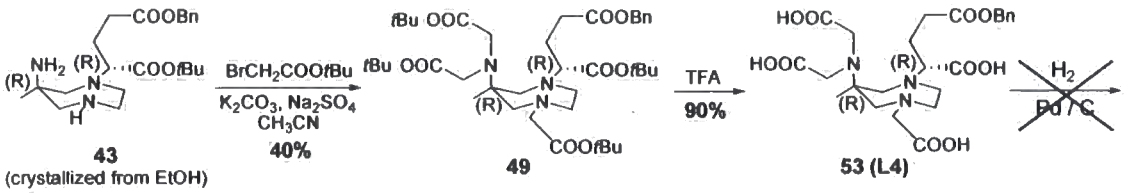

Scheme IV.8: Preparation of ligand L4 from diastereoisomer 43 (crystallized from ethanol).

The Eu^{III} complex was prepared from ligand **L4**, and rate constants for depopulation of the excited states were measured in H_2O and D_2O at 20 °C: $k_{(H_2O)} = 4.7$ ms^{-1} and $k_{(D_2O)} = 3.11$ ms^{-1}. Consequently, the degree of hydration, q, of the complex was estimated [6] to be 1.6.

IV.3.3 Preparation of the $[Ln^{III}(Glu)_2(RS)\text{-AAZTA}]^{3-}$ complexes

To conclude the work on the amide derivatives of AAZTA-diglutarates, to investigate if the nature of the isomers can play a determinant role in the water exchange rate dynamics, it was decided to prepare the *(RS)*-diglutarate AAZTA isomer (**Figure IV.15**) and examine the properties of the $Eu^{III}/Yb^{III}/Gd^{III}$ complexes derived from it.

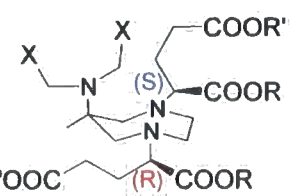

Figure IV.15: The $(Glu)_2(RS)$-AAZTA isomer.

The enantiopure *(R)*-2-bromo amino acid diester **46** was prepared in two steps from the D-glutamic acid 5-benzyl ester (**Scheme IV.9**) following the same experimental procedure already used for the synthesis of the corresponding (*S*)-enantiomer **41** (synthesis reported in **Scheme IV.3**).

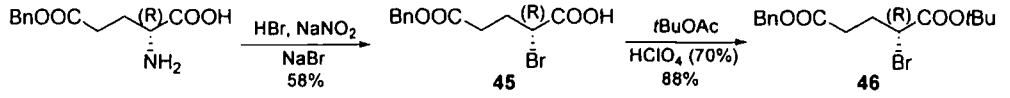

Scheme IV.9: Synthesis of (2*R*)-2-Bromo pentanedioic acid 1-(1,1-dimethylethyl) 5-(phenylmethyl) diester, 46.

Stereoselective alkylation of the secondary amine of the monoalkylated AMPED diastereoisomer soluble in ethanol (**42**), as shown in **Scheme IV.10**, led to the disubstituted AMPED derivative **47**, whose primary amine was then dialkylated using *tert*-butyl bromo acetate (**Figure IV.16**). Further deprotection of the *tert*-butyl and benzyl groups led to ligand **L6**.

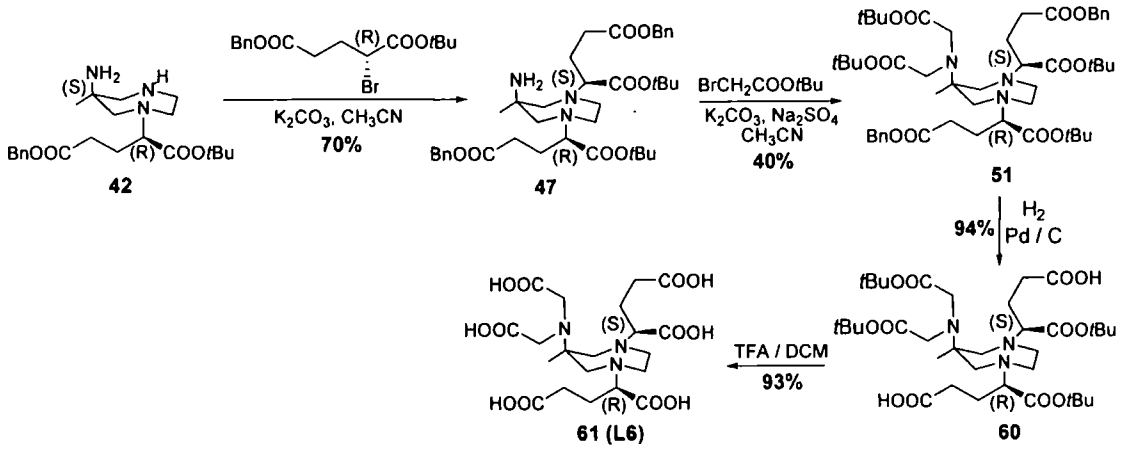

Scheme IV.10: Preparation of ligand (Glu)$_2$(*RS*)-AAZTA, L6, from the ethanol soluble diastereoisomer 42.

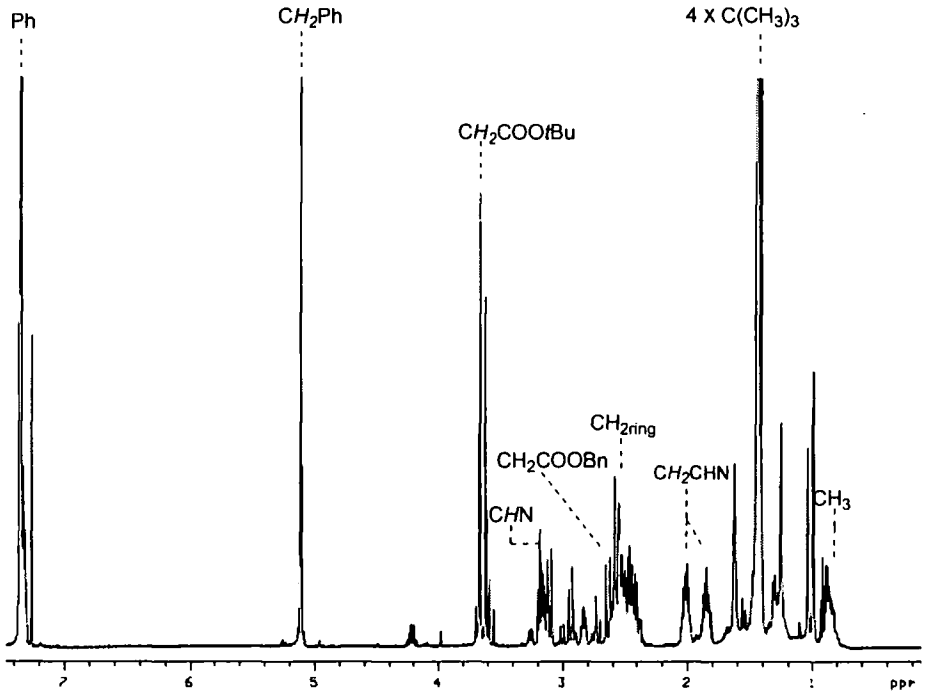

Figure IV.16: ^{1}HNMR spectrum of the fully functionalized ligand structure 51 (700 MHz, $CDCl_3$).

The lanthanide (Yb^{III}, Eu^{III}, Gd^{III}) complexes were prepared following the classical procedure of slowly adding an aqueous solution of the hexahydrate lanthanide salt ($LnCl_3 \cdot 6H_2O$) to the ligand, also dissolved into water. The pH value was kept constant at ~ 5.5 by adding aqueous potassium hydroxide solution, and stirring of the reaction mixture at 50 °C overnight led to formation of the lanthanide complex. As already observed with $[Ln^{III}(Glu)_2$*racemic*-AAZTA$]^{3-}$, the precipitation of a white solid straight after the addition of the metal ion solution was observed. The resulting solid was, once again, soluble only in acidic water and from ES-MS it was determined to be a mixture of lanthanide complex (which it was not possible to separate from the other components of the precipitate), salts and a 2:1 metal:ligand species (LM_2). The lanthanide complex was dissolved in the supernatant, and the excess lanthanide was removed as the corresponding hydroxide by raising the pH of the solution to ~ 10 with aqueous potassium hydroxide solution.

^{1}H NMR analysis of the Yb^{III} and Eu^{III} complexes (shown in **Figure IV.17** and **IV.18**, respectively) showed that two species were in solution, in approximately a 1:4 ratio (Yb^{III} complex) and 1:3 (Eu^{III} complex). The chemical shifts observed for the isomers of the Yb^{III} (*RS*)-complex correspond to those found for the (*RR*)-diastereoisomer. Noticeably, the diastereomeric mixture of the $[Yb^{III}(Glu)_2$*(RS)*-AAZTA$]^{3-}$ complexes was enriched in the same isomer as the racemic mixture $[Yb^{III}(Glu)_2$*racemic*-AAZTA$]^{3-}$, just the isomeric abundance in solution was different ($[Yb^{III}(Glu)_2$*(RS)*-AAZTA$]^{3-}$ 1:4 / $[Yb^{III}(Glu)_2$*racemic*-AAZTA$]^{3-}$ 9:4).

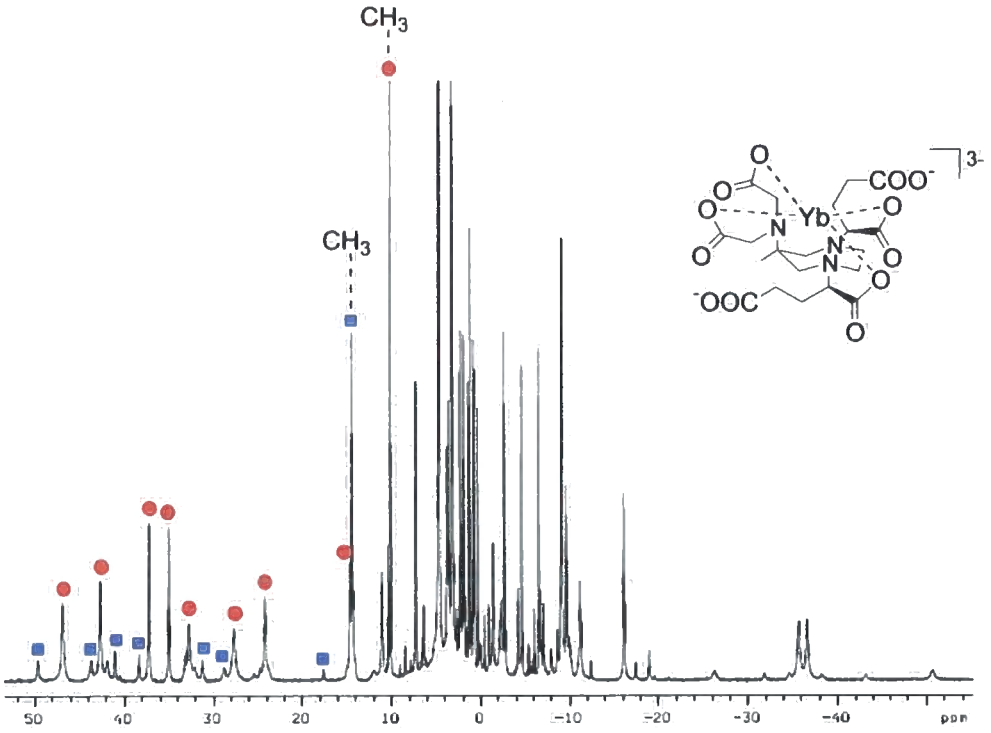

Figure IV.17: ^{1}H NMR spectrum of $[Yb^{III}(Glu)_2$*(RS)*-AAZTA$]^{3-}$ (700 MHz, D_2O, pD 5.4, 24 °C).

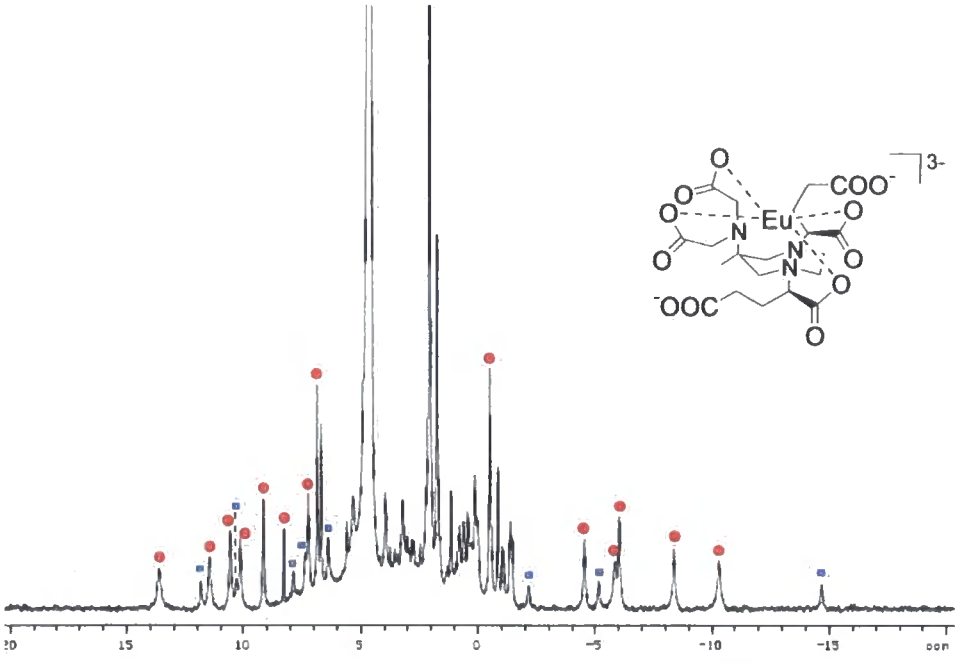

Figure IV.18: ^{1}H NMR spectrum of [Eu^{III}(Glu)$_2$*(RS)*-AAZTA]$^{3-}$ (700 MHz, D_2O, pD 5.4, 24 °C).

Magnetic and luminescence measurements were performed on the Gd^{III} and Eu^{III} complexes, respectively. Rate constants for the depopulation of the excited states of [Eu^{III}(Glu)$_2$*(RS)*-AAZTA]$^{3-}$ (k_{H2O} = 3.34 ms^{-1} and k_{D2O} = 1.27 ms^{-1}) allowed an estimation of the degree of hydration of the complex,[6] giving a q = 2.18.

An r_{1p} value of 7.5 mM^{-1}s^{-1} was measured for the [Gd^{III}(Glu)$_2$*(RS)*-AAZTA]$^{3-}$ complex at 20 MHz, 25 °C. Variable temperature ^{17}O NMR R_{2p} measurements (600 MHz, neutral pH, 25 °C) gave a water exchange rate at the Gd^{III} centre of 243 ns. This τ_m value is the lowest of those measured for the other AAZTA-diglutarates, *i.e.* [Gd^{III}(Glu)$_2$*(RR)*-AAZTA]$^{3-}$ and [Gd^{III}(Glu)$_2$*racemic*-AAZTA]$^{3-}$.

IV.4 Summary and analysis of the results obtained for the glutarated AAZTA derivatives

In **Table IV.1** the best fitting parameters determined by analysis of the $1/T_1$ NMRD and VT ^{17}O NMR R_{2p} profiles are reported and compared to the Gd^{III} chelates based

on the AAZTA core structure (molecular structures in **Figure IV.19**) discussed in this chapter.

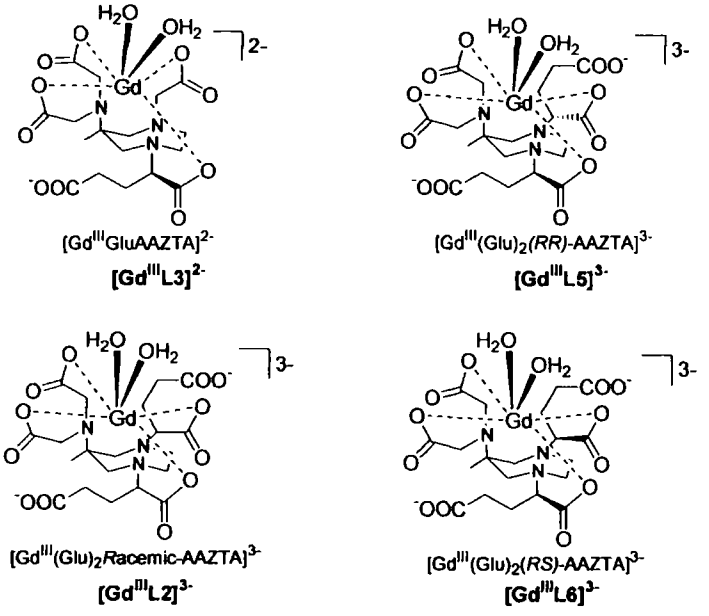

Figure IV.19: The four synthesized Gd^{III}chelates based on the AAZTA core structure.

Gd^{III} chelate	r_{1p} ($mM^{-1}s^{-1}$) -20 MHz, 298K-	τ_m (ns)	$\Delta^2(s^{-2})$	τ_V (s)
$[Gd^{III}GluAAZTA]^{2-}$	7.3	115	3.4×10^{19}	2.1×10^{-13}
$[Gd^{III}(Glu)_2(RR)AAZTA]^{3-}$	8.6	720	2.2×10^{19}	6.3×10^{-13}
$[Gd^{III}(Glu)_2(rac.)AAZTA]^{3-}$	8.0	414	2.7×10^{19}	2.8×10^{-13}
$[Gd^{III}(Glu)_2(RS)AAZTA]^{3-}$	7.5	243	1.57×10^{19}	2.8×10^{-13}

$[Gd^{3+}]$ have been determined by mineralization with HCl 37% at 120°C overnight

Table IV.1: Best fitting parameters determined by analysis of NMRD profiles and VT ^{17}O NMR R_{2p} experiments.

IV.4.1 Diglutarate AAZTA adducts: summary of observations

The diglutarate ligand exists as *(RR)*- and *(RS)*- isomers. Both structures were prepared by alkylation of the AMPED secondary amines with the enantiopure α-bromo diester **41** (in the case of the *(RR)*-isomer) and **46** (used only in the second

alkylation step for the preparation of the *(RS)*-isomer). A mixture of stereoisomers (*RR/SS-RS=SR*) was also prepared from the racemic α-bromo diester **35** (**Figure IV.20**).

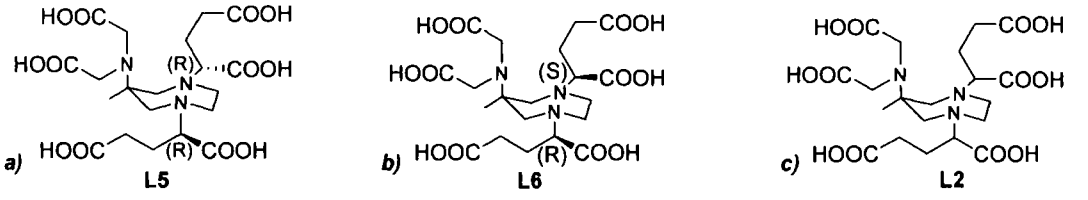

Figure IV.20: Diglutarate derivatives based on AMPED: *a) (RR)*-isomer, *b) (RS)*-isomer and *c) racemic* isomeric mixture.

The ligands used to prepare the complexes were shown to be one isomeric species, as deduced by TLC and NMR analysis. Yb^{III} complexes based on the *(RR)*-ligand system gave rise to a $\geq$ 9:1 mixture of complex stereoisomers, while the *(RS)*-system afforded a 1 : 4 mixture of the same isomeric types. In the ^1H NMR spectra of the corresponding Eu^{III} complexes, these two isomeric complexes could also be identified, present in ratio 8:1 (*(RR)*-isomer) and 1:3 (*(RS)*-isomer), displaying identical chemical shifts. With Yb^{III} complexes prepared from the racemic ligand (mixture of the *RR/SS-RS=SR* isomers), a 9:4 ratio is obtained, in perfect agreement with the 9+1 : 1+4 ratios mentioned for the (*RR)*- and (*RS)*- systems (this comparison between relative isomeric abundances is shown in **Figure IV.21**). Attempts to epimerise the statistical complex isomeric mixture in the Yb^{III} or Eu^{III} complexes did not seem to work: over the pH range 2.5 to 6 no change in the complex isomer ratio was observed on prolonged heating. Each of the examined Yb^{III} complexes (*(RR)*-, *(RS)*- and *racemic*- mixture) appears in the NMR analysis as a mixture of two complex stereoisomers, in slightly different ratio to the correspondent Eu^{III} complexes. The two stereoisomeric species show similar chemical shift behaviour. However, the small differences in the chemical shifts of their resonances allow the distinction of the two species. In the Yb^{III} complexes ^1H-NMR spectra, for example, the C-Me group resonates at about 10 ppm for one species and at 14 ppm for the other one.

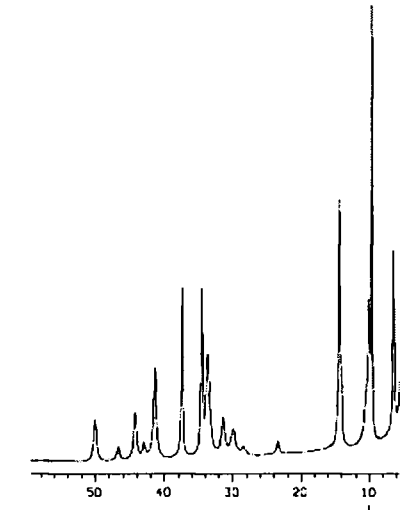

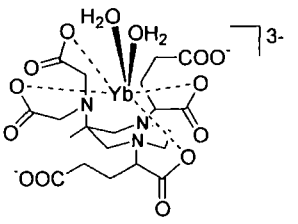

a) ^{1}H NMR spectrum (200 MHz, 20 °C, pH 5.5) of the $[Yb^{3+}(Glu)_2$*racemic*-AAZTA$]^{3-}$ complex (9 : 4 ratio).

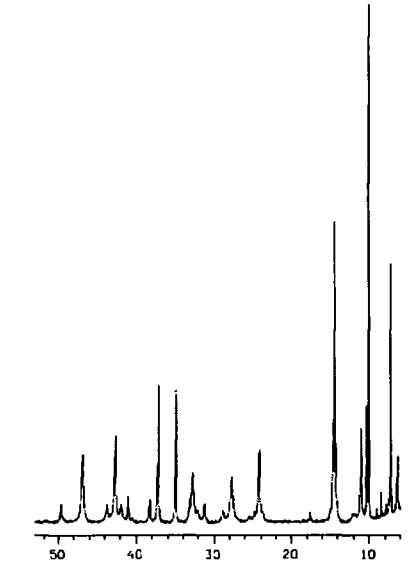

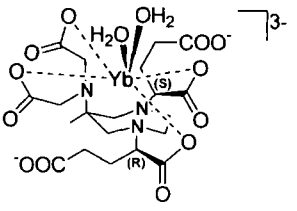

b) ^{1}H NMR spectrum (700 MHz, 20 °C, pH 5.5) of the $[Yb^{3+}(Glu)_2$*(RS)*-AAZTA$]^{3-}$ complex (1 : 4 ratio).

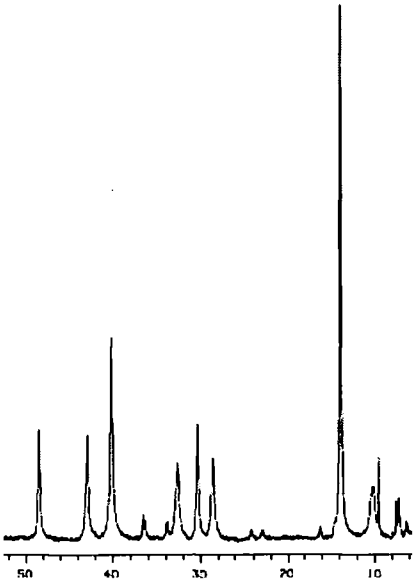

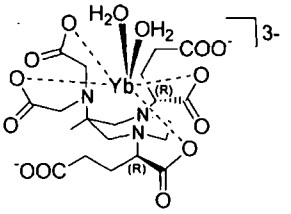

c) ^{1}H NMR spectrum (700 MHz, 20 °C, pH 5.5) of the $[Yb^{3+}(Glu)_2$*(RR)*-AAZTA$]^{3-}$ complex (≥ 9 : 1 ratio).

Figure IV.21: Sections of ^{1}H NMR spectra (700 and 200 MHz, D_2O, 20 °C) showing the most shifted resonances for the Yb^{III} diglutarated AAZTA complexes *a), b)* and *c).*

In the Gd^{III} complexes, the measured relaxivities at 20 MHz, 25 °C were about 8.0 $mM^{-1}s^{-1}$, typical values for a diaqua complex of this molecular volume.

From the VT ^{17}O NMR R_{2p} measurements, undertaken at 600 MHz and neutral pH, the water exchange rates associated with each Gd^{III} complex were obtained. The *(RR)*-system (8:1 isomeric mixture from ^1H NMR of the Eu^{III} complex) possesses a slow rate of water exchange (k_{ex}) of $1.4 \cdot 10^6$ s^{-1}. The *(RS)*-system (1:3 isomeric mixture, from ^1H NMR of the Eu^{III} complex) showed a k_{ex} of $4.1 \cdot 10^6$ s^{-1} and for the Gd^{III} complex derived from the statistical mixture of isomers, a k_{ex} of $2.4 \cdot 10^6$ s^{-1} was measured.

Solving the simultaneous equations **(1)** and **(2)** related to the *(RR)*- and *(RS)*-systems and using mole fractions to weight the contributions of the individual isomers (*x* and *y*):

$$(RR) \quad 1.4 \cdot 10^6 = 0.88\,x + 0.11\,y \qquad \textbf{(1)}$$

$$(RS) \quad 4.1 \cdot 10^6 = 0.25\,x + 0.75\,y \qquad \textbf{(2)}$$

allows the identification of the rate of water exchange of the individual complex stereoisomers. Thus, one isomer exchanges water more slowly than the other, as in gDOTA[9] and analogues:[2] a factor of six separates the two water exchange rates, which correspond to (*x*) $k_{ex} = 9.2 \cdot 10^5$ s^{-1} and (*y*) $k_{ex} = 5.4 \cdot 10^6$ s^{-1}. These results lead to the conclusion that in the *(RS)*-system, the more abundant stereoisomer (in the 8:1 mixture) is also the one possessing the faster water exchange rate, while in the *(RR)*-system the major isomer in the 1:3 mixture is the one possessing the slower exchange rate. The analysis is consistent (± 10%) also using mole fractions derived from the ratios determined by ^1H NMR of the Yb^{III} analogue mixture of isomers.

A comparison between the ^{17}O NMR R_{2p} *vs* temperature profiles of the three synthesized di-glutarate Gd^{III} AAZTA derivatives is shown in **Figure IV.22** and in **Figure IV.23**. It highlights the higher transverse relaxation time values (at different temperatures) shown by the enantiomerically pure *(RS)*- isomer $[Gd^{III}(Glu)_2$*(RS)*-

AAZTA]$^{3-}$ compared to the racemic isomeric mixture [$Gd^{III}(Glu)_2$*racemic*-AAZTA]$^{3-}$

.

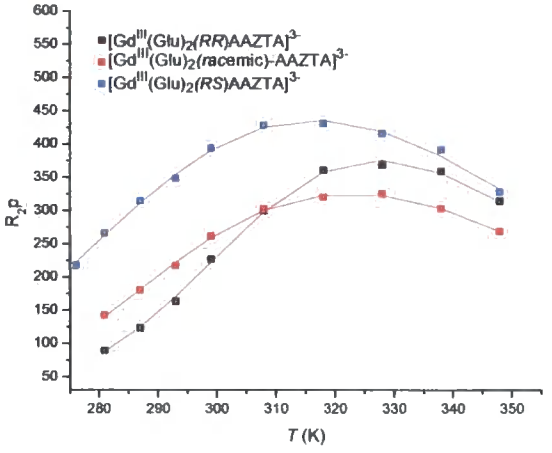

Figure IV.22: Comparison of the ^{17}O NMR R_{2p} /T profiles (600 MHz, pH 7) for [$Gd^{III}(Glu)_2$*(RS)*-AAZTA]$^{3-}$, [$Gd^{III}(Glu)_2$ *racemic.*-AAZTA]$^{3-}$ and [$Gd^{III}(Glu)_2$*(RR)*-AAZTA]$^{3-}$.

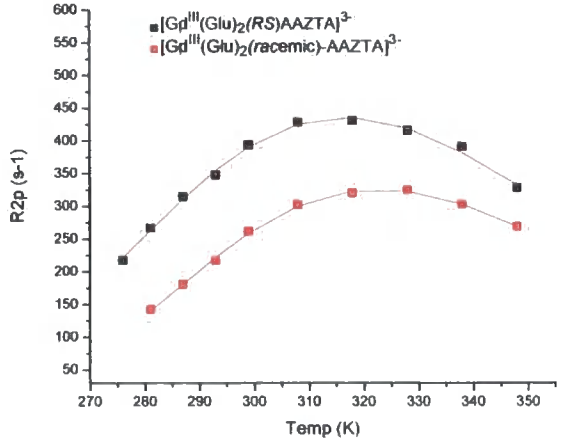

Figure IV.23: Comparison between ^{17}O NMR R_{2p} / T profiles (600 MHz, pH 7) of [$Gd^{III}(Glu)_2$*(RS)*-AAZTA]$^{3-}$ and [$Gd^{III}(Glu)_2$*(racemic)*-AAZTA]$^{3-}$.

IV.4.2 Monoglutarate AAZTA adducts: summary of observations

In the monosubstituted series, the *(RR)*- and *(SR)*- stereoisomers (**Figure IV.24**) were separated after monoalkylation of the AMPED core.

Figure IV.24: ***(RR)*- and *(SR)*- monoalkylated AMPED stereoisomers.**

The absolute configurations have still not been assigned, since no crystals of suitable quality for X-ray diffusion have been isolated. One diastereoisomer was taken forward (**42**, soluble in ethanol) and synthetically elaborated. The carboxymethyl groups were added, to obtain the ligand as one stereoisomer (as confirmed by ^{1}H NMR spectroscopy). Separately, the other isomer (**43**) was also brought forward. The Yb^{III} complex of the monoglutarated ligand **L3** (derived from isomer **42**) was initially promising, as one major complex isomer species (9:1) was observed, characterized by a chemical shift of 9 ppm for its methyl group.

The related Eu^{III} complex also formed one main complex species and the Gd^{III} complex had a relaxivity of 7.3 $mM^{-1}s^{-1}$ and a water exchange rate, $k_{ex} = 8.7 \cdot 10^{6}\ s^{-1}$.

In **Figure IV.25** is shown a comparison between the ^{17}O NMR R_{2p} / temperature profiles (600 MHz, pH 7) of two of the disubstituted $[Gd^{III}Glu_2$*(RR)*-AAZTA$]^{3-}$ and $[Gd^{III}Glu_2$*racemic*-AAZTA$]^{3-}$ complexes and the mono-substituted $[Gd^{III}GluAAZTA]^{2-}$.

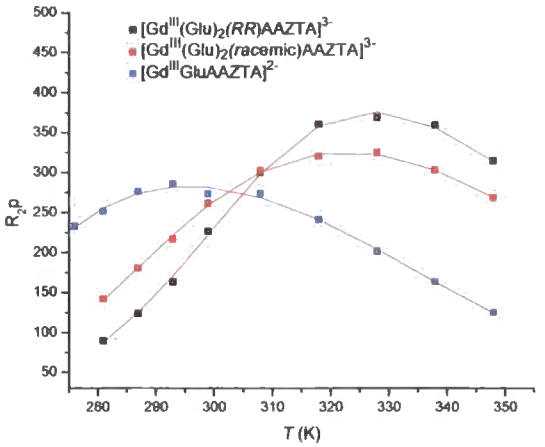

Figure IV.25: Comparison between ^{17}O NMR R_{2p} / T profiles (600 MHz, pH 7) of [Gd^{III}(Glu)$_2$*(RS)*-AAZTA]$^{3-}$, [Gd^{III}(Glu)$_2$*racemic*-AAZTA]$^{3-}$ and [Gd^{III}GluAAZTA]$^{2-}$.

The more concave shape shown by the VT ^{17}O NMR R_{2p} profile of the monoglutarate compared to the other diglutarated AMPED derivatives is consistent with its faster water exchange rate which, however, is not as fast as the target value of $\tau_m \sim 20$ ns.

IV.5 Amide derivatives of Gd^{III}AAZTA glutarated complexes

The main idea of this final work on the lanthanide AAZTA glutarate compounds is to adorn the periphery of the mono- and di-glutarate Gd^{III} chelates possessing faster water exchange rates (in **Figure IV.26**) with bulky, hydrophilic moieties.

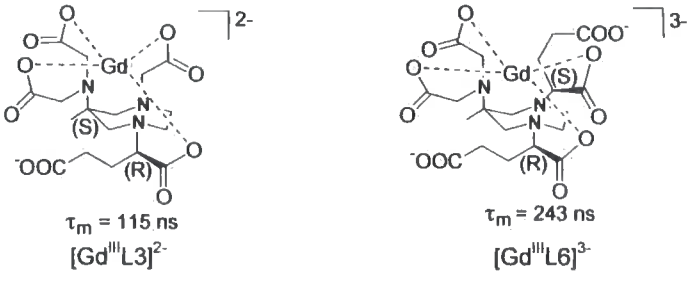

Figure IV.26: The two glutarate Gd^{III} chelates (pH 5.5) used for amide coupling with hydrophilic moieties.

It was thought that, in this way, the overall relaxivity would be enhanced, as a consequence of the increased molecular volume (*i.e.* slower molecular tumbling) and possibly of a more pronounced second sphere contribution to the overall relaxivity.
To test the reactivity of the free (*i.e.* not coordinated to the metal ion) carboxylated functions of the Gd^{III} chelates towards amide bond formation, a coupling reaction with the TRIS amino group was firstly attempted. Two different routes were explored: the first one is shown in **Scheme IV.11**, and it involves the direct coupling of the amine free carboxylate groups of the Yb^{III} chelate.

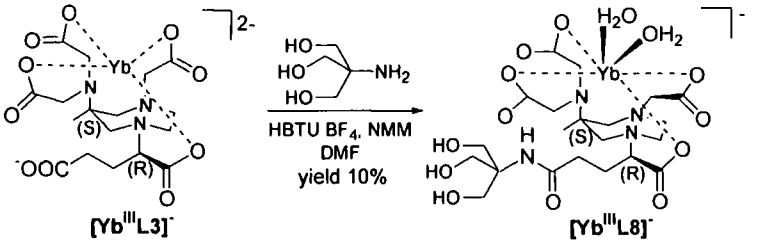

Figure IV.11: Direct coupling of TRIS to the Yb^{III} chelate free carboxylate pendant arm.

This one step synthetic pathway led to the product, **$[Yb^{III}L8]^-$**, which was obtained in modest yield. The same synthetic strategy did not afford the desired product when applied to the diglutarated complex $[Gd^{III}(Glu)_2$*(RS)*-AAZTA$]^{3-}$, and the alternative pathway shown in **Scheme IV.12** was therefore followed. This involved the functionalization of the carboxylic function of the ligand structure still *tert*-butyl protected, removal of the *tert*-butyl groups and finally complexation of the ligand **L7**.

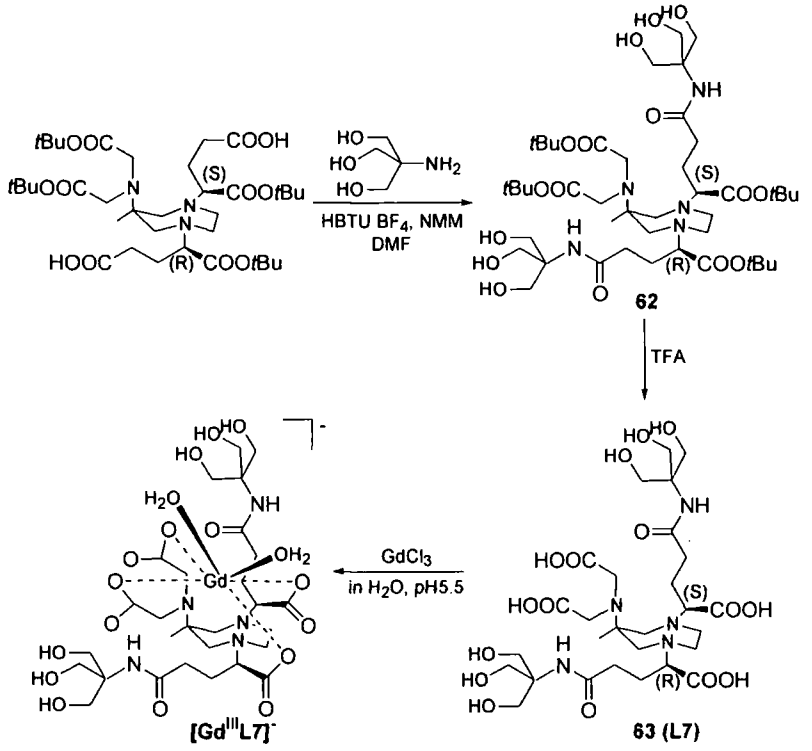

Scheme IV.12: The "long route" for functionalizing the glutamic carboxylate.

Relaxometric measurements were performed on the TRIS dialkylated adduct $[\mathbf{Gd^{III}L7}]^-$ and an r_{1p} of 7.7 $mM^{-1}s^{-1}$ (T_1 = 158.1 ± 0.2 ms at 60 MHz, 37°C; $[Gd^{3+}]_{ICP}$ = 0.12 mg / mL) was observed, disappointingly similar to the value found for the parent complex $[Gd^{III}(Glu)_2$*(RS)*-AAZTA$]^{3-}$, with r_{1p} was 7.5 $mM^{-1}s^{-1}$ (20 MHz, 25°C).

Other amide derivatives of Ln^{III} AAZTA glutarate complexes were prepared. Carbohydrate containing wedges were chosen as the bulky and hydrophilic substituents suitable to be attached to the lanthanide mono- and digluatarate AAZTA chelate cores. In **Scheme IV.13** the carbohydrate wedge was coupled to the free carboxylic side arm function by amide bond formation, promoted by the coupling agent HBTU · BF_4, using *N*-methylmorpholine as base.

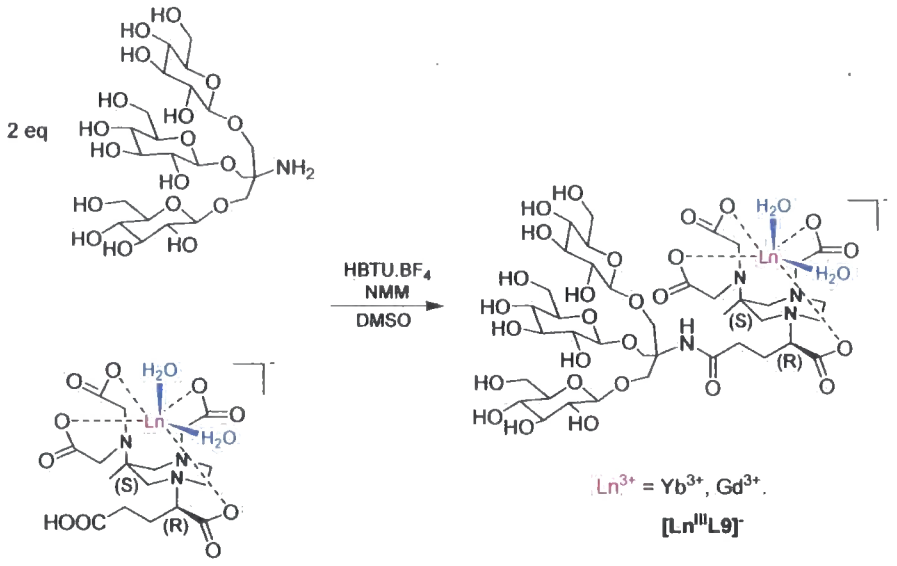

Scheme IV.13: Coupling reaction of carbohydrate wedges to $[Gd^{III}GluAAZTA]^-$.

Both ytterbium and gadolinium adducts were prepared and purified by HPLC (^1H NMR and ES-MS spectra are reported in the **Appendix**). Relaxometric measurements were performed on the analogue Gd^{III} adduct, but a low relaxivity value of 3.36 $mM^{-1}s^{-1}$ (at 20 MHz, 25 °C) was obtained. An r_{1p} value of 4.87 $mM^{-1}s^{-1}$ was found for the compound at 60 MHz, 37 °C.

An amide derivative of $[Gd^{III}(Glu)_2$*(RS)*-AAZTA$]^{3-}$ was also prepared, by using the same method previously described for $[Yb^{III}$(Gluco)GluAAZTA$]^-$: the primary amine was coupled to the glutaric carboxylate pendant arms of the Gd^{III} complex (**Scheme IV.14**).

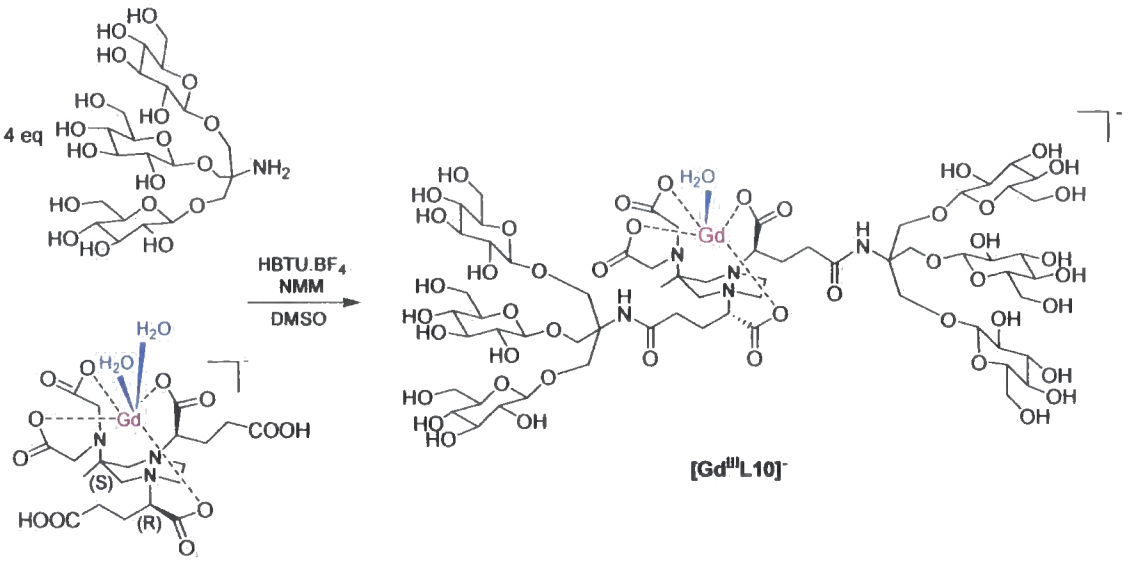

Scheme IV.14: Coupling reaction of carbohydrate wedges to $[Gd^{III}(Glu)_2$*(RS)*-AAZTA$]^-$.

An ES-MS of **$[Gd^{III}L10]^-$** is shown in the **Appendix**. Fitting of the VT ^{17}O NMR R_{2p} profile shown in **Figure IV.27** allowed an estimation of the water exchange rate, and the value of τ_m was determined to be 205 ns.

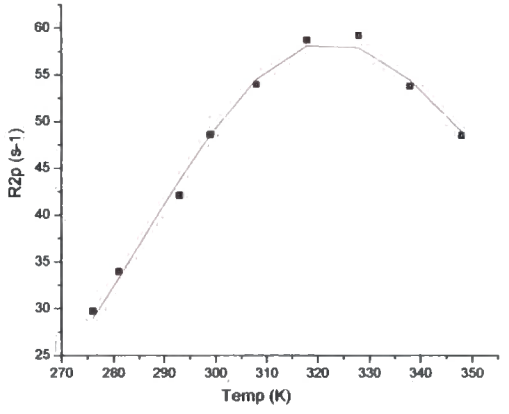

Figure IV.27: ^{17}O NMR R_{2p} / T profiles (600 MHz, pH 7) for $[Gd^{III}(Gluco)_2(Glu)_2$*(RS)*-AAZTA$]^{3-}$.

Relaxivity measurements on **$[Gd^{III}L10]^-$** gave an r_{1p} value of 15 $mM^{-1}s^{-1}$ (at 60 MHz, 37 °C). However, this value is in disagreement with the results obtained by our collaborators in University of Torino, who measured a relaxivity of 7.1 $mM^{-1}s^{-1}$ at 20

MHz, 25 °C. This last value is low with respect to the molecular weight of the complex (MW 1834), and making think of a reduction in the hydration number from $q = 2$ to $q = 1$ after coupling of the central diglutarate AAZTA chelate to the bulky carbohydrate substituents. $1/T_1$ NMRD profiles were measured for the **[Gd^{III}L10]$^-$** complex at 25 and 37 °C (**Figure IV.28**), and the fact that the relaxivity at 37 °C was lower than that at 25 °C indicates that there is not a kinetic limit to the relaxivity itself, and the τ_m is short enough not to limit this value.

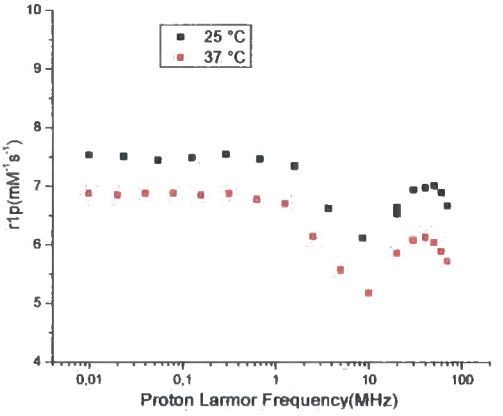

Figure IV.28: $1/T_1$ NMRD profiles for [Gd^{III}L10]$^-$ at 25 and 37 °C.

For purposes of comparison, the $1/T_1$ NMRD profile of **[Gd^{III}L10]$^-$** at 25 °C is shown in **Figure IV.29** with the $1/T_1$ NMRD profile of a $q = 2$ system of similar molecular weight prepared in the Bracco Imaging S.p.A. laboratories.

The two amide derivatives of Gd^{III} AAZTA glutarated complexes present $1/T_1$ NMRD profiles of similar overall form. However, the lower relaxivity measured for **[Gd^{III}L10]$^-$** can only be explained by setting a value of $q = 1$ in the fitting. In **Table IV.2** are reported the main parameters obtained from the fitting.

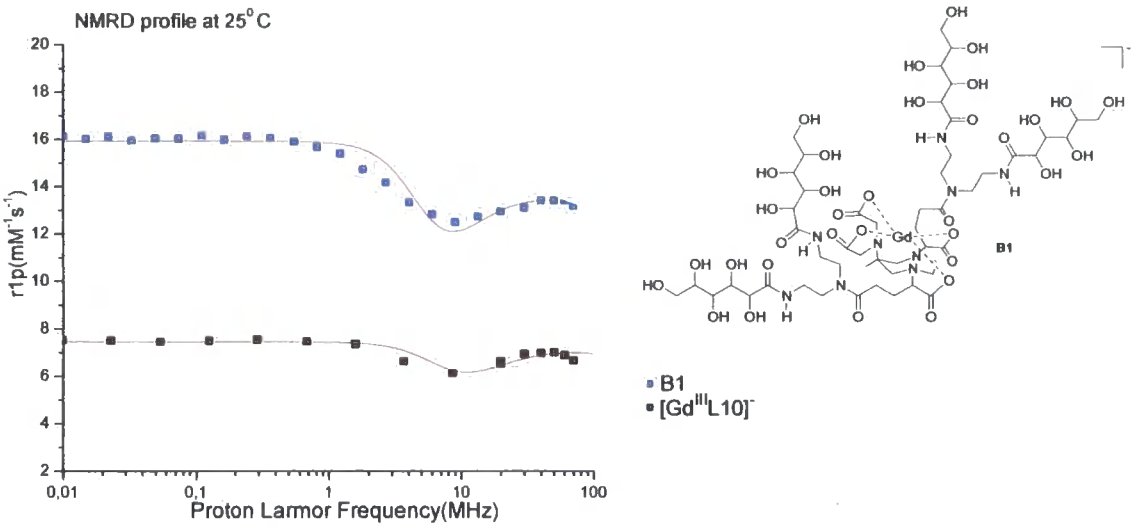

Figure IV.29: Comparison between $1/T_1$ NMRD profile of $[Gd^{III}L10]^-$ and that of a $q = 2$ Bracco Imaging S. p. A. compound (B1) of similar molecular volume.

	r_{1p} (20 MHz, 298K) $mM^{-1}s^{-1}$	τ_m (ns)	$\Delta^2(s^{-2})$	τ_V (s)	τ_R(ps)	q
B1	13.3	1760	2.6×10^{19}	2.8×10^{-11}	316	2
$[Gd^{III}L10]^-$	7.1	205	7.05×10^{19}	2.12×10^{-11}	167	1

$[Gd^{3+}]$ have been determined by mineralization with HCl 37% at 120°C overnight.

Table IV.2: Main parameters obtained from the fitting of $1/T_1$ NMRD profile and VT ^{17}O R_{2p} profile of $[Gd^{III}L10]^-$ and a $q = 2$ Bracco Imaging S. p. A. compound of similar molecular volume.

IV.6 Conclusions

A series of lanthanide AAZTA complexes with glutarate substituents has been prepared, and their magnetic properties have been defined. Measurement of the NMRD profiles has allowed an estimation of the relaxivity values at different magnetic field strengths and the fitting of the VT ^{17}O R_{2p} profiles afforded the water exchange rates at the paramagnetic centre of each Gd^{III} complex. Gd^{III} complexes of the *(RR)*, *(RS)* and the *racemic-* ligands were isolated and their Eu^{III} and Yb^{III} analogues characterized by NMR. This allowed a measurement of the ratio of the individual complex (Δ / Λ) stereoisomers in solution.

A difference exists between the water exchange rates measured for the different isomers: the fastest τ_m value is exhibited by the "diglutarated" AAZTA derivative $[Ln^{III}(Glu)_2$*(RS)*-AAZTA$]^{3-}$ (τ_m = 243 ns, where $\tau_m = 1/k_{ex}$). More precisely, this water exchange is given by the contribution of the τ_m values of the two complex stereoisomers constituent the $[Ln^{III}(Glu)_2$*(RS)*-AAZTA$]^{3-}$ system. Solving the simultaneous equations (as reported in **section IV, XX**) related to the (*RS*)-system allowed an evaluation of the contribution of the individual isomers to the observed water exchange rate. The more abundant isomer possesses a $k_{ex} = 5.4 \cdot 10^6$ s^{-1}, six times faster than the other, which shows a $k_{ex} = 9.2 \cdot 10^5$ s^{-1}. This noticeable difference among water exchange rates of complex stereoisomers suggested that further systems could be developed based upon this particular isomeric structure. However, the water exchange rate value found to be the fastest among these glutarated AAZTA based systems does not seem so extraordinary when compared with other similar sized systems, for example the q = 1 *(RRRR-SSSS)* $[Gd^{III}$gDOTA$)]^{5-}$, which exhibits a $k_{ex} = 1.85 \cdot 10^7$ s^{-1}.

The molecular volume of the faster water exchanging "diglutarated" $[Ln^{III}(Glu)_2$*(RS)*-AAZTA$]^{3-}$ and "monoglutarated" $[Ln^{III}$(Glu)AAZTA$]^{2-}$ complexes was increased by functionalization of their free carboxylate pendant arms with carbohydrates

containing wedges. The relaxivity values measured for these amide derivatives were not as high as expected for systems of such molecular volume (MW 1834 and 1175 g / mol, respectively). An explanation of this result is a decrease in the hydration number: the number of inner sphere water molecules decreases from $q = 2$ to $q = 1$ as the steric demand increases at the Ln^{III} centre. This increases from Eu^{III} to Yb^{III}, and has been observed, very recently, in the analysis of the X-ray structures of Eu^{III} ($q = 2$) and Yb^{III} ($q = 1$) complexes of related AAZTA complexes.[15] Thus, the functionalization of the AAZTA system with sterically demanding substituents may cause a change in the coordination sphere around the metal ion, hindering the access of a second water molecule to the lanthanide ion.

List of references

[1] Aime, S.; Calabi, L.; Cavallotti, C; Gianolio, E.; Giovenzana, G. B.; Losi, P.; Maiocchi, A.; Palmisano, G.; Sisti, M. *Inorg. Chem.* **2004**, *43*, 7588.

[2] Messeri, D.; Lowe, M. P.; Parker, D.; Botta, M. *Chem. Commun.* **2001**, 2742.

[3] Lowe, M. P. *Aust. J. Chem.* **2002**, *55*, 551.

[4] Hoye, T. R.; Caruso, A. J.; Magee, A. S. *J. Org. Chem.* **1982**, *47*, 4152.

[5] Thompson, N. C.; Parker, D.; Scmitt-Willich, H.; Slzle, D.; Muller, G.; Riehl, J. P. *Dalton Trans.* **2004**, 1892.

[6] Beeby, A.; Clarkson, I. M.; Dickins, R. S.; Faulkner, S.; Parker, D.; Royle, L.; de Sousa, A. S.; Williams, J. A. G.; Woods, M. *J. Chem. Soc., Perkin Trans. 2* **1999**, 493.

[7] Jocher, C. J.; Botta, M.; Avedano, S.; Moore, E. G.; Xu. J.; Aime, S.; Raymond, K. N. *Inorg. Chem.* **2007**, *46*, 4796.

[8] Aime, S.; Gianolio, E.; Corpillo, D.; Cavallotti, C.; Palmisano, G.; Sisti, M.; Giovenzana, G. B.; Pagliarin, R. *Helv. Chim. Acta* **2003**, *86*, 615.

[9] Woods, M.; Aime, S.; Botta, M.; Howard, J. A. K.; Moloney, J. M.; Navet, M.; Parker, D.; Port, M.; Rousseaux, O. *J. Am. Chem. Soc.* **2000**, *122*, 9781.

[10] Aime, S.; Barge, A.; Bruce, J. I.; Botta, M.; Howard, J. A. K.; Moloney, J. M.; Parker, D.; De Sousa, A. S.; Woods, M. *J. Am. Chem. Soc.* **1999**, *121*, 5762.

[11] Aime, S.; Barge, A.; Botta, M.; De Sousa, A. S.; Parker, D. *Angew. Chem. Int. Ed.* **1998**, *37*, 2673.

[12] Batsanov, A. S.; Beeby, A.; Bruce, J. I.; Howard, J. A. K.; Kenwright, A. M.; Parker, D. *Chem. Commun.* **1999**, 1011 – 1012.

[13] Dickins, R. S.; Howard, J. A. K.; Maupin, C. L.; Moloney, J. M.; Parker, D.; Riehl, J. P.; Siligardi, G.; Williams, J. A. G. *Chem. Eur. J.* **1999**, *5*, 1095.

[14] Lattuada, L. (Bracco S.p.A.) personal communication.

[15] Aime, S. (University of Torino) personal communication.

IV.7 Final Conclusions and Future Work

The aim of this research project has been the development of new gadolinium chelates exhibiting good solubility, stability (thermodynamic and kinetic) and paramagnetic properties (*i.e.* relaxivity) which can make them possible candidates for future applications in diagnostic medicine as CAs for MRI.

The challenge was to design innovative systems with superior performance compared to those already on the market. At the outset, a gadolinium chelate possessing carbohydrate containing dendrons coupled to a GdgDOTA core was synthesized. The effective motional coupling obtained with this system, together with its relatively high molecular weight (~3400 $gmol^{-1}$) translated into a slower molecular tumbling (*i.e.* lower τ_R values) and therefore enhanced efficacy of the contrast agent at the magnetic fields typically used for MRI applications. An alternative strategy was investigated using a series of new heptadentate ligands based on a 1,4-diazepine core structure. Phosphinate groups were attached to the endocyclic nitrogens, but the resultant di-aqua complexes of Ln^{III} ions were not sufficiently stable with respect to competitive anion coordination. Alternative structures using appended glutarate groups were synthesized in a stereocontrolled manner. However, although these systems were stable to added anions, the water exchange rate of the Gd^{III} complexes was not sufficiently fast to allow their exploitation in higher molecular weight derivatives. Significant differences in water exchange rate were identified for particular stereoisomeric complexes, suggesting that caution needs to be exercised to consider this issue in designing such systems. Future strategies to develop high relaxivity di-aqua systems require a di-aqua binding site that is further away from the site of ligand functionalization (to increase molecular volume), without compromising motional coupling. Such a system has been achieved, of course, for a mono-aqua system, as described in Chapter 2.

Chapter 5

Experimental

Experimental Methods

5.1 Experimental Details

All reagents were used as supplied by commercial sources unless otherwise stated. Solvents were dried over the appropriate drying agents when required. Water and H_2O refer to high purity water with conductivity ≤ 0.04 μScm^{-1}, obtained from the "Purite$_{STILL}$ Plus" purification system.

Reactions requiring anhydrous conditions were carried out using Schlenk-line techniques under an atmosphere of dry argon. Anhydrous solvents when required were freshly distilled over the appropriate drying agent as indicated below:
dichloromethane and triethylamine were dried over calcium hydride; *N,N*-dimethylformamide over molecular sieves; nitromethane was dried over calcium chloride and left to stand over molecular sieves; THF, methanol, acetonitrile were used as received from the solvent purification system "Pure Solv".

All pH measurements were performed using a Jenway 3320 pH meter attached to an Aldrich Chemical Company micro–pH combination electrode, calibrated using pH 4, 7 and 10 buffer solutions.

Chromatography

Thin-layer chromatography was carried out on silica plates (Merck 5554) and visualised under UV light (254 nm) or by washing in a bath of ethanol/sulphuric acid 5% or permanganate or by staining with iodine. Preparative column chromatography was performed using neutral aluminium oxide (Merck Aluminium Oxide 90, activity II–III, 70–230 mesh) washed in ethyl acetate, or silica (Merck Silica Gel 60, 230–400 mesh).

Gel filtration chromatography (GPC): used a P6 Biogel stationary phase, eluting with water, 0.7 mL/min.

The HPLC analysis and separation was carried out on a Perkin Elmer system comprising a Perkin Elmer Series 200 Pump, Perkin Elmer Series 200 Autosampler, Perkin Elmer Series 200 Fluorescence detector. GILSON-FC203B fraction collector was used in separation procedures. The stationary phase was a Phenomenex Synergi 4μ Fusion-RP 80, and the size of the column used was 150x4.6 mm (flow rate 1mL/min). The methods used are described below.

- **Chromatographic method A1 (HPLC)**

Perkin Elmer Series 200 Pump

Perkin Elmer Series 200 Autosampler

Perkin Elmer Series 200 Diode array detector

Column: Phenomenex Synergi 4μ Fusion-RP 80

Column dimensions: 150*4.6 mm

Particle size: 4 μm

Flow rate: 1 ml/min

Detection (UV): 210 nm, 254 nm.

Injection volume: 100 μl

Mobile phase:

A: H_2O
B: Acetonitrile

Programme A1:

Time (min)	Solvent A (%)	Solvent B (%)	Gradient
0	100	0	0
10	100	0	0
20	0	100	1
22	0	100	0
24	100	0	-3
28	100	0	0

- **Chromatographic method A-2 (HPLC)**

Stationary phase: Lichrosorb 60 RP-Select B 5 µm

75 x 4 mm column packed by Merck KGaA

Temperature: 45 °C

Mobile phase: gradient elution

A = 0.01 M KH_2PO_4 and 0.017 M H_3PO_4 in water

B = CH_3CN

Gradient timetable:

min	% A	% B
0	95	5
15	20	80
20	20	80

Flow rate: 1 mL min^{-1}

Detection (UV): 210 nm

Injection: 10 µL

Sample conc.: 1 mg mL^{-1}

Instrumentation : VWR Elite LaChrom- Hitachi high pressure gradient pump system (L-2100), VWR Elite LaChrom - Hitachi L-2200 autosampler, VWR Elite LaChrom - Hitachi L 2300 column oven, VWR Elite LaChrom - Hitachi L 2400 UV detector

Spectroscopy

^{1}H and ^{13}C NMR spectra were recorded on a Varian Unity-300 spectrometer (^{1}H at 299.908 MHz, ^{13}C at 75.412 MHz), Varian VXR 400 (^{1}H at 399.968 MHz, ^{13}C at 100.572 MHz), Bruker AMX 500 spectrometer or Varian Unity-700 spectrometer (^{1}H at 699.73 MHz). Spectra were referenced internally to the residual proton-solvent resonances and are reported in ppm relative to TMS, with coupling constants in Hz (typically ±0.4 Hz).

Electrospray mass spectra were recorded on a VG Platform II (Fisons Instruments), operating in positive or negative ion mode, with methanol as the carrier solvent. Accurate masses were recorded on a Thermo Finnigan LTQ instrument.

Luminescence spectra of the Eu^{III} complexes were recorded using a direct excitation of the Eu^{III} ion at 255 nm or 397 nm.

Lifetime measurements of the Eu^{III} complex were recorded on a Perkin Elmer LS55 luminescence spectrometer using FL Winlab software. The Eu^{III} ion was excited directly at 255 nm or 397 nm, with an excitation slit width of 10 nm. Lifetime values were measured following excitation of the sample by a short pulse of light, monitoring the integrated intensity of light (613 nm for europium) emitted during a fixed gate time, t_g, a delay time, t_d, later. A gate time of 0.1 ms was used. The data obtained follow an exponential decay:

$$I = A_0 e^{(-kt)}$$

where I = intensity at time t after the flash

A_0 = a pre-exponential factor

k = rate constant for the decay of the excited state

A linear form of the relationship was obtained:

$$\ln I = \ln A_0 - kt$$

The data were fitted with this equation in Microsoft Excel. The excited state lifetime, τ, is the inverse of the rate constant, k.

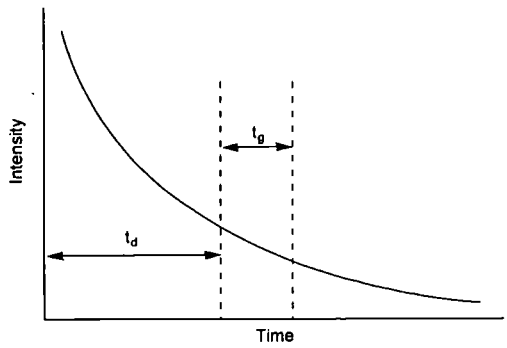

Figure 1: Measured parameters for lifetime measurement.

Experimental Procedures

_N_-(Benzyloxycarbonyl)tris(hydroxymethyl)methylamine (1)

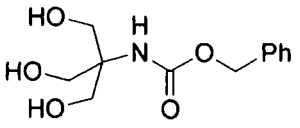

1

Benzyloxycarbonyl chloride (12 mL, 0.084 mol) was added dropwise over 0.5 h to a stirred solution of TRIS (6.7 g, 0.056 mol) in H_2O (30 mL) cooled at 0 ^{0}C. The pH of the medium was maintained at 8-10 by addition of Na_2CO_3. After 1 h of stirring at 0^{0}C, the reaction was allowed to warm to room temperature and left to stir overnight. The white slurry was filtered, washed with H_2O (2×30 mL) and dried for one day under high vacuum. The solid was ground up with a spatula, the water still present was removed by azeotropic evaporation with toluene (2 × 200 mL) and the white powder obtained was dried under high vacuum to afford the product (3.1g, 22%). R_f ($CHCl_3$ / MeOH 9:1, SiO_2) = 0.84 (UV). M.p. = 102 – 104 ^{0}C (lit. 102-104 ^{0}C).[1] δ_H ($CDCl_3$, 300 MHz): 3.71 (6H, s, 3×CH_2), 5.10 (2H, s, O-CH_2-Ph), 5.77 (1H, br s, NH), 7.36 (5H, m, Ph-H). δ_C ($CDCl_3$, 75.41 MHz): 61.7 (C(quat)), 63.0 (CCH_2), 67.0 (CH_2Ph), 128.9, 129.0, 129.5, 138.2 (Ph ring carbons), 157.4 (CO). ES-MS: *m/z* 256 $[M+H]^+$.

1,2,3,4,6-Penta-*O*-benzoyl-α-D-glucopyranose [2] (2)

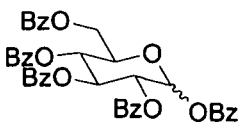

2

Benzoyl chloride (18 mL, 0.15 mol) was added dropwise to a suspension of glucose (5.0 g, 0.027 mol) in pyridine (95 mL) at 0 ^{0}C. The reaction mixture was stirred overnight at room temperature and then washed with H_2O (400 mL) and left to stand

for 1 h. The white precipitate was filtered, washed with HCl (0.2 M, 500 mL) and recrystallized from a mixture of Me_2CO (120 mL) and MeOH (350 mL). The solid obtained was filtered and washed with MeOH (2 × 20 mL) to afford a white solid (13.1 g, 67%). R_f (EtOAc / Hex 3:7, SiO_2) = 0.38 (UV). M.p. 180 - 184 °C (lit. 184 – 186 °C).[2] δ_H ($CDCl_3$, 300 MHz): 4.51 (1H, dd, J = 4.5, 12.6, H-5), 4.65 (2H, dd, J = 1.8, 9.3, H-6), 5.71 (1H, dd, J = 3.7, 10.0, H-2), 5.89 (1H, t, J = 10.0, H-4), 6.35 (1H, t, J = 10.0, H-3), 6.9 (1H, d, J = 3.7, H-1), 7.28 – 7.75 (15H, m, Ph-H), 7.89 – 8.21 (10H, m, Ph-H). δ_C ($CDCl_3$, 75.41 MHz): 62.6 (C-6), 67.1 (C-4), 69.0 (C-2), 70.7 (C-5), 90.3 (C-3), 95.1 (C-1), 128.3 – 130.3 (Ph ring carbons), 133.4, 133.6, 133.8, 134.2 (Ph ring carbons), 164.6, 165.4, 165.6, 166.1, 166.3 (*C*OPh). ES-MS: *m/z* 724 $[M + Na]^+$.

2,3,4,6–Tetra-*O*-benzoyl-α-D-glucopyranosyl bromide [2] (3)

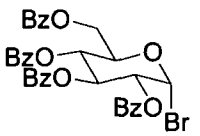

3

1,2,3,4,6-Penta-*O*-benzoyl-α-D-glucopyranose (13.1 g, 0.018 mol) was dissolved in freshly distilled CH_2Cl_2 (20 mL) and treated with 33% HBr in CH_3COOH (20 mL). After standing for 1.5 h at room temperature, the reaction mixture was diluted with CH_2Cl_2 (100 mL) and washed successively with a saturated solution of aqueous $NaHCO_3$ (3 × 100 mL) and with H_2O (100 mL). The organic phase was dried over Na_2SO_4 and concentrated *in vacuo* to afford a light yellow solid (11.6 g, 0.017 mol). The product was recrystallized from a mixture of Et_2O (30 mL) and petroleum ether (12 mL) and left to stand for 0.5 h. The white precipitate was filtered and washed with petroleum ether to afford a white crystalline solid (9.37 g, 79%). R_f (EtOAc / Hex 3:7, SiO_2) = 0.66 (UV). M.p. 127 – 130 °C (lit. 129-130 °C).[2] δ_H ($CDCl_3$, 300 MHz): 4.54 (1H, dd, J = 4.5, 12.3, H-5), 4.66 – 4.78 (2H, m, H-6), 5.34 (1H, dd, J = 4.0, 10.0, H-2), 5.84 (1H, t, J = 10.0, H4), 6.28 (1H, t, J = 10.0, H3), 6.88 (1H, d, J = 4.0, H1), 7.27 – 7.62 (15H, m, Ph-H), 7.88 – 8.10 (10H, m, Ph-H). δ_C ($CDCl_3$, 75.41

MHz): 62.2 (C-6), 68.2 (C-4), 70.8 (C-2), 71.7 (C-5), 72.9 (C-3), 87.1 (C-1), 128.6 - 130.3 (Ph ring carbons), 133.5, 133.6, 133.9, 134.1 (4 × Ph ring carbons), 165.3, 165.6, 165.8, 166.3 (*C*OPh). ES-MS: *m/z* 672 $(M + Na)^+$.

_N_-(Benzyloxycarbonyl)tris(2,3,4,6-tetra-_O_-benzoyl-β-D-glucopyranosyloxymethyl)-methylamine (4)

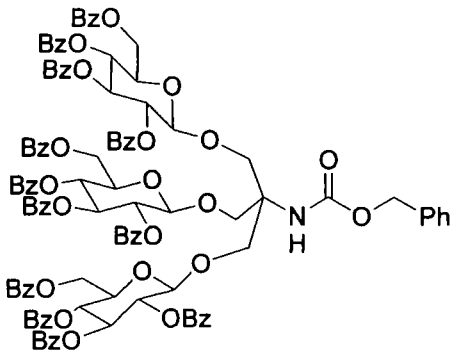

4

AgOTf (0.690 g, 2.654 mmol) was activated by dissolving in anhydrous toluene (10 mL) and the solvent was removed under vacuum. This procedure was repeated a further two times. A mixture of **1** (0.171 g, 0.67 mmol), AgOTf and 2,4,6-collidine (0.255 ml, 1.93 mmol) in CH_2Cl_2 (5 mL) and $MeNO_2$ (5 mL) was stirred at -30 ^{0}C under an argon atmosphere. A solution of 2,3,4,6-tetra-*O*-benzoyl-α-D-glucopyranosyl bromide, **3**, (1.4 g, 2.12 mmol) in CH_2Cl_2 (5 mL) was added dropwise over 20 min to the reaction mixture, which was stirred for 30 min at the same temperature, then for 2 h at 0 ^{0}C and finally left stirring overnight at room temperature. After completion of the reaction (TLC), C_5H_5N (1.0 mL) was added to the reaction mixture, which was left to stir for 30 min and then diluted with CH_2Cl_2 (20 mL), before being filtered through Celite. The filtrate was washed successively with aqueous $Na_2S_2O_3$ solution (1 M, 2 × 50 mL), aqueous HCl solution (0.1 M, 2 × 50 mL), saturated aqueous $NaHCO_3$ solution (2×50 mL) and H_2O (2×50 mL). The organic phase was dried over Na_2SO_4 and the solvent was removed in *vacuo*, to

afford crude product (2.20 g), the TLC of which showed a main product (R_f (EtOAc/Hex 3:7) = 0.11; H_2SO_4), in addition to a few other minor components (R_f = 0.28, 0.48; H_2SO_4). The main product was separated by column chromatography (SiO_2, EtOAc / Hex, 3:7) to yield the product (0.600 g, 45%) as a white foamy solid. R_f (EtOAc / Hex 1:1, SiO_2) = 0.49 (UV, H_2SO_4). δ_H ($CDCl_3$, 500 MHz): 3.55-3.61 (6H, m, $C_{(quat)}CH_a$), 4.03 (3H, d, $^2J_{CHa,CHb}$ = 8.0, $C_{(quat)}CH_b$), 4.31 (3H, d, $^3J_{1,2}$ = 10.5, H-1), 4.37 (3H, dd, $^3J_{5,6a}$ = 6.0, $^2J_{6a,6b}$ = 12.0, H-6a), 4.56 (3H, dd, $^3J_{5,6b}$ = 2.5 $^2J_{6a,6b}$ = 12.0, H-6b), 4.80 (1H, d, $^2J_{Ha,Hb}$ = 12.0, CH_bPh), 4.86 (1H, d, $^2J_{Ha,Hb}$ = 12.0, CH_aPh), 5.36 (3H, dd, $^3J_{1,2}$ = 8.0, $^3J_{2,3}$ = 9.5, H-2), 5.50 (3H, app. t, $^3J_{3,4} \sim {}^3J_{4,5}$ = 9.5, H-4), 5.65 (3H, app. t, $^3J_{2,3} \sim {}^3J_{3,4}$ = 9.5, H-3), 7.29 – 8.12 (65H, br.m., Ph-*H*). δ_C ($CDCl_3$, 125.68 MHz): 59.15 ($C_{(quat)}$), 60.66 (C-6), 63.35 (CH_2Ph), 68.77 ($C_{(quat)}CH_2$), 69.76 (C-4), 72.08 (C-5), 72.18 (C-2), 72.79 (C-3), 101.79 (C-1), 128.45 – 130.34 (Ph ring carbons), 155.15 (urethane *C*O), 164.94, 165.53, 165.98, 166.40 (*C*OPh). ES-MS: *m/z* 2014 $[M+Na]^+$.

_N_-(Benzyloxycarbonyl)tris(β-D-glucopyranosyloxymethyl)methylamine (5)

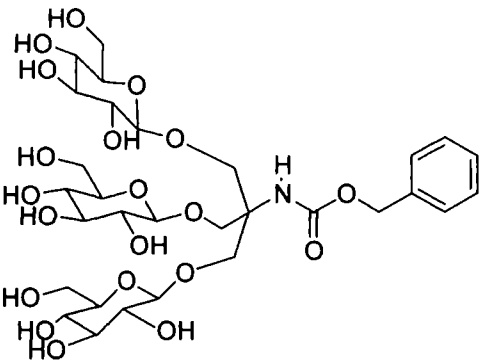

5

A solution of **4** (0.600 g, 0.301 mmol) in methanolic NaOMe (0.1 M, 20 mL) was stirred at room temperature for 6 h, then neutralized with Amberlite IR-120(H^+ form) ion-exchange resin and filtered. The solvents were removed *in vacuo* and the resulting white powder was partitioned between H_2O (20 mL) and Et_2O (15 mL). The aqueous layer was washed with further Et_2O (3 × 15 mL) and then freeze-dried

to obtain **5** as a colourless glass (0.22 g, 98%). R_f (EtOAc / Hex 1:1, SiO_2) = 0.05 (UV, H_2SO_4). δ_H (D_2O, 300 MHz): 3.08 (3H, $^3J_{1,2}$ = 8.7, $^3J_{2,3}$ = 7.5, H-2), 3.18 - 3.22 (6H, br. m, H-4 and H-5), 3.25 (3H, app.t, $^3J_{2,3}$ = 9.3, H-3), 3.47 (3H, br.d, $^2J_{6a,6b}$ = 12.3, H-6a), 3.70 (3H, br.d, $^2J_{6a,6b}$ = 12.3, H-6b), 3.98 (3H, d, $^2J_{Ha,Hb}$ = 10.5, $C_{(quat)}CH_aH_b$), 4.20 (3H, d, $^3J_{1,2}$ = 7.5, H-1), 4.88 (2H, s, CH_2Ph), 7.23 (5H, s, Ph). δ_C (D_2O, 75.41 MHz): 58.79 ($C_{(quat)}$), 60.8 (C-6), 66.86 (CH_2Ph), 67.95 ($C_{(quat)}CH_2$), 69.72 (C-4), 73.16 (C-2), 75.60 (C-3), 75.96 (C-5), 103.12 (C-1), 128.00, 128.58, 128.93 (Ph ring carbons), 156.76 (urethane *C*O). ES-MS: *m/z* 742 $[M+H]^+$.

Tris-(β-D-glucopyranosyloxymethyl)-methylamine (6)

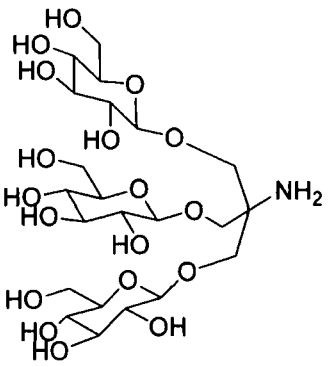

6

A suspension of **5** (0.22 g. 0.296 mmol) in H_2O / EtOH (10 mL, 1:1) and 20% $Pd(OH)_2/C$ (0.05 g) was hydrogenolysed overnight using a Parr hydrogenator (40 psi H_2). The reaction mixture was filtered over Celite, the solvent was evaporated in *vacuo* and the residue was dissolved in H_2O (15 mL) and freeze-dried to afford a white powder (0.196 g, 100%). δ_H (D_2O, 400 MHz): 3.14 (3H, dd, J = 8.0, 9.0, H-2), 3.19 (3H, app. t, J = 9.0, H-4), 3.26 - 3.29 (3H, m, H-5), 3.32 (3H, app.t, J = 9.0, H-3), 3.54 (3H, dd, J = 6, 12.5, H-6a), 3.58 (3H, d, J = 11.2, $CH_2C_{(quat)}$), 3.74 (3H, dd, J = 2, 12.5, H-6b), 3.83 (3H, dd, J = 10.4, $C_{(quat)}CH_aH_b$), 4.29 (3H, d, J = 8.0, H-1). δ_C (D_2O, 100.57 MHz): 59.0 ($C_{(quat)}$), 60.75 (C-6), 69.75 (C_4 & C_7), 73.17 (C-2), 75.57 (C-3), 76.02 (C-5), 102.93 (C-1). ES-MS: *m/z* 608 $[M+H]^+$.

_N_-(Benzyloxycarbonyl)-_N_-[tris(hydroxymethyl)methyl]glycinamide (7)

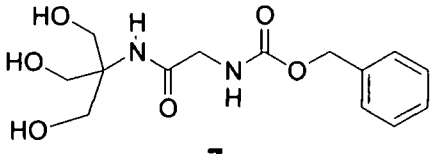

7

Hydroxybenzotriazole (1.35 g, 9.99 mmol) was added to a solution of carbobenzyloxyglycine (2.00 g, 9.56 mmol) and 1,3-dicyclohexylcarbodiimide (2.06 g, 9.98 mmol) in DMF (20 mL). When all reagents were dissolved, TRIS (2.32 g, 19.15 mmol) was added. The reaction mixture was stirred overnight at room temperature, under an atmosphere of argon. After completion of the reaction (TLC), DMF was removed under vacuum and the white solid obtained was dissolved in EtOH (20 mL). The white slurry was filtered and the filtrate evaporated to dryness. The product was purified by column chromatography (SiO_2, CH_2Cl_2 / MeOH 1%→ CH_2Cl_2 / MeOH 5%) to yield a white solid (0.86 g, 28%). R_f (CH_2Cl_2 / MeOH 1%, SiO_2) = 0.4 (UV, H_2SO_4). δ_H (DMSO, 300 MHz): 3.51 (6H, d, J = 6, C*H*$_2$OH), 3.62 (2H, d, J = 6, C*H*$_2$NH), 4.69 (3H, t, J = 6, 3 × O*H*), 5.02 (2H, s, C*H*$_2$Ph), 7.13 (5H, bs, Ph-H), 7.32 (1H, s, C(quat)N*H*), 7.44 (1H, m, CH$_2$N*H*). δ_C (DMSO, 75.41 MHz): 44.19 (*C*H$_2$NHCO), 61.04 (*C*H$_2$OH), 62.44 (CH$_2$*C*(quat)), 66.81 (*C*H$_2$Ph), 127.74, 127.96, 128.39 (Ph-*C*), 136.90 (Ph-*C*(quat)), 158.05 (*C*OCH$_2$NH), 171.63 (*C*OOCH$_2$Ph). ES-MS: *m/z* 335 [*M* + Na]$^+$, 647 [2×*M* + Na]$^+$.

N^{α}-(Benzyloxycarbonyl)-*N*-[Tris(2,3,4,6-tetra-*O*-benzoyl-β-D-glucopyranosyloxymethyl)methyl]glycinamide (8)

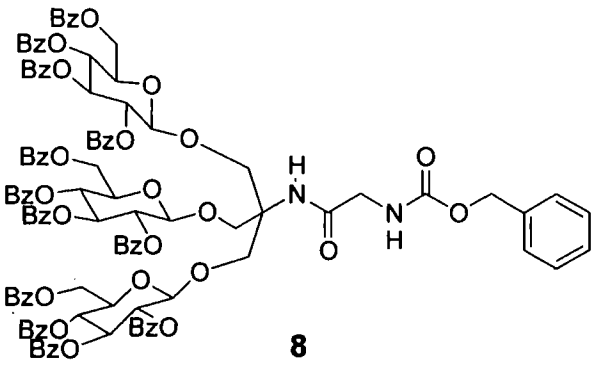

8

AgOTf (0.50 g, 1.94 mmol) was activated by dissolving in anhydrous toluene (10 mL) and the solvent was removed under vacuum. This procedure was repeated a further two times. A mixture of **7** (0.147 g, 0.471 mmol), AgOTf and 2,4,6-collidine (0.19 mL, 1.44 mmol) in CH_2Cl_2 (4.4 mL) and $MeNO_2$ (4.4 mL) was stirred at -30 ^{0}C. A solution of 2,3,4,6-tetra-*O*-benzoyl-α-D-glucopyranosyl bromide, **3**, (1.10 g, 1.67 mmol) in CH_2Cl_2 (4.4 mL) was added dropwise over 20 min to this suspension. Stirring was continued for 30 min at the same temperature and then the reaction mixture was stirred for 2 h at 0 °C, then overnight at room temperature. After completion of the reaction (TLC), C_5H_5N (1.0 mL) was added to the reaction mixture, which was left to stir for 30 min and then diluted with CH_2Cl_2 (20 mL) before being filtered through Celite. The filtrate was washed successively with aqueous $Na_2S_2O_3$ solution (1 M, 2 × 50 mL), aqueous HCl solution (0.1 M, 2 × 50 mL), saturated aqueous $NaHCO_3$ solution (2 × 50 mL) and H_2O (2 × 50 mL). The organic phase was dried over Na_2SO_4 and the solvent was removed in *vacuo* to afford crude product, the TLC of which showed a main product (R_f (EtOAc / Hex 3:7) = 0.2; H_2SO_4) and a few other minor components (R_f = 0.46, 0.51; H_2SO_4). The main product was separated by column chromatography (SiO_2, EtOAc / Hex, 3:7) to afford the product as a white foamy solid (0.47 g, 49%). R_f (EtOAc / Hex 4:6, SiO_2) = 0.30 (UV, H_2SO_4). δ_H ($CDCl_3$, 300 MHz): 3.50 (3H, d, $^2J_{CHa,CHb}$ = 10.2,

C(quat)CH_a), 3.60 – 3.70 (5H, m, H-5), 4.16 (3H, d, $^3J_{1,2}$ = 9.0, H-1), 4.24 (3H, d, $^2J_{CHa,CHb}$ = 10.2, $C_{(quat)}CH_b$), 4.38 (3H, dd, $^3J_{5,6a}$ = 4.5, $^2J_{6a,6b}$ = 12.0, H-6a), 4.54 (3H, app.d, $^2J_{6a,6b}$ = 12.0, H-6b), 5.18 (2H, s, CH_2Ph), 5.35 (4H, app.t, $^3J_{1,2} \sim {}^3J_{2,3}$ = 8.5, H-2 and CH_2NH), 5.55 (3H, app. t, $^3J_{3,4} \sim {}^3J_{4,5}$ = 9.6, H-4), 5.69 (3H, app. t, $^3J_{2,3} \sim {}^3J_{3,4}$ = 9.6, H-3), 6.01 (1H, s, N*H* carbamate), 7.28 – 8.06 (60H, m, Ph-*H*). δ_C ($CDCl_3$, 75.41 MHz): 58.37 ($C_{(quat)}$), 59.26 (*C*H_2NHCO), 61.91 (C-6), 65.89 (*C*H_2Ph), 66.86 ($C_{(quat)}CH_2$), 68.54 (C-4), 70.92 (C-5), 70.97 (C-2), 71.50 (C-3), 100.29 (C-1), 127.26 – 128.87 (Ph ring carbons), 132.13 (Ph$C_{(quat)}$), 164.04 (*C*OCH_2NH), 165.01 (*C*$OOCH_2$Ph). ES-MS: *m/z* 2071 $[M + Na]^+$, 4119 $[2\times M + Na]^+$; (Found: $[M + Na]^+$, 2070.6128. $C_{116}H_{98}N_2O_{33}$ requires $[M + Na]^+$, 2070.5984).

_N_-(Benzyloxycarbonyl)-_N_-[tris(β-D-glucopyranosyloxymethyl)-methyl]glycinamide
(9)

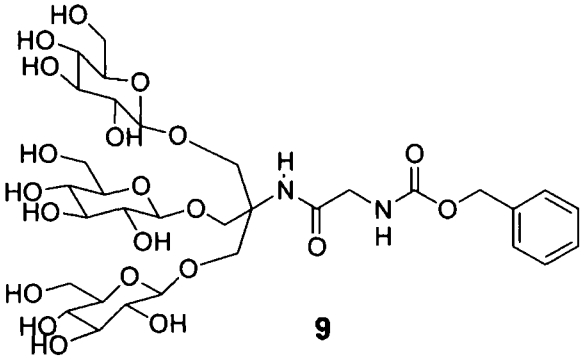

9

A solution of **8** (0.47 g, 0.23 mmol) in 0.10 M methanolic NaOMe (20 mL) was stirred at room temperature overnight. It was then neutralized with Amberlite IR-120(PLUS) ion-exchange resin, filtered and the solvents were removed *in vacuo*. The solvents were removed *in vacuo* and the resulting white powder was partitioned between H_2O (20 mL) and Et_2O (15 mL). The aqueous layer was washed with further Et_2O (3 × 15 mL) and then freeze-dried to obtain **9** (0.16 g, 87%). R_f ($CHCl_3$ / MeOH / H_2O 6:4:1, SiO_2) = 0.45 (UV, H_2SO_4). δ_H (D_2O, 500 MHz): 3.11 (3H, app. t, H-2), 3.19 – 3.32 (9H, m, H-3, H-4, H-5), 3.55 (3H, dd, $^3J_{5,6a}$ = 5.5, $^2J_{6a,6b}$ = 12.0, H-6a) 3.66 (2H, s, CH_2NHCO), 3.74 (3H, dd, H-5, $^3J_{5,6b}$ = 2, $^2J_{6a,6b}$ = 12.0, H-6b),

3.78 (3H, d, $^{2}J_{CHa,CHb}$ = 10.5, C(quat)CH_a), 4.08 (3H, d, $^{2}J_{CHa,CHb}$ = 10.5, C(quat)CH_b), 4.28 (3H, d, $^{3}J_{1,2}$ = 8.0, H-1), 5.00 (2H, s, CH_2Ph), 7.29 (5H, m, Ph-H). δ_C (D_2O, 125.67 MHz): 44.1 (Gly-CH_2), 59.1 (C(quat)), 60.8 (C-6), 67.6 (CH_2Ph), 67.7 (C(quat)CH_2), 69.8 (C-4), 73.2 (C-2), 75.6 (C-3), 76.1 (C-5), 103.1 (C-1), 127.9 – 128.6 – 128.1 (Ph ring carbons), 157.8 ($COCH_2NH$), 172.2 (Gly-CO). ES-MS: *m/z* 821 $[M + Na]^+$, 1619 $[2\times M + Na]^+$. (Found: $[M + Na]^+$, 820.9684 $C_{32}H_{50}N_2O_{21}{}^{23}Na_1$ 820.9682).

_N_-[Tris(β-D-glucopyranosyloxymethyl)methyl]glycinamide (10)

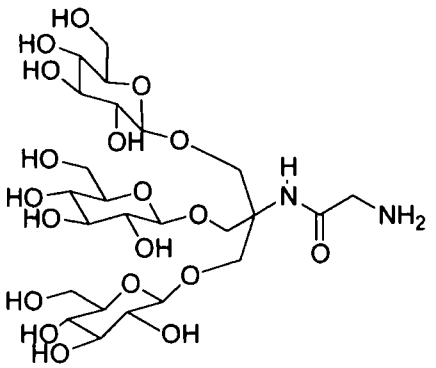

10

A suspension of **9** (0.47 g. 0.23 mmol) in 10 mL of H_2O/ EtOH (1:1) and $Pd(OH)_2/C$ (0.17 g) was hydrogenolysed overnight using a hydrogenator (40 psi H_2). The reaction mixture was filtered over Celite, the solvent was evaporated under reduced pressure and the residue was dissolved in H_2O (15 mL) and freeze-dried, to afford a white powder (0.146 g, 96%). δ_H (D_2O, 500 MHz): 3.14 (3H, app. t, $^{3}J_{1,2}$ = 8.0, H-2), 3.22 (3H, app. t, $^{3}J_{3,4}$ = 9.5, H-4), 3.28 – 3.34 (8H, m, H-3, H-5, CH_2NH_2), 3.55 (3H, d, $^{2}J_{6a,6b}$ = 12.5, H-6a), 3.76 (3H, d, $^{2}J_{6a,6b}$ = 12.5, H-6b), 3.79 (3H, d, $^{2}J_{CHaCHb}$ = 10.0, C(quat)CH_a), 4.12 (3H, d, $^{2}J_{CHa,CHb}$ = 10.0, C(quat)CH_b), 4.31 (3H, d, $^{3}J_{1,2}$ = 8.0, H-1). δ_C (D_2O, 125.67 MHz): 42.93 (Gly-CH_2), 57.56 (C(quat)), 60.82 (C-6), 67.76 (C(quat)CH_2), 69.79 (C-4), 73.17 (C-2), 75.66 (C-3), 76.07 (C-5), 100.12 (C-1), 172.30 (CONH). ES-MS: *m/z* 687 $[M + Na]^+$, 1351 $[2\times M + Na]^+$. (Found: $[M+H]^+$,

665.2614. $C_{24}H_{45}O_{19}N_2$ requires $[M+H]^+$, 665.2611; $[M + Na]^+$, 687.2438. $C_{24}H_{44}O_{19}N_2{}^{23}Na_1$ requires $[M + Na]^+$, 687.2430).

Tetraamide Dendrimer (11)

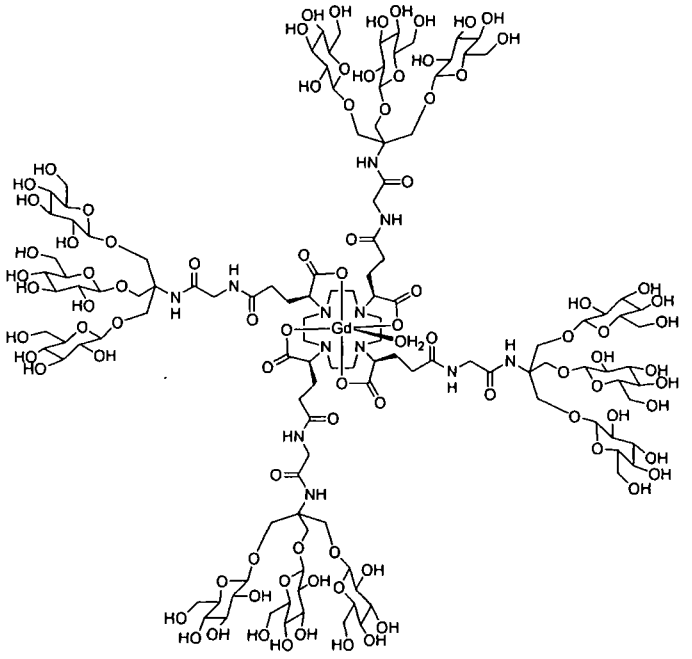

11

To a suspension of GdgDOTA (15 mg, 0.017mmol) in *N*-methylmorpholine (0.012 mL, 0.11 μmol) and DMF (0.82 mL) was added *O*-benzotriazol-1-yl-*N*, *N*, *N'*, *N'*-tetramethyluronium tetrafluoroborate (40 mg, 0.12 mmol) and the mixture allowed to stir for a few minutes. A solution of the amine **10** (70 mg, 0.13 mmol) was added to the reaction and the mixture allowed to stir overnight at 40 °C, under an atmosphere of dry argon. The reaction was partitioned between water (10 mL) and CH_2Cl_2 (10 mL). The aqueous layer was washed with CH_2Cl_2 (10 mL) and freeze-dried. The crude of the reaction is a mixture of the fully substituted tetraamide (major product) and the under-substituted triamide and diamide (minor products). Purification by gel-filtration chromatography afforded the pure product (19 mg,

32%), as confirmed by electrospray analysis. ES-MS: $[M]^{2-}$ = 1715.07, $[M]^{3-}$ = 1143.04 (tetraamide product).

$1/T_1$ NMRD and VT ^{17}O NMR R_{2p} analysis

A solution of the Gd^{III}-complex (0.016 g, 4.6 μmol) in water (25 mL) was prepared. The concentration of Gd^{III} in the sample was assessed by ICP-optical emission spectroscopy, and was found to be: $[Gd^{III}]$ = 0.15 mM. Relaxivity value found by $1/T_1$ NMRD analysis: r_{1p} = 19.6 $mM^{-1}s^{-1}$ (298 K, pH 7, 20 MHz). Fitting of the $1/T_1$ NMRD profile gave estimated τ_R = 318 ns.

The concentration of Gd^{III} in the sample prepared for the VT ^{17}O NMR R_{2p} analysis, assessed by ICP-optical emission spectroscopy: $[Gd^{III}]$ = 6.0 mM. Fitting of the ^{17}O NMR R_{2p} data gave τ_M = 221 ns.

(*N'-tert*-Butoxycarbonyl-*N*-methoxycarbonylmethyl-hydrazino)-acetic acid methyl ester (12)

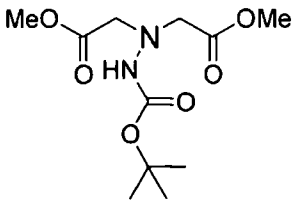

12

To a stirred solution of *t*-butylcarbazate (0.50 g, 3.67 mmol) in DMF (10 mL), methylbromoacetate (1.40 mL, 14.80 mmol) and K_2CO_3 (2.04 g, 14.80 mmol) were added dropwise, and the reaction mixture was stirred at 40 °C, under an argon atmosphere. The progress of the reaction was monitored by TLC, and after 48 h the solvent was removed under reduced pressure. Extraction of the residue in H_2O / CH_2Cl_2 (2 × 10 mL) followed by purification of the crude of reaction by column chromatography (SiO_2, Hex / EtOAc 5 % → 20 %) gave the product as a brown coloured gum (0.44 g, 43 %). R_f (Hex / EtOAc 20%, SiO_2) = 0.35 (Permanganate).

δ_H ($CDCl_3$, 300 MHz): 1.34 (9H, s, $C(CH_3)_3$), 3.63 (6H, s, 2 × OCH_3), 3.72 (4H, br d, CH_2N), 6.75 (1H, br s, N*H*). δ_C (D_2O, 100.61 MHz): 28.36 ($C(CH_3)_3$), 51.87 (OCH_3), 52.67 (CH_2CO), 57.09 ($C(CH_3)_3$, 156.49, 171.66 (C=O). ES-MS: *m/z* 276 $[M]^+$, 299 $[M+Na]^+$. (Found: $[M]^+$, 275.9975. $C_{11}H_{20}N_2O_6$ requires $[M]^+$, 275.9985).

(*N'-tert*-Butoxycarbonyl-N-methoxycarbonylmethyl-hydrazino)-acetic acid (13)

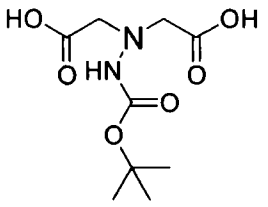

13

The ester, **12** (0.44 g, 1.59 mmol), was dissolved in MeOH (5 mL), and 5 mL of 1 M aq KOH was slowly added. After 7 h stirring at room temperature, the solution was acidified to pH 4.5 with 1M HCl and extracted with EtOAc (2 × 5 mL). The solvent was removed under reduced pressure and a white powder was obtained as the product of reaction (0.38 g, 97%). δ_H ($CDCl_3$, 400 MHz): 1.43 (9H, s, $C(CH_3)_3$), 3.71 (4H, s, 2 × CH_2COOH), 5.42 (1H, br s, N*H*). δ_C (CD_3CN, 100.61 MHz): 27.12 ($C(CH_3)_3$, 29.59 ($C(CH_3)_3$), 58.37 (2 × CH_2COOH), 170.59 (C=O), 206.27 (C=O). ES-MS: *m/z* 271 $[M+Na]^+$.

***tert*-Butoxycarbonyl-5-bromo-pentanoate [3] (14)**

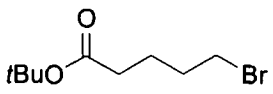

14

5-Bromovaleric acid (18.32 g, 0.10 mol) was dissolved in CH_2Cl_2 (50 mL) and oxalyl chloride (25 ml, 0.286 mol) was added. The resulting yellow solution was

stirred at room temperature for 3 h. Excess acid chloride was removed by distillation, the reaction mixture was washed with CH_2Cl_2 (4 x 50 mL) and a mixture consisting of pyridine (4.6 mL, 0.057 mol), *t*-butyl alcohol (6.4 ml, 0.069 mol) in (5 mL) was slowly added, at -78°C. The reaction mixture was allowed to warm to room temperature whilst stirring overnight under an argon atmosphere. The crude product was purified by column chromatography to remove any pyridinium salts (SiO_2, 10% ethyl acetate in hexane → 50% EtOAc in Hex), to yield a yellow oil, **14** (20.0 g, 85 %). δ_H ($CDCl_3$, 400 MHz): 1.31 (9H, s, $C(CH_3)_3$), 1.66 (2H, m, CH_2), 1.82 (2H, m, CH_2), 2.18 (2H, t, CH_2CO, J = 7.7), 3.34 (2H, t, CH_2Br, J = 6.8). δ_C ($CDCl_3$, 100.61 MHz): 23.74 (CH_2), 28.19 (CH_3), 32.11 (CH_2), 33.25 (CH_2Br), 34.56 (CH_2CO), 80.23 (($C_{(quat)}$), 172.40 (*C*=O). ES-MS: *m/z* 259.0 [^{79}Br M + Na]$^+$, 261.1 [^{81}Br M + Na]$^+$. (Found: [M+Na]$^+$, 258.0213, $C_9H_{16}O_2BrNa$ requires [M+Na]$^+$, 258.0231).

***Tert*-butyl-5-(diethoxy-phosphonyl)-pentanoate (15)**

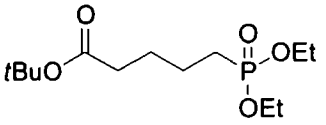

15

14 (8.10 g, 0.027 mol) was dissolved in triethylphosphite (25 mL) and heated at reflux for 18 h under an argon atmosphere. The crude product was distilled under reduced pressure (78 °C, 1.0 mmHg) to yield **15** as a clear oil (7.0 g, 89 %). δ_H ($CDCl_3$, 400 MHz): 1.22 (6H, t, OCH_2CH_3, J = 7.2), 1.33 (9H, s, $C(CH_3)_3$), 1.53 (6H, m, CH_2), 2.12 (2H, t, CH_2CO, J = 7.6), 3.98 (4H, m, CH_2OP). δ_C ($CDCl_3$, 125.6 MHz): 16.61 ($POCH_2CH_3$), 24.14 (CH_2), 25.86 (CH_2), 26.29 (CH_2), 27.97 ($C(CH_3)_3$), 35.06 (CH_2CO), 61.53 ($POCH_2$, J_{CP} = 6.5), 80.21 (*C*(quat)), 176.6 (C=O). ^{31}P NMR ($CDCl_3$, 80.9 MHz,) δ_p: 32.91. ES-MS: *m/z* 295.2 [M + H]$^+$, 317.2 [M + Na]$^+$, 611.4 [2M + Na]$^+$. (Found: [M+Na]$^+$, 317.1525. $C_{13}H_{27}O_5PNa$ requires [M+Na]$^+$, 317.1494).

5-(Diethoxy-phosphonyl)-pentanoic acid (16)

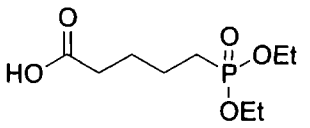

16

15 (4.04 g, 0.014 mmol) was suspended in CF_3COOH (2.0 mL) and CH_2Cl_2 (2.0 mL). The resulting solution was stirred under argon at room temperature overnight. The reaction mixture was concentrated under reduced pressure and the residue washed using CH_2Cl_2 (3 x 10 mL), to give **16** in near quantitative yield (3.20 g, 96 %). δ_H ($CDCl_3$, 400 MHz): 1.28 (6H, t, CH_2CH_3, J = 7.0), 1.71 (6H, m, CH_2), 2.42 (2H, t, CH_2CO, J = 7.0), 4.16 (4H, m, CH_2PO), 12.56 (1H, s, O*H*). δ_C ($CDCl_3$, 100.6 MHz): 16.41 (CH_3), 21.75 (CH_2), 24.72 (CH_2), 25.46 (CH_2), 35.55 (CH_2CO), 63.01 ($POCH_2CH_3$), 179.77 (*C*=O). ^{31}P NMR ($CDCl_3$, 80.9 MHz,) δ_p: 33.53 (*P*=O). ES-MS: *m/z* 237.1 [*M*]$^-$. (Found: [M]$^-$, 237.0905. $C_9H_{19}O_5P$ requires [M]$^-$, 237.0907).

(±) Ethyl-2-bromo-5-(diethoxy-phosphonyl)-pentanoate (17)

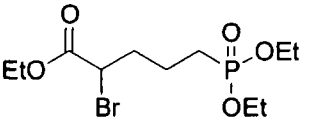

17

16 (5.29 g, 0.022 mmol) was dissolved in $SOCl_2$ (10 mL) and heated under reflux for approximately 1 h. Liquid bromine (3.53g, 0.021 mmol) was carefully added and the resulting brown solution was heated under reflux, under an argon atmosphere overnight. The reaction mixture was cooled in an ice bath and slowly added to a cooled solution of anhydrous EtOH (~ 20 mL). The resulting yellow solution was stirred under argon for 30 min and then poured onto crushed ice (100 g) and stirred until fully melted. The product was extracted using Et_2O (3 × 50 mL) and the organic phase was dried over $MgSO_4$. The solvent was filtered and then removed

under reduced pressure to yield **17** as a yellow oily product (4.9 g, 65%). δ_H ($CDCl_3$, 500 MHz): 1.04 (6H, t, J = 8.5, $POCH_2CH_3$), 1.13 (3H, m, CH_2CH_3), 1.79 (4H, m, 2 CH_2), 2.12 (2H, CH_2CO), 3.90 (4H, m, $POCH_2CH_3$), 4.04 (3H, m, $COOCH_2CH_3$ & CHBr). δ_C ($CDCl_3$, 125.6 MHz): 13.90 (CH_3), 16.33 (CH_3, $J_{C\text{-}P}$ = 5.7), 20.34 (CH_2), 23.88-25.01 (CH_2, J_{CP} = 141), 35.10 (CH_2CHBr), 45.32 (CHBr), 62.20 (CH_3CH_2OCO), 62.22 (CH_3CH_2OP), 169.60 (C=O). ^{31}P NMR ($CDCl_3$, 80.9 MHz,) δ_P: 32.50. ES-MS: *m/z* 345.1 [^{79}Br, M]$^+$, 347.2 [^{81}Br, M]$^+$, 367.2 [M + Na]$^+$. (Found: [M]$^+$, 345.0461, $C_{11}H_{23}O_5PBr$ requires [M]$^+$, 345.0466).

1,4,7-Tris-trifluoromethyl carbonyl-1,4,7,10-tetraazacyclododecane[4] (18)

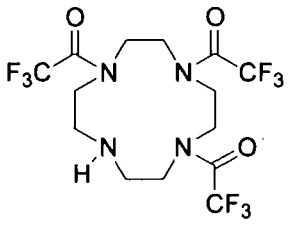

18

1,4,7,10-Tetraazacyclododecane (3.68 g, 21.39 mmol1.01 g, 5.87 mmol) and NEt_3 (0.8 ml, 6.98 mmol) was dissolved into anhydrous MeOH (100 mL) and cooled to 0 °C. Ethyl trifluoroacetate (12.17 g, 0.086 mmol) was added dropwise over a 30 min and the mixture was left stirring for 4 h under an argon atmosphere, at room temperature. Removal of the solvent under reduced pressure gave the crude of reaction. Purification by flash column chromatography (SiO_2, 1% MeOH in DCM → 3% MeOH in DCM) gave **18** (4.74 g, 45 %). R_f (EtOAc, SiO_2) = 0.30 (UV). δ_H ($CDCl_3$, 400 MHz): 1.49 (1H, br s, NH), 2.87 (4H, m, NCH_2), 3.52-3.65 (8H, m, NCH_2), 3.85 (4H, m, NCH_2). δ_C ($CDCl_3$,100.6 MHz): 20.93 (CH_2), 46.91-52.81 (m, NCH_2), 116.44 (q, CF_3, $J_{C\text{-}F}$ ~ 278, further split due to conformers), 156.78-158.22 (m, C=O, existence of conformers and long range C-F coupling). ES-MS: *m/z* 483.3 [M + Na]$^+$, 943.1 [2M +Na]$^+$.

1-*tert*-Butoxycarbonyl-4,7,10-tris-trifluoromethylcarbonyl-1,4,7,10 tetraazacyclododecane (19)

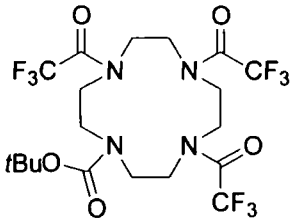

19

To a stirred solution of **18** (2.0 g, 4.44 mmol) in dry MeOH (20 mL) di-tert-butyl-dicarbonate (1.11 g, 5.28 mmol) was added. The resulting mixture was left stirring for 5 h at room temperature under an argon atmosphere. The solvent was removed under reduced pressure to yield the crude mixture, which was then purified by flash column chromatography (SiO_2, CH_2Cl_2 → 2% EtOAc in CH_2Cl_2) to give the product as a colourless oil (1.60 g, 65%). R_f (EtOAc / CH_2Cl_2 1:9, SiO_2) = 0.54 (UV). δ_H ($CDCl_3$, 400 MHz): 1.33 (9H, s, $C(CH_3)_3$), 3.34-3.73 (16H, m, NCH_2). δ_C ($CDCl_3$,100.6 MHz): 20.62 (CH_2), 27.98 ($C(CH_3)_3$), 48.54-50.70 (m, NCH_2), 81.04 ($C(CH_3)_3$), 116.03 (q, CF_3, J_{C-F} ~ 287 Hz, further split due to conformers), 156.67-158.70 (m, C=O, existence of conformers and long range C-F coupling). ES-MS: *m/z* 583.3 $[M + Na]^+$, 1152.3 $[2M + Na]^+$. (Found: $[M + Na]^+$, 583.1617, $C_{19}H_{25}O_5N_4F_9Na$ requires $[M + Na]^+$, 583.1579).

1-*tert*-Butoxycarbonyl- 1, 4, 7, 10-tetraazacyclododecane (20)

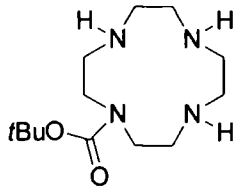

20

19 (1.60 g, 0.0028 mmol) was dissolved in MeOH (20 mL) and water (5 mL). Aqueous KOH solution (2 M, 1.0 mL) was added and the mixture was stirred for 3 h at room temperature. The solvent was removed under reduced pressure and a pale yellow oil was obtained. This crude material was suspended in CH_2Cl_2 (50 mL), washed with saturated $NaHCO_3$ solution (10 mL) and then with saturated aqueous NaCl solution (10 mL). The organic layer was dried over K_2CO_3 and solvent removed by reduced pressure to yield the product as a clear oil (0.75 g, 98%). δ_H ($CDCl_3$, 400 MHz): 1.21 (9H, s, $C(CH_3)_3$), 2.45 (4H, br m, NCH_2), 2.56 (8H, br m, NCH_2), 3.17 (4H, br m, NCH_2), 3.37 (3H, br s, NH). δ_C ($CDCl_3$,100.6 MHz): 28.29 ($C(CH_3)_3$), 46.46 (NCH_2), 48.06 (NCH_2), 48.56 (NCH_2), 48.68 (NCH_2), 48.94 (NCH_2), 79.38 (q, $C(CH_3)_3$), 156.38 (C=O). ES-MS: *m/z* 295.1 $[M + Na]^+$ (Found: $[M]^+$, 273.2302, $C_{13}H_{29}O_2N_4$ requires $[M]^+$, 273.2291).

1-*tert*-Butoxycarbonyl-4,7,10-tris-ethyl-2-bromo-5-(diethoxy-phosphonyl-pentanoate-1,4,7,10-tetraazacyclododecane (21)

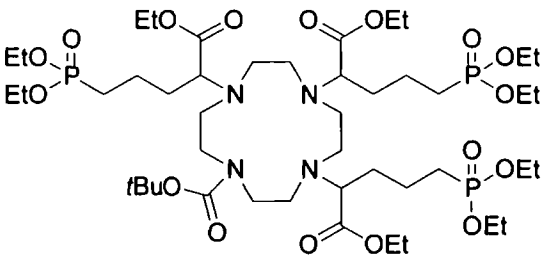

21

To a suspension of 1-*t*-butoxycarbonyl-1,4,7,10-tetraazacyclododecane (**20**) (0.17 g, 0.65 mmol) in dry MeCN, Cs_2CO_3 (0.74g, 2.27 mmol) and **17** were added. The reaction mixture was stirred under reflux for 72 h, under an argon atmosphere. The particulate matter was removed by filtration and the solvent removed under reduced pressure. The crude mixture was purified by column chromatography (SiO_2, CH_2Cl_2 → 3% MeOH in CH_2Cl_2), to yield the product as a brown oil (150 mg, 22%). R_f (CH_2Cl_2 / MeOH 3%, SiO_2) = 0.62. δ_H ($CDCl_3$, 499.77 Mz): 1.24 – 1.31 (27H, m,

18H $POCH_2CH_3$ + 9H $COCH_2CH_3$), 1.43 (9H, s, $C(CH_3)_3$), 1.74 – 1.77 (34H, m, 16H NCH_2 + 18H CH_2), 4.07 (21H, m, 12H $POCH_2CH_3$ + 6H $COCH_2CH_3$ + 3H CH). δ_C ($CDCl_3$, 125.67 Mz): 13.17 (CH_3), 15.46 (CH_3 J_{CP} = 3.8 Hz), 17.21 (CH_2), 23.75 (CH_2), 24.82 (CH_2), 27.42 ($C(CH_3)_3$), 33.76 (CH_2), 60.50 – 60.55 (m, $POCH_2CH_3$ J_{CP} = 6.2 Hz: long range CP coupling). δ_P ($CDCl_3$, 80.90 Mz): 31.83 – 32.66. ES-MS: *m/z* 1087.4 $[M + Na]^+$ (Found: $[M + Na]^+$, 1087.5555, $C_{46}H_{91}O_{17}N_4P_3Na$ requires $[M +Na]^+$, 1087.5496).

Benzyl-2-[(*tert*-butoxycarbonyl)amino]-4-oxoserinate [5] (22)

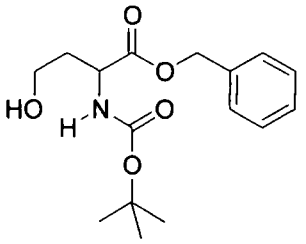

22

To a stirred solution of *N*-Boc-aspartic-acid-benzyl-ester (2.0 g, 6.20 mmol) in anhydrous THF (6.0 mL) cooled at -10 °C, *N*-methylmorpholine (0.66 mL, 6.20 mmol) was added dropwise. After 1 minute at -10 °C, ethyl chloroformate (1.84 mL, 19.17 mmol) was added dropwise and the mixture stirred at -5 °C for a further 15 min. *N*-methylmorpholine hydrochloride was removed by filtration and the filtrate was immediately added to $NaBH_4$ (0.30 mg, 7.93 mmol) . The reaction mixture was stirred at room temperature for 4 h, cooled to 5 °C, acidified to pH ~ 4 with HCl (1M, a few drops) and the solvent was evaporated. The residue, a white powder, was dissolved in EtOAc (20 mL), washed with water and then brine, dried (Na_2SO_4) and the solvent evaporated under reduced pressure to give a yellow oil (1.76 g). Purification by column chromatography (SiO_2, EtOAc / Hex, 3 : 7) gave the product as a colourless oil (0.60 g, 31 %). R_f (EtOAc / Hex 1 : 1) = 0.64 (UV). δ_H ($CDCl_3$, 400 MHz): 1.32 (9H, s, $C(CH_3)_3$), 1.61 (1H, m, CH_b), 2.04 (1H, m, CH_a), 3.16 (1H, br. s, OH), 3.57 (2H, m, CH_2OH), 4.40 (1H, m, CHCOO), 5.07 (2H, d, $^2J_{Ha,Hb}$ = 6.4,

C*H*$_2$Ph), 5.51 (1H, d, $^3J_{1,2}$ = 7.6, N*H*), 7.23 (5H, m, Ph*H*). δ_C ($CDCl_3$, 100.62 MHz): 28.25 (C(*C*H$_3$)$_3$), 35.54 (*C*H$_2$CH$_2$OH), 51.01 (*C*(CH$_3$)$_3$), 58.34 (*C*H$_2$OH), 65.65 (*C*HNH), 80.22 (*C*H$_2$Ph), 128.21, 128.47, 128.57 (Ph ring carbons), 135.34 ((Ph*C*(quat)), 156.27 (*C*OCH$_2$Ph), 172.68 (*C*O*O*t*Bu). ES-MS: *m/z* 332 [*M* + Na]$^+$, 641 [2×*M* + Na]$^+$.

Benzyl-2-[(*tert*-Butoxycarbonyl)amino]-4-oxobutanoate [6] (23)

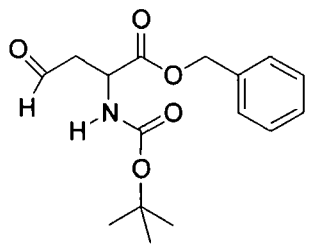

23

To a solution of oxalyl chloride (34.0 µL, 0.38 mmol) in CH_2Cl_2 (3 mL) at -78 °C was added DMSO (70.0 µL). To this mixture, a solution of **22** (0.11 g, 0.35 mmol) in CH_2Cl_2 (2 mL) was added. After stirring for 30 min NEt_3 was added dropwise to the mixture, which was left to stir for 5 min at -78 °C and then allowed to warm to room temperature. After 2 h the reaction mixture was diluted with CH_2Cl_2 (10 mL) and washed with brine (10 mL). The organic layer was dried over Na_2SO_4, concentrated under reduced pressure and the crude mixture purified by column chromatography (SiO_2, EtOAc / Hex, 3:7) to afford **23** (0.1 g, 86 %) as a white powder. R_f (EtOAc/Hex 4:6) = 0.35 (UV). M.p. 58 - 61°C (lit. 60 – 62 °C). δ_H ($CDCl_3$, 400 MHz): 1.35 (9H, s, C(C*H*$_3$) × 3), 2.96 (1H, br. dd, C*H*$_b$), 2.99 (1H, br. dd, C*H*$_a$), 4.56 (1H, m, C*H*COO), 5.09 (2H, s, C*H*$_2$Ph), 5.35 (1H, br. d, N*H*), 7.23 (5H, m, Ph*H*), 9.63 (1H, s, C*H*O). δ_C ($CDCl_3$, 100.62 MHz): 28.25 (C(*C*H$_3$)$_3$), 45.97 (*C*H$_2$COH), 48.81 (*C*(CH$_3$)$_3$), 67.55 (**C*HNH), 80.27 (*C*H$_2$Ph), 128.25, 128.48, 128.60 (Ph ring carbons), 135.14 (Ph*C*(quat)), 155.36 (*C*OOCH$_2$Ph), 170.88 (*C*ONH), 199.23 (*C*OH). ES-MS: *m/z* 330 [*M* + Na]$^+$, 639 [2×*M* + Na]$^+$.

Benzyl-2-[(*tert*-Butoxycarbonyl)amino]-4-oxobutanoate[7] (24)

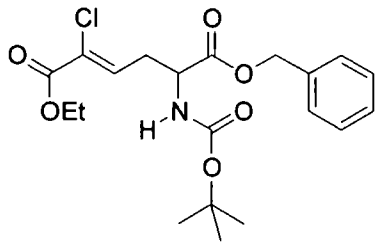

24

To a suspension of NaH (0.22 g, mol) in THF (20 mL) at 0 °C, triethyl-2chloro-phosphonoacetate (1.9 mL, 6.17 mmol) was added and the mixture was stirred at room temperature. After 30 min, a solution of the aldehyde **23** (0.88 g, 2.83 mmol) in THF (7 mL) was added to the reaction mixture at 0 °C , then stirred at room temperature for 2 h. Saturated aqueous $NaHCO_3$ (15 mL) and aq. $Na_2S_2O_3$ (10 mL) were added, and the mixture extracted with Et_2O (20 mL × 2). The organic layer was washed with brine (10 mL × 2), dried over Na_2SO_4, filtered and the solvent evaporated to dryness to give the crude mixture. Purification by column chromatography (EtOAc / Hex 9 : 1 → EtOAc / Hex 8 : 2) afforded the product **24** as a pale brown oil (0.24 g, 21%). δ_H ($CDCl_3$, 300 MHz): 1.30 (3H, t, J = 7, OCH_2CH_3), 1.43 (9H, s, $C(CH_3)_3$), 2.65-3.04 (2H, m, $NCHCH_2$), 4.24 (2H, q, J = 7, OCH_2CH_3), 4.52 (1H, br. m, NCH), 5.17 (3H, s, NH, CH_2Ph), 6.98 (1H, t, J = 7 Hz, CH=CCl), 7.34 (5H, s, Ph). δ_C ($CDCl_3$, 75 MHz): 14.00 (CH_3CH_2), 28.23 ($C(CH_3)_3$), 32.81 (OCH_2), 52.20 ($C(CH_3)_3$), 62.22 (CHN), 67.56 (CH_2CHN), 80.27 (CH_2Ph), 127.58, 128.38, 128.55 (Ph ring carbons), 135.74 (ClC=CH), 137.94 (ClC=C), 155.07 (C=OCH_2Ph), 161.81 (C=OOEt), 171.11 (C=OO*t*Bu). ES-MS: *m/z* 434.2 [*M* + Na]$^+$.

(Hydroxymethylene)methyl-phosphinic acid ethyl ester [10] (25)

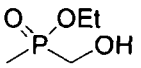

25

A suspension of methyldiethoxyphosphine (2.00 g, 14.70 mmol) and an excess of paraformaldehyde (0.55 g, 18.33 mmol) in THF (10 mL) over molecular sieves was stirred overnight at 50 °C under an argon atmosphere. After 15 h, the solvent was removed under reduced pressure and the residue dissolved in CH_2Cl_2. Salts were filtered off and the filtrate evaporated to dryness to give the crude product, which was purified by column chromatography (Al_2O_3, $CH_2Cl_2 \rightarrow CH_2Cl_2$ / MeOH 1.5 %), to afford the product as a colourless oil (1.12 g, 65%). R_f (CH_2Cl_2 / MeOH 3 % , SiO_2) = 0.30. δ_H ($CDCl_3$, 200 MHz): 1.29 (3H, t, J = 7, OCH_2CH_3), 1.50 (3H, d, J = 13.8, CH_3P), 3.81 (2H, m, PCH_2OH), 4.07 (2H, m, OCH_2CH_3). δ_C ($CDCl_3$, 100 MHz): 12.82 (d, J = 96 Hz, PCH_3), 16.45 (OCH_2CH_3), 63.63 (OCH_2CH_3), 63.68 (d, J = 98 Hz, CH_2OH).^{31}P NMR ($CDCl_3$, 161.97 MHz,) δ_P: 53.15. ES-MS: *m/z* 161.0 $[M+Na]^+$.

(*O*-Mesylmethylene)methylphosphinic ethyl ester (26)

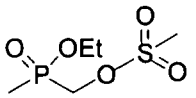

26

To a suspension of **25** (1.12 g, 8.11 mmol) and Et_3N (2.01 g, 19.90 mmol) in THF (50 mL) at 0 °C, MsCl (2.3 g, 20.17 mmol) was added dropwise and the reaction mixture was left stirring for 2 h. The reaction was quenched with EtOH (10 mL) and left stirring for a further 20 min, then the solvents removed under reduced pressure. The residue was dissolved in EtOAc (25 mL), the salts were filtered off and the solvent evaporated to dryness, to give the crude product. Purification by column chromatography (SiO_2, EtOAc) afforded the desired product as a pale brown oil

(1.22 g, 70%). R_f(EtOAc, SiO_2) = 0.30 (permanganate). δ_H($CDCl_3$, 400 MHz): 1.29 (3H, br. t, OCH_2CH_3), 1.56 (3H, br. d, J = 13.80, CH_3P), 3.08 (3H, s, OCH_2P), 4.07 (2H, m, OSO_2CH_3), 4.37 (2H, m, OCH_2CH_3). δ_C ($CDCl_3$, 100.61 MHz): 12.31 (d, J_{CP} = 100 Hz, PCH_3), 16.43 (OCH_2CH_3), 37.57 (CH_3S), 61.84 (OCH_2CH_3), 63.02 (d, J_{CP} = 106 Hz, CH_2OMs). ^{31}P NMR ($CDCl_3$, 161.97 MHz,) δ_P: 45.00. ES-MS: *m/z* 217 $[M+H]^+$.

1,4-Dibenzyl-6-methyl-6-nitroperhydro-1,4-diazepine [8] (27)

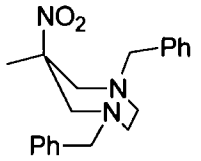

27

A suspension of *N,N'*-dibenzylethylenediamine (5.0 mL, 0.02 mol) and *para*-formaldehyde (1.91 g, 0.06 mmol) in EtOH (50 mL) was refluxed for 6 h. Nitroethane (1.52 mL, 0.02 mol) was added dropwise, and the reaction mixture was heated at reflux overnight, under an argon atmosphere. The progress of the reaction was monitored by TLC, and after 16 h the solvent removed under reduced pressure and the residue partitioned between CH_2Cl_2 / sat. aq. Na_2CO_3. The organic extracts were washed with water, dried, filtered, evaporated and purified through column chromatography (SiO_2, CH_2Cl_2) to afford a light brown waxy solid (6.50 g, 96 %) as the product of reaction. R_f(CH_2Cl_2, SiO_2) = 0.4 (UV). m.p. 49.5 – 50 °C. δ_H($CDCl_3$, 300 MHz): 1.34 (3H, s, $CH_3C_{(quat)}$), 2.59 (4H, m, 2 × CH_2N), 2.95 (2H, d, 14.1), 3.60 (2H, d, J = 14.1), 3.65 (2H, d, J = 13.2) , 3.78 (2H, d, J = 13.2), 7.26-7.33 (10H, m, 2 × Ph-*H*). ES-MS: *m/z* 339.3 $[M]^+$, 340.3 $[M+H]^+$, 361.4 $[M+Na]^+$.

6-Amino-6-methylperhydro-1,4-diazepine (AMPED) [8] (28)

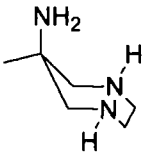

28

A suspension of **27** (2.27 g, 6.69 mmol) in MeOH (10 mL) and 20% $Pd(OH)_2/C$ (1.88 g, 13.4 mmol) was hydrogenated overnight using a Parr hydrogenator (10 psi H_2). The reaction mixture was filtered over Celite, the solvent was evaporated under reduced pressure and a yellow oil (0.850 g, 98 %) was obtained as the only product of reaction. R_f (CH_2Cl_2 / MeOH 19% / NH_3 1%, SiO_2) = 0.10 (Iodine). δ_H ($CDCl_3$, 400 MHz): 0.85 (3H, s, $CH_3C_{(quat)}$), 1.86 (br. s, 4H, exch. with D_2O), 2.50 (4H, m, 2 × $CH_{2(ring)}$ H-5a, 5b and H-7a, 7b), 2.63 - 2.69 (2H, m, $CH_{2(ring)}$ H-2a, 3a), 2.74 – 2.80 (2H, m, $CH_{2(ring)}$ H-2b, 3b). δ_C ($CDCl_3$, 100.6 MHz): 26.81 ($CH_3C_{(quat)}$), 52.06 (*C-2* and *C-3*), 54.15 ($C_{(quat)}$), 62.42 (C-5 and C-7). ES-MS: *m/z* 130 $[M+H]^+$.

6-Amino-6-methyl, 1, 4-bis(ethoxymethylphosphinoxymethyl)-diazepine (29)

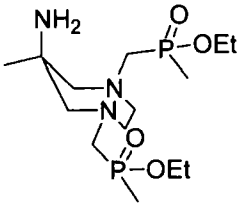

29

To a solution of **28** (0.85 g, 6.59 mmol) in 20 mL of CH_3CN at 85 °C, a suspension of paraformaldehyde (0.39 g, 13.22 mmol) in CH_3CN (5 mL) was slowly added. After heating at reflux for 30 min, the solution was allowed to cool to room temperature and left to stir for 40 min. Methyldiethoxyphosphine (2.0 mL, 13.22 mmol) dissolved in CH_3CN (10 mL) was added dropwise and the reaction mixture was left stirring overnight at room temperature. The solvent was removed under reduced pressure and the resulting yellow oil purified by column chromatography

(SiO_2, CH_2Cl_2 / MeOH 6% / NH_3 1% → CH_2Cl_2 / MeOH 15% / NH_3 1%) to yield the desired product (1.045 g, 43 %) as a mixture of *(RR)/(SS)* and *(RS)/(SR)* stereoisomers. R_f (CH_2Cl_2 / MeOH 19% / NH_3 0.5%, SiO_2) = 0.50 (Iodine). δ_H ($CDCl_3$, 300 MHz): 0.78 (3H, s, $CH_3C_{(quat)}$), 1.08 (6H, t, J = 7, 2 × OCH_2CH_3), 1.27 (3H, d, J = 18 Hz, PCH_3), 1.32 (3H, d, J = 18 Hz, PCH_3), 2.36 - 2.84 (12H, br. m, 4 × $CH_{2(ring)}$ and 2 × CH_2N), 3.82 - 3.92 (4H, m, 2 × OCH_2CH_3). δ_C ($CDCl_3$, 100.6 MHz): 13.51 (d, J_{CP} = 100 Hz, PCH_3), 16.73 (OCH_2CH_3), 21.11 ($CH_3C_{(quat)}$), 52.57 (*C2* and *C3*), 56.51 ($C_{(quat)}$), 57.74 (d, J_{CP} = 120 Hz, PCH_2N), 60.75 (*C5* and *C7*), 65.89 and 66.21 (OCH_2CH_3). ^{31}P NMR ($CDCl_3$, 121.42 MHz,) δ_P: 52.66, 52.58, 52.45. ES-MS: *m/z* 370.3 $[M+H]^+$. (Found: $[M + H]^+$, 370.2020. C_{14} H_{34} N_3 O_4 P_2 requires 370.2019).

6-*N*-bis(*t*-Butoxycarbonylmethyl)-6-methyl 1,4bis(ethoxymethylphosphinoxymethyl)-diazepine (30)

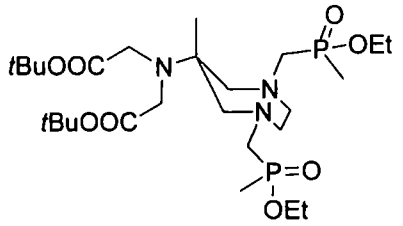

30

t-Butylbromoacetate (0.85 mL, 5.82 mmol) was added dropwise to a stirred solution of **29** (0.86 g, 2.33 mmol), K_2CO_3 (0.69 g, 4.99 mmol) and Na_2SO_4 (0.46 g, 3.24 mmol) in CH_3CN (20 mL) cooled to 0 °C. After the addition, the reaction mixture was allowed to warm to room temperature and then heated at reflux overnight. The solvent was then removed under reduced pressure and the residue suspended in 100 mL of petroleum ether / EtOAc (8 : 2). Salts were filtered off and the filtrate evaporated to dryness. The crude of the reaction was purified by column chromatography (SiO_2, CH_2Cl_2 / MeOH 5%), to afford the product as a pale brown oil (0.53 g, 38%). R_f (CH_2Cl_2 / MeOH 10%, SiO_2) = 0.45 (Iodine). δ_H ($CDCl_3$, 300

MHz): 1.14 (3H, s, $CH_3C_{(quat)}$), 1.34 (6H, br. t, 2 × OCH_2CH_3), 1.46-1.67 (24H, m, 2 × PCH_3 and 2 × $C(CH_3)_3$), 2.69 (4H, br.s, $CH_2CO_2C(CH_3)_3$), 2.80-3.08 (12H, m, 4 × $CH_{2(ring)}$ and 2 × CH_2P), 4.08 (4H, br. m, 2 × OCH_2CH_3). δ_C ($CDCl_3$, 100.6 MHz): 13.37 (d, J_{CP} = 91 Hz, PCH_3), 13.47 (d, J_{CP} = 91 Hz, PCH_3), 16.64 (OCH_2CH_3), 24.50 ($CH_3C_{(quat)}$), 28.18 ($C(CH_3)_3$), 51.53 (*C2* and *C3*), 58.65 ($C_{(quat)}$), 59.27 (NCH_2P), 59.81 (*C5* and *C7*), 60.71 (OCH_2CH_3), 70.44 ($RingNCH_2$), 80.57 ($C(CH_3)_3$, 172.49 (*C*=O). ^{31}P NMR ($CDCl_3$, 121.42 MHz,) δ_P: 53.09, 53.05, 52.80. *m/z* 598 $[M+H]^+$, 620 $[M+Na]^+$. (Found: $[M + H]^+$, 598.3381. $C_{26}H_{54}N_3O_8P_2$ requires 598.3385).

6-*N*-bis(Hydroxycarbonylmethyl)-6-methyl-1,4bis((hydroxymethylphosphinoxymethyl)-diazepine-dihydrochloride (31, L1)

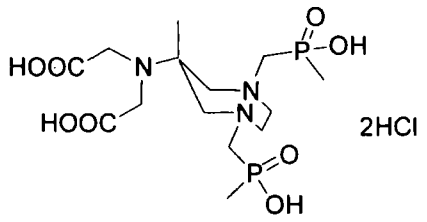

31

TMSI (0.44 g, 2.18 mmol) was slowly added to a solution of **30** (0.07 g, 0.165 mmol) in CH_3CN (10 mL) cooled at 5 °C, and the reaction mixture was left to stir at room temperature for 36 h. The dark red solution was diluted with H_2O (5 mL) and treated with aqueous $NaHSO_3$ (1 M, ~ 5 mL), until the solution became yellow in colour. Purification through Amberlite XAD 16 (chloride form, washed with water until pH 7) gave the product of reaction as a white powder (0.049 g, 70 %). δ_H (D_2O, 300 MHz): 1.19 (s, 3H, CH_3), 1.34 (d, 6H, J_{CP} = 15, 2 × PCH_3), 2.82 - 3.90 (m, 16H, 4 × $CH_{2(ring)}$, 2 × CH_2P, 2 × CH_2COOH), 3.88 (br s, 4H, 2 × CH_2P). ^{31}P NMR (D_2O, 121.42 MHz,) δ_P: 35.63.

Eu^{III}-AAZTA $[Eu^{III}L1]^-$

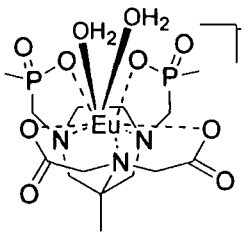

$[Eu^{III}L1]^-$

A solution of **31** (50.0 mg, 0.12 mmol) and $Eu(OAc)_3 \cdot 6H_2O$ (100.32 mg, 0.23 mmol) in water (4.0 mL) at pH 5.5 *ca.* was stirred at 60 °C for 18 h. The solvent was removed under reduced pressure, the residue redissolved in H_2O / MeOH (1 : 1, 4.0 mL) and aqueous KOH solution (1M, 450 μL) was added to give a solution pH of *ca.* 9. The solution was then centrifuged, the supernatant brought back to pH 6 and the solvent removed under reduced pressure to yield a light brown powder (75.0 mg).

The compound revealed exchange broadened ^1H NMR signals consistent with a paramagnetic shift due to the presence of europium. ^{31}P NMR (D_2O, 121.4 MHz,) δ_P: 54.8 (broad). $\tau_{(H_2O)} = 0.38$ ms, $\tau_{(D_2O)} = 1.25$.

Gd^{III}-AAZTAP $[Gd^{III}L1]^-$

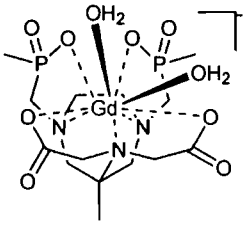

$[Gd^{III}L1]^-$

A solution of **27** (0.11 g, 0.34 mmol) and $GdCl_3 \cdot 6H_2O$ (0.19 g, 0.50 mmol) in water (6.0 mL) at pH 5.5 *ca.* was left stirring at 60 °C overnight. The solvent was removed under reduced pressure, the residue redissolved in 6.0 mL of H_2O / MeOH (1 : 1)

and aqueous KOH solution (1M, 370 μL) was added to give a solution pH of *ca.* 9. The solution was centrifuged, and the supernatant readjusted to pH 6 and the solvent removed under reduced pressure to yield 0.13 g of a yellow-brown powder. r_{1p} = 5.8 $mM^{-1}s^{-1}$ (20 MHz, 37 °C).

_N_-Allylbenzamide [9] (32)

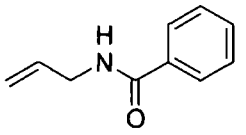

32

Benzoyl chloride (3.83 mL, 32.94 mmol) was slowly added to a solution of allylamine (2.63 mL, 35.02 mmol) and NEt_3 (9.22 mL, 66.24 mmol) in CH_2Cl_2 (25 mL) at 0 °C. The reaction mixture was stirred for 18 h under at room temperature under an argon atmosphere. Extractive work-up with H_2O (20 mL) and aqueous NH_4Cl solution (2 × 20 mL) followed by distillation gave *N*-Allylbenzamide (5.24 g) as a colorless oil in 93 % yield. b.p. 101 °C, P = 0.2 atm. δ_H ($CDCl_3$, 200 MHz): 3.93 (t, 2H, J = 5.6, CH_2NH), 5.08 (br dd, 2H, CH_2CH), 5.82 (m, 1H, $CHCH_2$), 7.30 (m, 3H, PhH), 7.79 (2H, dd, J = 1.2, 8 *o*-Ar).

3-Benzamidopropyl(hydroxymethyl)phosphinic acid [10] (33)

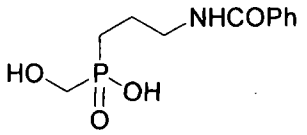

33

To a solution of *N*-Allylbenzamide **32** (0.6 g, 3.72 mmol) in dioxane (10 mL) hypophosphorous acid (0.69 g, 50 % aq. sol) and benzoyl peroxide (0.024 g, 0.01 mmol) were added. The reaction mixture was heated to reflux for 18 h, then the solvent was removed under reduced pressure and the residue redissolved in dioxane (5 mL). Excess paraformaldehyde (1.50 g) was added and the mixture heated to

reflux for further 48 h. After removal of the solvent, the residue was purified by column chromatography (SiO_2, CH_2Cl_2 / MeOH 28 % / 2 % aq NH_4OH → 3 % aq NH_4OH) to yield the desired product as the ammonium salt of the acid **33**, as a hygroscopic colourless glass, yield: 0.46 g (50 %). ES-MS: *m/z* 257 [M], 256 [M-1]. δ_H (D_2O, 200 MHz): 1.50 (2H, m, CCH_2C), 1.63 (2H, m, PCH_2C), 3.24 (2H, t, J = 7 Hz, CH_2N), 3.48 (2H, d, J = 6 Hz, HOCH_2P), 7.31 (2H, t, J = 8 Hz, Ph-*m*), 7.39 (1H, t, J = 8 Hz, Ph-*p*), 7.54 (2H, d, J = 8 Hz, Ph-*o*). δ_C (D_2O, 100.61 MHz): 21.7 (*C*H_2CH_2P), 25.0 (d, J_{CP} = 90 Hz, *C*H_2P), 40.9 and 41.0 (*C*H_2NHCO E and Z), 59.7 (d, J_{CP} = 108 Hz, P*C*H_2OH), 127.0 (Ph-*m*) , 128.7 (Ph-*o*), 132.0 (Ph-*p*), 133.7 (Ph-*i*), 170.7 (*C*ONH). ^{31}P NMR (D_2O, 161.9 MHz) δ_P: 40.5 (m).

Ethyl 3-Benzamidopropyl(hydroxymethyl)phosphinate (34)

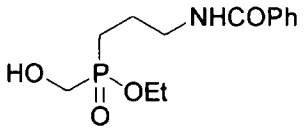

34

To a solution of the ammonium salt of **33** (0.23 g, 0.89 mmol) in water (2 mL) was added a strong acid ion-exchange resin (Dowex 50W, H^+ form, 1.43 g) and after filtration and evaporation, the residue was treated with triethyl orthoformate (1.15 mL) and the mixture was heated to reflux for 96 h. After evaporation, the residue was purified by column chromatography (SiO_2, CH_2Cl_2 / MeOH 5 % → 10 % MeOH), to yield the desired product **36**, mixed with its orthoformate ester [ES-MS: *m/z* 387; ^{31}P NMR ($CDCl_3$): δ 52.00]. Transesterification was performed by boiling the mixture in EtOH (10 mL) in the presence of conc. H_2SO_4 (500 mL) for 36 h. Evaporation and purification by column chromatography (SiO_2, CH_2Cl_2 / MeOH 5 %) yielded the desired product as a pale oil (0.15 g, 60 %). ES-MS: *m/z* 286 [M + H]$^+$. δ_H ($CDCl_3$, 400 MHz): 1.13 (t, 3H, CH_3), 1.85 (m, 4H, CH_2CH_2P), 3.56 (dt, 2H, CH_2NHCO), 3.82 (br d, 2H, CH_2OH), 3.90 (m, 2H, CH_2O), 7.25 (m, 3H), 7.77 (dd, 2H, *o*-Ar). ^{31}P NMR ($CDCl_3$, 121.42 MHz,) δ_P: 53.7.

(±)Dimethyl-2-bromo-pentanedioate (35)

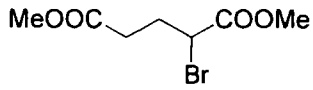

35

Thionyl chloride (30 mL) was added over a period of 20 min to monomethylglutaric acid (19.55 g, 146 mmol). After heating at reflux for 30 min, the reaction mixture was cooled to room temperature, Bromine (7.5 mL, 146 mmol) was added dropwise and then heated at reflux for 3 h. After cooling to 0 °C, methanol (30 mL) was added slowly and the solution stirred for 30 min. Water (200 mL) and $Na_2S_2O_3$ (5 g) were added and the mixture was extracted sequentially with petroleum ether (150 mL), ether (75 mL) and CH_2Cl_2 (75 mL). The combined organic extracts were washed with $NaHCO_3$ (2×100mL) and brine (50 mL), dried over Na_2SO_4 and evaporated under reduced pressure to give an oil, from which a solid separated. The oil was distilled using a Vigreux column at ~ 0.05 mmHg (60 – 95 °C), to give the product of reaction as a clear oil (12 g, 50.4 mmol, 35 %). δ_H ($CDCl_3$, 400.13 MHz): 2.15 – 2.22 (1H, m, CH_aCHBr), 2.28 – 2.34 (1H, m, CH_bCHBr), 2.42 – 2.46 (2H, m, CH_2COOCH$_3$), 3.61 (3H, s, CH$_2$COOCH_3), 3.70 (3H, s, CHBrCOOCH_3), 4.31 (1H, dd, J = 6, CHBr). δ_C ($CDCl_3$, 100.62 MHz): 29.5 (*C*H$_2$CHBr), 31.2 (*C*H$_2$CO), 44.45 (CH$_2$COO*C*H$_3$), 51.73 (CHBrCOO*C*H$_3$), 53.3 (*C*HBr), 169.75 (CH$_2$*C*=O), 173.0 (CHBr*C*=O). *m/z* (ES+): 261.3 $[M+Na]^+$. (Found: $[M+Na]^+$, 260.9733 $C_7H_{11}O_4{}^{79}Br_1{}^{23}Na_1$ requires $[M]^+$, 260.9733).

6-Amino-6-methylperhydro-1,4-bis(1'-methoxycarbonyl-3'methoxycarbonylpropyl)diazepine (36)

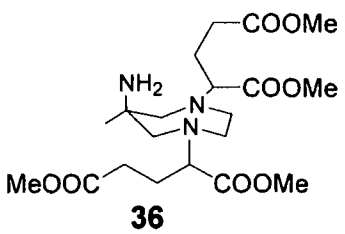

36

The ester **35** (1 g, 4.18 mmol) dissolved in CH_3CN (10 mL) was added over a period of 10 min to a suspension of AMPED, **28**, (0.257 g, 1.99 mmol) and K_2CO_3 (0.55 g, 3.98 mmol) in MeCN (10 mL). After 24 h stirring at 75 °C, the solvent was removed under reduced pressure and the residue dissolved in EtOAc (15 mL), washed with water/brine (80:20 v/v, 3×15 mL) and dried over Na_2SO_4. Evaporation of the solvent to dryness gave **36** (0.74 g, 1.66 mmol, 84 %) as dark yellow oil. R_f ($CHCl_3$/MeOH/NH_3 9:1:0.1, SiO_2) = 0.2 (UV, $KMnO_4$). δ_H ($CDCl_3$, 399.96 MHz): 0.91 (3H, s, CH_3), 1.73 – 1.88 (2H, m, 2 × C$H_a$$CH_2CO_2CH_3$), 1.89 – 2.04 (2H, m, 2 × C$H_b$$CH_2CO_2CH_3$), 2.37 – 2.42 (4H, m, 2 × C$H_2$$CO_2CH_3$), 2.42 – 2.80 (8H, br. m, 4 × CH_{2ring}), 3.15 – 3.23 (1H, br. dd, CH_XN), 3.23 – 3.30 (1H, br. dd, CH_YN), 3.58 – 3.60 (12H, m, 4 × OCH_3). δ_C ($CDCl_3$, 75 MHz): 24.42 (*C*H_3), 25.0 - 25.5 (*C*$H_2CH_2CO_2CH_3$), 30.8 (*C*$H_2CO_2CH_3$), 51.8 (O*C*H_3), 49.9 – 55.4 (*C*H_{2ring}), 67.41 (*C*HN), 173.0 (*C*=O), 173.6 (*C*=O). *m/z* (ES+): 446.3 $[M + H]^+$, 468.3 $[M + Na]^+$. (Found: $[M + H]^+$, 446.2493 $C_{20}H_{36}N_3O_8$ requires $[M + H]^+$, 446.2497).

6-Bis(*tert*-butoxycarbonylmethyl)amino-6-methyl-1,4-bis(1'-methoxycarbonyl-3'methoxycarbonylpropyl)- diazepine (37)

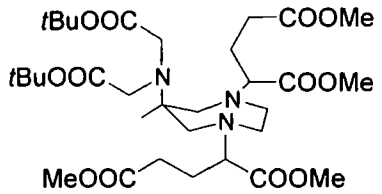

37

t-Butyl bromoacetate (d = 1.321, 0.8 mL, 5.49 mmol) was added to a stirred suspension of **36** (0.7 g, 1.57 mmol) and K_2CO_3 (0.86 g, 6.20 mmol) in CH_3CN (15 mL) cooled to 0 °C. The reaction mixture was allowed to warm to room temperature, Na_2SO_4 (0.20 g, 1.41 mmol) was added and the suspension heated at reflux overnight. After cooling to room temperature, salts were filtered off and the mother liquor evaporated to give the crude product (0.85 g, 1.26 mmol). Purification by flash chromatography (SiO_2, 20 % EtOAc in Hexane → 50 % EtOAc in Hexane)

gave the product, **37**, as a yellow oil (0.37 g, 0.55 mmol, 35 %). R_f (Hexane/EtOAc 7:3, SiO_2) = 0.2 (UV, Iodine). δ_H ($CDCl_3$, 399.95 MHz): 0.95 (3H, s, CH_3), 1.34 – 1.35 (18H, s, $C(CH_3)_3$), 1.73 – 1.85 (2H, m, 2 × $CH_{2a}CH_2CO_2CH_3$), 1.86 – 1.98 (2H, m, 2 × $CH_{2b}CH_2CO_2CH_3$), 2.31 – 2.36 (4H, m, 2 × $CH_2CO_2CH_3$), 2.36 – 3.05 (8H, br. m, 4 × CH_{2ring}), 3.17 – 3.23 (1H, br. dd, CH_XN), 3.26 – 3.31 (1H, br. dd, CH_YN), 3.51 (2H, d, J = 12.4, $CH_2COOtBu$), 3.56 (2H, d, J = 12.4, $CH_2COOtBu$), 3.56 – 3.60 (12H, m, 4 × OCH_3). δ_C ($CDCl_3$, 125.66 MHz): 23.9 (CH_3), 24.20 ($CH_2CH_2CO_2CH_3$), 28.3 ($CH_2CO_2CH_3$), 51.8 (OCH_3), 51.40 – 51.87 (CH_{2ring}), 54.03 ($C_{qual}CH_3$), 68.42 ($CH_2COOtBu$), 68.5 (*C*HN), 80.71 ($C_{qual}(CH_3)_3$), 172.6 – 172.9 (*C*=O), 173.19 (C=O), 173.75 (*C*=O). *m/z* (ES-): 674.2 $[M + H]^+$, 696.3 $[M + Na]^+$. (Found: $[M + H]^+$, 674.3858. $C_{32}H_{56}O_{12}N_3$ requires $[M + H]^+$, 674.3856; found: $[M + Na]^+$, 696.3678. $C_{32}H_{55}O_{12}N_3{}^{23}Na_1$ requires $[M + Na]^+$, 696.3676).

6-Bis(carboxymethyl)amino-6-methyl-1,4-bis[1',3'-(dimethoxycarbonyl)propyl]- diazepine (38)

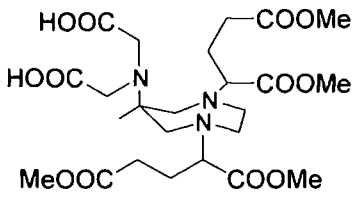

38

A solution of **37** (0.2 g, 0.29 mmol) in TFA/CH_2Cl_2 (1:1, 3.0 mL) was stirred at room temperature for 24 h. The solvent was removed under high vacuum (KOH pellets in the traps), the residue was dissolved in CH_2Cl_2 (3 mL) and the solution evaporated under reduced pressure. This procedure was repeated twice. The residue was washed twice with diethyl ether (2 × 2 mL) and a precipitated white solid was obtained (**38**, 0.146 g, 0.26 mmol, 90 %). δ_H ($CDCl_3$, 399.96 MHz): 1.2 (3H, br. s, CH_3), 1.96 – 2.11 (4H, m, 2 × $CH_2CH_2CO_2CH_3$), 2.38 – 2.55 (4H, m, 2 × $CH_2CO_2CH_3$), 2.80 – 3.35 (8H, br. m, 4 × CH_{2ring}), 3.46 (1H, br. dd, CH_XN), 3.48 (1H, br. dd, CH_YN), 3.6 (2H, br. d, 2 × CH_2COOH), 3.69 – 3.72 (12H, m, 4 × OCH_3).

6-Bis(carboxymethyl)amino-6-methyl-1,4-bis[1',3'(dimethoxycarbonyl)propyl]-diazepine : a statistical mixture of RR/SS and RS isomers (39, L2)

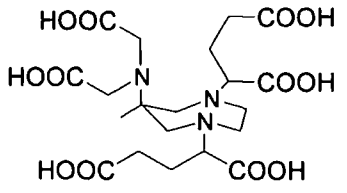

L2

KOD (1M solution in D_2O, 1mL) was added to **38** (0.15 g, 0.27 mmol) and the solution was stirred at 40 °C. The reaction's progress was checked by ^1H NMR. After 7 days, the solvent was removed under reduced pressure and a white glassy solid was obtained, which was used directly for the next complexation reaction (**L2**, 0.13 g, 0.26 mmol, 96 %). δ_H (D_2O, 399.96 MHz): 1.1 (3H, s, CH_3), 1.6 – 1.88 (4H, m, 2 × $CH_2CH_2CO_2H$), 2.03 – 2.15 (4H, m, 2 × $CH_2CH_2CO_2H$), 2.45 – 3.32 (8H, br. m, 4 × CH_{2ring}), 3.55 (1H, br. dd, CH_XN), 3.67 (1H, br. dd, CH_YN), 3.7 (4H, br. d, 2 × CH_2COOH).

$[Ln^{III}(Glu)_2$*racemic*-AAZTA$]^{3-}$

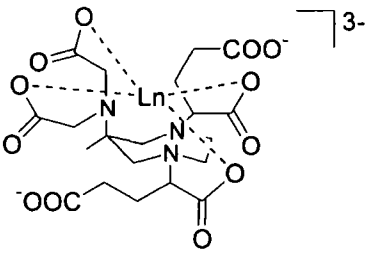

$[Ln^{III}L2]^{3-}$

An aqueous solution of $LnCl_3 \cdot 6H_2O$ (0.8 eqv) was added dropwise to a solution of **39** (1 eqv, dissolved in the minimum volume of H_2O). The pH was adjusted to ~ 5.5 with aqueous KOH solution (1M) and the mixture was left to stir at 50 °C. After 48h, the reaction mixture was cooled to room temperature and the pH of the solution raised to ~ 10 (using aqueous KOH, 1M). The white powder that precipitated was

isolated by centrifugation and the pH of the supernatant readjusted to ~ 5.5. Freeze drying of the liquid gave the complex as a white crystalline solid, together with KCl. The properties of the complex were examined in the presence of the salt.

$[Yb^{III}L2]^{3-}$

m/z (TOF MS ES-): 672.5 $[M]^-$. (Found: $[M]^-$, 668.4998. $C_{20}H_{27}N_3O_{12}{}^{170}Yb_1$ requires $[M]^-$, 668.4998 and $[M]^-$, 672.5007. $C_{20}H_{27}N_3O_{12}{}^{174}Yb_1$ requires $[M]^-$, 672.5067).

$[Gd^{III}L2]^{3-}$

m/z (TOF MS ES-): 659.0 $[M]^-$. (Found: $[M]^-$, 659.0304 $C_{20}H_{27}N_3O_{12}{}^{158}Gd_1$ requires $[M - H]^-$, 659.0309; $[M]^-$, 655.0465 $C_{20}H_{27}N_3O_{12}{}^{154}Gd_1$ requires $[M - H]^-$, 655.0470; $[M]^-$, 656.0506 $C_{20}H_{27}N_3O_{12}{}^{155}Gd_1$ requires $[M - H]^-$, 656.0510).

Relaxivity value found by NMRD analysis: r_{1p} = 8.02 $mM^{-1}s^{-1}$ (20 MHz, 298 K). The $[Gd^{3+}]$ was determined by mineralization with 37% HCl at 120°C overnight.

$[Eu^{III}L2]^{3-}$

m/z (TOF MS ES-): 652.2 $[M]^-$. (Found: $[M]^-$, 652.0795 $C_{20}H_{27}O_{12}N_3{}^{151}Eu_1$ requires $[M]^-$, 652.0798; $[M]^-$, 654.0808 $C_{20}H_{27}O_{12}N_3{}^{153}Eu_1$ requires $[M]^-$, 654.0813).

$\tau_{(H_2O)}$ = 0.20, $\tau_{(D_2O)}$ = 0.35.

(2S)-2-Bromo pentanedioic acid 5-(phenylmethyl)ester (40)

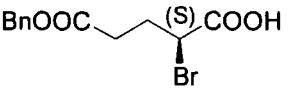

40

A solution of $NaNO_2$ (5.5 g, 80.1 mmol) in water (50 mL) was added dropwise over 30 minutes to a mixture of L-glutamic acid 5-benzyl ester (10.0 g, 42.1 mmol) and NaBr (16 g, 155.9 mmol) in 1M HBr (250 mL) cooled at -5 °C. After 7 h, conc. H_2SO_4 (4 mL) was slowly added to the solution, which was then extracted with Et_2O (3 x 300 mL). The combined organic phases were washed with brine (2 x 200 mL), dried (Na_2SO_4) and evaporated under reduced pressure. The crude product was purified by flash chromatography (SiO_2, 10 % EtOAc in *n*-Hexane → 20% EtOAc in *n*-Hexane) to give **40** as a light yellow oil (7.4 g, 24.6 mmol, 57.8%). R_f (*n*-Hexane /

EtOAc 15%, SiO_2) = 0.25 (UV, $KMnO_4$). HPLC (Chromatographic method A2): t_r: 8.8 min. δ_H ($CDCl_3$, 699.73 MHz): 2.29 - 2.34 (1H, m, CH_{2a}CHBr), 2.41 – 2.46 (1H, m, CH_{2b}CHBr), 2.57 – 2.63 (2H, m, CH_2CO), 4.41 (1H, dd, ^{3}J = 6.0, ^{3}J = 8.8, C*H*Br), 5.14 (2H, s, CH_2Ph), 7.33 – 7.39 (5H, m, Ph-*H*); δ_C ($CDCl_3$, 175.95 MHz): 29.73 (*C*H_2COOBn), 31.64 (*C*H_2CHBr), 44.18 (*C*HBr), 66.91 (*C*H_2Ph), 128.52 – 128.86 (Ph – *C*), 135.78 ($C_{(quat)}$), 172.09 (*C*OBn), 173.37 (*C*OOH); *m/z* (ES+) 323.2 $[M + Na]^+$; (Found: C, 47.97; H, 4.57; Br, 26.01%. $C_{12}H_{13}BrO_4$ requires C, 47.86; H, 4.35; Br, 26.53%).

(2S)-2-Bromo pentanedioic acid 1-(1,1-dimethylethyl) 5-(phenylmethyl) diester (41)

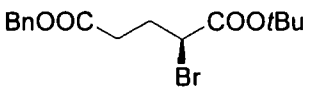

41

A solution of compound **40** (2 g, 6.85 mmol) in *t*-butyl acetate (24 mL) and $HClO_4$ 70% in water (25 µL, 0.34 mmol) was stirred at room temperature for 16 h. Water (35 mL) was added to the reaction mixture and the separated organic phase was washed successively with water (25 mL), 5 % aqueous Na_2CO_3 solution (25 mL, neutral pH) and dried over Na_2SO_4. After the solvent was removed under reduced pressure, **41** was obtained as a pale yellow oil (2.15 g; 6.03 mmol, 88%). R_f (*n*-Hexane / EtOAc 5%, SiO_2) = 0.44 (UV, $KMnO_4$). HPLC (Chromatographic method A2): t_r: 13.1 min. δ_H ($CDCl_3$, 699.73 MHz): 1.48 (9H, s, C(CH_3)$_3$), 2.24 – 2.29 (1H, m, CH_{2a}CHBr), 2.34 – 2.39 (1H, m, CH_{2b}C*H*Br), 2.52 - 2.60 (2H, m, CH_2CO), 4.25 (1H, dd, $^3J_{2,3a}$ = 5.6, $^3J_{2,3b}$ = 8.4, C*H*Br), 5.13 (2H, s, CH_2Ph), 7.31 – 7.38 (5H, m, Ph - *H*); δ_C ($CDCl_3$, 175.95 MHz): 27.95 (C(*C*H_3)$_3$), 29.95 (*C*H_2COOBn), 31.86 (*C*H_2CHBr), 46.85 (*C*HBr), 66.77 (*C*H_2Ph), 82.86 ($C_{(quat)}$ (CH_3)$_3$), 128.46 – 128.83 (Ph - *C*), 135.94 ($C_{(quat)}$Ph), 168.56 (*C*OBn), 172.26 (*C*OOH); *m/z* (ES+) 379.2 $[M + Na]^+$; (Found: C, 52.73; H, 5.58; Br, 22.30%; $C_{16}H_{21}BrO_4$ requires: C, 52.49; H, 5.58; Br, 23.28%).

(*1'R,6S*)-(1'-*t*-Butoxycarbonyl-3'-benzyloxycarbonylpropyl)-6-amino-6-methylperhydro-1,4-diazepine, (42); (*1'R,6R*)-1'-*t*-butoxycarbonyl-3'-benzyloxycarbonylpropyl) 6-amino-6-methylperhydro-1,4-diazepine, (43); (*R,R*)- 1,4-bis(1'-*t*-butoxycarbonyl-3'-benzyloxycarbonylpropyl)-6-amino-6-methylperhydro-1,4-diazepine, (44)

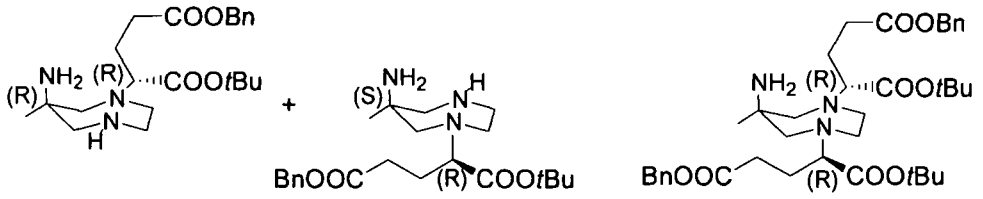

42 **43** **44**

A suspension of **41** (2.25 g, 6.32 mmol), **28** (5.4 g, 41.82 mmol) and K_2CO_3 (0.87 g; 6.32 mmol) in MeCN (80 mL) was stirred at room temperature for 18 h. The solvent was removed under reduced pressure and the residue dissolved in EtOAc (80 mL), washed with water / brine (80 : 20 v/v, 2 × 70 mL), dried over Na_2SO_4 and evaporated to dryness. The residue was dissolved in EtOAc (50 mL), washed with aqueous HBr (1M) (10 : 1 v/v, 3 × 40 mL), dried over Na_2SO_4 and evaporated to dryness, to give **44** as a pale brown oil (1.19 g, 1.76 mmol, 28 %). Concentrated aqueous ammonia (5.2 mL) was added dropwise to the aqueous phase (till pH ~ 9), which was then extracted with EtOAc (4 × 40 mL). The organic phase was washed with H_2O / brine (4 : 1 v/v, 3 × 50 mL), dried over Na_2SO_4 and evaporated to dryness to give an oil (1.5 g, 3.7 mmol), a mixture of **42** and **43**. Crystallization from EtOH and washing of the precipitated solid with CH_3CN gave a yellow oil (1.02 g, 2.52 mmol, 40 %) and a crystalline white solid (0.250 g, 0.61 mmol, 10 %).

***44:* (*R,R*) 1,4-Bis(1'-*t*-Butoxycarbonyl-3'-benzyloxycarbonylpropyl)-6-amino-6-methylperhydro-1,4-diazepine**

R_f ($CHCl_3$/EtOH/NH_3 95:5:0.1, SiO_2) = 0.2 (UV, $KMnO_4$).

HPLC (Chromatographic method A2): 70 % (Area %); t_r: 14 min. δ_H ($CDCl_3$, 399.9 MHz): 0.91 (3H, s, CH_3), 1.40 (9H, s, $C(CH_3)_3$), 1.42 (9H, s, $C(CH_3)_3$), 1.82 – 2.19 (4H, br. m, $2\times CH_2CHN$), 2.35 – 2.72 (8H, m, CH_{2ring}), 2.88 – 3.0 (4H, m, $2\times CH_2COOBn$), 3.44 – 3.5 (2H, m, $2\times CHN$), 5.10 (4H, d, J = 7.2, $2\times CH_2Ph$), 7.29 – 7.35 (10 H, m, 2×Ph – *H*). δ_C ($CDCl_3$, 75 MHz): 25.10 (CH_3), 26.08 (CH_2CHN), 28.56 ($C(CH_3)_3$), 32.11 (CH_2COOBn), 49.10 ($CH_{2(ring)}N$), 51.75 ($CH_{2(ring)}C_{quat}$), 66.54 (CH_2Ph), 68.33 (*C*HN), 128.5 – 129.08 (C_{arom}), 136.33 ($C_{quat\ arom}$), 171.98 ($C_{quat}NH_2$), 173.21 ($C{=}O_{Bn}$), 174.00 ($C{=}O_{tBu}$). *m/z* (ES+): 682.4 $[M + H]^+$, 704.3 $[M + Na]^+$, 626.33 $[M - tBu]^+$. (Found: C, 64.27; H, 8.15; N, 5.90% · 1½ H_2O; $C_{38}H_{55}N_3O_8 \cdot 3/2\ H_2O$ requires: C, 64.4; H, 8.19; N, 5.93%).

***42:* (*1'R,6S*)-(1'-*t*-Butoxycarbonyl-3'-benzyloxycarbonylpropyl)-6-amino-6-methylperhydro-1,4-diazepine - *Diastereoisomer soluble in EtOH* –**

R_f ($CHCl_3$/MeOH/NH_3 86:12:1, SiO_2) = 0.35 (UV, $KMnO_4$). HPLC (Chromatographic method A2): t_r: 5 min. δ_H ($CDCl_3$, 699.73 MHz): 0.94 (3H, s, CH_3), 1.42 (9H, s, $C(CH_3)_3$), 1.81 - 1.91 (1H, m, $CH_{2a}CHN$), 1.96 – 2.03 (1H, m, $CH_{2b}CHN$), 2.45 - 2.54 (2H, m, CH_2COOBn), 2.61 – 2.91 (8H, m, H_{ring}), 3.14 – 3.19 (1H, m, CHN), 5.09 (2H, s, CH_2Ph), 7.31 - 7.33 (5H, m, Ph – *H*). δ_C ($CDCl_3$, 125.67 MHz): 25.42 (CH_2CHN), 25.7 (CH_3), 28.44 ($C(CH_3)_3$), 31.26 (CH_2COOBn), 49.42 (CH_2N), 54.3 (CH_2N), 56.8 (C_{quat}), 56.9 (CH_2C_{quat}), 60.0 (CH_2C_{quat}), 66.73 (CH_2Ph), 68.7 (*C*HN), 82.6 ($C(CH_3)_3$), 128.4 – 128.84 (C_{arom}), 136.0 ($C_{quat\ arom}$), 171.01 ($C{=}O_{Bn}$), 173.0 ($C{=}O_{tBu}$). m/z (ES+): 406.2 $[M+H]^+$, 428.3 $[M+Na]^+$.

***43:* (*1'R,6R*)-1'-*t*-butoxycarbonyl-3'-benzyloxycarbonylpropyl) 6-amino-6-methylperhydro-1,4-diazepine - *Crystalline solid insoluble in EtOH* -**

R_f ($CHCl_3$/MeOH/NH_3 86:12:1, SiO_2) = 0.35 (UV, $KMnO_4$). HPLC (Chromatographic method A2): t_r: 5 min. m.p. 117 – 124 °C. δ_H ($CDCl_3$, 699.73 MHz): 0.98 (3H, s, CH_3), 1.44 (9H, s, $C(CH_3)_3$), 1.82 - 1.89(1H, m, $CH_{2a}CHN$), 2.0 – 2.07 (1H, m, $CH_{2b}CHN$), 2.49 – 2.52 (2H, td, ^3J = 2.8, CH_2COOBn), 2.62 – 2.68 (m, 5H, H_{ring}), 2.71 – 2.75 (m, 1H, H_{ring}), 2.79 – 2.83 (m, 1H, H_{ring}), 2.91 – 2.95 (m, 1H, H_{ring}), 3.17 (1H, dd, ^3J = 6.3, ^3J = 9.1, *C*HN), 5.11 (2H, s, CH_2Ph), 7.33 - 7.35

(5H, m, Ph – *H*). δ_C ($CDCl_3$, 175.95 MHz): 25.73 (CH_2CHN), 26.41 (CH_3), 28.51 ($C(CH_3)_3$), 31.19 (CH_2COOBn), 51.84 (CH_2N), 53.62 (CH_2N), 55.5 (C_{quat}), 62.46 (CH_2C_{quat}), 66.54 (CH_2C_{quat}), 66.87 (CH_2Ph), 68.91 (*C*HN), 81.46 ($C(CH_3)_3$), 128.48 – 128.8 (C_{arom}), 136.13 ($C_{quat\ arom}$), 171.95 ($C{=}O_{Bn}$), 173.32 ($C{=}O_{tBu}$). *m/z* (ES+): 406.2 $[M + H]^+$, 428.3 $[M + Na]^+$.

(2R)-2-Bromo pentanedioic acid 5-(phenylmethyl)ester (45)

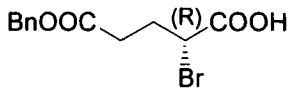

45

The same experimental procedure used for the synthesis of **40** was followed, and the analytical characterization of the molecule (ESMS, HNMR, ^{13}CNMR) is identical.

(2*R*)-2-Bromo pentanedioic acid 1-(1,1-dimethylethyl) 5-(phenylmethyl) diester (46)

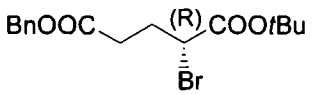

46

The same experimental procedure used for the synthesis of **41** was followed, and the analytical characterization of the molecule (ESMS, HNMR, ^{13}CNMR) is identical.

(*R,S*) 1,4-Bis(1'-*t*-Butoxycarbonyl-3'-benzyloxycarbonylpropyl)-6-amino-6-methylperhydro-1,4-diazepine (47)

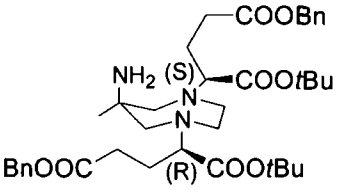

47

46 (0.73 g, 2.05 mmol) dissolved in CH_3CN (10mL) was added dropwise to a stirred solution of **42** (0.83 g, 2.05 mmol), K_2CO_3 (0.28 g, 2.05 mmol) and Na_2SO_4 (0.064 g, 0.45 mmol) in CH_3CN (10 mL) cooled at 0 °C. The reaction mixture was allowed to warm to room temperature and left stirring for 18 h. The solvent was removed under reduced pressure and the residue dissolved in EtOAc (30 mL), washed with water/brine (80 : 20 v/v, 2 × 30 mL), dried over Na_2SO_4 and evaporated to dryness. The residue was dissolved in EtOAc (20 mL), washed with H_2O / HBr (1M) (10 : 1 v/v, 3 × 20 mL), dried over Na_2SO_4 and evaporated to dryness, to give **47** as a yellow oil (0.97 g, 1.42 mmol, 70 %). R_f ($CHCl_3$/EtOH/NH_3 95:5:0.1, SiO_2) = 0.2 (UV, $KMnO_4$). δ_H ($CDCl_3$, 400.13 MHz): 1.40 – 1.46 (21H, br. s, 2 × $C(CH_3)_3$ + CH_3), 1.83 – 2.03 (2H, m, $CH_{2a}CHN$), 2.08 – 2.17 (2H, m, $CH_{2b}CHN$), 2.33 – 3.10 (12H, m, 2 × CH_2COOBn + H_{ring}), 3.46 (2H, dd, J = 6, J = 8.8, 2 × CHN), 5.10 - 5.12 (2H, s + s, 2 × CH_2Ph), 7.28 – 7.34 (10 H, m, 2 × Ph – *H*). δ_C ($CDCl_3$, 100 MHz): 24.72 (CH_3), 27.72 ($C(CH_3)_3$), 29.71 (CH_2CHN), 31.63 (CH_2COOBn), 48.8 ($CH_{2(ring)}N$), 52.61 ($CH_{2(ring)}C_{quat}$), 66.54 (CH_2Ph), 68.21 (CHN), 127.0 – 128.75 (C_{arom}), 136.0 ($C_{quat\ arom}$), 168.29 ($C{=}O_{Bn}$), 173.01 ($C{=}O_{tBu}$), 173.13 ($C_{quat}NH_2$). *m/z* (ES+): 682.4 $[M + H]^+$, 704.3 $[M + Na]^+$, 626.33 $[M - tBu]^+$.

(*1'R,6S*)-1-(1'-*t*-Butoxycarbonyl-3'-benzyloxycarbonylpropyl)-4-(*t*-butoxycarbonylmethyl)-6-bis(*t*-butoxycarbonylmethyl)amino-6-methylperhydro-1,4-diazepine, (**48** and **49**)

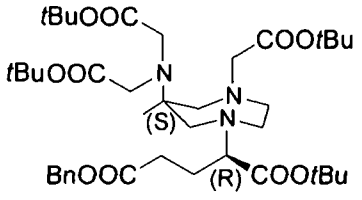

48

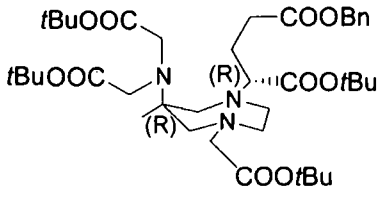

49

t-Butyl bromoacetate (0.26 mL, 1.75 mmol) was added dropwise to a stirred solution of **48** (0.20 g , 0.5 mmol), K_2CO_3 (0.27 g, 1.95 mmol) and Na_2SO_4 (0.064 g, 0.45 mmol) in CH_3CN (10 mL) cooled at 0°C. The reaction mixture was allowed to warm to room temperature, boiled under reflux for 6 h and then left stirring overnight at room temperature. The mixture was evaporated under reduced pressure and the residue treated with petroleum ether / EtOAc 8 : 2 (20 mL). Salts were filtered off and the mother liquor evaporated to give the crude product (0.6 g). Purification by flash chromatography (SiO_2, 10 % EtOAc in petroleum ether → 20 % EtOAc in petroleum ether) gave the product as a yellow oil (0.22 g, 0.3 mmol, 60%). R_f (petroleum ether/EtOAc 8:2, SiO_2) = 0.3 (UV, $KMnO_4$). HPLC (Chromatographic method A2): t_r: 19 min. δ_H ($CDCl_3$, 699.73 MHz): 0.99 (3H, s, CH_3), 1.42 – 1.47 (36H, m, C(CH_3)$_3$), 1.81 - 1.91 (1H, m, CH_{2a}CHN), 1.94 – 2.04 (1H, m, CH_{2b}CHN), 2.45 - 2.76 (8H, m, 4×CH_{2ring}), 3.0 – 3.07 (2H, m, CH_2COOBn), 3.13 (1H, dd, J = 5.6, J = 10.5, C*H*N), 3.26 (1H, d, J = 14, C$H_{2a}N_{ring}$), 3.33 (1H, d, J = 14, C$H_{2b}N_{ring}$), 3.67 (2H, s, CH_2COO*t*Bu), 3.68 (2H, s, CH_2COO*t*Bu), 5.11 (2H, s, CH_2Ph), 7.31 - 7.35 (5H, m, Ph – *H*). δ_C ($CDCl_3$, 125.67 MHz): 24.38 (*C*H$_3$), 25.11 (*C*H$_2$CHN), 28.4 (C(*C*H$_3$)$_3$), 31.15 (*C*H$_2$COOBn), 51.84 ($C_{ring}H_2N$), 52.56 ($C_{ring}H_2N$), 60.1 (*C*H$_2$C$_{quat}$), 61.24 (C$_{quat}$), 62.07 (N*C*H$_2$COO*t*Bu), 66.52 (*C*H$_2$Ph), 67.33 (*C*H$_2$COO*t*Bu), 69.33 (*C*HN), 80.46 (*C*(CH$_3$)$_3$), 80.94 (*C*(CH$_3$)$_3$), 81.21 (*C*(CH$_3$)$_3$), 128.44 – 128.77 (C_{arom}), 136.18 ($C_{quat\ Ph}$), 171.24 (*C*=O$_{Bn}$), 172.07 (*C*=O$_{Bn}$), 172.88 (*C*=O$_{tBu}$), 173.47 (*C*=O$_{tBu}$). *m/z* (ES+): 748.4 $[M + H]^+$, 770.4 $[M + Na]^+$.

The same experimental procedure was followed using the Monoalkylated **49** as starting material for the reaction. Yield = 40%.

(*R,R*)1,4-Bis(1'-*t*-butoxycarbonyl-3'-benzyloxycarbonylpropyl)-6-bis(*t*-butoxycarbonlymethyl)amino-6-methylperhydro-1,4-diazepine (50)

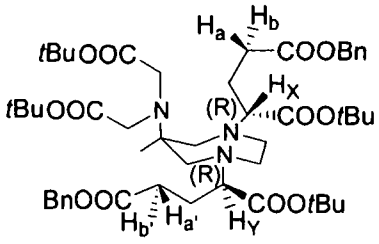

50

t-Butyl bromoacetate (0.13 mL, 0.88 mmol) was added to a stirred solution of **44** (0.24 g; 0.35 mmol) and K_2CO_3 (0.1 g; 0.7 mmol) in CH_3CN (5 mL) cooled to 0 °C. The reaction mixture was allowed to warm to room temperature and Na_2SO_4 (0.025 g, 0.17 mmol) was added. The suspension was boiled under reflux overnight and stirred at 60 °C for further 8 h. After addition of more *t*-butyl bromoacetate (0.13 mL, 0.88 mmol), the reaction mixture was boiled under reflux again overnight, than cooled to room temperature and left to stir for 5 h. The suspension was filtred, the solvent removed under reduced pressure and the residue was treated with petroleum ether / EtOAc 8 : 2 (10 mL). Salts were filtered off and the mother liquor evaporated to give the crude product (0.37 g) that was purified by flash chromatography (SiO_2, 5 % EtOAc in petroleum ether → 15 % EtOAc in petroleum ether) to give **50** as a yellow oil (0.2 g, 0.23 mmol, 65 %). R_f (petroleum ether / EtOAc 8 : 2, SiO_2) = 0.5 (UV, $KMnO_4$). HPLC (Chromatographic method A2): t_r: 21 min. δ_H ($CDCl_3$, 699.74 MHz): 0.99 (3H, s, CH_3), 1.40 – 1.43 (36H, m, 4×C(CH_3)$_3$), 1.82 – 1.87 (1H, m, CH_{2a}CH$_X$N), 1.88 – 1.94 (1H, m, CH_{2b}CH$_X$N), 1.98 – 2.05 (2H, m, C$H_{2a,b}$CH$_Y$N), 2.35 – 2.59 (8H, m, CH_{2ring}), 2.71 (1H, d, J = 14.7, CH_{2a}COOBn), 2.74 (1H, d, J = 12.6, CH_{2b}COOBn), 2.90 (1H, d, J = 12.6, CH_{2b}COOBn), 3.00 (1H, d, J = 14.7, CH_{2a}COOBn), 3.14 (1H, dd, J = 5.6, J = 10, CH_XN) 3.25 (1H, dd, J = 5.6, J = 10, CH_YN), 3.57 (2H, d, J = 17.5, CH_{2b}COO*t*Bu), 3.67 (2H, d, J = 17.5, CH_{2a}COO*t*Bu),

5.10 (4H, m, $J_{H_aH_b}$ = 15, $CH_{2(a,b)}$Ph + $CH_{2(a',b')}$Ph), 7.31 – 7.35 (10H, m, 2×Ph – *H*). δ_C ($CDCl_3$, 125.67 MHz): 25.23 (CH_3), 26.14 (CH_2CHN), 28.32 – 28.53 ($C(CH_3)_3$), 31.13 (CH_2COOBn), 51.7 – 54.2 (CH_{2ring}), 61.74 ($C_{quat}CH_3$), 66.6 (CH_2Ph), 68.13 ($CH_2COOtBu$), 69.23 (*C*HN), 80.58 ($C(CH_3)_3$), 81.26 ($C(CH_3)_3$), 81.33 ($C(CH_3)_3$), 128.44 – 128.79 (C_{arom}), 136.15 ($C_{quat\ Ph}$), 172.0 ($C{=}O_{Bn}$), 172.21 ($C{=}O_{Bn}$), 172.64 ($C{=}O_{tBu}$), 173.38 ($C{=}O_{tBu}$). *m/z* (ES+): 910.5 $[M + H]^+$, 932.5 $[M + Na]^+$. (Found: C, 62.20; H, 8.10; N, 4.11 %; $C_{50}H_{75}N_3O_{12} \cdot 3H_2O$ requires: C, 62.28; H, 8.41; N, 4.36 %).

(*R,S*)-1,4-Bis(1'-*t*-butoxycarbonyl-3'-benzyloxycarbonylpropyl)-6-bis(*t*-butoxycarbonylmethyl)amino-6-methylperhydro-1,4-diazepine, (51)

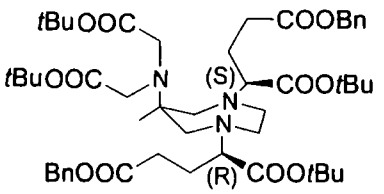

51

t-Butyl bromoacetate (0.53 mL, 3.56 mmol) was added to a stirred solution of **47** (0.97 g, 1.42 mmol) and K_2CO_3 (0.57 g, 4.12 mmol) in CH_3CN (10 mL) cooled to 0 °C. The reaction mixture was allowed to warm to room temperature, Na_2SO_4 (0.025 g, 0.17 mmol) was added and then refluxed overnight and stirred for further 6 h at 60 °C. The solvent was removed under reduced pressure and the residue treated with petroleum ether / EtOAc 8 : 2 (15 mL). Salts were filtered off and the mother liquor evaporated to give the crude product (1.05 g). Purification by flash chromatography (SiO_2, 5 % EtOAc in petroleum ether → 20 % EtOAc in petroleum ether) gave **51** as a yellow oil (0.52 g, 0.57 mmol, 40 %). R_f (petroleum ether/EtOAc 8:2, SiO_2) = 0.4 (UV, $KMnO_4$). δ_H ($CDCl_3$, 400.13 MHz): 1.01 (3H, s, CH_3), 1.43 – 1.46 (36H, s + s, 4×$C(CH_3)_3$), 1.89 – 1.95 (2H, m, CH_2CHN), 1.98 – 2.10 (2H, m, CH_2CHN), 2.36 – 2.57 (8H, m, CH_{2ring}), 2.62 - 2.87 (1H, m, 2×CH_2COOBn), 3.01 - 3.12 (2H, m, 2×*CH*N), 3.63 (2H, d, J = 17.6, $CH_2COOtBu$), 3.69 (2H, d, J = 17.6, $CH_2COOtBu$),

5.13 (4H, d, J = 2.4, $CH_{2(a,b)}$Ph + $CH_{2(a',b')}$Ph), 7.30 – 7.37 (10H, m, 2×Ph – *H*). δ_C ($CDCl_3$, 125.67 MHz): 25.22 (CH_3), 25.8 (CH_2CHN), 28.31 – 28.52 ($C(CH_3)_3$), 31.40 (CH_2COOBn), 31.52 (CH_2COOBn), 51.1 – 54.1 (CH_{2ring}), 61.74 ($C_{quat}CH_3$), 66.51 (CH_2Ph), 66.73 (CH_2Ph), 68.13 (CH_2COO*t*Bu), 68.38 (CH_2COO*t*Bu), 69.23 (*C*HN), 69.3 (*C*HN), 80.44 ($C(CH_3)_3$), 80.57 ($C(CH_3)_3$), 81.26 ($C(CH_3)_3$), 81.33 ($C(CH_3)_3$), 128.43 – 128.78 (C_{arom}), 136.15 (C_{quatPh}), 136.20 (C_{quatPh}), 171.73 ($C{=}O_{Bn}$), 172.0 ($C{=}O_{Bn}$), 172.64 ($C{=}O_{tBu}$), 173.38 ($C{=}O_{tBu}$). *m/z* (ES+): 910.3 [M + H]$^+$, 932.4 [M + Na]$^+$. (Found: MH$^+$, 910.5427. $C_{50}H_{76}N_3O_{12}$ requires MH$^+$, 910.5423; Found: [M + Na]$^+$, 932.5250. $C_{50}H_{75}N_3O_{12}Na$ requires [M + Na]$^+$, 9932.5243).

(1*R*,6*R*)-6-Bis(carbonylmethyl)amino-4-[(carboxymethyl)-1(1'- carbonyl)-3'-benzyloxycarbonylpropyl)-tetrahydro -6-methyl-1H-1,4-diazepine (53 *or* GluAAZTABn, L4)

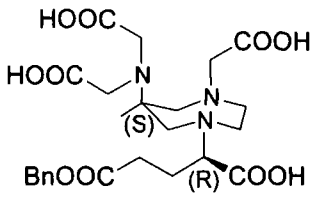

52

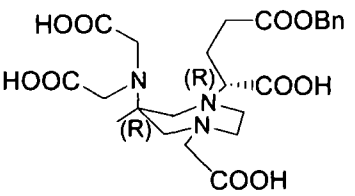

L4

A solution of **48** (0.10 g, 0.13 mmol) in TFA / DCM (1 : 1, 5.0 mL) was stirred at room temperature for 24 h. The solvent was removed under high vacuum (KOH pellets in the traps), the residue taken up with CH_2Cl_2 (3×8 mL) and the solution evaporated under reduced pressure for three times. The product of reaction, **52**, was obtained as a yellow oil (0.073 g; 0.14 mmol, 93 %).

A solution of **49** (0.020 g, 0.03 mmol) in TFA/DCM (1:1, 1.0 mL) was stirred at room temperature for 24 h. The solvent was removed under high vacuum (KOH pellets in the traps), the residue taken up with CH_2Cl_2 (3×2 mL) and the solution

evaporated under reduced pressure for three times. The product of reaction, **L4**, was obtained as a yellow oil (0.17 g, 0.33 mmol, 90 %).

52 δ_H (D_2O, 199.99 MHz): 0.95 (3H, br. s, CH_3), 1.73 - 1.9 (2H, m, CH_2CHN), 2.34 - 2.40 (2H, m, CH_2COOBn), 2.7 – 3.9 (13 H, br. m, 8×H_{ring}, CHN, 2×CH_2COOH), 4.94 (2H, s, CH_2Ph), 7.2 (5H, br. s, Ph – *H*).

53, L4 δ_H (D_2O, 399.96 MHz): 1.14 (3H, br. s, CH_3), 2.0 – 2.15 (2H, m, CH_2CHN), 2.53 - 2.59 (2H, m, CH_2COOBn), 2.96 – 3.8 (9 H, br. m, 8×H_{ring}, CHN), 3.92 – 4.0 (4H, m, 2×CH_2COOH), 5.14 (2H, s, CH_2Ph), 7.31-7.37 (5H, m, Ph – *H*). δ_C ($CDCl_3$, 125.67 MHz): 24.50 (CH_3), 25.24 (CH_2CHN), 31.15 (CH_2COOBn), 52.0 ($C_{ring}H_2N$), 52.60 ($C_{ring}H_2N$), 60.1 (CH_2C_{quat}), 61.24 (C_{quat}), 62.07 (NCH_2COOH), 66.52 (CH_2Ph), 67.33 (CH_2COOH), 69.33 (CHN), 128.3 – 128.6 (C_{arom}), 136.18 ($C_{quat\ Ph}$), 171.25 ($C{=}O_{Bn}$), 173.0 (C=OOH), 172.90 (C=OOH), 173.50 (C=OOH).

(*1'R,6S*)-6-[Bis(carboxymethyl)]-4-[(carboxymethyl) –1-(1'-carboxy-3'-carboxypropyl)-tetrahydro-6-amino-6-methyl-1H-1,4-diazepine (54 *or* GluAAZTA, L3)

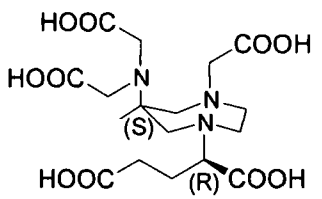

L3

10% Pd/C (0.005 g) was added to a solution of compound **52** (0.05 g, 0.067 mmol) in EtOH (4 mL) and H_2O (0.5 mL). The reaction mixture was stirred under a hydrogen atmosphere for 48 h using a hydrogenator (30 psi H_2). The catalyst was filtered over Celite and the solvent evaporated under reduced pressure, to afford the product as a white glassy solid (**L3**, 0.047 g, 0.07 mmol, 96%). δ_H (D_2O, 199.99 MHz): 1.05 (3H, br. s, CH_3), 1.92 – 2.01 (2H, m, CH_2CHN), 2.42 – 2.49 (2H, br. m,

CH_2COOH), 3.06 – 3.57 (8 H, br. m, $4\times CH_{2ring}$), 3.67 (4H, br. s, $2\times CH_2COOH$), 3.7 (2H, br. s, CH_2COOH). *m/z* (ES-MS): 453 $[M + Na]^+$.

(*RR*)-6-Bis(*t*-butoxycarbonylmethyl)amino-4-[*t*-(butoxycarboxymethyl)-1(1'-*t*-butoxycarbonyl)-3'-carboxypropyl)-tetrahydro -6-methyl-1H-1,4-diazepine (55)

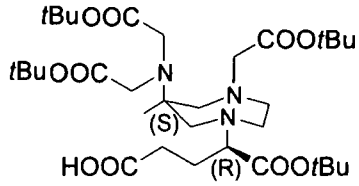

55

10% Pd/C (0.005 g) was added to a solution of compound **48** (0.05 g, 0.067 mmol) in EtOH (4 mL) and H_2O (0.5 mL). The reaction mixture was stirred under hydrogen atmosphere for 48 h using a hydrogenator (30 psi H_2). The catalyst was filtered over Celite and the solvent evaporated under reduced pressure, to afford the product of reaction as a white glassy solid (**55**, 0.047 g, 0.07 mmol, 96%).

δ_H (CD_3OD, 199.99 MHz): 1.06 (3H, br. s, CH_3), 1.46-1.48 (36H, m, $4\times C(CH_3)_3$), 1.77 – 2.0 (4H, m, $2 \times CH_2CHN$), 2.39 - 2.46 (2H, m, CH_2COOH), 3.0-3.6 (H, m, 9 H, br. m, $8\times H_{ring}$ + CHN), 3.7 (4H, dd, $2\times CH_2COOtBu$). *m/z* (ES+): 658.2 $[M + H]^+$.

(*RR*)-6-Bis(carboxymethyl)amino-1,4-bis(1'-carboxy-3'-carboxypropyl)-tetrahydro-6-methyl-1H-1,4-diazepine (56 *or* Glu AAZTA, L3)

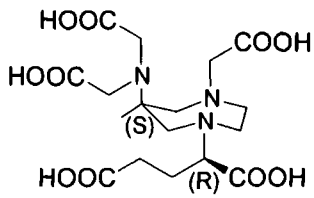

L3

A solution of **55** (0.047 g, 0.07 mmol) in TFA / CH_2Cl_2 (1 : 1, 2.5 mL) was stirred at room temperature for 24 h. The solvent was removed under high vacuum (KOH pellets in the traps), the residue taken up with CH_2Cl_2 (3 × 4 mL) and the solution evaporated under reduced pressure for three times. The residue was washed twice with diethyl ether (2×2 mL) and a precipitated white solid was obtained as the

product of reaction (**56**, 0.03 g, 0.068 mmol, 97%). δ_H (D_2O, 399.96 MHz): 1.04 (3H, br. s, CH_3), 1.91 - 1.93 (2H, m, CH_2CHN), 2.41 (2H, br. m, CH_2COOH), 3.0 – 3.49 (8 H, br. m, $4\times CH_{2ring}$), 3.62 (4H, br. s, $2\times CH_2COOH$), 3.82 (2H, br. s, CH_2COOH). *m/z* (ES+): 453.4 $[M + Na]^+$.

(*RR*)-6-Bis(carbonylmethyl)amino–1,4-bis(1'- carbonyl)-3'-benzyloxycarbonylpropyl)-tetrahydro -6-methyl-1H-1,4-diazepine (57)

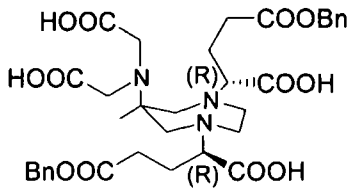

57

A solution of compound **50** (0.07 g, 0.077 mmol) in TFA and CH_2Cl_2 (1:1, 2 mL) was stirred at room temperature for 24 h. The mixture was then evaporated, the residue taken up with CH_2Cl_2 (2 mL) and the solution evaporated under reduced pressure. This operation was repeated three times, then the residue was washed twice with diethyl ether (2×2 mL) and a precipitated white solid was obtained as the product of reaction (**57**, 0.06 g, 0.087 mmol, 88%). δ_H (D_2O, 399.96 MHz: 1.05 (3H, s, CH_3), 1.98 – 2.06 (4H, m, 2 × CH_2CHN), 2.50 – 2.80 (4H, m, 2 × CH_2COOBn), 3.0 – 3.75 (10H, br. m, $4\times CH_{2ring}$ + 2 × CHN), 3.80 – 3.90 (4H, m, NCH_2COOH), 5.14 (4H, d, J = 4, 2 × CH_2Ph), 7.33 – 7.36 (10H, m, 2 × Ph – *H*).

(*RR*)-6-Bis(*t*-butoxycarbonylmethyl)amino–1,4-bis(1'-*t*-butoxycarbonyl)-3'-carboxypropyl)-tetrahydro -6-methyl-1H-1,4-diazepine (58)

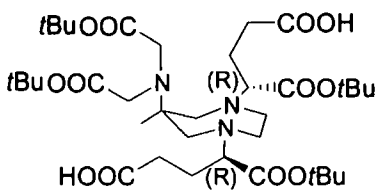

58

10% Pd/C (0.008 g) was added to a solution of compound **50** (0.08 g, 0.12 mmol) in EtOH (10 mL) and H_2O (1 mL). The reaction mixture was stirred under a hydrogen atmosphere for 48 h using a hydrogenator (30 psi H_2). The catalyst was filtered over Celite and the solvent evaporated under reduced pressure, to afford the product of reaction as a white glassy solid (0.08 g, 0.11 mmol, 92%). δ_H (CD_3OD, 699.73 MHz): 1.18 (3H, br. s, CH_3), 1.48 (21H, s, $C(CH_3)_3$), 1.56 (15H, m, $C(CH_3)_3$), 1.96 – 1.99 (2H, m, CH_2CHN), 2.07 – 2.1 (2H, m, CH_2CHN), 2.1 - 2.18 (4H, m, $2\times CH_{2ring}$), 2.47 – 2.58 (4H, m, $2\times CH_{2ring}$), 2.65 (2H, dd, J = 14, CH_2COOH), 2.96 (1H, d, J = 14, $CH_{2a}COOH$), 3.10 (1H, d, J = 14, $CH_{2b}COOH$), 3.25 – 3.28 (2H, m, $2\times CHN$), 3.50 (2H, d, J =17.5, CH_2COO*t*Bu), 3.61 (2H, d, J = 17.5, CH_2COO*t*Bu). δ_C (CD_3OD, 125.67 MHz): 25.8 (CH_3), 26.9 (CH_2CHN), 27.04 – 27.31 ($C(CH_3)_3$), 29.92 (CH_2COOH), 30.17 (CH_2COOH), 50.68 (CH_{2ring}), 65.40 ($C_{quat}CH_3$), 67.41 – 67.61 (CH_2COO*t*Bu), 82.23 ($C(CH_3)_3$), 82.54 ($C(CH_3)_3$), 167.45 ($C{=}O_{tBu}$), 170.8 ($C{=}O_{tBu}$), 174.7 (C=OOH), 174.9 (C=OOH). *m/z* (ES+): 730.3 $[M + H]^+$. *m/z* (ES-): 728.5 $[M - H]^-$. (Found: MH^+, 730.4493. $C_{36}H_{64}N_3O_{12}$ requires MH^+, 730.4485).

(*RR*)-6-Bis(carboxymethyl)amino–1,4-(bis1'-carboxy-3'-carboxypropyl)-tetrahydro-6-methyl-1H-1,4-diazepine: (59 *or* (Glu)$_2$*RR*-AAZTA, L5)

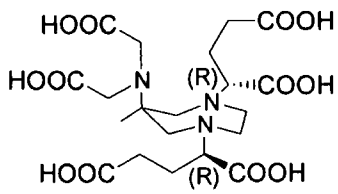

L5

10% Pd/C (0.006 g) was added to a solution of compound **57** (0.06 g, 0.087 mmol) in EtOH (3 mL) and H_2O (0.4 mL). The reaction mixture was stirred under hydrogen atmosphere for 24 h using a hydrogenator (30 psi H_2). The catalyst was filtered over Celite and the solvent evaporated under reduced pressure, to afford the product as a white glassy solid (**L5**, 0.044 g, 0.088 mmol, 98%). δ_H (D_2O, 399.96 MHz): 1.06 (3H, s, CH_3), 1.8 – 2.05 (4H, m, $2\times CH_2CHN$), 2.40 – 2.55 (4H, m, 2 × CH_2COOH),

2.95 – 3.40 (10H, br. m, 4 × CH_{2ring} + 2 × C*H*N), 3.62 – 3.75 (4H, m, 2×NCH_2COO*H*). *m/z* (ES-): 504.3 $[M - H]^-$.

(*RS*)-6-Bis(*t*-butoxycarbonylmethyl)amino–1,4-bis(1'-t-butoxycarbonyl)-3'-carboxypropyl)-tetrahydro -6-methyl-1H-1,4-diazepine (60)

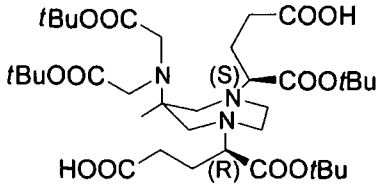

60

10% Pd/C (0.03 g) was added to a solution of compound **51** (0.30 g, 0.33 mmol) in EtOH (8 mL) and H_2O (1 mL). The reaction mixture was stirred under hydrogen atmosphere for 48 h using a hydrogenator (30 psi H_2). The catalyst was filtered over Celite and the solvent evaporated under reduced pressure, to afford the product of reaction as a white glassy solid (0.48 g, 0.35 mmol, 94%). δ_H (CD_3OD, 499.77 MHz): 1.09 (3H, s, CH_3), 1.48 – 1.50 (36H, m, 4×C(CH_3)$_3$), 1.85 – 1.89 (2H, m, CH_2CHN), 1.95 – 2.0 (2H, m, CH_2CHN), 2.36 – 2.48 (4H, m, 2×CH_{2ring}), 2.66 – 2.77 (4H, m, CH_{2ring}), 3.0 (2H, d, J = 14, CH_2COOH), 3.16 (2H, d, J = 14, CH_2COOH), 3.26 - 3.36 (2H, m, 2×C*H*N), 3.6 (2H, d, J =17.75, CH_2COO*t*Bu), 3.75 (2H, d, J = 17.75, CH_2COO*t*Bu). δ_C (CD_3OD, 125.67 MHz): 25.7 (*C*H$_3$), 26.04 (*C*H$_2$CHN), 27.26 – 27.43 (C(*C*H$_3$)$_3$), 31.0 (*C*H$_2$COOH), 51.5 – 53.68 (*C*H$_{2ring}$), 64.55 (C_{quat}CH$_3$), 68.8-69.3 (*C*H$_2$COO*t*Bu), 67.9 (*C*HN), 80.73 (*C*(CH$_3$)$_3$), 80.9 (*C*(CH$_3$)$_3$), 81.13 (*C*(CH$_3$)$_3$), 81.37 (*C*(CH$_3$)$_3$), 171.73 (*C*=O$_{tBu}$), 171.95 (*C*=O$_{tBu}$), 173.10 (*C*=OOH). *m/z* (ES+): 730.3 $[M + H]^+$, 752.4 $[M + Na]^+$. (Found: MH^+, 730.4475. $C_{36}H_{64}N_3O_{12}$ requires MH^+, 730.4484; Found: MNa^+, 752.4303. $C_{36}H_{63}N_3O_{12}Na$ requires MNa^+, 752.4304).

(*RS*)-6-Bis(carboxymethyl)amino–1,4-(bis1'-carboxy-3'-carboxypropyl)-tetrahydro-6-methyl-1H-1,4-diazepine: (61 *or* (Glu)$_2$*RS*-AAZTA, L6)

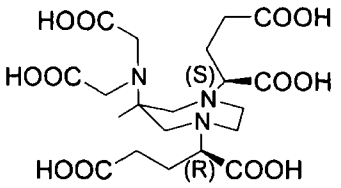

L6

A solution of **60** (0.24 g, 0.33 mmol) in TFA / CH_2Cl_2 (1:1, 4.0 mL) was stirred at room temperature for 24 h. The solvent was removed under high vacuum (KOH pellets in the traps), the residue taken up with CH_2Cl_2 (4 mL) and the solution evaporated under reduced pressure. This procedure was repeated three times, then the residue was washed twice with diethyl ether (2×2 mL) and a precipitated white solid was obtained as the trifluoroacetate salt of the product (**L6**, 0.18 g, 0.36 mmol, 93 %). δ_H (D_2O, 499.77 MHz): 1.05 (3H, s, CH_3), 1.92 – 2.06 (4H, m, 2×CH_2CHN), 2.36 – 2.50 (4H, m, 2×CH_2COOH), 3.02 – 3.32 (8H, m, CH_{2ring}), 3.54 - 3.58 (2H, m, 2×C*H*N), 3.59 (2H, d, J =11.5, NCH_2COO*H*), 3.65 (2H, d, J = 11.5, NCH_2COOH). δ_C (D_2O, 125.67 MHz): 22.01 (*C*H$_3$), 24.37 (*C*H$_2$CHN), 30.65 (*C*H$_2$COOH), 50.65 – 51.61 (*C*H$_{2ring}$), 61.61 (C_{quat}CH$_3$), 66.17 (NCH$_2$COOH), 67.81 (*C*HN), 173.08 (CH*C*=OOH), 176.1 (NCH$_2$*C*=OOH), 177.0 (CH$_2$)$_2$*C*=OOH). *m/z* (ES-): 504.3 [M - H]$^-$. (Found: [M-H]$^-$, 504.1835. $C_{20}H_{30}N_3O_{12}$ requires [M-H]$^-$, 504.1836).

Ln^{III} complexes

^1H NMR spectra were recorded for the Eu^{III} and Yb^{III} complexes of AMPED based ligands. In this section are listed selected chemical shifts corresponding to the major and minor isomers of each complex

- **From GluAAZTA, L3**

$[Ln^{III}(Glu)AAZTA]^{2-}$

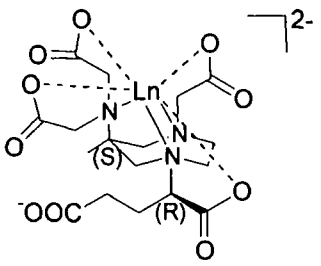

$[Ln^{III}L3]^{2-}$

An aqueous solution of $LnCl_3 \cdot 6H_2O$ (0.8 eqv) was added dropwise to a solution of **L3** in H_2O / MeOH 5% solution (1 eqv, dissolved in the minimum volume). The pH was adjusted to ~ 5.5 with aqueous KOH solution (1M) and the mixture was left to stir at 50 °C. After 48h, the reaction mixture was cooled to room temperature and the pH of the solution raised to ~ 10 (using aqueous KOH solution, 1M). The white powder precipitated was isolated by centrifugation and the pH of the supernatant readjusted to ~ 5.5. Freeze drying of the liquid gave the complex as a white crystalline solid, together with KCl. The properties of the complex were examined in the presence of the salt.

$[Yb^{III}(Glu)AAZTA]^{2-}$ or **$[Yb^{III}L3]^{2-}$**

HPLC (Chromatographic method A1): 100% (Area %); t_r: 1.5 min.

m/z (ES-): 603.07 $[M - H]^-$ (Found: $[M - H]^-$, 599.0737. $C_{17}H_{23}N_3O_{10}{}^{170}Yb_1$ requires $[M - H]^-$, 599.0737 and $[M - H]^-$, 603.0777. $C_{17}H_{23}N_3O_{10}{}^{174}Yb_1$ requires $[M - H]^-$,

603.0777). $\delta_{H\ (Major\ isomer)}$ (D_2O, 499.79 MHz): -36.05, -28.62, -8.72, -5.69, -5.47, -3.84, -3.38, -2.21, -1.07, -1.17, 5.65, 6.01, 8.88, 10.66, 27.26, 29.54, 30.92, 32.51, 36.09, 42.33.

$\delta_{H\ (Minor\ isomer)}$ (D_2O, 499.79 MHz): -41.85, -25.32, -8.14, -6.31, -3.82, -3.81, -3.62, -2.50, -1.11, -0.89, 0.70, 7.62, 9.1, 12.03, 28.43, 33.85, 34.25, 36.23.

$[Gd^{III}(Glu)AAZTA]^{2-}$ or $[Gd^{III}L3]^{2-}$

HPLC (Chromatographic method A1): 100% (Area %); t_r: 1.5 min. *m/z* (ES-): 587.1 $[M - H]^-$ (Found: $[M - H]^-$, 587.0618. $C_{17}H_{23}N_3O_{10}{}^{158}Gd_1$ requires $[M - H]^-$, 587.0630; $[M - H]^-$, 583.0590. $C_{17}H_{23}N_3O_{10}{}^{154}Gd_1$ requires $[M - H]^-$, 583.0597); $[M - H]^-$, 584.0607. $C_{17}H_{23}N_3O_{10}{}^{155}Gd_1$ requires $[M - H]^-$, 584.0615).
Relaxivity value found by NMRD analysis: $r_{1p} = 7.3\ mM^{-1}s^{-1}$ (20 MHz, 298 K). The $[Gd^{3+}]$ have been determined by mineralization with 37% HCl at 120°C overnight. Fitting of the ^{17}ONMR R_{2p} *vs* T (K) profile gave $\tau_M = 115$ ns.

$[Eu^{III}(Glu)AAZTA]^{2-}$ or $[Eu^{III}L3]^{2-}$

$\tau_{(H_2O)} = 0.33$ ns, $\tau_{(D_2O)} = 0.86$ ns.

$\delta_{H\ (Major\ isomer)}$ (D_2O, 499.79 MHz): -14.03, -12.96, -12.34, -5.95, -5.14, -4.96, -3.33, -2.55, -2.34, -1.20, -0.97, -0.86, -0.23, 0.28, 0.67, 1.24, 5.40, 5.45, 6.34, 6.84, 7.92, 8.88, 10.51, 11.72, 14.31.

$\delta_{H\ (Minor\ isomer)}$ (D_2O, 499.79 MHz): -10.71, -7.72, -7.23, -3.09, -1.98, 6.74, 7.08, 7.21, 9.43, 9.66, 15.01.

- From GluAAZTABn, L4

$[Eu^{III}(Glu)AAZTABn]^-$

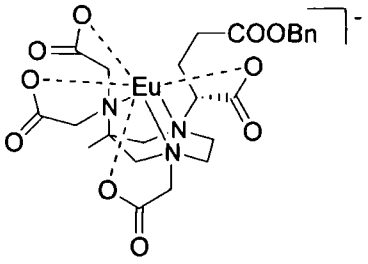

$[Eu^{III}L4]^-$

A solution of $LnCl_3 \cdot 6H_2O$ (0.8 eqv) in H_2O was added dropwise to an aqueous solution of **L4** (1 eqv, dissolved in the minimum volume of a solution of H_2O / MeOH 10%). The pH was adjusted at ~ 5.5 with KOH (1M). After 48h stirring at 50 °C, the reaction mixture was cooled to room temperature, the pH raised to ~ 10 (using aqueous KOH solution, 1M), the white powder precipitated was isolated by centrifugation and the pH of the supernatant was than readjusted to ~ 5.5. Freeze drying of the liquid gave a white glassy solid, mixture of the complex and KCl salt.

$[Eu^{III}(Glu)\,AAZTABn]^-$ or $[Eu^{III}L4]^-$

$\tau_{(H_2O)}$ = 0.21 ns, $\tau_{(D_2O)}$ = 0.32 ns.

$\delta_{H\ (Major\ isomer)}$ (D_2O, 499.79 MHz): -14.04, -12.96, -12.77, -7.93, -5.14, -4.31, -3.43, -2.46, -2.06, -1.58, -0.79, 0.18, 1.30, 1.84, 3.21, 5.36, 6.24, 7.26, 8.09, 9.02, 10.39, 11.51, 14.00.

- From $(Glu)_2$*(RR)*-AAZTA, L5

$[Ln^{III}(Glu)_2$ *(RR)*-AAZTA$]^{3-}$

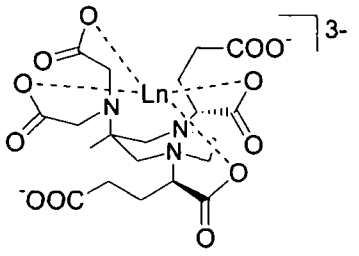

$[Ln^{III}L5]^{3-}$

$[Eu^{III}(Glu)_2$ *(RR)*-AAZTA$]^{3-}$ or $[Eu^{III}L5]^{3-}$

A solution of $EuCl_3 \cdot 6H_2O$ (0.018g, 0.048 mmol) in H_2O (1 mL) was added dropwise to an aqueous solution of **L5** (0.045g, 0.053mmol in 1.5 mL H_2O). The pH was adjusted to ~ 5.5 using KOH (1M). After 48h stirring at 50 °C, the supernatant was separated from a white precipitate and freeze dried. A white crystalline solid, mixture of the complex and KCl salt, was obtained (0.053g, 0.08 mmol, crude yield 60%). *m/z* (ES+): 652.2 $[M]^-$. (Found: $[M]^-$, 652.0794. $C_{20}H_{27}O_{12}N_3{}^{151}Eu_1$ requires $[M]^-$, 652.0798; $[M]^-$, 654.0806 $C_{17}H_{27}O_{10}N_3{}^{153}Eu_1$ requires $[M - H]^-$, 654.0813). $\tau_{(H_2O)}$ = 0.28 ns, $\tau_{(D_2O)}$ = 0.87 ns.

$\delta_{H\ (Major\ isomer)}$ (D_2O, 699.73 MHz): -14.65, -5.19, -2.21, -1.59, -1.03, -1.59, -1.03, -0.62, 0.09, 0.43, 0.69, 1.86, 1.96, 4.90, 6.63, 7.29, 7.79, 10.29, 11.77.

$\delta_{H\ (Minor\ isomer)}$ (D_2O, 499.79 MHz): -10.27, -8.39, -5.89, -4.64, 0.09, 0.89, 2.32, 2.46, 3.84, 5.52, 9.23, 13.76.

$[Gd^{III}(Glu)_2$*(RR)*-AAZTA$]^{3-}$ or $[Gd^{III}L5]^{3-}$

A solution of $GdCl_3 \cdot 6H_2O$ (0.007 g, 0.017 mmol) in H_2O (0.5 mL) was added dropwise to an aqueous solution of **L5** (0.016 g, 0.019 mmol in 1.5 mL H_2O). The pH was adjusted to pH = 5.5 using an aqueous solution of KOH (1M). After 48h stirring at 50°C, the supernatant was separated from a white precipitate and freeze dried, to yield a white crystalline solid, as a mixture of the complex and the KCl salt (0.024 g, 0.036 mmol, crude yield 47%). *m/z* (ES+): 658.9 $[M - H]^-$ (Found: $[M - H]^-$, 659.0831. $C_{20}H_{27}N_3O_{12}{}^{158}Gd_1$ requires $[M-H]^-$, 659.0841; $[M - H]^-$, 655.0801.

$C_{17}H_{27}N_3O_{10}{}^{154}Gd_1$ requires [M - H]$^-$, 655.0809; [M - H]$^-$, 656.0817. $C_{17}H_{27}N_3O_{12}{}^{155}Gd_1$ requires [M - H]$^-$, 656.0813).

Relaxivity value found by NMRD analysis: r_{1p} = 8.65 $mM^{-1}s^{-1}$ (20 MHz, 298 K). The [Gd^{3+}] have been determined by mineralization with 37% HCl at 120°C overnight.

Fitting of the ^{17}O NMR R_{2p} *vs* T (K) profile gave τ_M= 720 ns.

[Yb^{III}(Glu)$_2$*(RR)*-AAZTA]$^{3-}$ or [Yb^{III}L5]$^{3-}$

The same experimental procedure followed for the synthesis of **[Gd^{III}L5]$^{3-}$** was used in the synthesis of **[Yb^{III}L5]$^{3-}$**, and approximately the same crude yield (50%) was obtained.

$\delta_{H\ (Major\ isomer)}$ (D_2O, 699.73 MHz): -50.83, -26.87, -18.45, -17.30, -9.92, -8.53, -8.08, -7.41, -5.43, -4.29, -1.62, -0.79, 10.41, 14.03, 28.65, 30.38, 32.69, 40.18, 42.95, 48.55.

$\delta_{H\ (Minor\ isomer)}$ (D_2O, 499.79 MHz): -36.32, -33.80, -22.23, -14.76, -13.55, -9.22, 9.64, 16.31, 22.93, 24.27, 33.87, 36.58.

- From (Glu)$_2$*(RS)*-AAZTA, L6

[Ln^{III}(Glu)$_2$*(RS)*-AAZTA]$^{3-}$

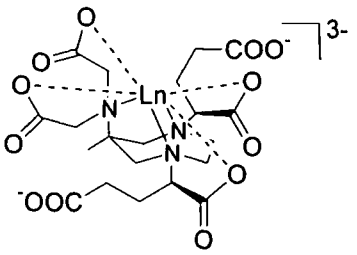

[Ln^{III}L6]$^{3-}$

A solution of $LnCl_3 \cdot 6H_2O$ (0.8 eqv) in H_2O was added dropwise to an aqueous solution of **L6** (1 eqv, dissolved in the minimum volume of a solution H_2O / MeOH 5%). The pH was adjusted to ~ 5.5 with KOH (1M). After 48h stirring at 50 °C, the reaction mixture was cooled to room temperature, the pH raised to ~ 10 (using an aqueous KOH solution, 1M), the white powder precipitated was isolated by

centrifugation and the pH of the supernatant was than readjusted to ~ 5.5. Freeze drying of the liquid gave the complex as a white crystalline solid, plus KCl salt.

$[Gd^{III}(Glu)_2$*(RS)*-AAZTA$]^{3-}$ or $[Gd^{III}L6]^{3-}$

Crude yield: 50%. HPLC (Chromatographic method A1): t_r: 1.55 min. *m/z* (ES-): 659.2 [M - H]$^-$. (Found: [M - H]$^-$, 659.0845. $C_{20}H_{27}N_3O_{12}{}^{158}Gd_1$ requires [M-H]$^-$, 659.0841).

Relaxivity value found by NMRD analysis: r_{1p} = 7.5 $mM^{-1}s^{-1}$ (20 MHz, 298 K). The [Gd^{3+}] have been determined by mineralization with 37% HCl at 120°C overnight.

Fitting of the ^{17}O NMR R_{2p} *vs* T (K) profile gave τ_M= 246 ns.

$[Yb^{III}(Glu)_2$*(RS)*-AAZTA$]^{3-}$ or $[Yb^{III}L6]^{3-}$

Crude yield: 60%. *m/z* (ES-): 675.3 [M]$^-$. (Found: [M]$^-$, 675.0996. $C_{20}H_{27}N_3O_{12}{}^{174}Yb_1$ requires [M-H]$^-$, 675.0989).

$\delta_{H\ (Major\ isomer)}$ (D_2O, 699.73 MHz): -51.48, -37.01, -35.99, -26.08, -19.10, -16.28, -11.24, -9.67, -9.27, -7.18, -4.77, -2.69, -1.48, 0.23, 0.64, 0.82, 1.88, 3.56, 7.25, 10.10, 10.98, 14.85, 24.39, 28.16, 33.13, 35.07, 37.44, 43.18, 47.42, 50.24.

$\delta_{H\ (Minor\ isomer)}$ (D_2O, 699.73 MHz): -55.84, -49.92, -43.70, -38.62, -34.93, -32.15, -21.73, -19.96, -17.60, -12.45, -10.03, -7.99, -5.87, -4.4, -0.53, 6.14, 9.00, 10.32, 14.56, 17.59, 25.82, 29.22, 31.49, 38.50, 41.43, 44.32, 52.14.

$[Eu^{III}(Glu)_2$*(RS)*-AAZTA$]^{3-}$ or $[Eu^{III}L6]^{3-}$

Crude yield: 45%. $\tau_{(H_2O)}$ = 0.38, $\tau_{(D_2O)}$ = 1.27.

$\delta_{H\ (Major\ isomer)}$ (D_2O, 699.73 MHz): -10.32, -8.37, -6.03, -5.86, -4.54, -1.46, -1.38, -0.85, -0.51, 0.11, 1.75, 2.07, 3.21, 3.95, 5.31, 6.38, 6.84, 7.23, 8.29, 9.17, 10.14, 10.57, 11.45, 13.64.

$\delta_{H\ (Minor\ isomer)}$ (D_2O, 699.73 MHz): -14.66, -5.16, -2.16, -1.09, -1.04, 5.56, 8.29, 11.83.

(*γR,γ'S*)-6-[bis[2(1,1-dimethylethoxy)-2oxoethyl]amino]-*γ,γ'*-bis[(1,1dimethylethoxy) carbonyl]tetrahydro-6-methyl-1H-1,4-diazepine-1,4(5H)-dibutanoic acid bis ((trihydroxymethyl)aminomethane)amide (62)

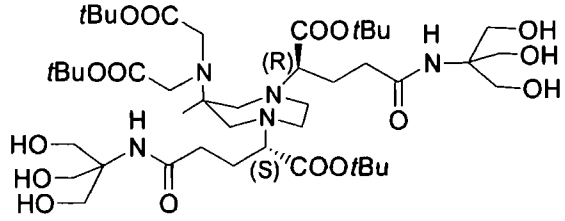

62

To a solution of **60** (0.015 g, 0.021 mmol) in DMF (0.5 mL), *N*-methylmorpholine (11.5 μL, 0.12 mmol) was added and the mixture was stirred at 50 °C for 20 min. After cooling to 10 °C, *O*-benzotriazol-1-yl-*N*, *N*, *N'*, *N'*- tetramethyluronium tetrafluoroborate (0.023 g, 0.072 mmol) was added and after a few minutes a solution of TRIS (0.0075 g, 0.061 mmol) in DMSO (0.5 mL) was dripped into the reaction mixture, which was than left to stir at 40 °C for 72 h. The reaction mixture was cooled to room temperature and the solvent removed under reduced pressure (high vacuum line, 0.6 mBar, at ambient temperature). The residue was dissolved in CH_2Cl_2 (8 mL) and washed with HCl 0.1 M (5 mL), saturated $NaHCO_3$ solution (5 mL), H_2O (2 × 5 mL) and brine (5 mL). Removing of the solvent under reduced pressure gave **62** as a colourless oil (0.015 g, 0.016 mmol, 76%). R_f (CH_2Cl_2/MeOH 2%, SiO_2) = 0.5 (UV). δ_H (CD_3OD , 399.96 MHz): 1.18 (3H, s, CH_3), 1.46 - 1.48 (36H, br. s, $C(CH_3)_3$), 1.77 – 1.88 (2H, m, CH_2CHN), 1.91 – 2.03 (2H, m, CH_2CHN), 2.32 - 2.41 (4H, m, 2 × CH_{2ring}), 2.54 – 2.70 (4H, m, 2 × CH_{2ring}), 2.80 – 3.10 (4H, m, 2 × CH_2CONH), 3.10 – 3.30 (2H, m, 2 × CHN), 3.60 (2H, br. d, $CH_2COOtBu$), 3.70 (2H, br. d, $CH_2COOtBu$), 3.68 – 3.75 (12H, m, 6 × CH_2OH). *m/z* (ES-): 935 $[M]^-$.

$TRIS_2(Glu)_2$*(RS)*-AAZTA, L7

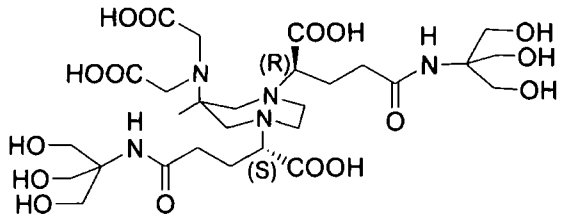

L7

A solution of **62** (0.015 g, 0.016 mmol) in TFA / CH_2Cl_2 (1:2, 3 mL) was stirred at room temperature for 24 h. The solvent was removed under reduced pressure (with KOH pellets in the traps), the residue dissolved in CH_2Cl_2 (4 mL) and the solution evaporated under reduced pressure. This procedure was repeated three times, and the residue was washed twice with diethyl ether (2 × 2 mL) and a precipitated white powder was obtained as the product of the reaction (**L7**, 0.010 g, 9.49×10^{-3} mmol, 60%). δ_H (D_2O, 499.79 MHz): 1.11 (3H, s, CH_3), 1.92 – 2.10 (4H, br. m, 2 × CH_2CHN), 2.78 (4H, br. d, CH_2CONH), 2.9 (1H, d, J = 4, CH_aCONH), 2.93 (1H, d, J = 4, CH_bCONH), 3.0 – 3.34 (8H, br. m, 4 × CH_{2ring}), 3.39 – 3.47 (2H, m, 2 × C*H*N), 3.62 (4H, d, J = 2.5, 2 × CH_2COOH), 3.67 – 3.75 (12H, m, 6 × CH_2OH). *m/z* (ES-): 710.4 $[M-H]^-$. (Found: $[M-H]^-$, 710.3105. $C_{28}H_{48}N_5O_{16}$ requires $[M-H]^-$, 710.3102).

$[Gd^{III}TRIS_2(Glu)_2$*(RS)*-AAZTA$]^-$

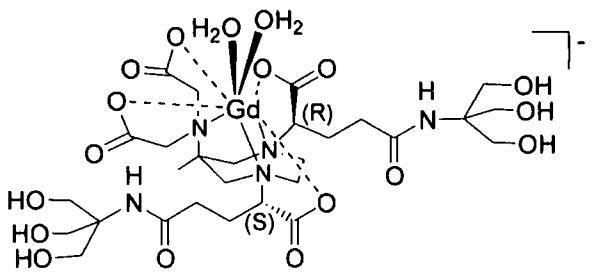

$[Gd^{III}L7]^-$

An aqueous solution of $LnCl_3 \cdot 6H_2O$ (0.0028 g, 7.59×10^{-3} mmol) was added dropwise to **L7** (0.010 g, 9.49×10^{-3} mmol) dissolved in H_2O (2 mL). The pH was

adjusted to ~ 5.5 with aqueous KOH solution (1M). After stirring at 50 °C for 48h, the reaction mixture was cooled to room temperature, the pH raised to ~ 10 (using KOH, 1M), the white precipitate was isolated by centrifugation and the pH of the supernatant was than readjusted to ~ 5.5. Freeze drying of the liquid gave the complex as a white powder (0.005 g, 5.78 $\times 10^{-3}$ mmol, crude yield 61%). HPLC (Chromatographic method A1): t_r: 1.7 min. *m/z* (ES-): 865.3 $[M]^-$.

T_1 (60MHz, 37 °C) = 158.1 ± 0.2 ms $[Gd^{3+}]_{ICP}$ = 0.12 mg/mL.

- Coupling reactions on $[Ln^{III}(Glu)AAZTA]^-$ complexes ($[Ln^{III}L3]^-$)

$[Yb^{III}TRIS(Glu)AAZTA]^-$

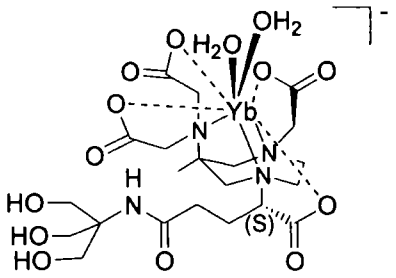

$[Yb^{III}L8]^-$

To a solution of $[Yb^{III}(Glu)AAZTA]^{2-}$ (**$[Yb^{III}L3]^-$**, 0.005 g, 8.3×10^{-3} mmol) in DMF (0.5 mL), *N*-methylmorpholine (2 μL, 1.64×10^{-2} mmol) was added, and the mixture was stirred at 50 °C for 20 min. After cooling to 10 °C, *O*-benzotriazol-1-yl-*N*, *N*, *N'*, *N'*- tetramethyluronium tetrafluoroborate (0.0065 g, 0.021 mmol) was added and after a few minutes a solution of TRIS (0.003 g, 2.5×10^{-2} mmol) in DMF (0.5 mL) was dripped into the reaction mixture, which was than left to stir at 40 °C for 10 days. The reaction mixture was cooled to room temperature, transferred in a small flask containing EtOH (7 mL) and the solid precipitated was separated from the supernatant, and a white powder was isolated as the product of reaction (0.008 g, 0.007 mmol, 10%), together with some starting material (**$[Yb^{III}L3]^-$**) and KCl salt. *m/z* (ES-): 705.9 $[M]^-$. (Found: $[M]^-$, 706.5033 $C_{21}H_{32}N_4O_{12}{}^{174}Yb_1$ requires $[M]^-$, 706.5033).

[Yb^{III}(Gluco)GluAAZTA]$^-$

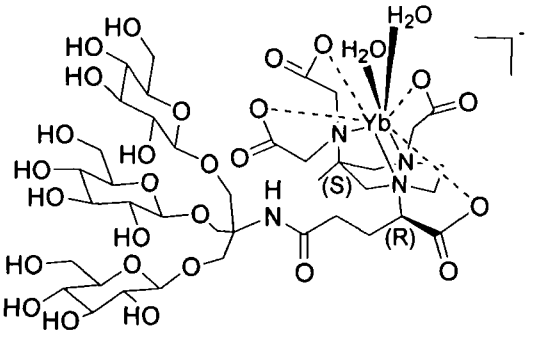

[Yb^{III}L9]$^-$

To a solution of [Yb^{III}(Glu)AAZTA]$^{2-}$ (**[Yb^{III}L3]$^-$**, 0.0058 g, 9.6×10^{-3} mmol) in DMSO (0.5 mL), *N*-methylmorpholine (20 μL, 1.8×10^{-4} mmol) was added, and the mixture was stirred at 50 °C for 20 min. After cooling to 10 °C, *O*-benzotriazol-1-yl-*N*, *N*, *N'*, *N'*- tetramethyluronium tetrafluoroborate (0.0077 g, 0.024 mmol) was added and after a few minutes a solution of *N*-[tris(*β*-glucopyranosyloxymethyl)methyl]glycinamide (**10**, 0.012 g, 0.019 mmol) in DMSO (0.5 mL) was dripped into the reaction mixture, which was than left to stir at 40 °C for 3.5 weeks. The reaction mixture was cooled to room temperature, transferred in a small flask containing EtOH (7 mL) and the solid precipitated was separated from the supernatant, dissolved in water and purified by HPLC, to obtain a light yellow solid as product of reaction (0.008 g, 0.007 mmol, 61%). *m/z* (ES-): 1192.5 [M]$^-$. (Found: [M]$^-$, 1192.3042. $C_{39}H_{62}N_4O_{27}Yb_1$ requires [M]$^-$, 1192.2995; [M + H]$^-$, 1193.3068. $C_{39}H_{63}N_4O_{27}Yb_1$ requires [M + H]$^-$, 1193.3073). HPLC (Chromatographic method A1): 100% (Area %); t_r: 1.5 min.

$\delta_{H\ (Major\ isomer)}$ (D_2O, 399.95 MHz): -39.95, -35.22, -29.34, -26.59, -8.32, -5.97, -5.37, -4.74, -3.67, -2.84, -1.28, 1.00, 6.73, 7.25, 8.94, 9.59, 11.20, 29.00, 29.51, 30.19, 36.32, 42.15.

$\delta_{H\ (Minor\ isomer)}$ (D_2O, 399.95 MHz): -41.50, -41.26, -27.88, -23.78, -18.17, -12.56, -8.83, -6.32, -5.23, -4.37, -2.42, -0.41, 0.10, 8.72, 10.03, 16.10, 27.37, 28.20, 36.02, 42.72.

$[Gd^{III}(Gluco)GluAAZTA]^-$

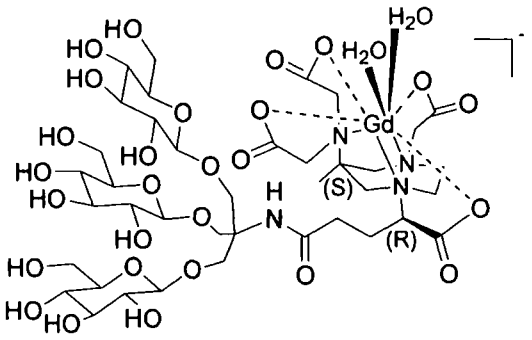

$[Gd^{III}L9]^-$

To a solution of $[Gd^{III}(Glu)AAZTA]^{2-}$ (**$[Gd^{III}L3]^-$**, 0.0068 g, 11.5 × 10^{-3} mmol) in DMSO (0.5 mL), *N*-methylmorpholine (20 μL, 1.8 × 10^{-4} mmol) was added, and the mixture was stirred at 50 °C for 20 min. After cooling to 10 °C, *O*-benzotriazol-1-yl-*N*, *N*, *N'*, *N'*- tetramethyluronium tetrafluoroborate (0.009 g, 0.028 mmol) was added and after a few minutes a solution of the amine **10** (0.014 g, 0.023 mmol) in DMSO (0.5 mL) was dripped into the reaction mixture, which was than left to stir at 40 °C for 2 weeks. The reaction mixture was cooled to room temperature, transferred in a small flask containing EtOH (7 mL) and the solid precipitated was separated from the supernatant, dissolved in water and freeze dried, to give the product as a light yellow solid (0.007 g, 5.95×10^{-3} mmol, 52%). HPLC (Chromatographic method A1): 80% (Area %); t_r: 1.5 min. *m/z* (ES-): 1175.6 $[M]^-$. (Found: $[M]^-$, 1175.5205. $C_{39}H_{62}N_4O_{27}{}^{158}Gd$ requires $[M]^-$, 1175.5206). Relaxivity value found by NMRD analysis: r_{1p} = 3.36 $mM^{-1}s^{-1}$ (20 MHz, 298 K). The $[Gd^{3+}]$ was determined by mineralization with 37% HCl at 120°C overnight. Measurements performed in University of Turin (Italy): $[Gd^{3+}]$ = 0.23 mM; R_{1obs}= 1.15 s^{-1} (25 °C, 20MHz). r_{1p}= 3.36 $mM^{-1}s^{-1}$.

Measurements in Durham (U.K.): $[Gd^{3+}]_{ICP}$ = 0.426 mM; T_1(60MHz) = 430 ms. R_{1p} ($1/T_1$- R_D 0.25) = 2.07 s^{-1}. r_{1p}= 4.87 $mM^{-1}s^{-1}$.

-Coupling reaction on $[Gd^{III}(Gluco)_2(Glu)_2(RS)\text{-}AAZTA]^-$ complexes ($[Gd^{III}L6]^-$)

$[Gd^{III}(Gluco)_2(Glu)_2AAZTA]^-$

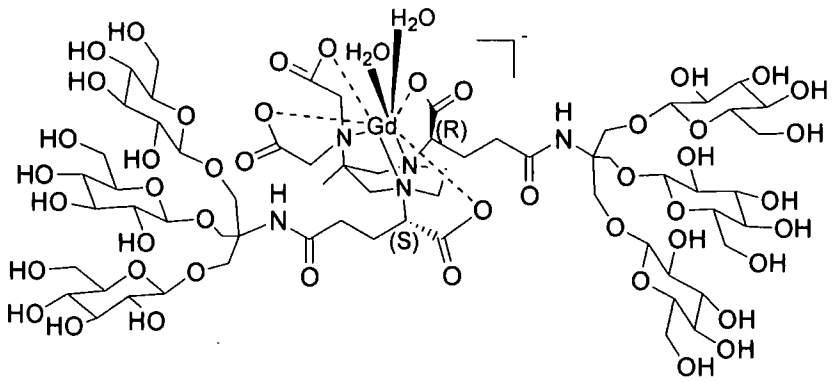

$[Gd^{III}L10]^-$

To a solution of $[Gd^{III}(Glu)_2(RS)\text{-}AAZTA]^{3-}$ (**$[Gd^{III}L6]^-$**, 0.0015 g, 0.023 mmol) in DMSO (0.5 mL), *N*-methylmorpholine (60 μL, 5.4×10^{-4} mmol) was added, and the mixture was stirred at 50 °C for 20 min. After cooling to 10 °C, *O*-benzotriazol-1-yl-*N*, *N*, *N'*, *N'*- tetramethyluronium tetrafluoroborate (0.033 g, 0.103 mmol) was added and after a few minutes a solution of the amine **10** (0.056 g, 0.092 mmol) in DMSO (0.5 mL) was dripped into the reaction mixture, which was than left to stir at 40 °C for 2 weeks. The reaction mixture was cooled to room temperature, transferred in a small flask containing EtOH (7 mL) and the solid precipitated was separated from the supernatant, dissolved in water and freeze dried, to give the product, a light yellow solid (0.014 g, 0.0076 mmol, 33%). HPLC (Chromatographic method A1): 100% (Area %); t_r: 1.6 min. *m/z* (TOF MS ES-): 1837.4 $[M + 3H]^-$, 918.4 $[M/2]^-$. (Found: $[M]^-$, 1834.5304 $C_{64}H_{105}N_5O_{46}{}^{154}Gd$ requires $[M]^-$, 1834.5262).

***N*-(*t*-Butyloxycarbonyl)tris(acetoxymethyl)methylamine**

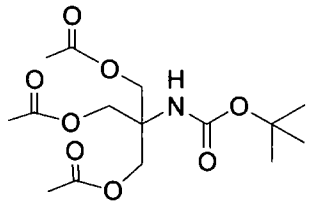

64

A solution of Boc-protected TRIS (1 g, 4.53 mmol) in $CHCl_3$ (5 mL) was cooled to 0 °C and Ac_2O (1.30 mL, 13.6 mmol) and Py (1.09 mL, 13.6 mmol) were slowly added. After 18 h stirring at room temperature, aqueous $CuSO_4$ solution (0.25 M, 3×8 mL) was added to the reaction mixture and the organic phase was separated, dried over Na_2SO_4 and evaporated to dryness, to give **64** as a clear oil (1.96 g, 5.66 mmol, 80%). R_f (Hex/EtOAc 1:1, SiO_2) = 0.5 (UV, Iodine). δ_H ($CDCl_3$, 399.96 MHz): 1.35 (9H, s, 3×CH_3), 2.01 (9H, s, C(CH_3)$_3$), 4.28 (6H, s, 3×CH_2O). δ_C ($CDCl_3$, 125.67 MHz): 20.92 (3×CH_3), 28.41 (C(CH_3)$_3$), 31.08 (C_{quat}But), 56.73 (C_{quat}NH), 63.05 (3×CH_2O), 154.42 (C=ONH), 170.63 (C=OCH_3). *m/z* (ES-): 348.2 $[M+H]^+$. (Found: $[M+Na]^+$, 370.1473. $C_{15}H_{25}N_1O_8{}^{23}Na_1$ requires $[M+Na]^+$, 370.1472).

2-Bromo-4-(1,3-dioxo-1,3-dihydro-isoindol-2-yl)-pentanedioic acid diethyl ester [11] (65)

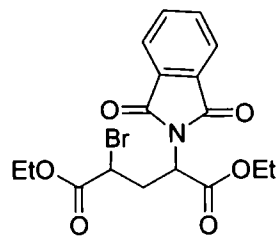

65

PBr_5 (4.0 g, 9.29 mmol), Br_2 (0.28 mL, 5.46 mmol) and *N*-phthaloyl-L-glutamic acid (1.0 g, 3.61 mmol) were stirred and heated (irradiated by a 200W lamp) overnight at 65 °C.

After cooling in an ice bath, absolute EtOH (10 mL) was added dropwise to the mixture under vigorous stirring and the solution was boiled under reflux for 5 h. The solvent was removed and the residue extracted with EtOAc (3 × 7 mL). The organic layer was washed with H_2O (2 × 5 mL), Na_2CO_3 aq. (2 × 5 mL), then again with H_2O (2 × 5 mL), dried over $MgSO_4$ and concentrated under reduced pressure. Column chromatography (SiO_2, Hexane/EtOAc 10% → Hexane/EtOAc 20%) of the residue, gave the two separated diastereomers (*erythro, S/R*) **65a** (0.526 g, 24 %) and (*threo S/S*) **65b** (0.154g, 11 %) as light yellow oils.

m/z 598 $[M+H]^+$, 620 $[M+Na]^+$.

R_f(Hexane/EtOAc 20%, SiO_2) = 0.4 **65a** and **65b** 0.45 (UV).

Erythro (*S/R*)

δ_H ($CDCl_3$, 500 MHz): 1.22 (6H, m, 2 × OCH_2CH_3), 2.90-3.05 (2H, m, $CH_2C_{(quat)}$), 4.08-4.22 (5H, m, 2 × OCH_2CH_3), 4.36 (1H, t, J = 10, H4), 4.98 (H2), (1H, dd, H-2), 7.72-7.86 ($4H_{arom}$, m). δ_C ($CDCl_3$, 100.61 MHz): 14.1 (Me), 14.3 (Me), 33.7 (CH_2), 42.7 (CH_2CHBr), 50.5 (CHN), 62.5 (OCH_2), 123.9 (CHC_{quat}), 131.8 (C_{quat}), 134.7 ($CHCHC_{quat}$), 167.7 (NCO), 168.4 (NCO), 169.0 (C=O), 169.1 (C=O).

Threo (*S/S*)

δ_H ($CDCl_3$, 500 MHz): 1.22 (6H, m, 2 × OCH_2CH_3), 2.90-3.05 (2H, m, $CH_2C_{(quat)}$), 4.08-4.22 (5H, m, 2 × OCH_2CH_3 and H4), 5.13 (H2) (1H, dd, H-2), 7.72-7.86 ($4H_{arom}$, m). δ_C ($CDCl_3$, 100.61 MHz): 14.1 (Me), 14.3 (Me), 34.7 (CH_2), 42.1 (CH_2CHBr), 50.0 (CHN), 62.5 (OCH_2), 123.9 (CHC_{quat}), 131.8 (C_{quat}), 134.7 ($CHCHC_{quat}$), 167.5 (NCO), 168.2 (NCO), 169.0 (C=O), 169.1 (C=O).

List of references

[1] Ashton, P. R.; Boyd, S. E., Brown, C. L.; Jayaraman, N.; Nepogodiev, S. A.; Stoddart, J. F. *Chem. Eur. J.* **1996**, *2*, 1115.

[2] Ness, R. K.; Fletcher Jr.; H. G.; Hudson C. S. *J. Am. Chem. Soc.* **1950**, *72*, 2200.

[3] Schmidt, U.; Braun, C.; Sutoris, H. *Synthesis* **1996**, 223.

[4] Atkinson, P. *Chemoselective Phospho-Anion Binding Studies*, **2005**, PhD Thesis, Durham University.

[5] Valerio, R. M.; Alewood, P.F.; Johns, R. B. *Synthesis* **1988**, 786.

[6] Ramsamy, K.; Olsen, R. K.; Emery, T. *Synthesis* **1982**, 42.

[7] Märkl, G. *Chem. Ber.* **1962**, *95*, 3003.

[8] Aime, S.; Calabi, L.; Cavallotti, C.; Gianolio, E.; Giovenzana, G. B.; Losi, P.; Maiocchi, A.; Palmisano, G.; Sisti, M. *Inorg. Chem.*, **2004**, *43*, 24.

[9] Kanoh, S.; Nishimura, T.; Mitta, Y.; Veyama, A.; Motoi, M. *Macromolecules*, **2002**, *Vol. 35,* 3.

[10] Broan, C. J.; Cole, E.; Jankowsky, K. J.; Parker, D.; Pulukkody, K.; Boyce, B. A.; Beeley, N. R. A.; Millar, K.; Millican, A. T. *Synthesis*, **1992**, 63.

[11] Krasnov, V. P.; Bukrina, I. M.; Zhdanova, E. A.; Kodess, M. I.; Korolyova, M. A. *Synthesis*, **1994**, 961.

Appendix

In this appendix are displayed the ES-MS, ^{1}H NMR and ^{1}H - ^{1}H COSY NMR spectra which were used in the characterization of selected lanthanide complexes discussed in Chapter II, III and IV.

Tetraamide dendrimer $[GdgDOTAGlu_{12}Gly_4(H_2O)]^-$

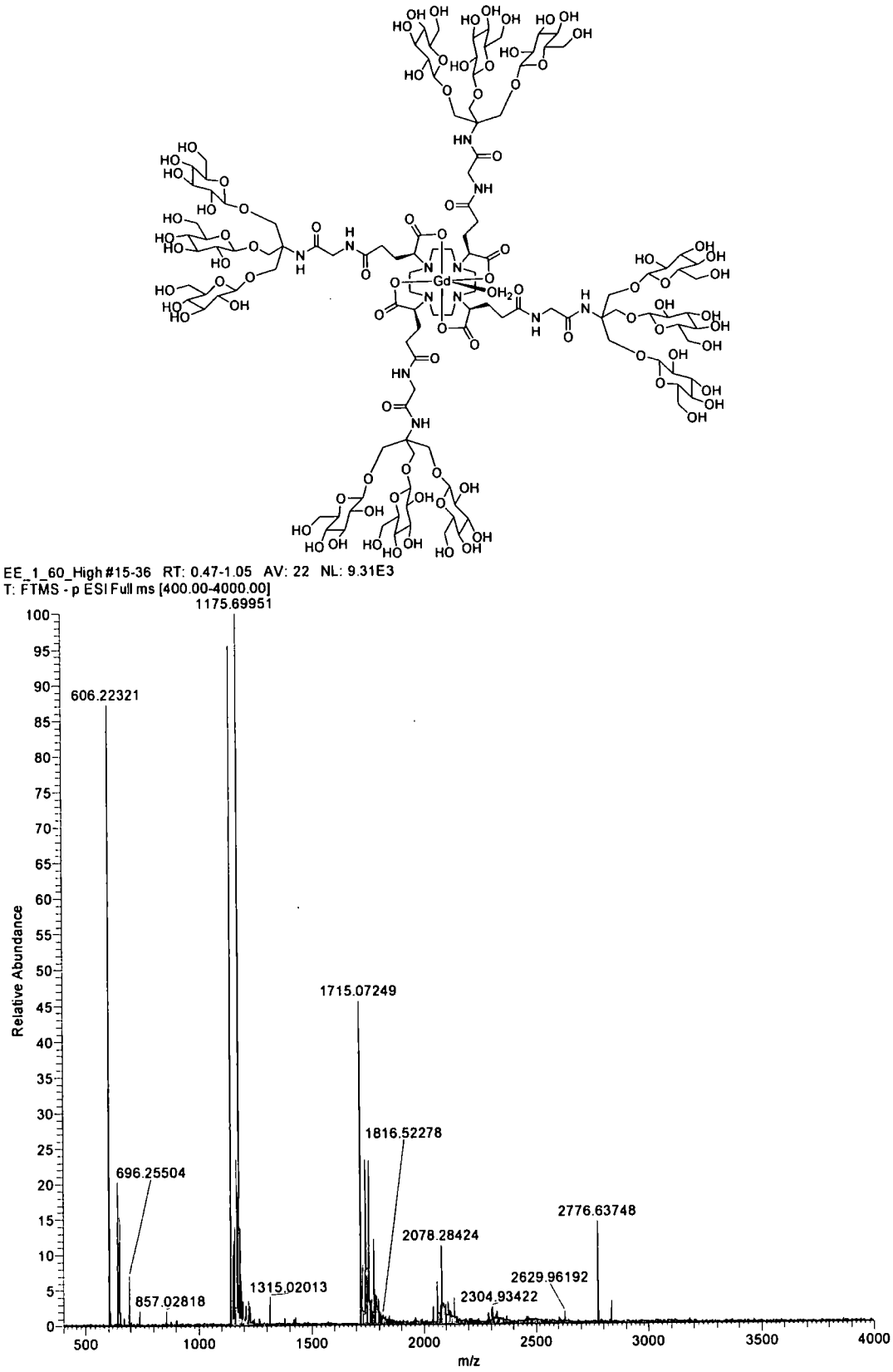

Figure 1: ES – MS spectrum of dendrimer $[GdgDOTAGlu_{12}Gly_4(H_2O)]^-$.

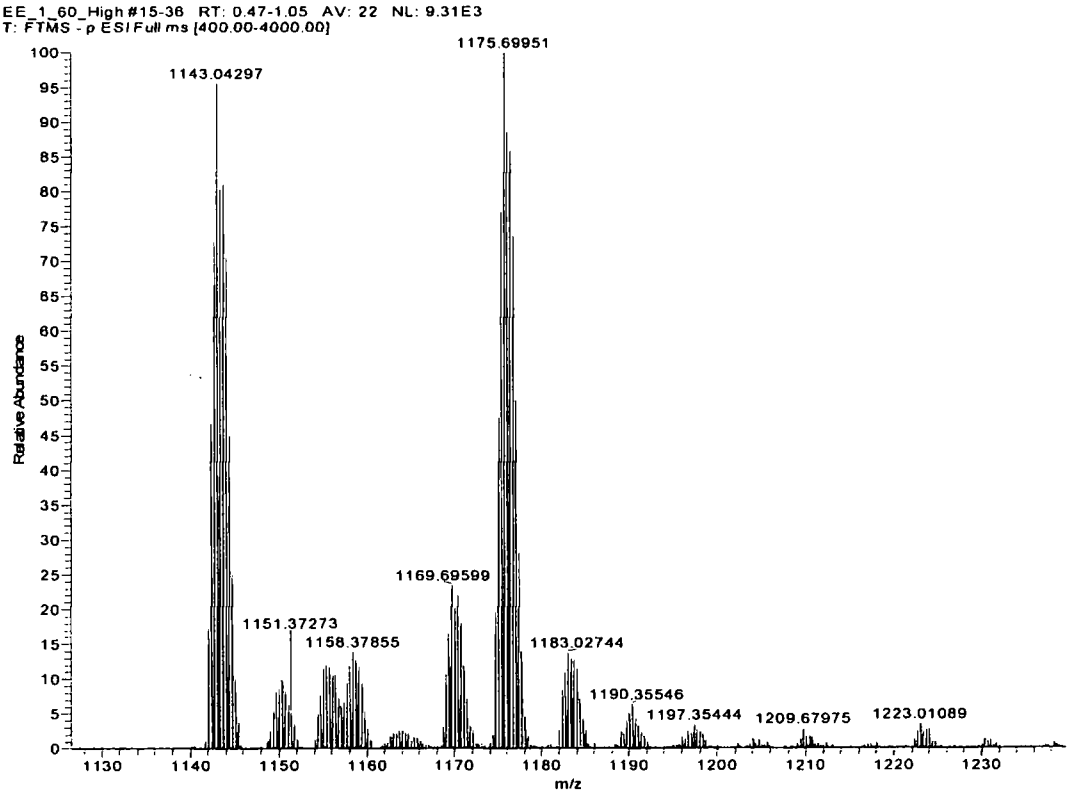

Figure 2: Expansion of the ES – MS spectrum of dendrimer [GdgDOTAGlu$_{12}$Gly$_4$(H$_2$O)]$^-$.

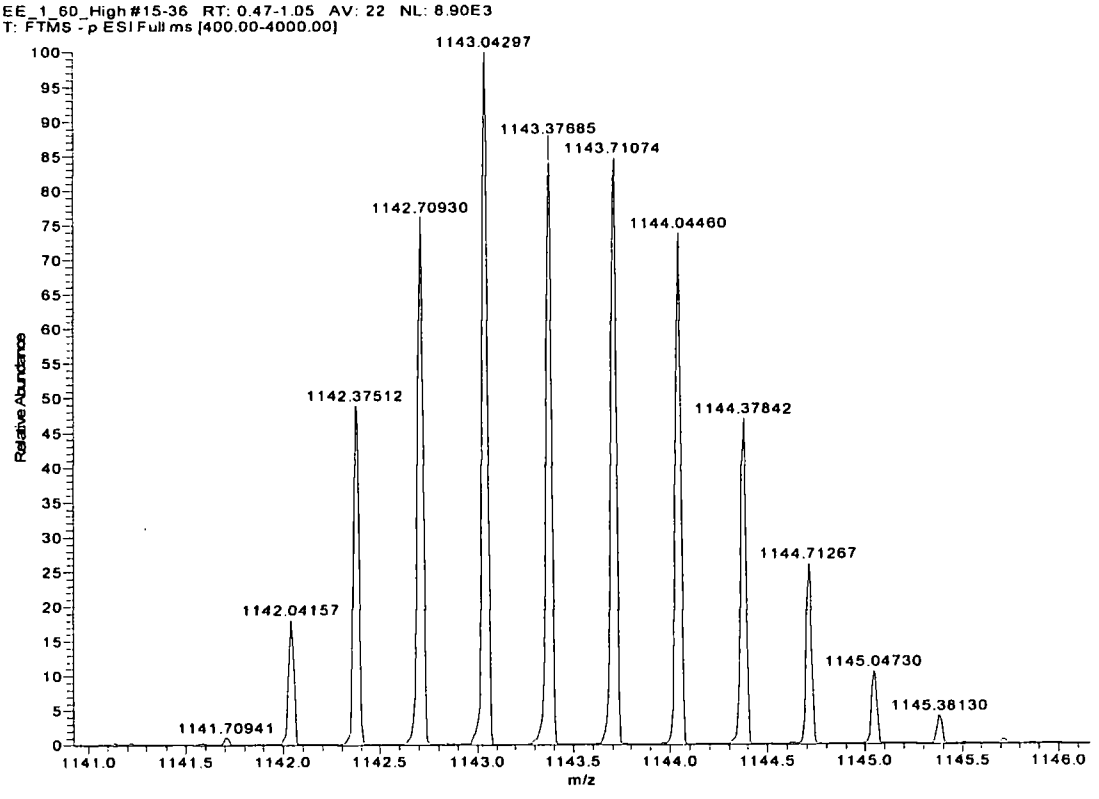

Figure 3: Expansion of the ES – MS spectrum of dendrimer [GdgDOTAGlu$_{12}$Gly$_4$(H$_2$O)]$^-$ highlighting the isotopic pattern of the molecular ion.

$[Ln^{III}(Glu)_2$*racemic*-AAZTA$]^{3-}$ or $[Ln^{III}L2]^{2-}$ systems

$[Eu^{III}(Glu)_2$*racemic*-AAZTA$]^{3-}$

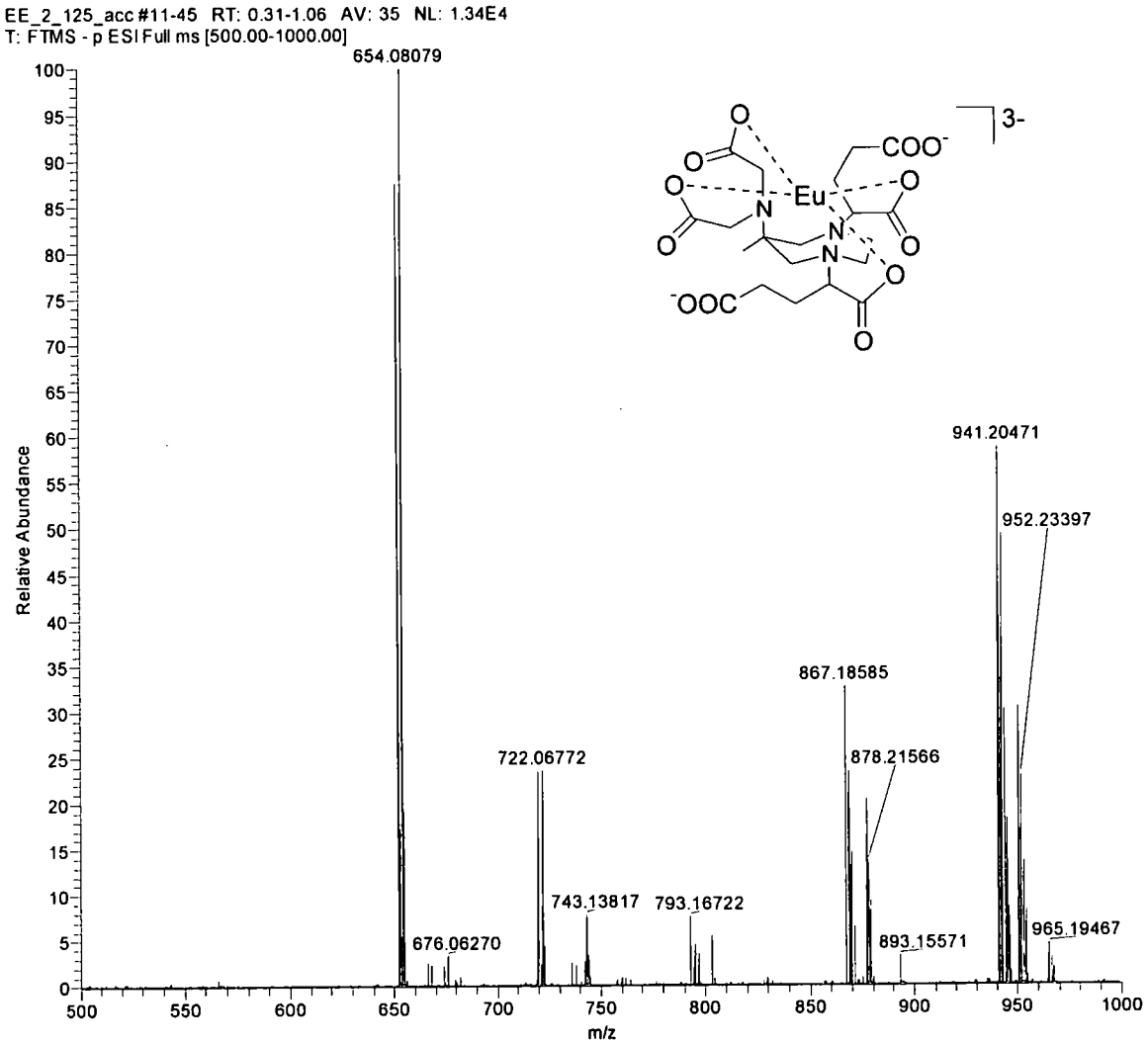

Figure 4: ES – MS spectrum of $[Eu^{III}(Glu)_2$*racemic*-AAZTA$]^{3-}$.

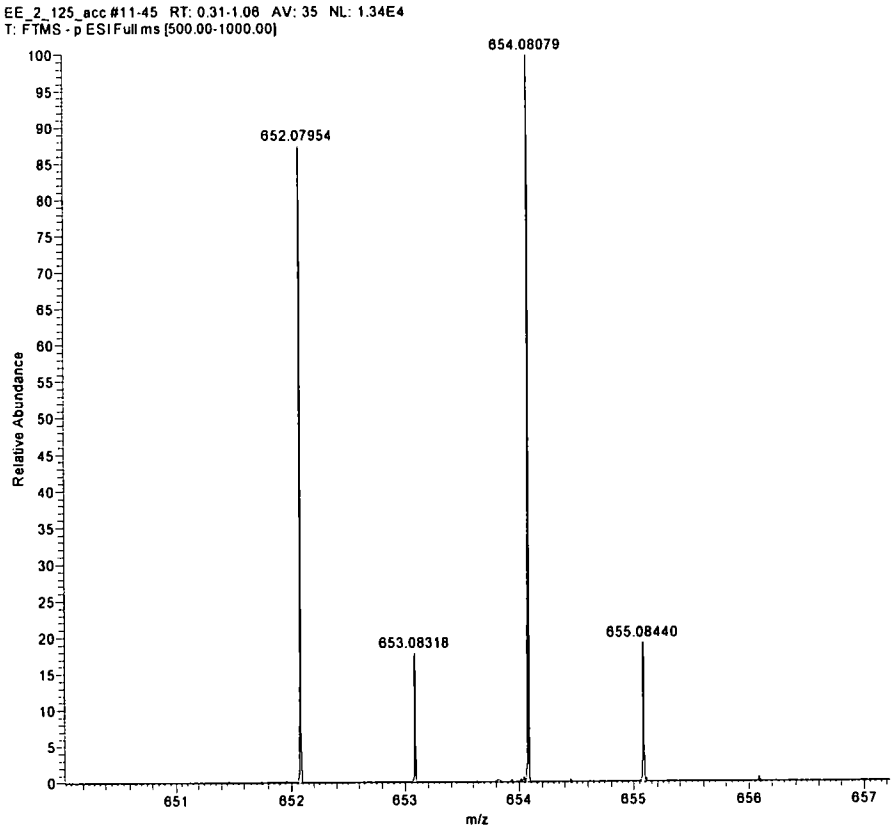

Figure 5: ES – MS spectrum of $[Eu^{III}(Glu)_2$*racemic*-AAZTA$]^{3-}$.

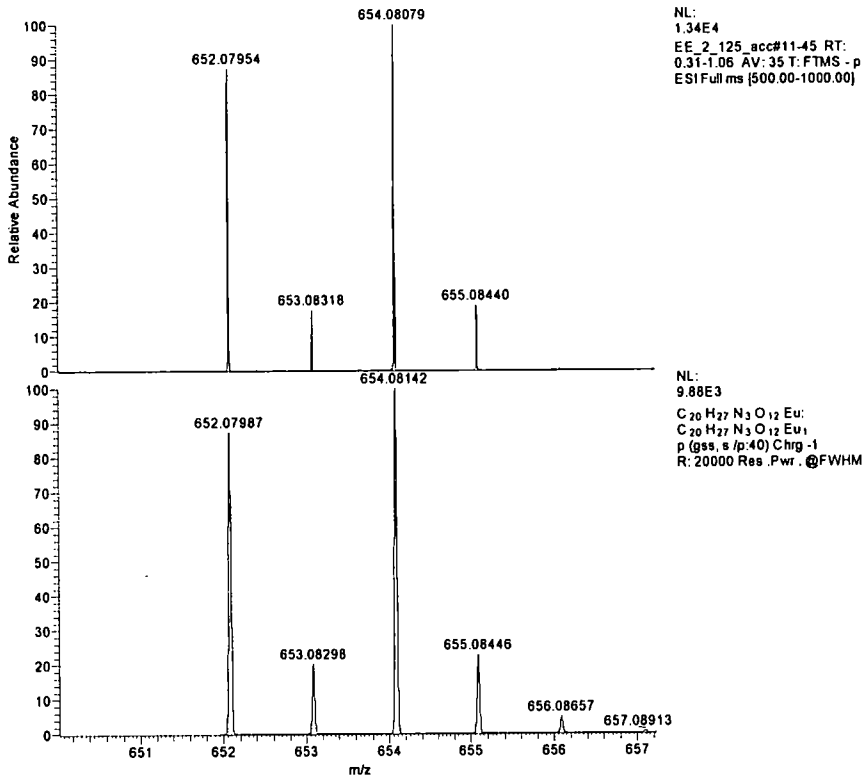

Figure 6: ES – MS spectrum of $[Eu^{III}(Glu)_2$*racemic*-AAZTA$]^{3-}$: expansion highlighting the isotopic pattern of the molecular ion.

$[Ln^{III}(Glu)_2(RR)\text{-AAZTA}]^{3-}$ or $[Ln^{III}L3]^{2-}$ systems

$[Gd^{III}(Glu)_2(RR)\text{-AAZTA}]^{3-}$

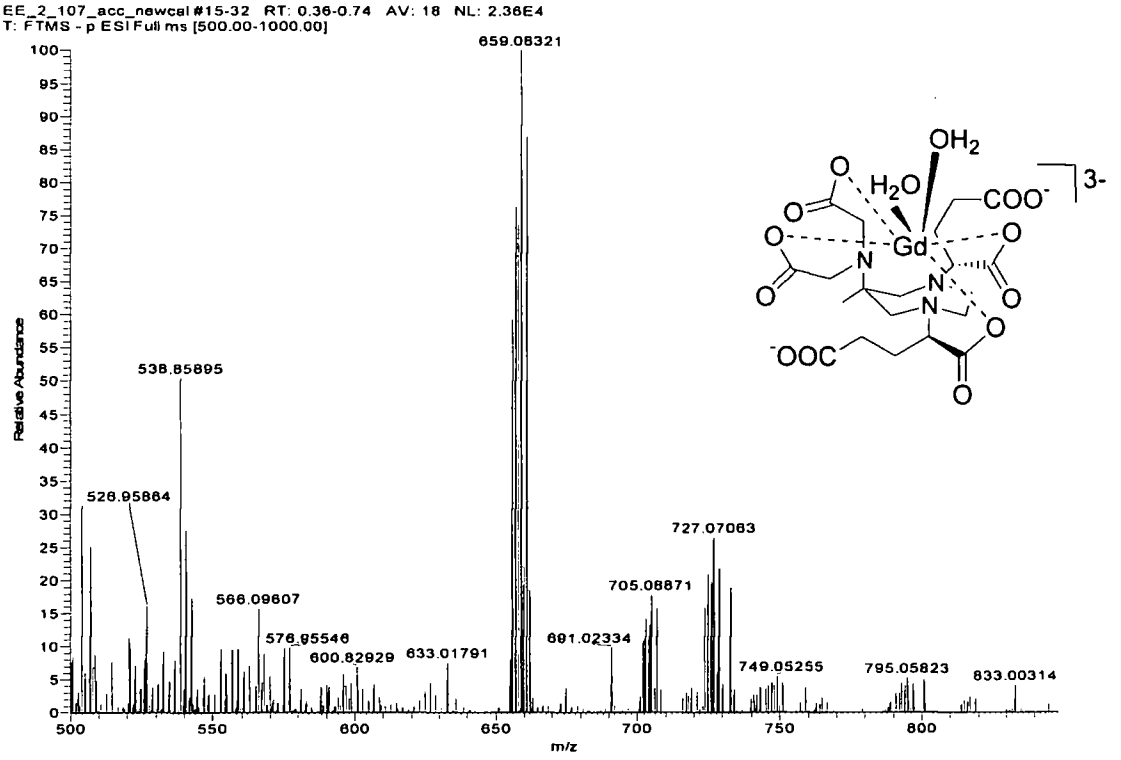

Figure 7: ES – MS spectrum of $[Gd^{III}(Glu)_2(RR)\text{-AAZTA}]^{3-}$.

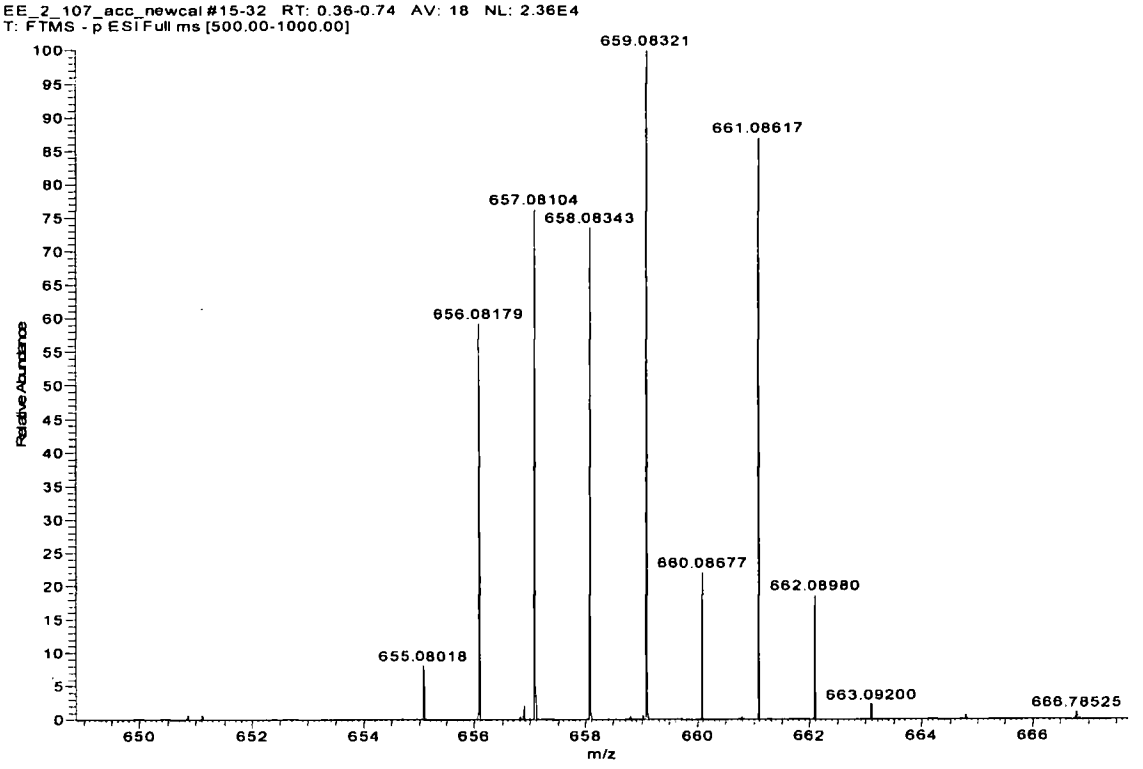

Figure 8: Expansion of the ES – MS spectrum of $[Gd^{III}(Glu)_2(RR)\text{-AAZTA}]^{3-}$, highlighting the isotopic pattern of the molecular ion.

$[Eu^{III}(Glu)_2$*(RR)*-AAZTA$]^{3-}$

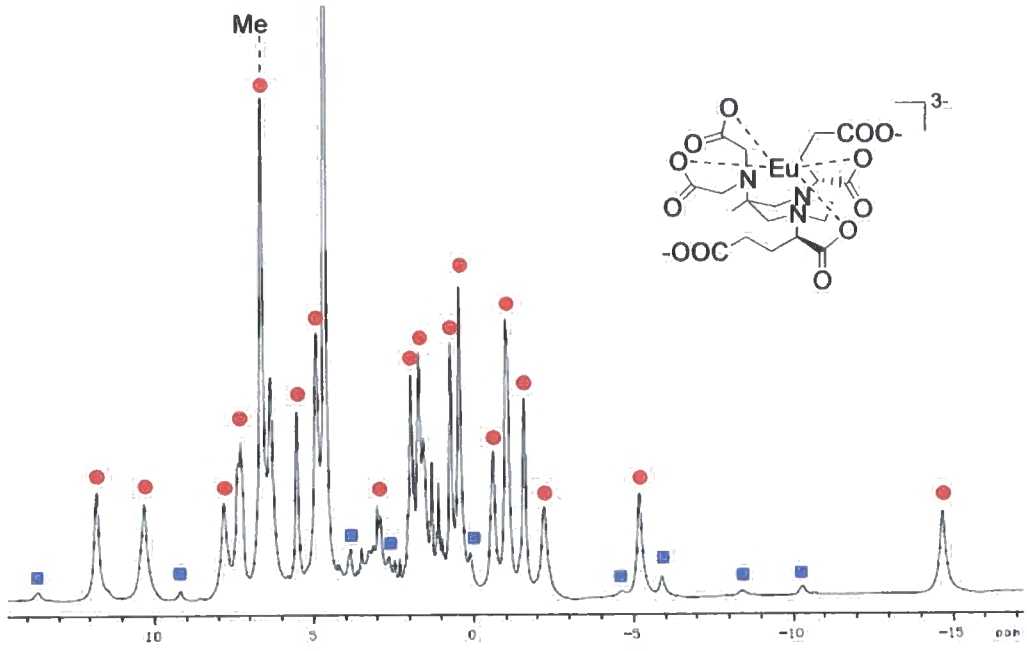

Figure 9: ^{1}H NMR spectrum of $[Eu^{III}(Glu)_2$*(RR)*-AAZTA$]^{3-}$ (700 MHz, D_2O, pD 5.4, 24 °C).

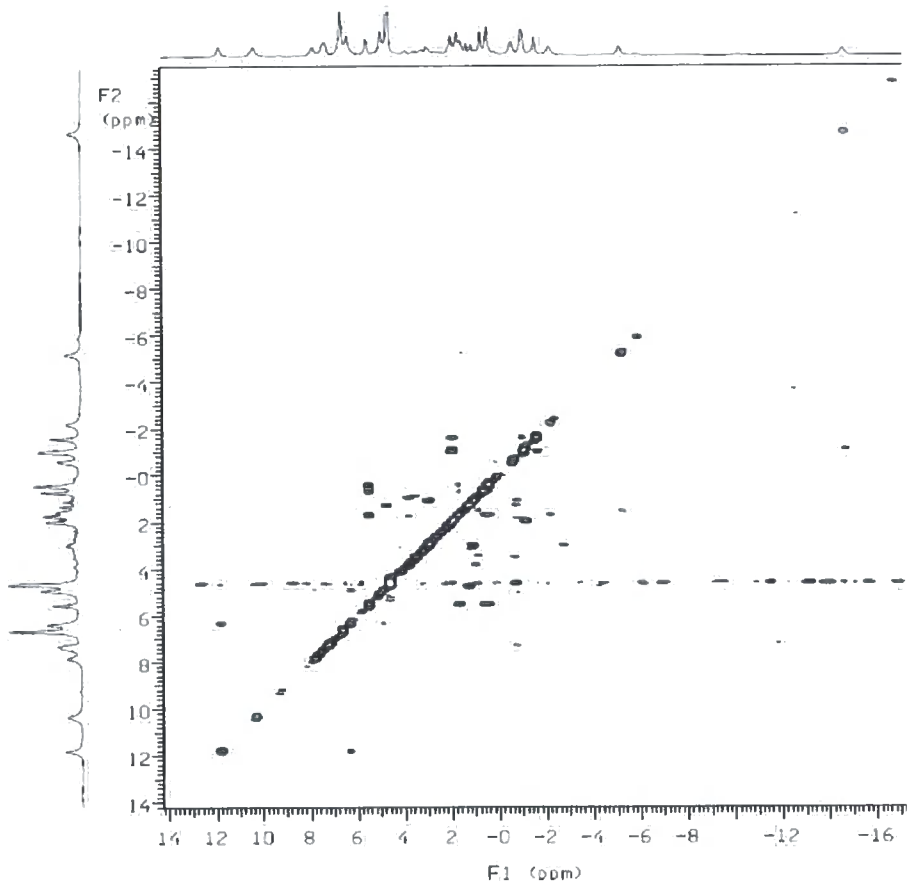

Figure 10: ^{1}H - ^{1}H COSY NMR spectrum of $[Eu^{III}(Glu)_2$*(RR)*-AAZTA$]^{3-}$ (700 MHz, D_2O, pD 5.4, 24 °C).

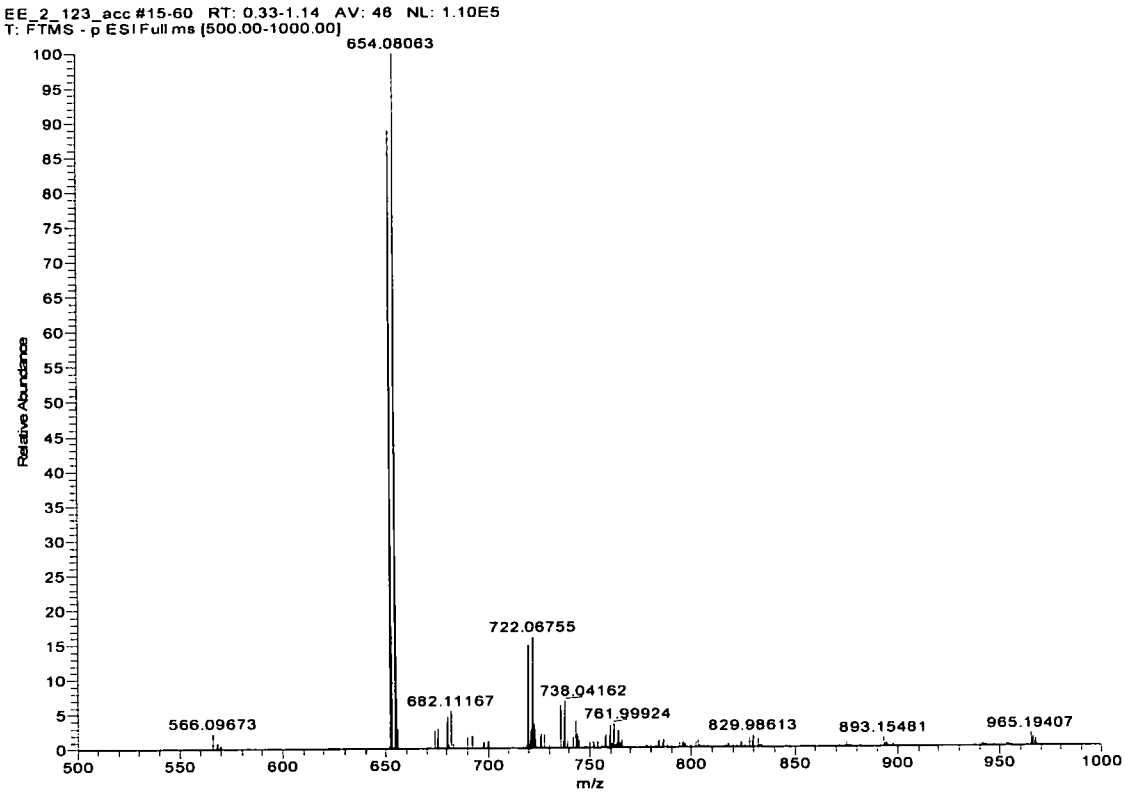

Figure 11: ES – MS spectrum of $[Eu^{III}(Glu)_2(RR)\text{-AAZTA}]^{3-}$.

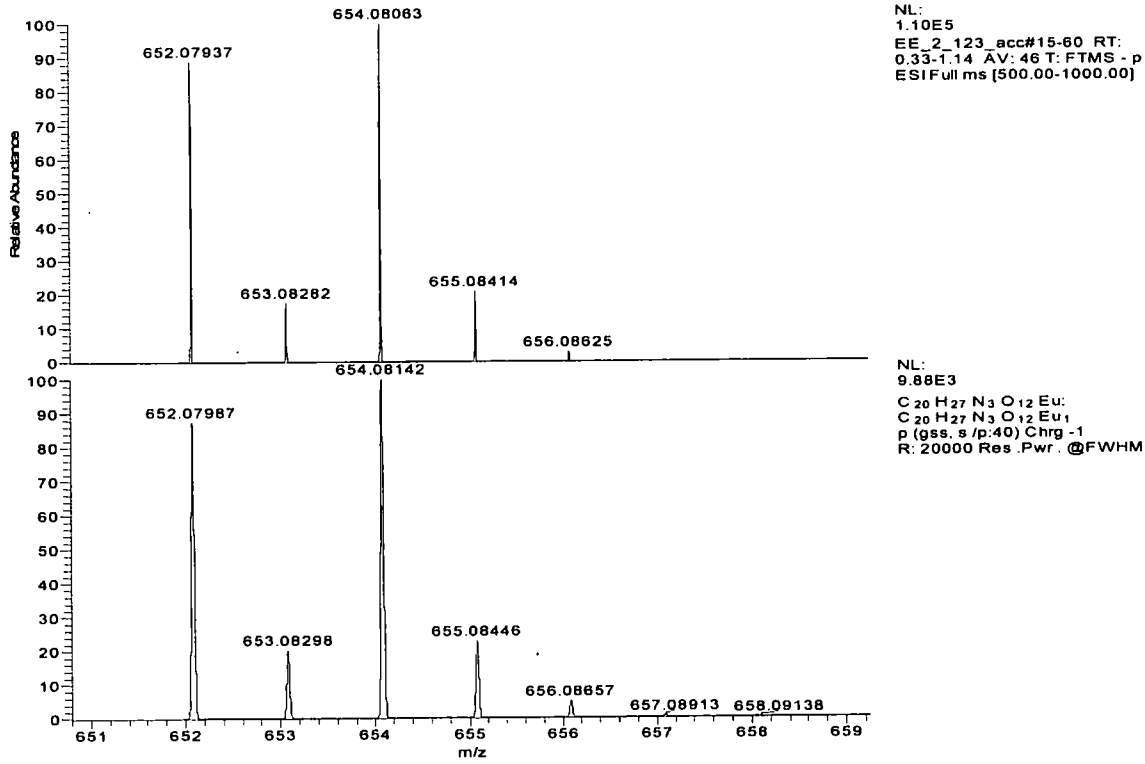

Figure 12: Expansion of the ES – MS spectrum of $[Eu^{III}(Glu)_2(RR)\text{-AAZTA}]^{3-}$, highlighting the isotopic pattern of the molecular ion.

$[Ln^{III}(Glu)AAZTA]^{2-}$ or $[Ln^{III}L3]^{2-}$ systems

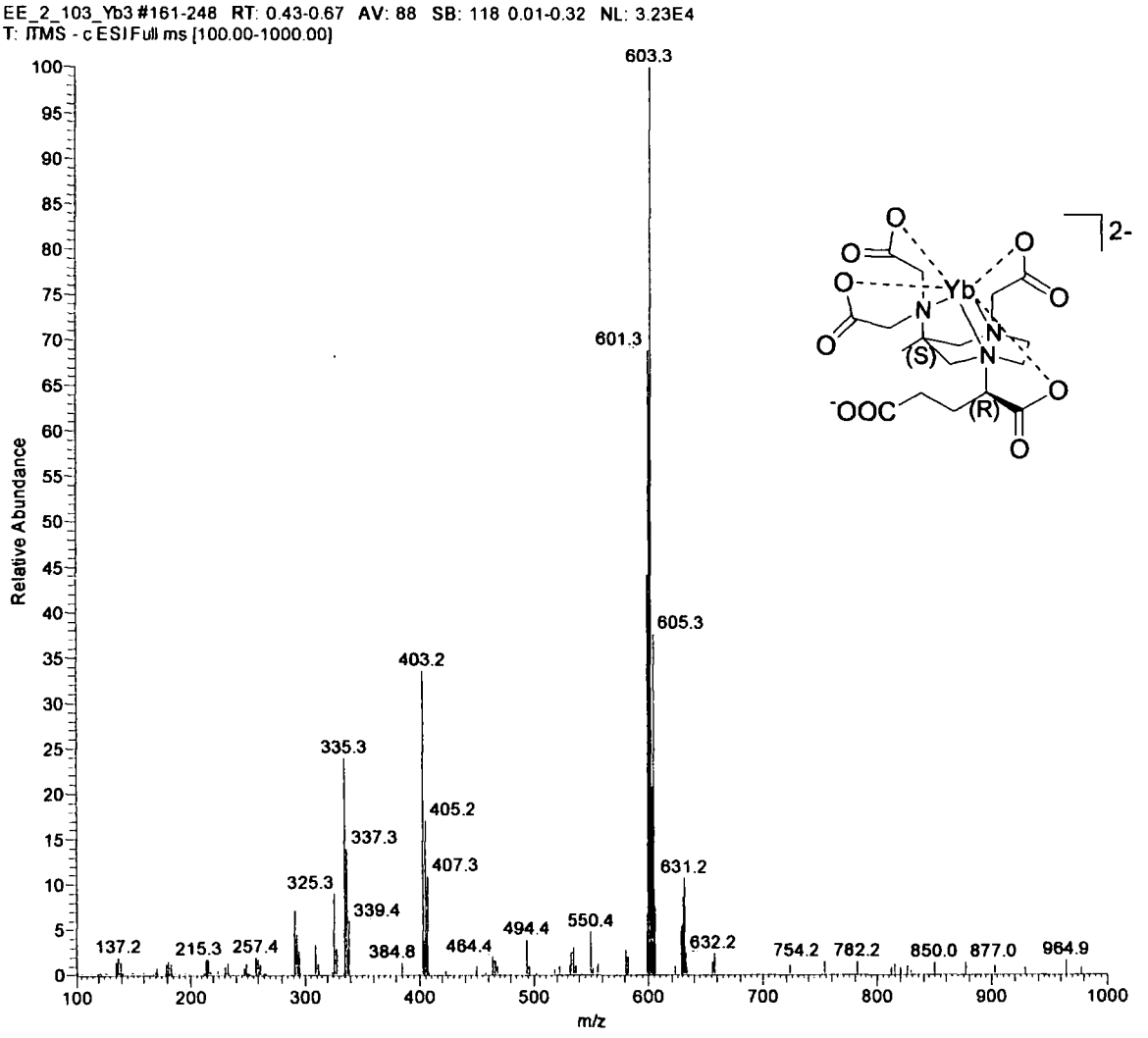

Figure 13: ES – MS spectrum of $[Yb^{III}(Glu)AAZTA]^{2-}$.

In the next two pages are shown the ^1H NMR and ^1H - ^1H COSY spectra of the complex $[Yb^{III}(Glu)AAZTA]^{2-}$ and of the analogue europium complex $[Eu^{III}(Glu)AAZTA]^{2-}$, both registered at in D_2O, 500 MHz, 20 °C, pD 5.4.

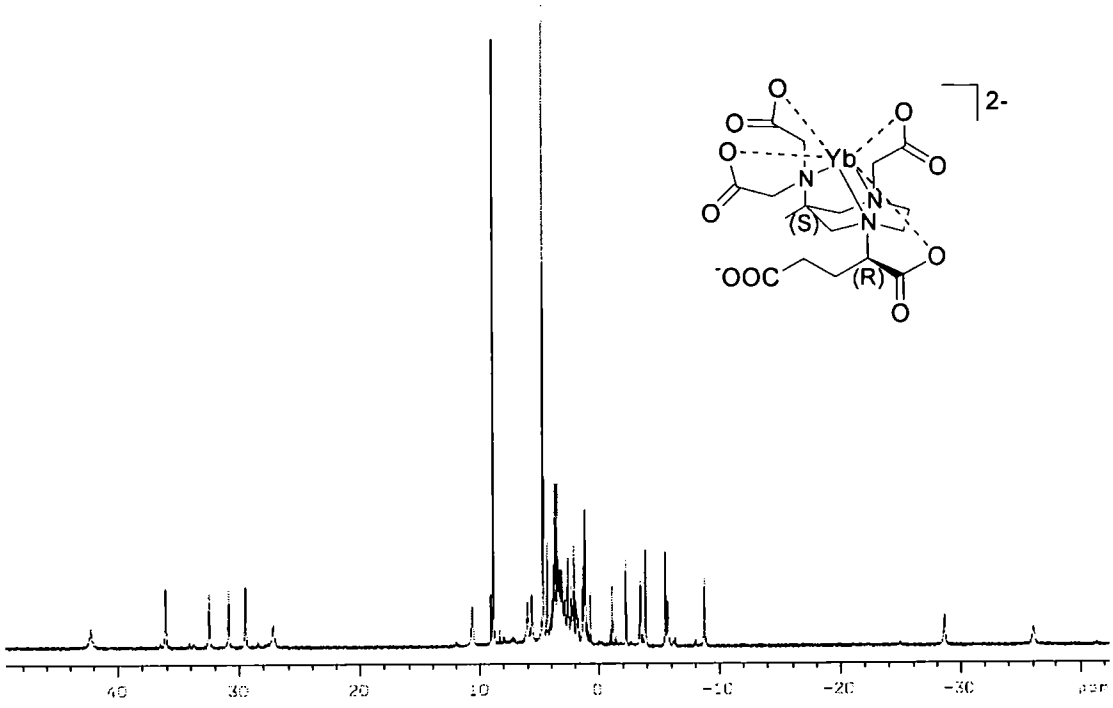

Figure 14: ^{1}H NMR spectrum of [Yb^{III}(Glu)AAZTA]$^{2-}$.

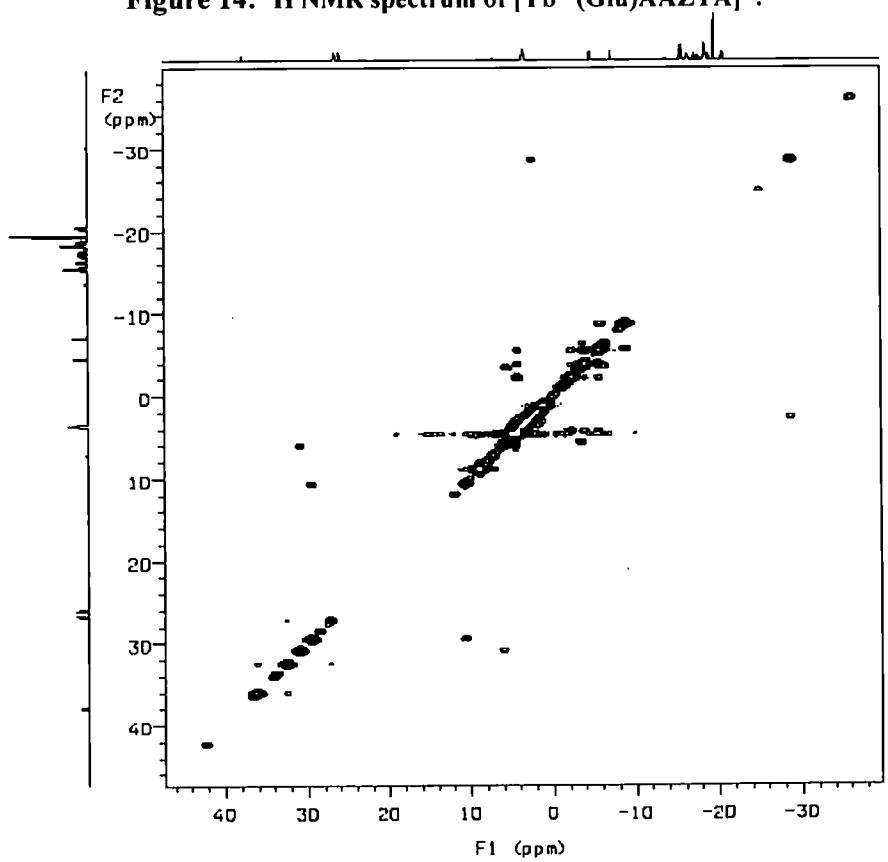

Figure 15: ^{1}H - ^{1}H COSY NMR spectrum of [Yb^{III}(Glu)AAZTA]$^{2-}$.

[Yb^{III}(Glu)AAZTA]$^{2-}$ or [Yb^{III}L3]$^{2-}$.

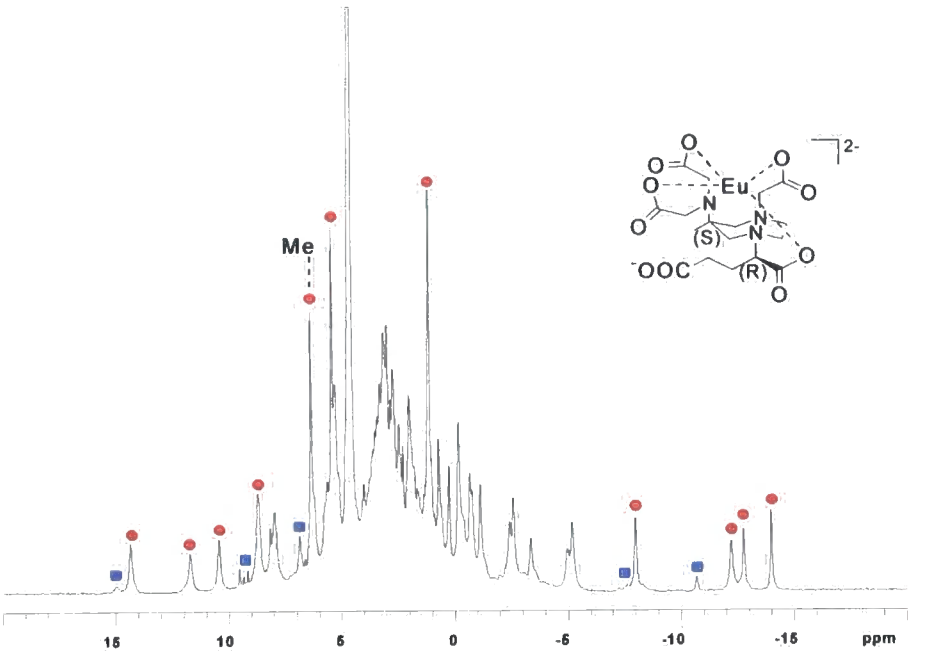

Figure 16: ^{1}H NMR spectrum of [Eu^{III}(Glu)AAZTA]$^{2-}$.

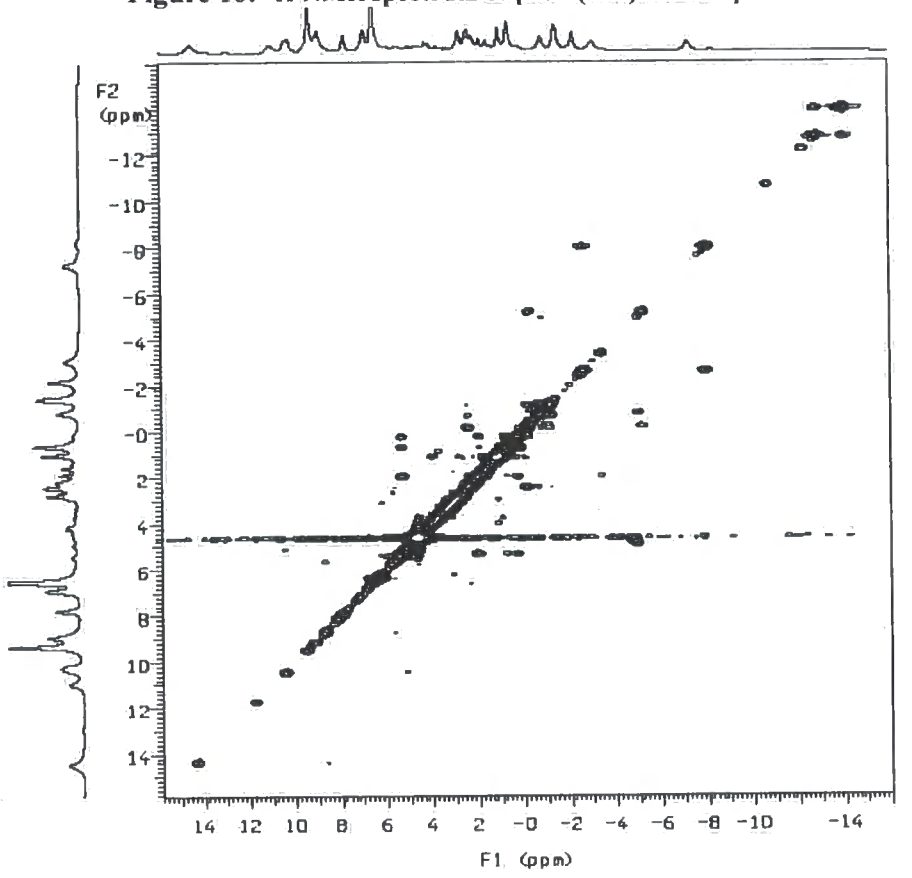

Figure 17: ^{1}H - ^{1}H COSY NMR spectrum of [Eu^{III}(Glu)AAZTA]$^{2-}$.

$[Gd^{III}(Glu)AAZTA]^{2-}$ or $[Gd^{III}L3]^{2-}$

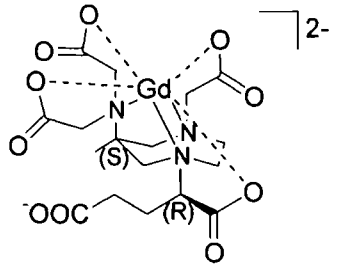

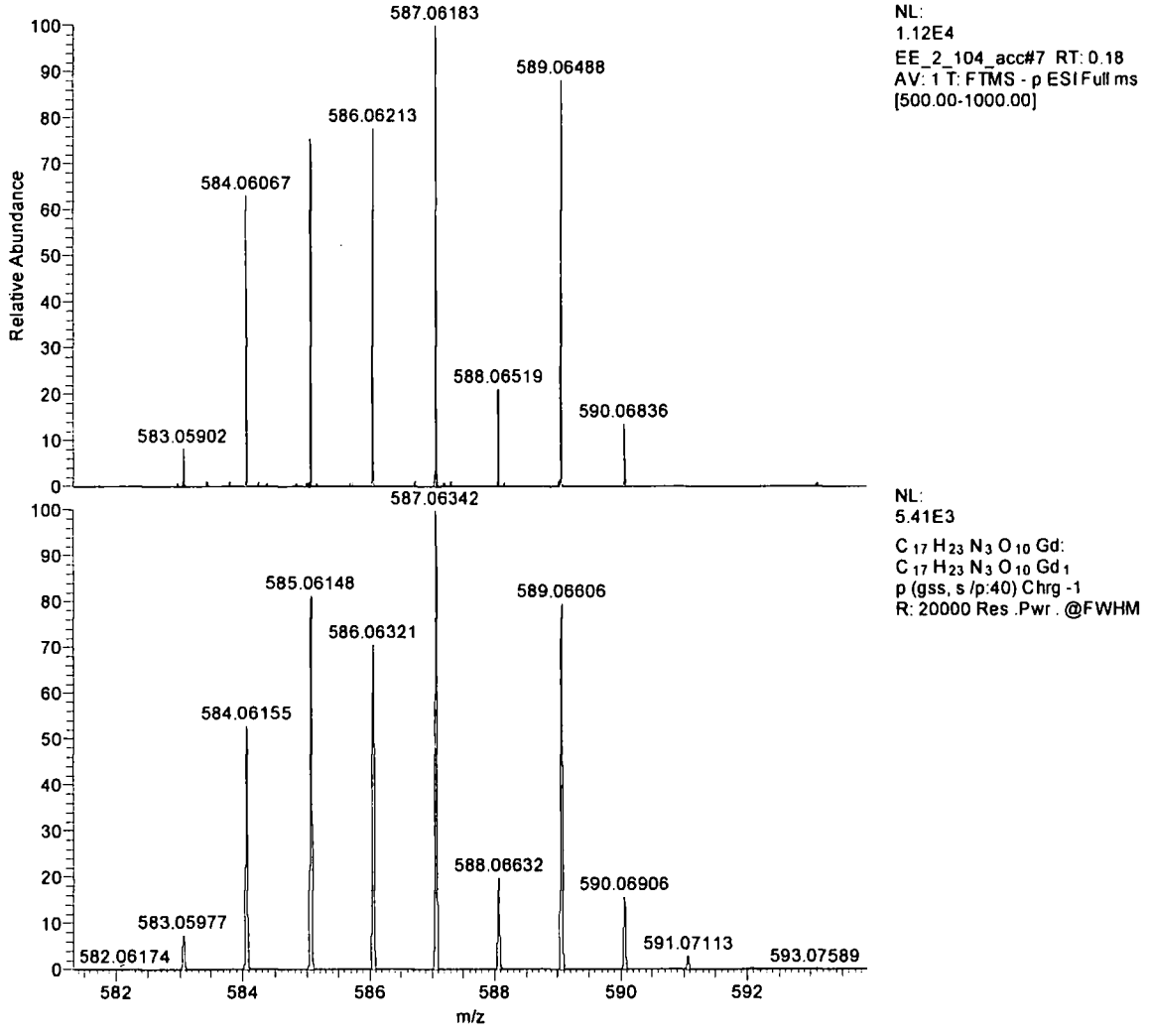

Figure 18: ES – MS of $[Yb^{III}(Glu)AAZTA]^{2-}$: a comparison between the measured (top) and the theoretical (bottom) mass-spectra.

$[Ln^{III}(Glu)_2(RS)\text{-AAZTA}]^{3-}$ or $[Ln^{III}L3]^{2-}$ systems

$[Gd^{III}(Glu)_2(RS)\text{-AAZTA}]^{3-}$

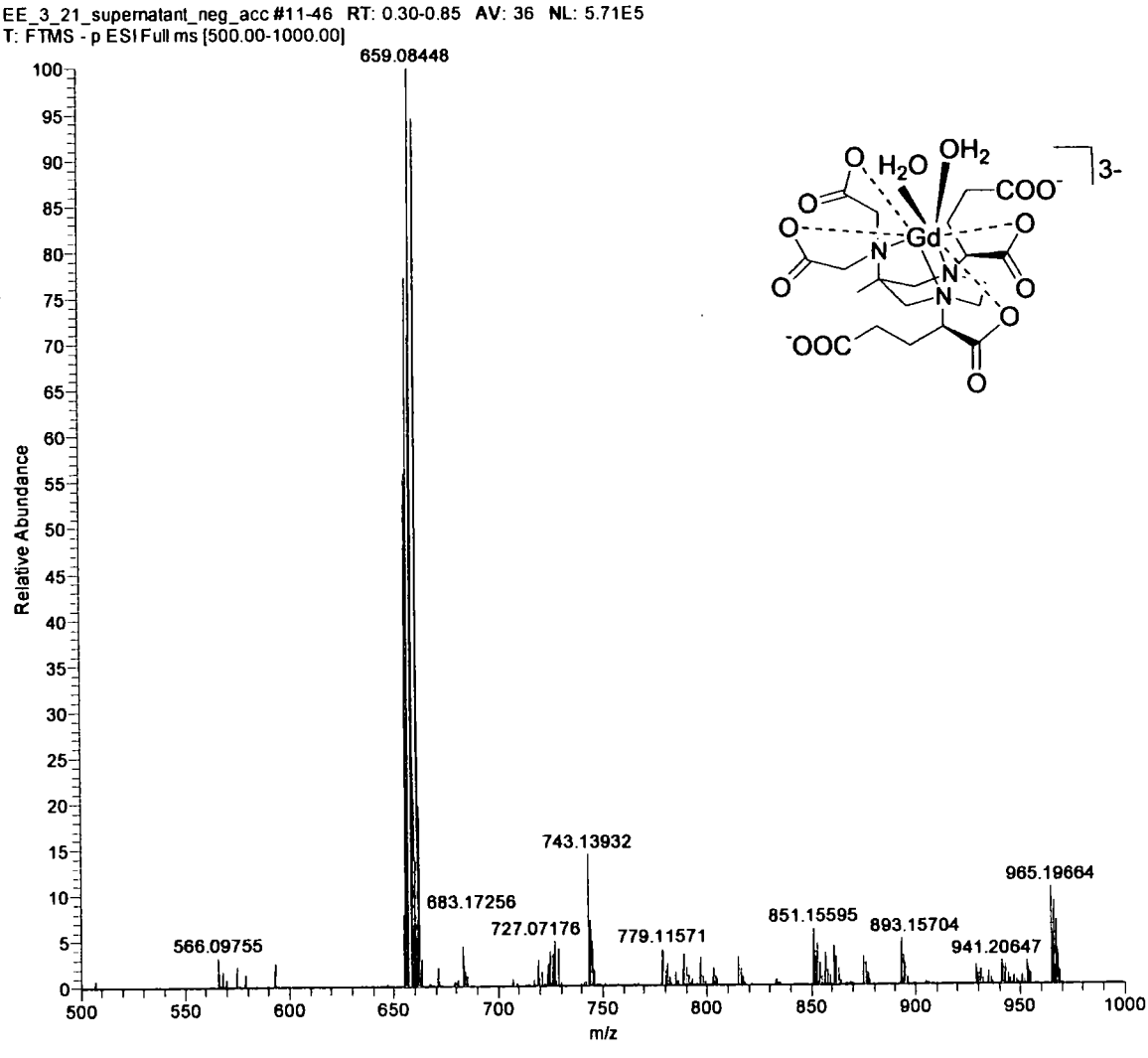

Figure 19: ES – MS of $[Gd^{III}(Glu)_2(RS)\text{-AAZTA}]^{3-}$

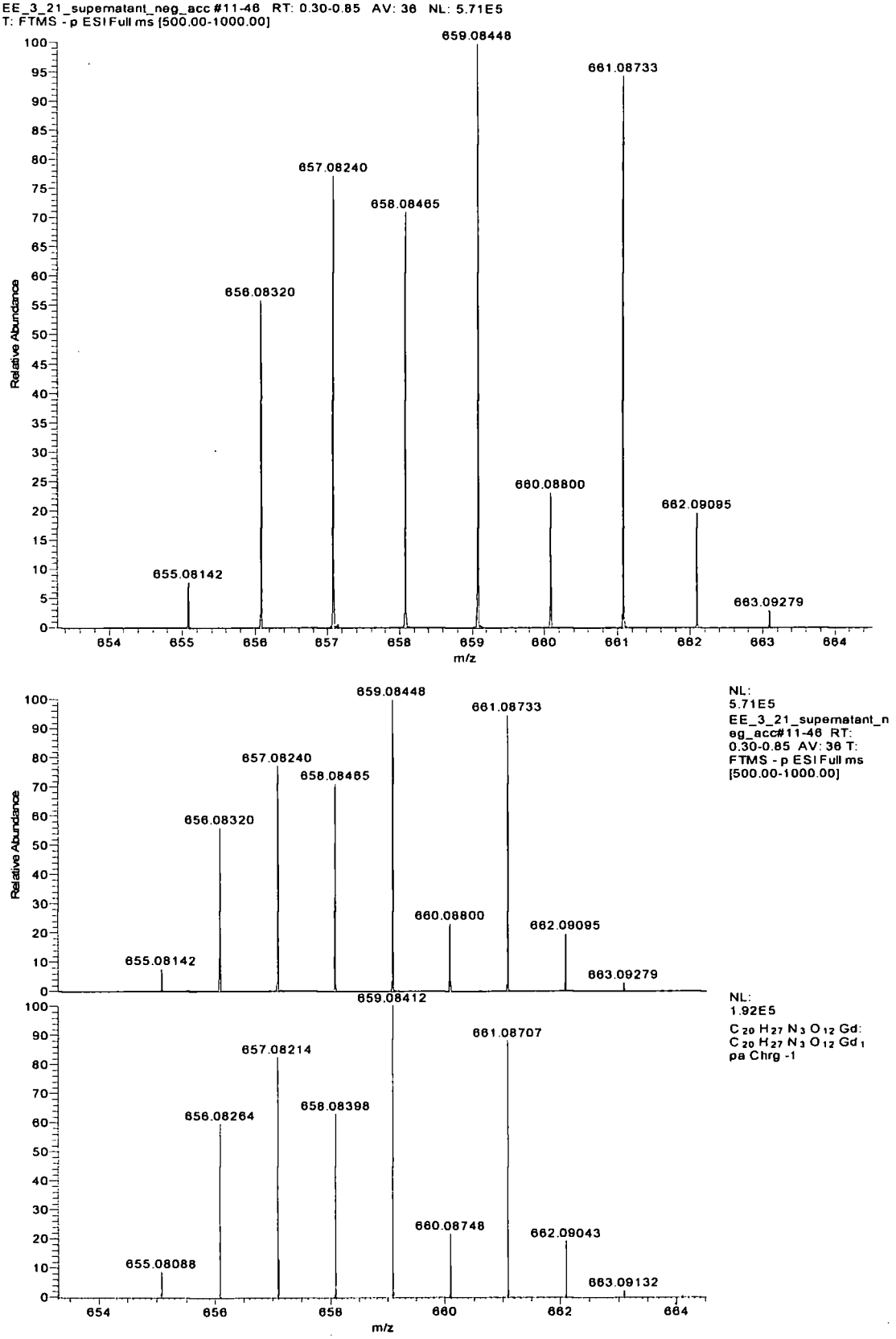

Figure 20: Expansion of ES-MS of $[Gd^{III}(Glu)_2$*(RS)*-AAZTA$]^{3-}$ highlighting the isotopic pattern of the molecular ion (top); a comparison between the measured and the theoretical mass-spectra (bottom part of the page).

$[Yb^{III}(Gluco)GluAAZTA]^-$ or $[Yb^{III}L9]^-$

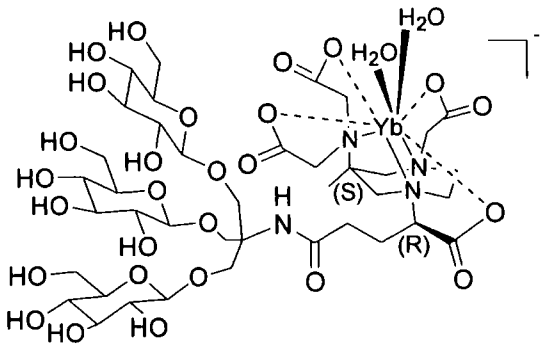

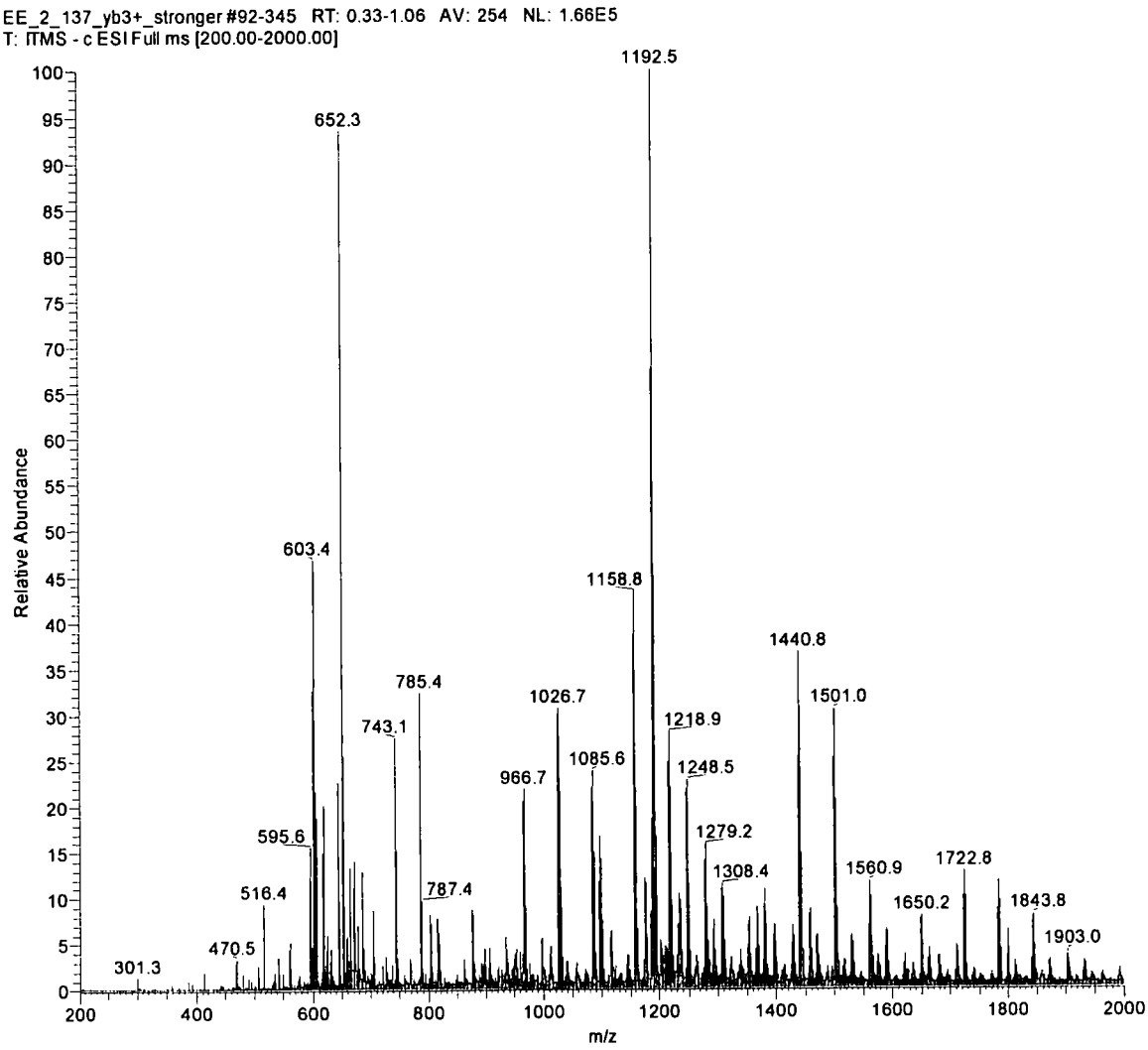

Figure 21: ES-MS of $[Yb^{III}(Gluco)GluAAZTA]^-$.

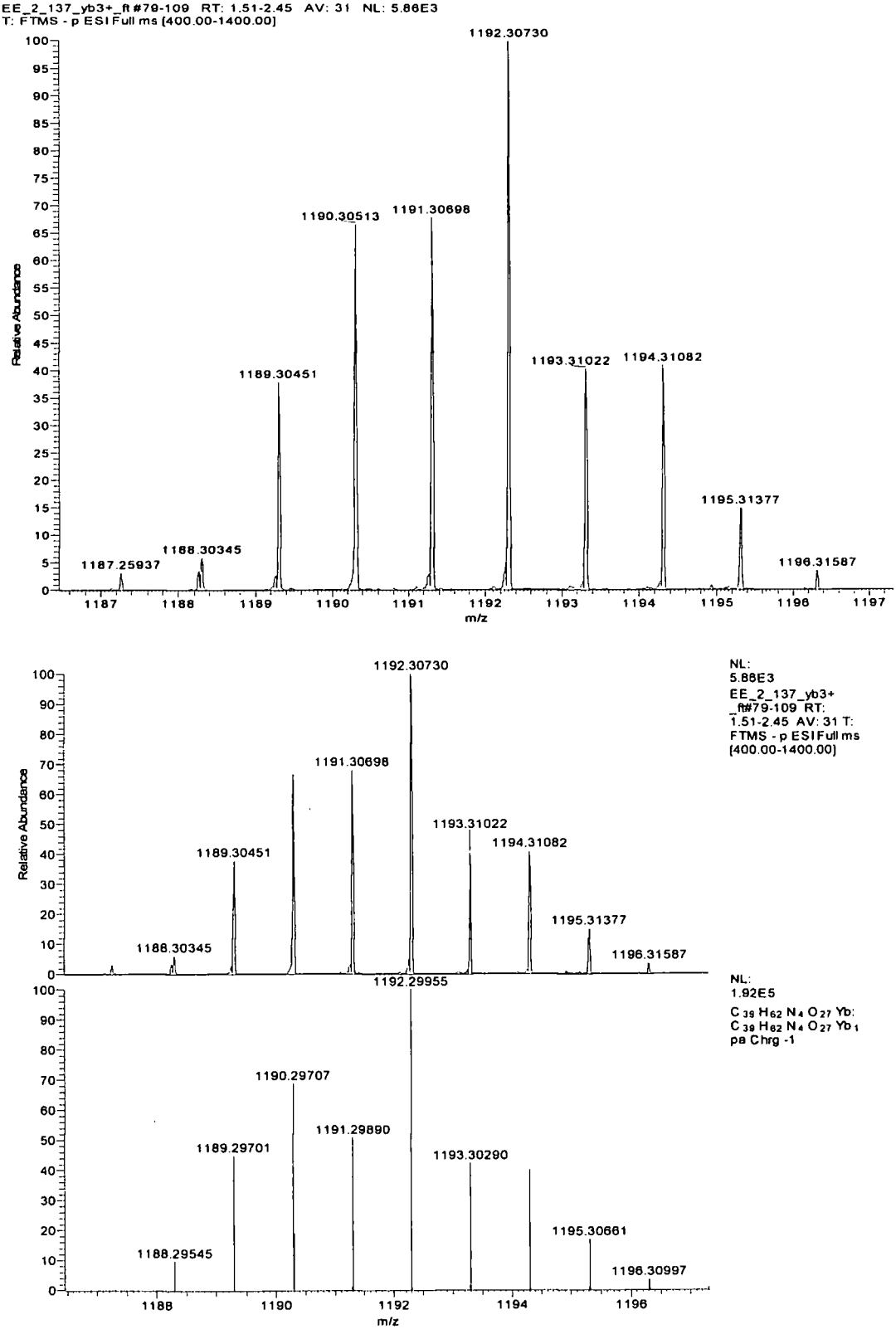

Figure 22: Expansion of ES-MS of $[Yb^{III}(Gluco)GluAAZTA]^-$ highlighting the isotopic pattern of the molecular ion (top); a comparison between the measured and the theoretical mass-spectra (bottom part of the page).

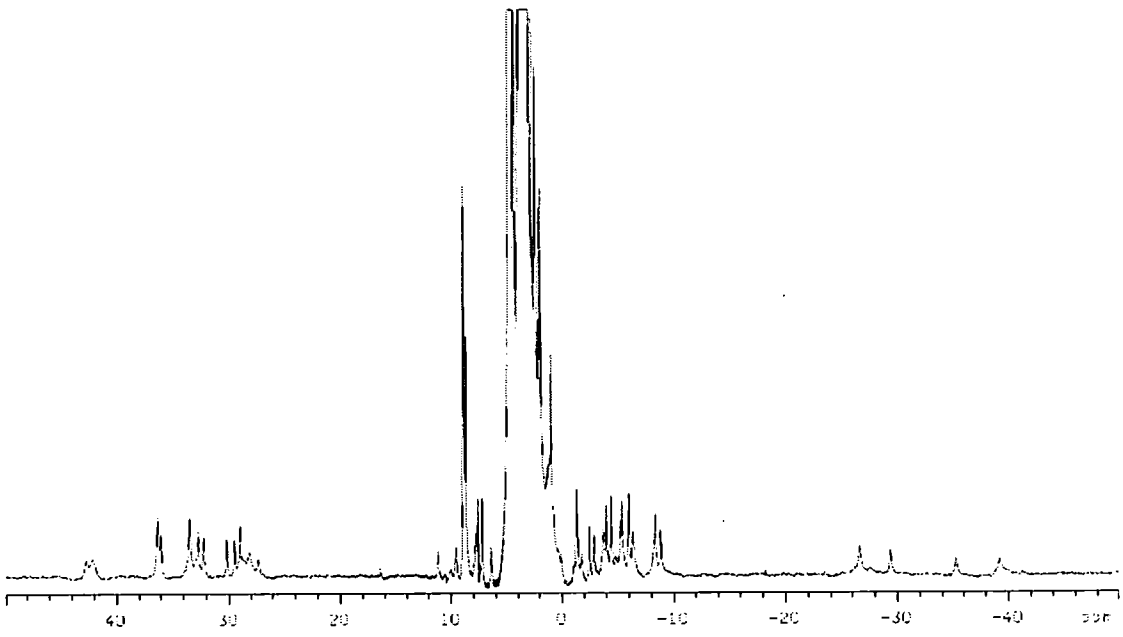

Figure 23: ^{1}H NMR spectrum of [Yb^{III}(Gluco)Glu-AAZTA]$^{-}$ (D_2O, 400 MHz, ambient temperature, pD 5.4).

[$Yb^{III}(Gluco)_2(Glu)_2$*(RS)*-AAZTA]$^-$ or [Yb^{III}L9]$^-$

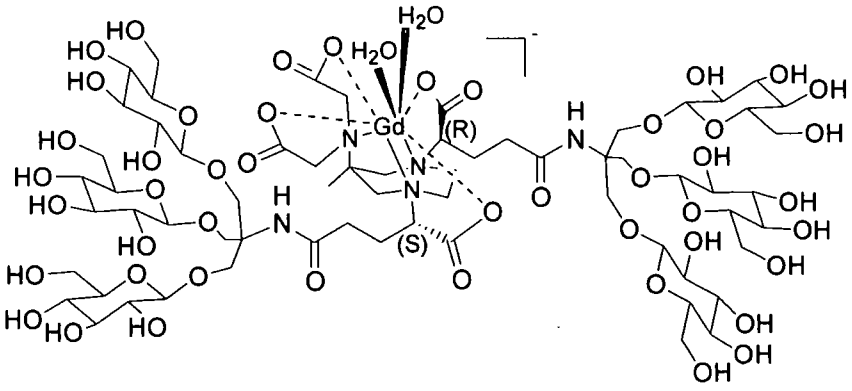

[Gd^{III}L10]$^-$

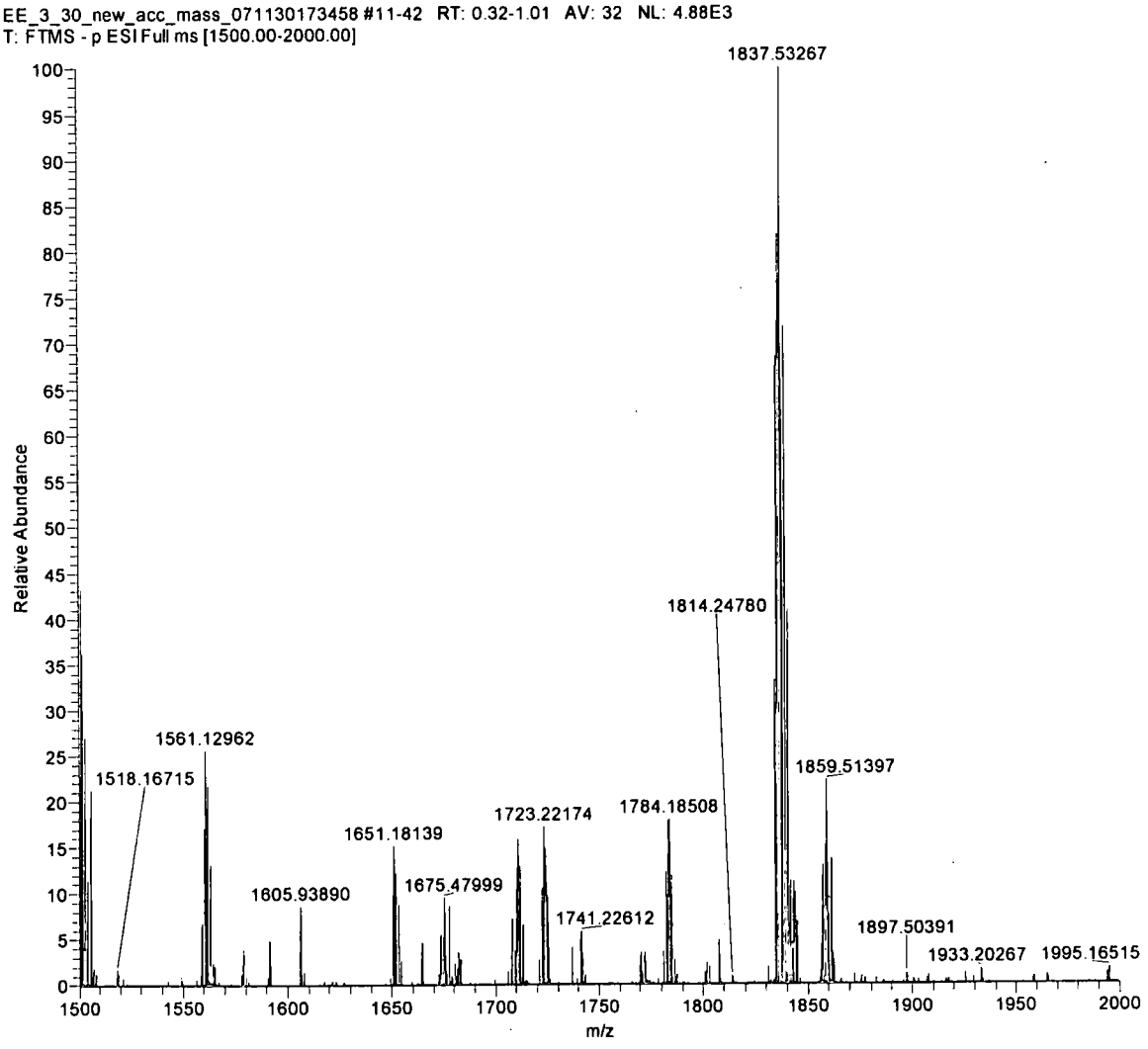

Figure 24: ES-MS of [$Yb^{III}(Gluco)_2(Glu)_2$*(RS)*-AAZTA]$^-$.

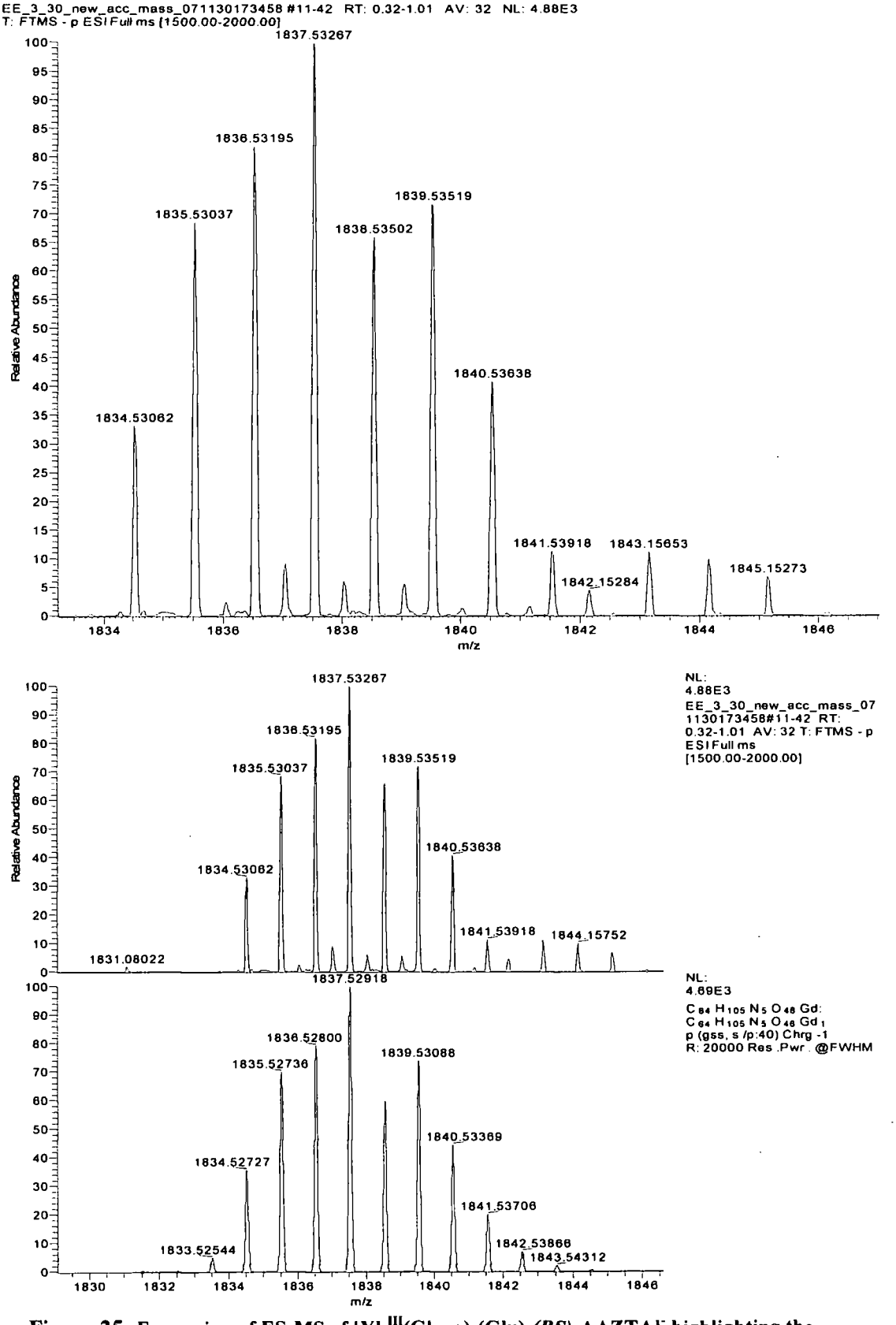

Figure 25: Expansion of ES-MS of $[Yb^{III}(Gluco)_2(Glu)_2$*(RS)*-AAZTA]$^-$ highlighting the isotopic pattern of the molecular ion (top); a comparison between the measured and the theoretical mass-spectra (bottom part of the page).